Lead and Cadmium Geochemistry of Corals : Reconstruction of Historic Perturbations in the Upper Ocean

by

Glen T. Shen

S.B., Massachusetts Institute of Technology

(1979)

SUBMITTED IN PARTIAL FULFILLMENT
OF THE REQUIREMENTS FOR THE DEGREE OF
DOCTOR OF PHILOSOPHY

at the

MASSACHUSETTS INSTITUTE OF TECHNOLOGY
and the
WOODS HOLE OCEANOGRAPHIC INSTITUTION

SEPTEMBER, 1986

Signature of Author_____
Department of Earth, Atmospheric, and Planetary Sciences,
Massachusetts Institute of Technology and the Joint Program in
Oceanography, Massachusetts Institute of Technology/Woods Hole
Oceanographic Institution, September 1986

Certified by_____
Edward A. Boyle, Thesis Supervisor

Accepted by_____
Edward A. Boyle, Chairman, Joint Committee for Chemical
Oceanography, Massachusetts Institute of Technology/Woods Hole
Oceanographic Institution

LEAD AND CADMIUM GEOCHEMISTRY OF CORALS: RECONSTRUCTION OF HISTORIC PERTURBATIONS IN THE UPPER OCEAN

by

Glen T. Shen

Submitted to the Department of Earth, Atmospheric and Planetary Sciences on August 8, 1986 in partial fulfillment of the requirements for the Degree of Doctor of Philosophy in Oceanography

Abstract

Twentieth century trace element chronologies for the western North Atlantic, Pacific, and Indian Oceans have been reconstructed from annually-banded scleractinian corals. Elements analyzed include lead (4-60 nmol/mol Ca), cadmium (0.3-6 nmol/mol Ca), barium (4-6 μmol/mol Ca), zinc (3-10 nmol/mol Ca), and vanadium (90-120 nmol/mol Ca). A rigorous preparative/cleaning protocol enabled removal of detrital, organic, and handling associated contaminants in five of seven coral genera studied. Prior to analysis, samples were dissolved and residual lattice bound metals (except Ba) non-selectively coprecipitated as dithiocarbamate chelates in the presence of a cobalt carrier. This procedure isolates metals of interest from the coral calcium matrix to allow more precise analysis by graphite furnace atomic absorption spectrophotometry. The cleaning techniques used also permitted determination of stable Pb isotopic distributions in a variety of corals. Samples analyzed by mass spectrometry were purified by anion exchange chromatography.

Measurements of lattice-bound Pb in sequential coral bands have revealed temporal changes in surface water Pb concentrations and Pb isotopic ratios. Perturbations are observable in all specimens studied, attesting to global augmentation of environmental Pb by industrialization. In the western North Atlantic, Pb perturbations have occurred in direct response to the American industrial revolution and the subsequent introduction and phasing-out of alkyl Pb additives in gasoline. Surface ocean conditions near Bermuda may be reliably reconstructed from the coral data via a lead distribution coefficient (K_D) of 2.3 for the species Diploria strigosa. Based on ^{210}Pb measurements, a similar distribution coefficient may be characteristic of corals in general. Surface Pb concentrations in the pre-industrial Sargasso Sea were about 15-20 pM. Concentrations rose to near 90 pM

by 1923 as a result of metals manufacture and fossil fuel combustion. Beginning in the late 1940's, increased utilization of leaded gasoline eventually led to a peak concentration of 240 pM in 1971, representing an approximate 15-fold increase over background. Surface ocean concentrations are presently declining rapidly (128 pM in 1984) as a result of curtailed alkyl Pb usage. Lead isotopic shifts parallel the concentration record indicating that characteristic industrial and alkyl Pb source signatures have not changed appreciably in time. Industrial releases recorded in the Florida Straits reflect a weaker source and evidence of recirculated Pb (5-6 yrs old) from the North Atlantic subtropical gyre. An inferred background concentration of 38 pM suggests influence of shelf and/or resuspended inputs of Pb to waters overlying this coral reef.

In remote areas of the tropical and South Pacific and Indian Oceans, industrial signals are fainter and the corals studied much younger than their Atlantic counterparts; consequently, historic trends are more difficult to ascertain. Contemporary Pb concentrations implied by coral measurements (assuming K_D=2.3) are 40-50 pM for surface waters near Tutuila and Galapagos in the South Pacific, and 25-29 pM near Mauritius in the Indian Ocean. A single coral band from Fiji (1920±5 yrs) suggests a pre-industrial surface water concentration of 16-19 pM Pb for the South Pacific. In view of actual surface water measurements (Flegal and Patterson, 1983) and the North Atlantic coral data, the past and present Pacific coral extrapolations may be slightly high (estimated minimum pre-industrial surface Pb concentration = 10 pM). This could be a result of small variations in K_D among different coral genera, or incorporation of diagenetic Pb by corals sampled in coastal environments.

Surface ocean Cd levels near Bermuda have also been enhanced by North American industrial activity. Three to four-fold peak increases over background occurred at ca. 1920 due to unexploited Cd-rich flue dusts originating from zinc production, and again near 1970 as a result of heightened metals production and waste incineration. Natural modulation of surface seawater Cd levels in the eastern Equatorial Pacific has also been measured in a Galapagos Islands coral, Pavona clavus. Implied dissolved Cd concentrations over the past 20 years of 15-65 pM based on K_D = 1.0 closely resemble the observed range in adjacent surface waters. Close correlation of the coral Cd record to sea surface temperature and Southern Oscillation indices suggests a route to paleo-ENSO (El Nino - Southern Oscillation) reconstruction.

Thus far, only Pb and Cd have demonstrated clear temporal variability associated with industrialization and/or natural perturbations in ocean circulation. Distributions of Zn and V in the Sargasso Sea and Ba and ^{210}Pb in Florida Straits surface waters appear to have undergone little or no change over the past century. Addition of Cd and particularly Zn (+2 ionic radius only 80% that of Ca^{2+}) to

the growing list of cations which appear to be indiscriminately precipitated by corals with respect to their seawater distributions, suggests a common incorporation mechanism. A thermodynamic basis is not evident since expected differences in chemical speciation favor widely varying K_D's. More likely, the precipitation process is kinetically controlled within the supersaturated, possibly reducing micro-environment of the coral ectoderm.

Application of the coral Pb concentration and isotopic record of Bermuda to the ventilated thermocline model of Jenkins (1980) and Boyle et al. (1986) places important constraints on the geochemical transport of Pb in the oceans. Conservative models dominated by lateral ventilation on ^{3}H and ^{3}He-based time scales cannot account for observed distributions of Pb and ^{210}Pb simultaneously. More compelling, though, are model discrepancies from the vertical distribution of Pb isotopes reported in this thesis. The measured $^{206/207}Pb$ profile below 600 m clearly requires mixing of ventilated Pb with Pb of more recent origin (ca. 1920-1965). Regeneration of surface-derived Pb in proportion to apparent oxygen utilization rates improves the model fit considerably. Beyond a 12% net recycling efficiency (balanced by a scavenging residence time time of 70 yrs), however, the fit to the data cannot be further improved. Diapycnal mixing may constitute a secondary mechanism which forces deep water $^{206/207}Pb$ ratios toward measured values by diminishing the influence of very recent (post-1965) Pb inputs. Alternatively, the possibility exists that Pb isotope fluxes exhibit mild spatial variability. Quantification of these variations along with source water Pb and ^{210}Pb concentration gradients will comprise the next step in model refinement.

Acknowledgments

Many individuals have left indelible marks on this thesis. To describe each contribution is impossible; in this respect, an acknowledgment seems an inadequate means of conveying heartfelt gratitude. A student can only hope that thanks can be repaid in small measure through the merit of his research and its usefulness to the scientific community.

Ed Boyle has been to me all things a thesis advisor should be. If I have managed to capture some of his scientific intensity and human kindness in working alongside him these past five years, I know I shall be well served. John Edmond, the force behind my arrival in oceanography, has encouraged and inspired me with his spontaneous insights as he did many years ago in Building 54 at M.I.T.

The members of my thesis committee, Ellen Druffel, Mike Bacon, Rick Fairbanks, and Karl Turekian have furnished important ideas and arranged useful talks which encouraged me to evaluate my work at intermediate stages. E. Druffel and R. Fairbanks are especially thanked for sharing their expertise in coral geochemistry and for their generosity in providing key samples. Conversations with M. Bacon on one of several WHOI - Bermuda transects are an especially fond memory.

Stan Hart introduced me to the world of isotope geochemistry, both in the classroom and his mass spectrometry lab. Many thanks are due him for the Pb isotope results produced on TIMER. Vincent Salters, Mary Reid, Brian Taras, and Levent Gullen are thanked for their help in the lab and for their friendship.

Coral sampling, x-radiography, and sectioning were aided immeasurably by the efforts of Sheila Griffin, Robbie Smith, John Goddard, Steve Smith, Randi Schneider, and Ted McConnaughey. Throughout my many vists to Woods Hole, S. Griffin's good humor and willingness to lend a hand never faltered. Robbie Smith helped me to sample Bermuda's many waterways and recovered important coral samples during his own studies at North Rock. Ted McConnaughey's Galapagos Islands coral section appears to have opened a whole new window to historic ocean/climate dynamics of the Eastern Equatorial Pacific.

Bob Buddemeier and Dick Dodge provided valuable reprints and suggestions as to additional sample contacts. Bob's visit to M.I.T. was very much appreciated.

I am grateful to Jim Bishop, Werner Deuser, and Craig Hunter for their recommendations regarding deployment of free-drifting sediment traps for particulate Pb isotope studies.

A very crowded laboratory was made a manageable work environment largely through the efforts of Susan Chapnick. Her accomplishments with seawater Pb analysis have a magical quality about them and continue to be a source of wonder and admiration. Art Spivack's departure to Cal Tech was keenly felt this past year. The support and friendship of my other student and work colleagues at M.I.T. made for an enjoyable time in Cambridge as well as at sea.

Cara Barton spent many dedicated hours typing tables and text for this thesis. Her warmth and cheerfulness throughout a most difficult period brightened my life. Chris Measures taught me to plot on the HP 85 and proved a most dependable consultant for all kinds of scientific problems encountered during my graduate career.

My parents have through the years shown their understanding of Western individualism in supporting me in whatever career paths I've contemplated. To simultaneously nurture the drive to always do one's best made for a delicate balancing act. I thank them for their great care in striking this balance and for their many sacrifices along the way.

Support for this research was furnished by the Office of Naval Research (grant # N 000014-80-C-0273) and the National Science Foundation (grant # OCE 8416382).

Dedicated to

C.L.W.

and to my parents

Table of Contents

List of Figures

List of Tables

CHAPTER 1

INTRODUCTION

1.1 General Introduction

Aeolian anthropogenic lead is a useful, largely unexploited tracer of chemical tranfer processes in the ocean. Since the source and non-conservative chemical behavior of Pb differs from that of other transient tracers (bomb-produced radionuclides and flourocarbons), new perspectives on particle interactions and fluid transport may be realized. The existence of four stable Pb isotopes and the decay product of ^{238}U, ^{210}Pb ($t_{1/2}$ = 22.5 yrs), add interpretive power to the use of Pb as an environmental marker. Because the largest industrial perturbations have occurred only over the last several decades, and the residence time of Pb in thermocline and deep waters is at least this long (as determined by ^{210}Pb studies -- Craig et al., 1973; Bacon et al., 1976; Nozaki and Tsunogai, 1976; Schaule and Patterson, 1981; and many others), the vertical distribution of Pb today is not in steady state. Furthermore, spatial heterogeneities in Pb concentrations and isotopic ratios have never been greater than at present, especially in surface waters. This is due to the diversity of modern industrial sources (emission volumes and isotopic signatures), and the fact that horizontal mixing time scales are long relative to the residence time of Pb in the upper ocean.

Application of the industrial Pb transient to oceanographic studies, however, hinges on recovery of accurate regional deposition records. Murozumi and coworkers (1969) successfully documented historic increases of Pb in snow strata cored in Greenland and Antarctica. Extrapolation of these fluxes to lower latitudes, though, is difficult. Subsequent studies have highlighted the severity of contamination problems associated with recovery and analysis of polar ice cores for trace metals (Wolff and Peel, 1985). Sediment chronologies have been informative only in nearshore environments where sedimentation rates are

high and signals have been amplified by local inputs (Chow et al., 1970; Bruland et al., 1974; Ng and Patterson, 1982).

Scleractinian corals offer more useful records of historic Pb fluxes in a wide range of tropical and subtropical locations. Lead and other metals possessing large +2 ionic radii (Sr, Ba, Ra, Nd, Co) appear to substitute for aragonitic calcium in direct proportion to their seawater concentrations. X-radiography provides an immediate and accurate means of sample dating by revealing high and low density annual banding patterns. In addition, cleaning and measurement techniques for Pb are directly applicable to other transition metals which are expected to be compatible in an aragonite lattice. Among these, cadmium demonstrates great potential as an indicator of paleo-fertility in surface waters subject to variable upwelling, as in the Eastern Equatorial Pacific. Records of other metals may eventually prove useful as additional markers of anthropogenic or natural perturbations to the surface ocean.

1.2 Lead

1.2.1 Atmospheric and oceanic lead

Lead fluxes carried by various marine air masses have been estimated by Settle and Patterson (1982) as part of the SEAREX program. Based largely on 1979 sample collections, these estimates (in units of $mg/m^2/yr$) are as follows: N. Atlantic Westerlies: 1.7; N. Pacific Westerlies: 0.5; N. Pacific Easterlies: 0.06-0.07; S. Pacific Easterlies: 0.03. The progression of highest fluxes in the N. Atlantic to lowest fluxes in the S. Pacific reflects the importance of industrial emissions originating from urban centers and prevailing atmospheric circulation patterns. Figures 1.1 and 1.2 depict the regularity and direction of winter and summer winds over the Atlantic, Pacific, and Indian Oceans. Atmospheric Pb fluxes to the Sargasso Sea have also been measured by Jickells et al. (1984) and Church et al. (1984) for the

Figure 1.1 Winds and pressures over the Atlantic Ocean during February and August. Note changing trajectories affecting Bermuda. (Source: Tchernia, 1980; (adapted from Schott, 1944)).

Figure 1.2 Winds and pressures over the Pacific and Indian Oceans during February and August. (Source: Tchernia, 1980; (adapted from Schott, 1944)).

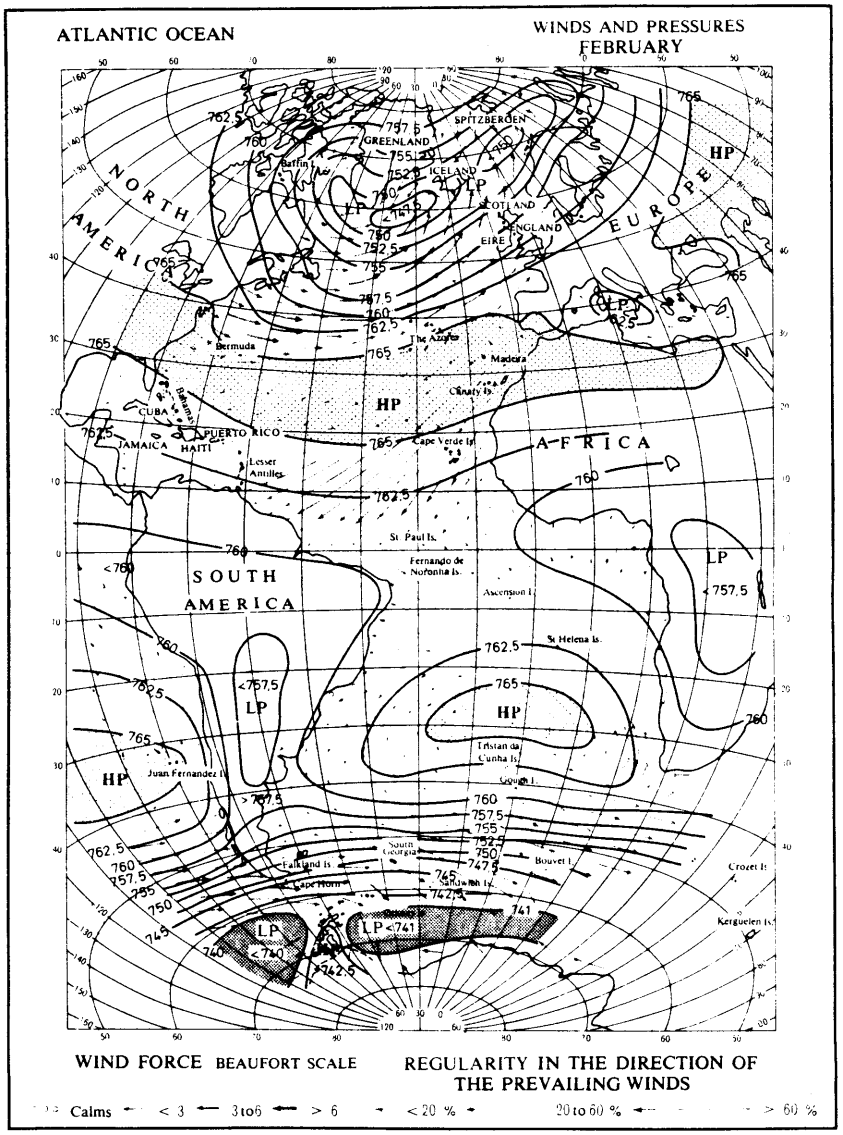

Adapted from G. SCHOTT (1944)

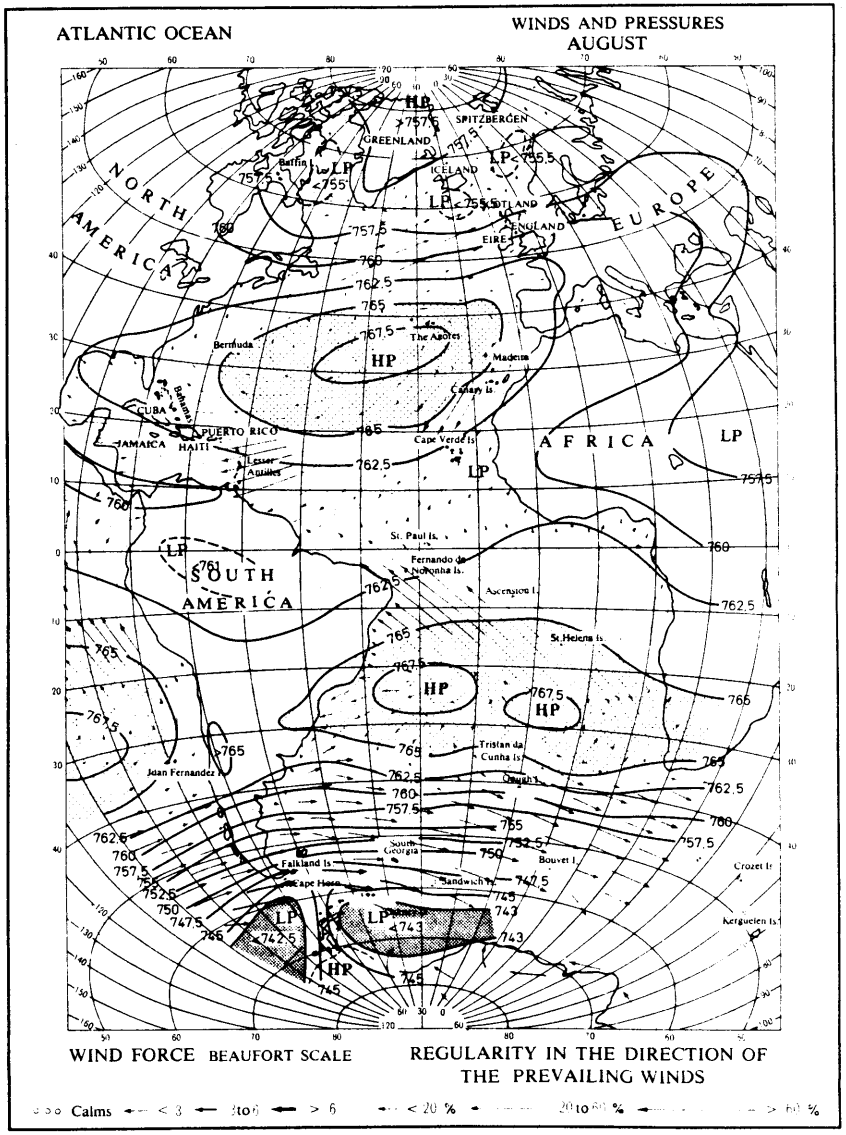

Adapted from G. SCHOTT (1944)

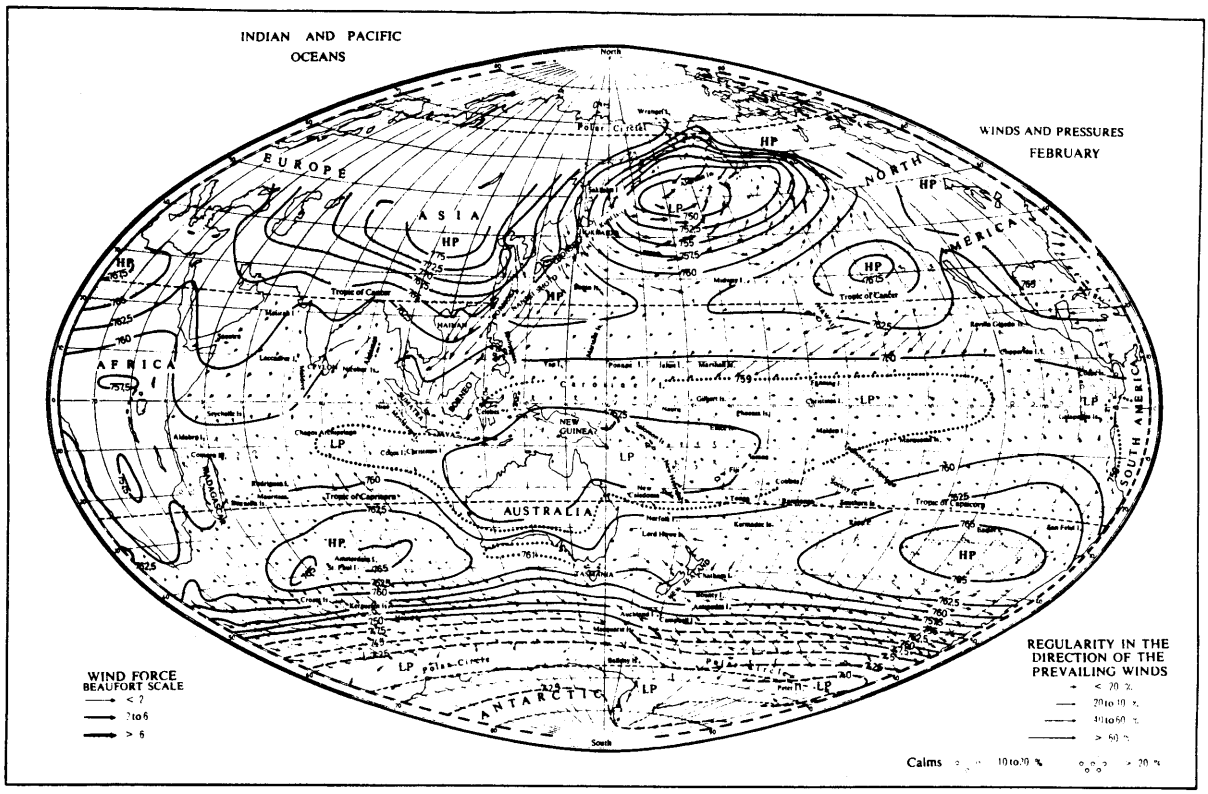

Adapted from G. SCHOTT (1935)

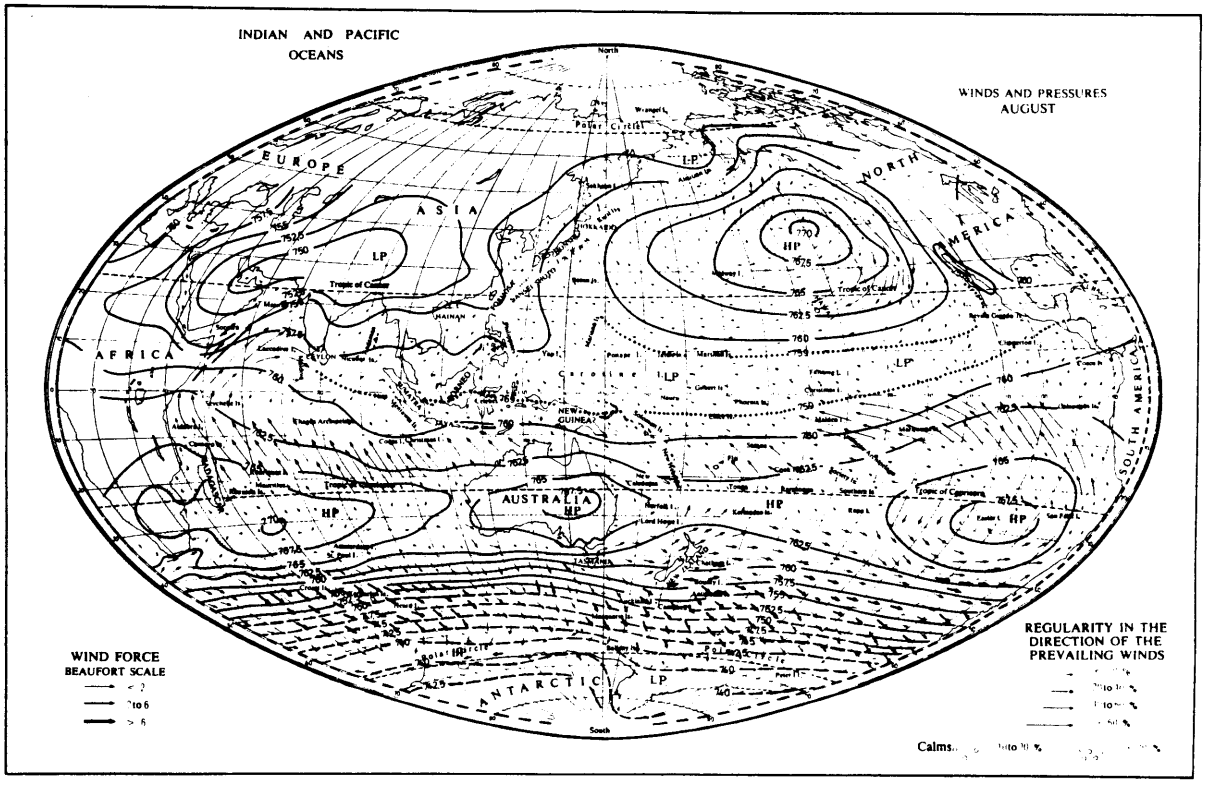

Adapted from G. SCHOTT (1935)

period 1981-1983. Annual averages of 1.1-1.2 $mg/m^2/yr$ are lower than Settle and Patterson's estimate for the western N. Atlantic, but part of this difference can be ascribed to declining emissions from the United States. It will become evident later in this thesis that temporal changes in industrial emissions over the last decade have been dramatic.

A consistent pattern is observed in the oceanic profiles presented in Fig. 1.3. Surface Pb concentrations are 2-to-3 fold higher in the western N. Atlantic than in the central N. Pacific, in rough accord with with aerosol measurements. Deep waters do not appear to converge until below 3000 m. Relative to the northern hemisphere measurements, the Pb profile at 20^oS in the S. Pacific shows greater isolation from industrial influence. The offset between the two Sargasso Sea profiles in the thermocline (Schaule and Patterson, 1983; Boyle et al., 1986) could clearly be attributed to a 5-year time lapse were it not for possible analytical biases between laboratories. The larger discrepancies in the mixed layer are likely due in part, to curtailed alkyl Pb usage in the U.S. Interpretation of surface ocean Pb changes, however, is complicated by extreme variability on seasonal and even subseasonal time scales. In the Sargasso Sea, Boyle et al. (1986) have documented variations of $\pm$25% from the annual average which occur as a result of mixed layer stratification and breakdown, biological removal, and seasonally-dependent input. ^{210}Pb fluctuations appear to occur in tandem, despite expected geographical differences between Pb and ^{210}Pb sources (Boyle et al., 1986; Talbot and Andren, 1983).

Oceanic Pb is primarily dissolved (>90% passes through 0.4 um nuclepore filter) except in coastal waters with higher suspended loads (Bacon et al., 1976; Schaule and Patterson, 1981, 1983). Principal dissolved Pb species in seawater as determined by Turner et al. (1981) are $PbCO_3^o$ (41%) and various chloride complexes (47%). Uncomplexed Pb^{2+} amounts to only 2-3% of the total.

The transport of Pb from surface ocean to sediments is most conveniently described in terms of residence times relative to particulate removal in different layers of the water column. Numerous

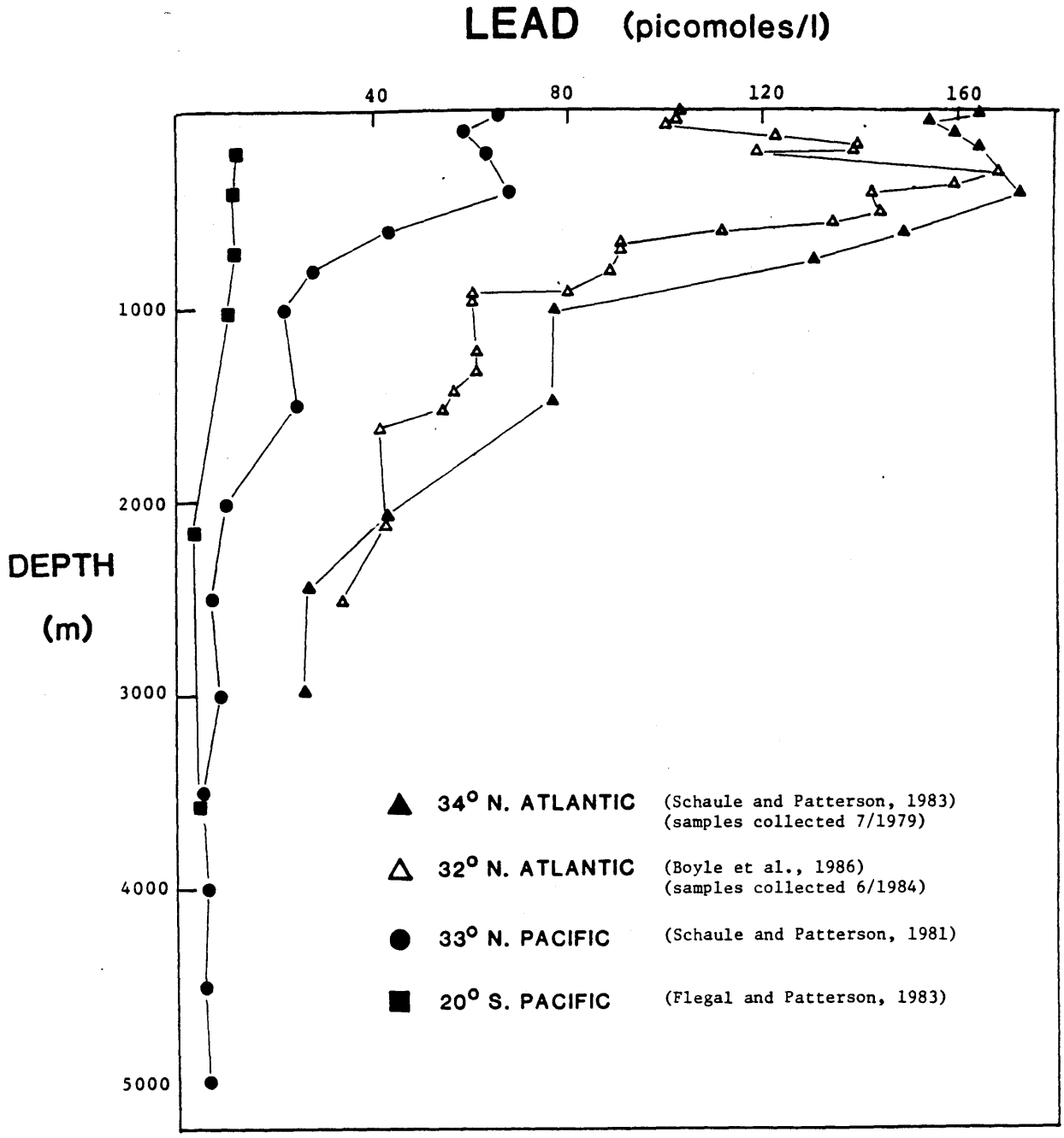

Figure 1.3 Vertical profiles of lead in the western North Atlantic and Pacific Oceans.

studies based on $^{210}Pb/^{226}Ra$ disequilibria and atmospheric ^{210}Pb flux measurements have yielded a range of Pb residence times for the mixed layer and deep ocean. For surface waters, the Pb residence time is well established with values consistently ranging from 1.7-2.5 years (Nozaki et al., 1976; Bacon et al, 1976). Deep water residence times are complicated by the probable existence of two Pb removal mechanisms -- in-situ scavenging by suspended particulate matter and interfacial scavenging at topographic margins (Bacon et al., 1976, Nozaki et al., 1980). The range of reported deep water residence times is 54-100 years, with values in the lower range generally computed from sites located closer to continental margins (Craig et al., 1973; Nozaki and Tsunogai, 1976; Thomson and Turekian, 1976; and others). Based on their central N. Pacific stable Pb profile, Schaule and Patterson (1981) constructed a stable Pb - ^{210}Pb model to estimate residence times of 20 years (minimum) in the thermocline (100-900 m) and 80-85 years in the deep ocean. Eleven measurements of Pb in particulate material trapped at 3200 m near Bermuda suggest that atmospheric fluxes are very nearly balanced by rapid delivery to the seafloor (1980-82 average sediment trap flux = 0.88 $mg/m^2/yr$; Jickells et al., 1984). When normalized to ^{210}Pb measurements in four of the same samples (8/80 - 7/81; Bacon et al., 1985), a surprisingly constant $Pb/^{210}Pb$ ratio results: 1140 $\pm$ 120 pM/dpm. This ratio closely resembles the 1979 surface water ratio of 1280 pM/dpm (Schaule and Patterson, 1983; Bruland, unpublished data).

1.2.2 Lead sources to the atmosphere and oceans

Worldwide emission estimates of Pb aerosols derived from natural sources such as windblown dusts, volcanogenic particles, and plant exudates are listed in Table 1.1 (Nriagu, 1979). The estimated background flux of Pb, 24.5 x 10^9 g/yr, is currently exceeded by anthropogenic releases which reached on the order of 450 x 10^9 g/yr in 1975 (Table 1.2). Combustion of leaded gasoline (61%) and primary metal/steel production (30%) accounted for most of the atmospheric Pb inputs in 1975. Historically, production and consumption of Pb extends back in time at least four-thousand years (Patterson et al., 1970),

Table 1.1 Worldwide emissions of trace metals from natural sources (from Nriagu, 1979)

Source	Global Production ($\times 10^9$kg yr^{-1})	Worldwide annual emissions ($\times 10^6$kg) Cd	Cu	Pb	Ni	Zn
Windblown dusts	500	0.1	12	16	20	25
Forest fires	36	0.012	0.3	0.5	0.6	2.1
Volcanogenic particles	10	0.52	3.6	6.4	3.8	7.0
Vegetation	75	0.2	2.5	1.6	1.6	9.4
Seasalt sprays	1,000	~0.001	0.08	0.02	0.04	0.01
Total		0.83	18.5	24.5	26.0	43.5

Table 1.2 Worldwide anthropogenic emissions of trace metals during 1975 (from Nriagu, 1979)

Source	Global Production or consumption ($\times 10^9$kg yr^{-1})	Trace metal emissions ($\times 10^6$kg) Cd	Cu	Pb	Ni	Zn
Mining, non-ferrous metals	16	0.002	0.8	8.2		1.6
Primary non-ferrous metal production						
Cd	0.0017	0.11				
Cu	7.9	1.6	19.7	27	1.5	6.6
Pb	4.0	0.20	0.29	31	0.34	0.44
Ni	0.8			2.5	7.2	0.68
Zn	5.6	2.8	0.78	16	0.36	99
Secondary non-ferrous metal production	4.0	0.60	0.33	0.77	0.2	9.5
Iron and steel production	1,300	0.07	5.9	50	1.2	35
Industrial applications		0.05	4.9	7.4	1.9	26
Coal combustion	3,100	0.06	4.7	14	0.66	15
Oil (including gasoline) combustion	2,800	0.003	0.74	273	27	0.07
Wood combustion	640	0.2	12	4.5	3.0	75
Waste incineration	1,500	1.4	5.3	8.9	3.4	37
Manufacture, phosphate fertilizers	118	0.21	0.6	0.05	0.6	1.8
Miscellaneous				5.9		6.7
Total		7.3	56	449	47	314

Table 1.3 All-time worldwide consumption and anthropogenic emissions of trace metals (from Nriagu, 1979)

Source	Global metal emissions ($\times 10^6$kg) Cd	Cu	Pb	Ni	Zn
Pre-1850	63	319	2,420		2,804
1850-1900	19	92	1,100	12	841
1901-10	8.9	53	471	8.2	392
1911-20	11	80	493	21	493
1921-30	14	96	1,120	21	622
1931-40	17	116	1,639	49	746
1941-50	22	169	1,672	80	959
1951-60	34	230	2,694	140	1,514
1961-70	54	435	3,704	257	2,372
1971-80	74	585	4,265	415	3,252
Total (all time)	316	2,175	19,578	1,003	13,995

however, the greatest emissions have occurred only within the last century (Table 1.3).

Due to its dominant role in the U.S. over past decades, automotive Pb emissions have frequently been assumed to outweigh all other atmospheric sources (Fig. 1.4). At its consumption peak in 1970, however, alkyl Pb probably accounted for only 65% of the total U.S. Pb aerosol release to the environment. The relative contributions by iron/steel, Pb, Cu, and Zn production, and coal combustion (in descending order of importance as per Nriagu, (1979)), must be gaining rapidly as alkyl leads are being phased out. Similarly, at the turn of the 19th century (before alkyl leads were invented in 1923), these industrial sources were responsible for all anthropogenic fluxes (Fig. 1.5). Temporal source variability is important as far as creation of isotopic heterogeneities in the environmental Pb signal, as will be seen.

On the basis of ^{210}Pb-^{210}Po disequilibrium measurements in rain, it has been estimated that lead aerosols reside in the troposphere for an average of only 9.6 $\pm$ 2 days (Francis et al., 1970). These aerosols exist as submicron-sized particles of a variety of compounds including PbO_x, PbS, $PbCO_3$, $PbSO_4$, and many halogenated compounds derived from engine exhausts (e.g. $PbCl_2$, $PbBr_2$, PbBrCl) (Nriagu, 1978, Biggins and Harrison, 1979). Apparently, these particles are readily soluble since filtration of surface seawater samples reveals consistently small (<10%) particulate fractions.

Riverine fluxes of Pb to the oceans, though large, are predominantly particulate (generally > 95%; $K_D \geq 10^5$; Trefry et al., 1985; Lee and Boyle, unpublished data). Trefry and coworkers estimated an average total Pb transport of 2×10^9 g/yr for the Mississippi River in 1982-83. Their measurements of dissolved Pb (530$\pm$240 pM), however, are high relative to recent measurements by Lee and Boyle which suggest an average value closer to 150 pM. This dissolved concentration is strikingly low in view of huge industrial inputs throughout the

Figure 1.4 Alkyl lead consumption in the Unites States: 1927-1984. (Source: testimony by Ethyl Corporation to EPA public hearing on proposed regulations on the lead content of gasoline, Aug. 31, 1984.)

Figure 1.5 Historical U.S. production of (a) primary lead (b) iron ore (c) coal (Source: Bureau of the Census of the U.S. Department of Commerce)

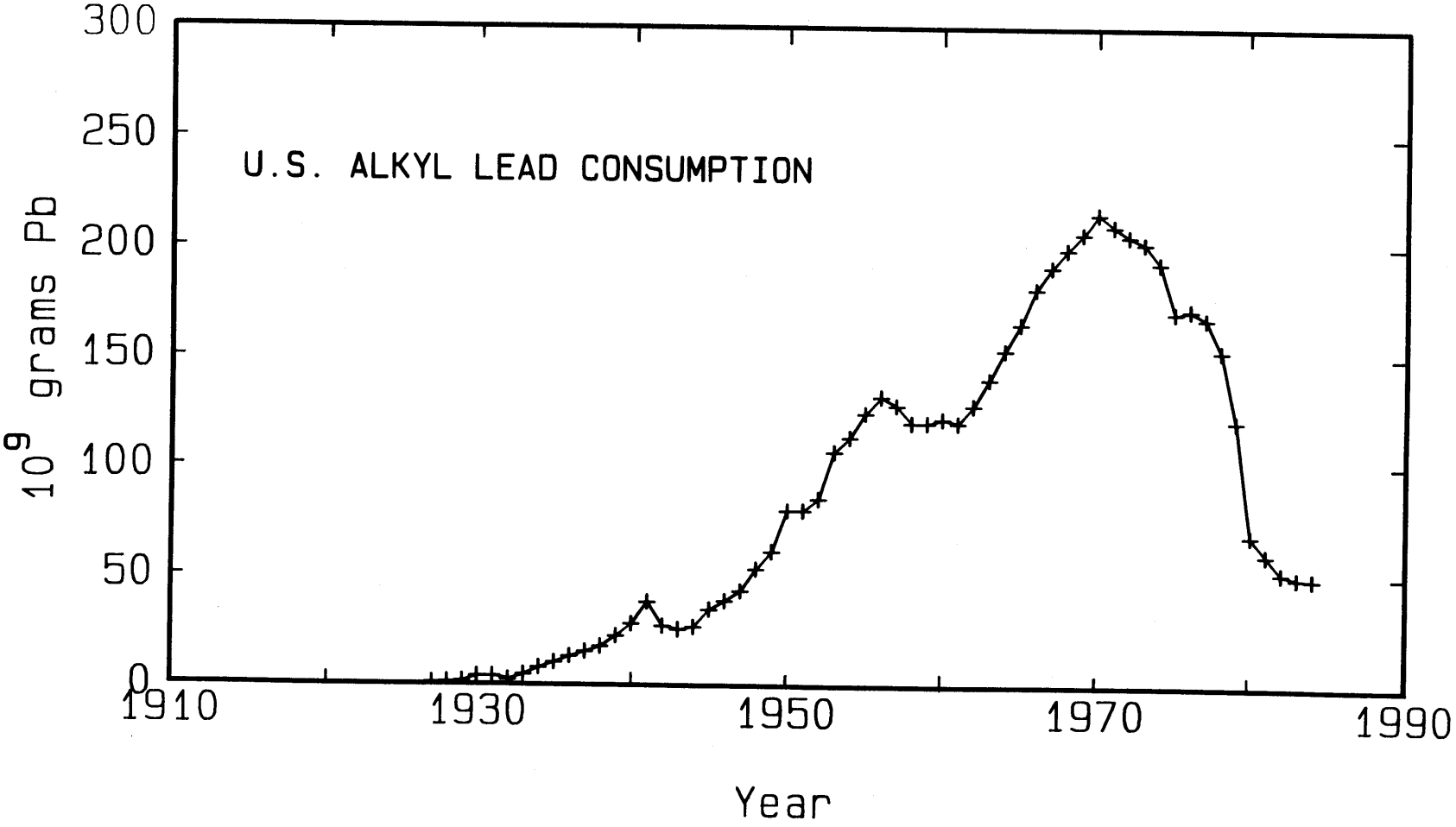
U.S. ALKYL LEAD CONSUMPTION
300
250
200
150
100
50
0
10^9 grams Pb
1910
1930
1950
1970
1990
Year

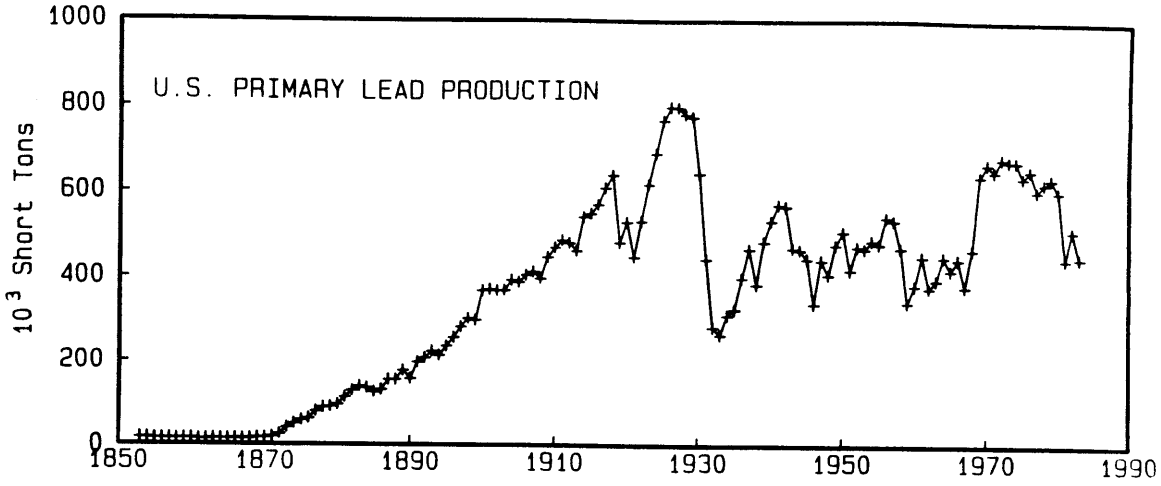
U.S. PRIMARY LEAD PRODUCTION
10^3 Short Tons
1000
800
600
400
200
0
1850
1870
1890
1910
1930
1950
1970
1990

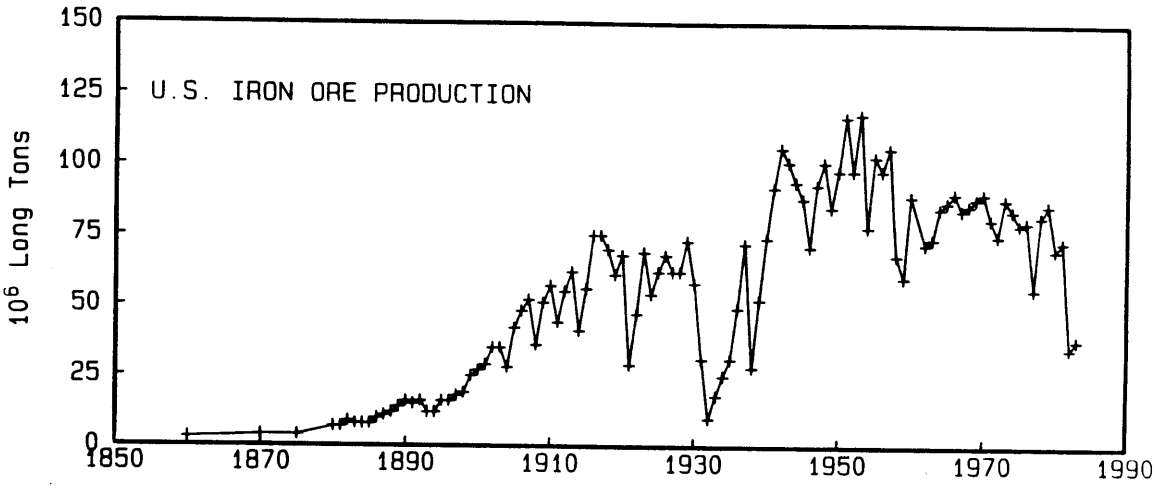
U.S. IRON ORE PRODUCTION
10^6 Long Tons
150
125
100
75
50
25
0
1850
1870
1890
1910
1930
1950
1970
1990

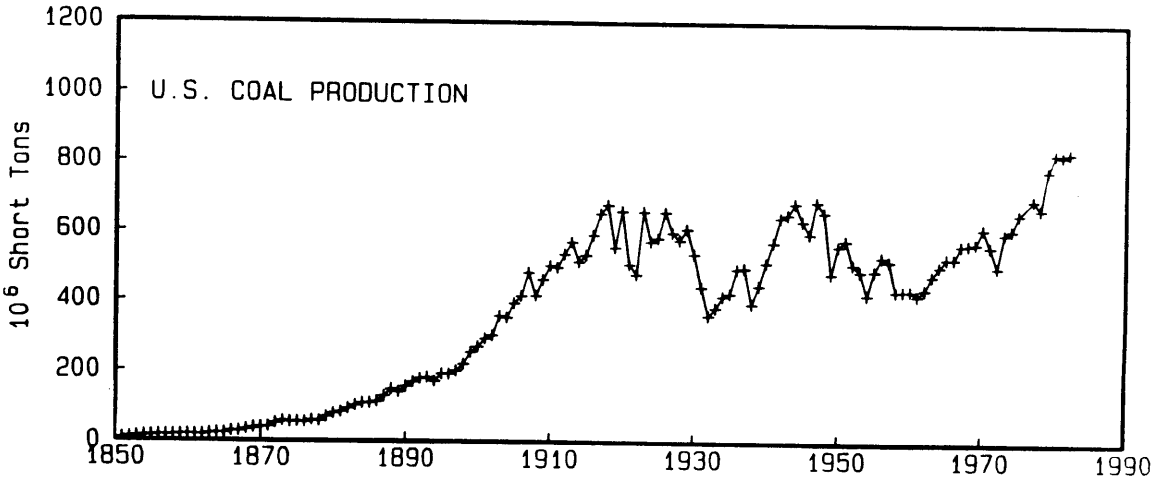
U.S. COAL PRODUCTION
10^6 Short Tons
1200
1000
800
600
400
200
0
1850
1870
1890
1910
1930
1950
1970
1990

Mississippi Valley, attesting to a very high particle affinity for Pb. Further, large-scale chemical removal of riverine Pb upon mixing with seawater is not evident (Lee and Boyle, unpublished data). Thus, if the Mississippi is typical of the world's rivers, contemporary fluvial inputs of dissolved Pb to the ocean amount to only about 10^9 g/yr (annual river discharge = 3.7×10^{16} liter/yr; Baumgartner and Reichel, 1975). Dispersal of this small dissolved input is further hindered by the brief residence time of Pb in coastal waters. Assuming a horizontal eddy diffusion coefficient of 10^{-6} cm^2/sec and a surface water residence time of one year, Schaule and Patterson (1983) estimated a transport limit of only 50-100 km.

Hydrothermal fluxes of Pb along mid-ocean ridges have been estimated by Von Damm (1983) as $0 - 2 \times 10^{10}$ g/yr. As for fluvial inputs, the influence of these fluxes is probably localized as Pb is rapidly precipitated as sulfide and deposited as metalliferous sediments.

Natural and pollutant Pb sources are potentially identifiable by their stable isotopic ratios. Of the four principal stable Pb isotopes, three are radiogenic and constitute the terminal products of the U and Th decay series: $^{238}U \rightarrow {}^{206}Pb$; $^{235}U \rightarrow {}^{207}Pb$; $^{232}Th \rightarrow {}^{208}Pb$. Primordial ^{204}Pb has no contemporary source and so its abundance remains invariant in time. The isotopic heterogeneity of lead ores is illustrated in Fig. 1.6. Commercially important deposits of the Mississippi Valley (U.S.) and Broken Hill Mine (southern Australia) span most of the observed Pb isotopic range. Subtle differences in weathered continental leads are expressed in oceanic pelagic sediments as distinct isotopic provinces (Chow and Patterson, 1962). High precision mass spectrometry is routinely capable of distinguishing ratio differences of only 0.05% per amu. Flegal et al. (1984, 1986) have applied Pb isotopes to deduce probable industrial sources of Pb in the northeast and central Pacific Ocean. Leaded gasoline and to a lesser extent, industrial sewage and mine tailings have also been directly implicated by isotopic measurements as key sources of sedimented and dissolved Pb in coastal

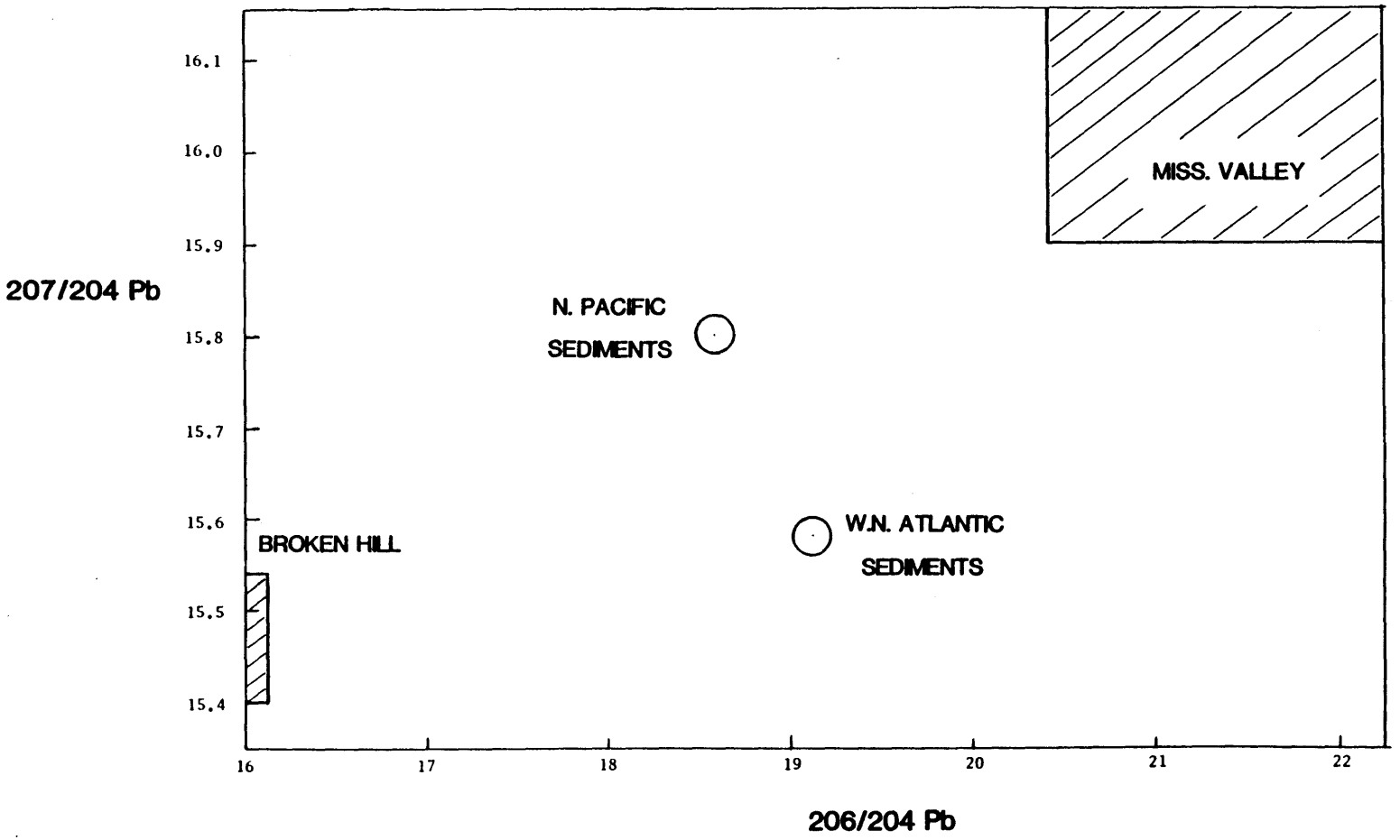

Figure 1.6 Heterogeneity of lead isotopes as indicated by two principal ore deposits and pelagic sediments (sediment fields from Chow and Patterson, 1962).

waters off southern California and British Columbia (Chow et al., 1973; Ng and Patterson, 1982; Stukas and Wong, 1981). Unfortunately, characteristic Pb isotopic ratios for historic and contemporary emissions are poorly known.

The fifth widely measured Pb isotope, ^{210}Pb, is derived as a decay product of ^{222}Rn which emanates from continental soils. Studies of the marine disequilibria of this radioactive isotope ($t_{1/2}$ = 22.5 yrs) have provided most of our present knowledge of the behavior of Pb in the oceans.

1.2.3 Historical records of anthropogenic lead

The most extensive records of atmospheric Pb inputs to the environment have been those found in snow and ice cores from Greenland and Antarctica (see review by Wolff and Peel, 1985). The records of Murozumi and coworkers (1969) reveal increases in northern Greenland (Camp Century) from less than 1 ng/kg at 800 B.C. to greater than 200 ng/kg in recently formed ice. Rapid increases near 1800 and 1950 signal the advent of the European and American industrial revolutions and widespread use of alkyl Pb gasoline additives. Maximum Antarctic Pb concentrations amount to only one-tenth the highest observed Greenland measurement, reflecting limited interhemispheric exchange of Pb through the atmosphere.

Sediments offer another repository for anthropogenic Pb. However, because of the brief time scale of recent perturbations, such records are useful only in areas of rapid sedimentation. Resolution in sediment cores is also easily obscured by bioturbation and sediment transport. The 20th century industrialization of southern California is recorded in sediment profiles of Pb in San Pedro, Santa Monica, and Santa Barbara Basins (Chow et al., 1973). These records compare favorably with deposition histories for Cr, Cd, Zn, Cu, Ag, V, and Mo in these same basins (Bruland et al., 1974).

1.3 Cadmium

1.3.1 Atmospheric and oceanic cadmium

Atmospheric Cd fluxes are best known over the western North Atlantic as a result of wet deposition measurements by Jickells et al. (1984a) and Church et al. (1984) and analysis of sediment-trapped material by Jickells et al. (1984b). The annual flux estimate computed from Cd concentrations in Bermuda rain is about 90 $\mu g/m^2/yr$ for the years 1981-82. Sediment trap measurements near Bermuda (depth = 3200 m), however, revealed a maximum flux to the deep ocean of only 10 $\mu g/m^2/yr$ in 1980-82 (including likely Cd contamination from PVC stabilizers). The large discrepancy is probably due to a large recycled sea salt component in the rain measurements.

Boyle et al. (1976) first recognized that the geochemical behavior of Cd in the oceans resembles that of the nutrients, phosphate and nitrate. That is, Cd is depleted in surface waters, increases rapidly across the thermocline, and then changes little with depth. A number of more recent hydrographic studies (Bruland and Franks, 1983; Boyle and Huested, 1983; and many others) have shown surface ocean Cd concentrations to vary from 2 pM in the N. Pacific and N. Atlantic central gyres, to 200 pM in shelf waters. At depths of 1-3 km, net accumulation of Cd in the N. Pacific can be observed as concentrations there are of order 900 pM compared to 300 pM in the Sargasso Sea. Corresponding PO_4 and NO_3 concentrations are of order 0.1 and 1 μM in oligotrophic surface waters, 1.1 and 18 μM in N. Atlantic waters of 1-3 km depth, and 2.8 and 40 μM in the mid-depth N. Pacific. Since Cd concentrations in oceanic surface waters are highly depleted by biological uptake (accidental or otherwise), industrial perturbations have neither been anticipated nor documented.

Like Pb, oceanic Cd is primarily dissolved. Cadmium speciation in seawater favors various chloride complexes ($CdCl_2^o$, $CdCl^+$, and $CdCl_3^-$) leaving only about 2-3% as uncomplexed Cd^{2+} (Turner et al., 1981; Zirino and Yamamoto, 1972).

1.3.2 Cadmium sources to the atmosphere and oceans

Global natural and anthropogenic emissions of Cd to the atmosphere have been estimated by Nriagu (1979) (Tables 1.1-1.3). These estimates suggest a nine-fold increase in the total aerosol flux of Cd from pre-industrial times to 1975 (0.83×10^9 g/yr to 7.3×10^9 g/yr). Mart (1983) measured Cd concentrations in near-surface snow from the eastern Arctic Ocean averaging 5 pg/g, but there exist no reliable data in old snow to shed light on historic increases due to industrialization.

Early industrial releases of Cd to the atmosphere resulted mainly from venting of Cd-rich flue dusts produced during Zn smelting (and to a lesser extent, Pb and Cu smelting). By the early 1900's, a large proportion of these flue dusts was recovered as industrial uses for Cd metal were conceived. Fig. 1.7 illustrates the historical timing and interdependence of Zn and Cd production in the U.S. Contemporary emissions may have significant contributions derived from waste incineration (20%), but the bulk of Cd releases continues to originate from metals manufacture (Nriagu, 1979).

1.4 Corals

The corals investigated in this thesis, like most reported in the literature, are among the dominant reef builders; order Scleractinia and class Anthozoa. These corals normally grow at shallow depths (0-40 m) in warm latitudes bounded roughly by the tropics of Cancer and Capricorn. Optimum growth conditions consist of 25-29°C water temperatures, 34-36‰ salinity, high turbulence (to supply nutrients and oxygen), and strong light intensity (for photosynthesis by symbiotic zooxanthellae) (Kinsman, 1964). The general distribution of corals is favored on western oceanic margins. Colder water temperatures due to upwelling and inhospitable topography inhibit growth along eastern margins near Africa and the Americas, although pockets of growth can be found (e.g. Galapagos Islands). Ahermatypic (non-reef building) corals are distributed worldwide and include many deep dwelling species. Growth

Figure 1.7 Historical U.S. production zinc and cadmium. (Sources: Bureau of the Census of the U.S. Department of Commerce; U.S. Department of the Interior - Minerals Yearbook)

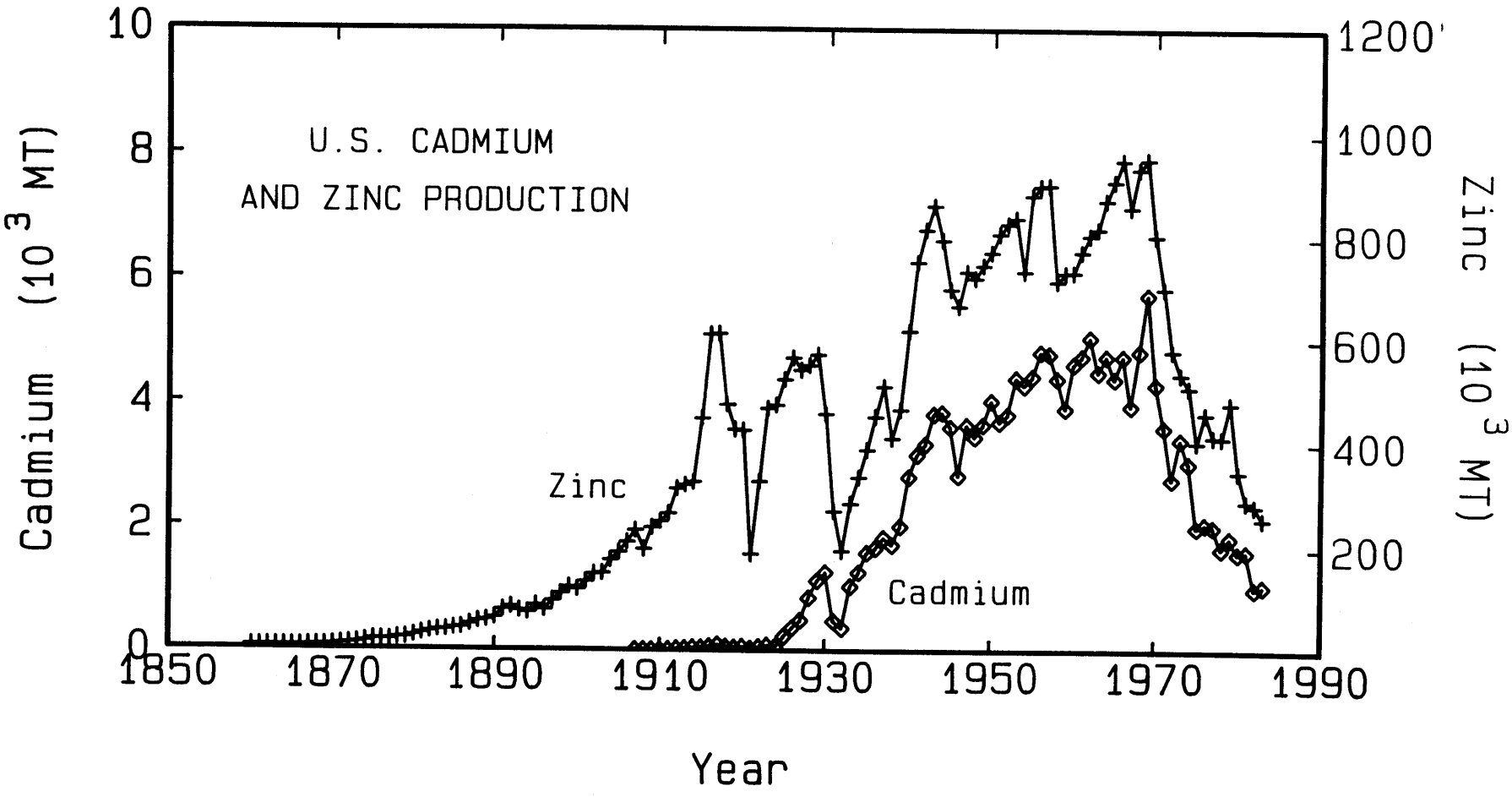
U.S. CADMIUM
AND ZINC PRODUCTION
Zinc
Cadmium
Cadmium (10 3 MT)
Zinc (10 3 MT)
Year
0
2
4
6
8
10
200
400
600
800
1000
1200
1850
1870
1890
1910
1930
1950
1970
1990

rates for ahermatypic corals are normally a small fraction of the 2-15 mm/yr annual growth rates found in hermatypes, thus making dating and sectioning difficult. As a result, geochemical and geophysical studies of corals have concentrated mainly on hermatypic genera.

The descriptive terms, hermatypic, reef-building, and zooxanthellate have frequently been used in the literature interchangeably. Recently, Schuhmacher and Zibrowius (1985) have proposed refinements to these terms since the previous generalizations abound with exceptions. The revised terminology distinguishes zooxanthellate (or azooxanthellate), from constructional (or non-constructional), from hermatypic (or ahermatypic). The difference between constructional and hermatypic is subtle; hermatypic signifying contribution to the framework of an actual reef, and constructional denoting the formation of a bioherm or durable carbonate structure. Hermatypic corals are always constructional, but constructional corals are not necessarily hermatypic.

The relation between a coral polyp and skeleton is shown in Fig. 1.8 (from Wells, 1956). Zooxanthellate corals house large numbers of unicellular dinoflagellate algae in their endoderm. The interaction of organic tissue with skeletal secretion is not well understood, however, specialized cells within the ectoderm are known to deposit minute crystalline fibers of aragonite. These fibers are actually orthorhombic crystals of about 2 microns diameter, which are arranged normal to the ectoderm surface (Wells, 1956). It has been hypothesized by many coral biologists that the calcification centers within corals constitute microenvironments which are supersaturated with respect to aragonite. Such conditions may be mediated in part by photosynthetic fixation of CO_2 by zooxanthellae, thus explaining why zooxanthellate hermatypic corals accrete $CaCO_3$ faster than their azooxanthellate counterparts (Goreau, 1963; Barnes, 1973).

When corals are x-rayed, bands of contrasting aragonite density may be distinguished (Fig. 1.9). Various mechanisms have been reported to account for these bands, including seasonal changes in light

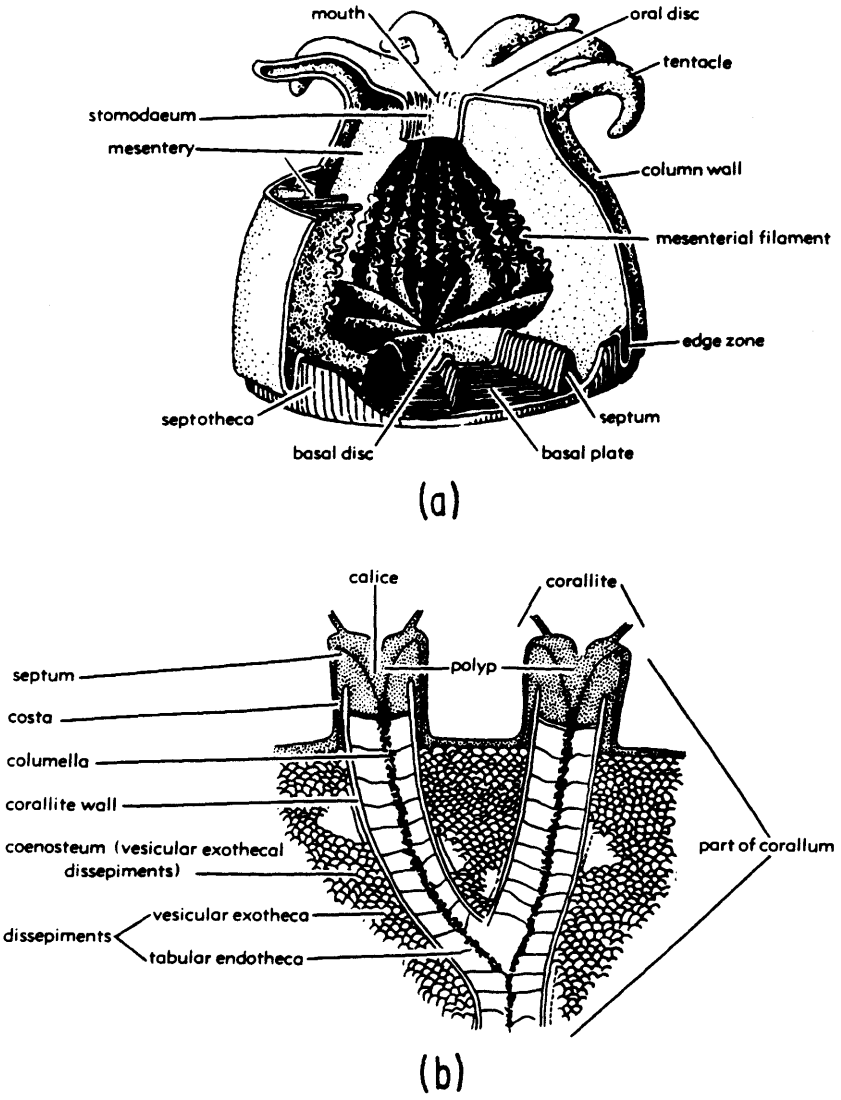

Figure 1.8 Relation of polyp and skeleton in scleractinian corals. (from Wells, 1956)

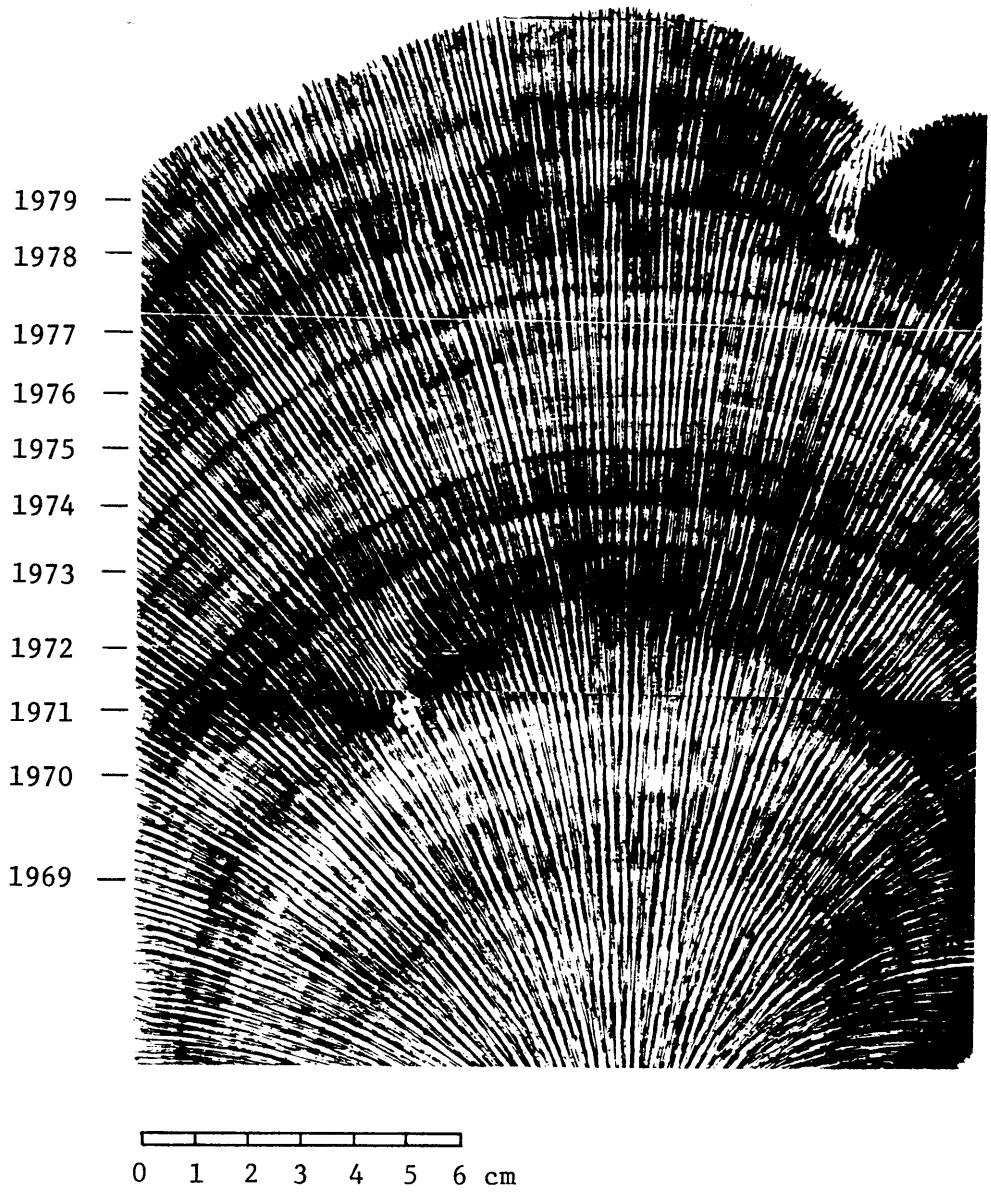

Figure 1.9 X-radiograph of Hydnophora microconos from Tutuila.

intensity, temperature, and salinity (due to seasonal rainfall or river discharge) (Buddemeier et al., 1974, 1976; Hudson et al., 1976; Dodge and Lang, 1983). Subannual bands are also a fairly common occurrence which have been ascribed to lunar periodicity and unusually stressful conditions (especially severe temperature changes) (Buddemeier, 1974; Buddemeier and Kinzie, 1975; Hudson, 1981). Generally, annual banding patterns are sufficiently regular to allow precise dating by simple counting. Radiometric methods applicable to specimens with ambiguous banding or discontinuities are described in section 2.2.5.

1.5 Existing Chemical Records in Corals

Chemical studies of corals have provided various records of modern and ancient surface ocean composition. Previous studies have traced isotopic variations resulting from natural processes (^{18}O, ^{13}C, ^{14}C, ^{210}Pb) and CO_2 and bomb radionuclide release to the atmosphere (^{14}C, ^{90}Sr, $^{239,240}Pu$). Elemental analyses have focused primarily on alkali and alkaline earth metals which are either very abundant in seawater or resemble Ca^{2+} in aragonite lattice compatibility. With the exception of uranium, chronological studies of trace elements have not been reported until very recently for Pb (Dodge and Gilbert, 1984; see Fig. 3.6).

Stable carbon and oxygen isotope studies in hermatypic corals have revealed complex fractionation patterns due to respiration, photosynthesis by zooxanthellae, temperature, salinity, and water composition (see review by Swart, 1983). The overall result is a depletion of ^{13}C and ^{18}O in coral aragonite due to metabolic effects. In some cases, $\delta^{13}C$ is reflective of water mass $\delta^{13}C$ (Nozaki et al., 1978, Druffel, unpublished data). Temperature effects on $\delta^{13}C$ are small and are masked by biological fractionation processes. ^{18}O paleothermometry, however, is preserved despite offsets in $\delta^{18}O$ vs. temperature curves for different coral genera (Weber and Woodhead, 1972). Apparently, relative contributions of CO_3^{2-} from seawater and metabolic CO_2 remain constant within a given genus, but may change from one genus to another.

Radioisotope measurements in corals have had a wide variety of applications. Radiocarbon has been used to reconstruct dilution of natural ^{14}C by fossil fuel CO_2 (Suess Effect), as well as to measure invasion rates of bomb-produced ^{14}C in the ocean (Druffel and Linick, 1978; Druffel and Suess, 1983; Nozaki et al., 1978; and many others). The ^{14}C half-life of 5,730 years is also suited for dating coral samples up to tens of thousands of years old. Other long term radiometric dating methods which have been attempted include $^{234}U/^{238}U$, $^{230}Th/^{234}U$, $^{231}Pa/^{235}U$, and He/U (see review by Veeh and Green, 1977). Shorter term radiometric techniques which have been applied with good success include ^{210}Pb (Dodge and Thomson, 1974), $^{228}Th/^{228}Ra$ (Moore and Krishnaswami, 1972), and identification of bands containing bomb produced ^{90}Sr and $^{239,240}Pu$ (Knutson et al., 1972; Toggweiler and Trumbore, 1985, Benninger and Dodge, 1983).

Measurements of alkali and alkaline earth elements in corals have usually been performed from the standpoint of identifying environmental controls. For example, temperature, light intensity, water chemistry, growth rate and phylogenetic effects on partition coefficients between corals and seawater have been sought for Na, K, Mg, Sr, and Ba (Cross and Cross, 1983; Houck et al., 1977; Weber, 1974; Smith et al., 1979; Swart, 1981; Goreau, 1977). Often, purported changes in elemental uptake by corals have not been traceable to simple causes since growth rate, temperature, insolation, etc. are inextricably linked. In general, though, coral habitat changes exert limited influence on major and minor element uptake ($\pm$ a few percent) -- especially for the alkaline earth metals which are thought to substitute for calcium (Sr, Ba, Ra). Probably the best established correlation is that of linearly decreasing Sr uptake by corals with increasing temperature. Over a 12°C range (laboratory mediated), the Sr/Ca distribution coefficient has been observed to change by about 10% (Houck et al., 1977, Smith et al., 1979). Inorganic calcite precipitation experiments by Lorens (1981) suggest that calcification rate can be an important factor in biogenic uptake of Sr and trace metals. Oomori et al. (1983) measured variations

of up to 30% for Mg incorporation in Porites lutea which were ascribable to temperature/growth rate changes. Alkali metals and Mg appear to display greater uptake variability (especially between different genera) than Sr, Ba, and Ra, presumably as a result of their incorporation in adsorbed sites or dispersed mineral phases (Amiel et al., 1973). Non-stoichiometric incorporation is indicated by very small and variable distribution coefficients for these elements relative to those for Sr, Ba, and Ra. Experimental results by Swart (1981) showing that neither Mg nor Na in corals correlate with Mg and Na seawater concentrations also imply a non-substitutive uptake mechanism.

1.6 Trace Elements in Corals

Although coralline aragonite is very nearly pure $CaCO_3$, trace levels of many contaminant cations and anions are detectable. Exact incorporation mechanisms are not well understood, but several distinct pathways are likely:

1) direct substitution for Ca^{2+} with full coordination
2) interstitial lattice substitution
3) surface adsorption
4) presence in organic coatings
5) presence in extraneous mineral phases

Amiel et al. (1973) and Livingston and Thompson (1971) attempted to determine the distribution of skeletal, detrital, and organic pools for a variety of elements and coral species. While analyses of constituents incorporated by any of the above mechanisms may yield useful information, however, isolation of specific contributions and measurement reproducibility are doubtful for all but perhaps (1) and (2). For these reasons, a variety of cleaning treatments were developed during this research in order to eliminate the presence of all trace element components associated with pathways 3-5. Further, elements studied were chosen largely for their substitution potential within aragonite.

Lattice substitution of metals in aragonite depends on a variety of factors including size compatibility, coordination number, charge balance, and chemical speciation. Among +2 cations which exhibit octahedral coordination, known and potential coral lattice substituents are listed in Table 1.4 along with effective ionic radii compiled by Shannon (1976). The most striking aspect of Table 1.4 is the agreement between trace element abundances in corals which have been measured and those which are estimated based on a coral:seawater distribution coefficient (K_D) of 1.0. The distribution coefficient is a standard means of expressing an enrichment or depletion of an element in a solid phase relative to its distribution in a surrounding liquid medium. In the case of corals:

$$K_D = \frac{([M]/[Ca])_{lattice}}{([M]/[Ca])_{seawater}}$$

The observation that K_D appears to be close to unity for five other elements resembling calcium suggests that precipitation is proportional to <u>total</u> dissolved metal concentrations. Solid solution thermodynamics would predict uptake proportional to the <u>uncomplexed</u> metal concentrations, thus resulting in a range of K_D's for various metals.

Measurements of Pb in corals have been reported by Livingston and Thompson (1971), but their results based on optical emission and γ-spectrometry only suggest a <u>maximum</u> concentration of 2 ppm, which is assuredly too high. The existence of apparent lattice-bound concentrations of Ra, Ba, Nd, and Sr in corals suggests that Pb, with an intermediate ionic radius (Pb^{2+} = 1.29 Å), should also demonstrate skeletal uptake. Limited solid solution of $PbCO_3$ (cerrusite) in inorganic aragonite (up to 3 mole %), has also been observed (Speer, 1983). Cadmium closely resembles calcium in +2 ionic radius, however, $CdCO_3$ commonly occurs in a rhombohedral calcite configuration. The utility of calcitic foraminiferal Cd in paleo-chemical reconstructions

Table 1.4 $^{+2}$ cations exhibiting octahedral coordination with effective ionic radii and abundances in corals.

Cation	Effective Ionic Radius (Å) (1)	Measured Abundance in Coral*			Predicted Abundance in Coral* (K_D=1)	
Ra^{2+}	1.48	6 dpm	^{226}Ra/100g	(2)	7.4 dpm	^{226}Ra/100g
→ Ba^{2+}	1.42	4	x 10^{-6}	(3)	3.6-4.4	x 10^{-6}
Pb^{2+}	1.29					
Nd^{2+}	1.29	0.3-6.6	x 10^{-9}	(4)	0.3-3.4	x 10^{-9}
Sm^{2+}	1.27	13-130	x 10^{-9}	(5)	0.06-0.6	x 10^{-9}
Sr^{2+}	1.26	7.5-8.5	x 10^{-3}	(6)	8.4	x 10^{-3}
Am^{2+}	1.26				0.01 dpm	^{241}Am/100g
Eu^{2+}	1.25				0.02-.08	x 10^{-9}
Hg^{2+}	1.14				1.5	x 10^{-9}
Yb^{2+}	1.14				0.08-.43	x 10^{-9}
→ Ca^{2+}	1.12	0.40			0.40	
→ Cd^{2+}	1.10				0.2-6.5	x 10^{-9}
Mn^{2+}	0.96				0.6-3.0	x 10^{-8}
Fe^{2+}	0.92				15	x 10^{-9}
Co^{2+}	0.90	1-10	x 10^{-9}	(7)	0.5-10	x 10^{-9}
Zn^{2+}	0.90				4-8	x 10^{-9}
Mg^{2+}	0.89	3-8	x 10^{-3}	(8)	5.3	

* Expressed as mole ratios relative to Ca. Seawater abundances used are simply predicted coral abundances multiplied by $[Ca]_{sw}$ or 0.0104.

Refs. (1) Shannon, 1976 (2) Dodge and Thomson, 1974 (3) Buddemeier et al., 1981 (4) Shaw and Wasserburg, 1985 (5) Scherer and Seitz, 1980 (6) Cross and Cross, 1983 (7) Veeh and Turekian, 1968 (8) Weber, 1974

has been amply demonstrated by Boyle (1986). Measurements of cobalt in corals by Veeh and Turekian (1968) suggest that the possibility of substitution exists even for cations with radii 20% smaller than the principal Ca^{2+} cation. Other elements with a high probability of residing in the coral lattice include Hg, Mn, Fe, Zn, and a number of the rare earth elements. Hg and Zn may be of particular interest insofar as possible perturbations to background environmental levels of these elements.

Apart from those elements whose presence in aragonite might be predicted on steric/charge bases, other elements may co-exist via different modes of lattice substitution. Uranium is a primary example. An abundance of U measurements in corals have been reported and are summarized by Broecker (1982) and Swart and Hubbard (1982). K_D's generally vary from 0.6-1.0. Swart and Hubbard (1982) estimate that dissolved U in seawater consists of 68% $UO_2(CO_3)_2^{2-}$ and 32% $UO_2(CO_3)_3^{4-}$. Thus, U uptake probably occurs as anionic complexes, possibly involving replacement of several $CaCO_3$ groups per atom of U substituted.

1.7 Research Strategy and Coral Study Sites

As previously discussed, the magnitude of historic and contemporary industrial perturbations to Pb and other trace element cycles are expected to be greatest in the western North Atlantic. The North Pacific should follow, with yet smaller perturbations expected in the ocean basins of the southern hemisphere. The intent of this research was first to produce historical records of Pb uptake in corals from around the world, in order to confirm the above expectations and thus validate the coral method. Additional verification of the method could be gained through measurement of chemical analogues of Pb which exhibit no industrial influence, such as Ba and ^{210}Pb. Having established that corals respond predictably to environmental changes in Pb, a detailed historical record was attempted for the highly perturbed western North Atlantic. Viewed as a regional source function, such a record would allow transport modeling of observed oceanic Pb distributions. A

complementary coral Pb isotopic record accompanied by seawater measurements would provide additional powerful constraints on Pb transport pathways.

A coral Pb concentration/isotope record spanning the years 1883-1982 was successfully reconstructed in the Sargasso Sea near Bermuda. Subsequently, seawater isotopic measurements were also undertaken at Station "S", 50 km southeast of Bermuda. A pair of younger North Pacific corals from Lisanski Island and Eniwetak Atoll proved the only specimens which failed to yield useful stable Pb data. Thus, a record detailing 20th century Asian industrial Pb inputs to the North Pacific is as yet, unavailable.

Measurements of barium, ^{210}Pb, and other potentially interesting trace metals (Cd, Zn, and V) were performed for certain corals. Among these were the same Bermuda corals which revealed temporal changes in Pb uptake, and a Galapagos Islands specimen cored in waters affected by variable upwelling (El Nino - Southern Oscillation influence).

A map and list of all coral sample locations are given in Fig. 1.10 and Table 1.5. Relevant information on species, sampling depth, and site proximity to land are also included.

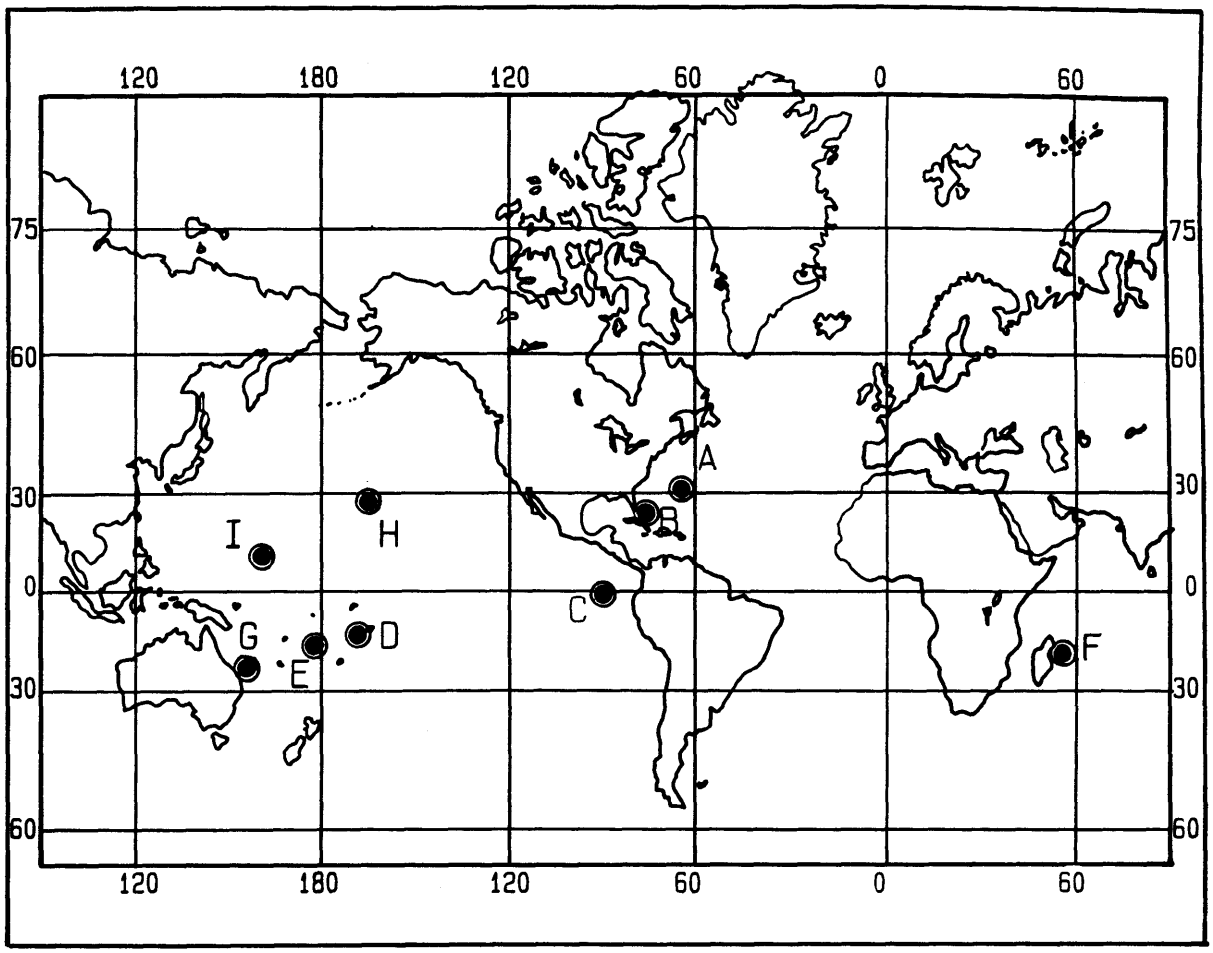

Figure 1.10 Coral sample locations: (A) Bermuda (B) Florida Straits (C) Galapagos (D) Tutuila (E) Fiji (F) Mauritius (G) Heron Island (H) Lisianski Island (I) Eniwetak

Table 1.5 Coral sample collection data

Location	Latitude	Longitude	Genus/Species	Water Depth (m)	Distance from Shore (km)	Collector
N. Atlantic						
Bermuda (North Rock)	32°29'N	64°48'W	Diploria strigosa	10	14	Druffel (1983)
Bermuda (Southern Preserve)	32°19'N	64°41'W	Diploria strigosa	9	0.5	Druffel (1983)
Florida Straits	24°57'N	80°33'W	Montastrea annularis	4	1	Hudson et al. (1978) Griffin and Druffel (1983)
Pacific						
Galapagos (San Cristobal Island)	0°45'S	89°36'W	Pavona clavus	15	1	McConnaughey (1982)
Tutuila (Aunuu)	14°20'S	170°40'W	Hydnophora microconos	5	1	Fairbanks (1979)
Fiji (Suva)	18°07'S	178°27'E	Platygyra rustica	5	2.5	Fairbanks (1979)
Eniwetak	11°20'N	162°20'E	Favia speciosa	8-9	0.5	Buddemeier (1973)
Lisianski Island (Hawaii)	26° 0'N	174° 0'W	Porites lobata	9	?	Buddemeier (1979)
Heron Island, (Great Barrier Reef)	23°14'S	152° 0'E	Porites australiensus	8	3	Druffel (1983)
Indian						
Mauritius	20° 0'S	57°30'E	Platygyra rustica	?	?	Toggweiler (1978)

References

Amiel, A.J., G.M. Friedman, and D.S. Miller (1973). Distribution and nature of incorporation of trace elements in modern aragonitic corals, Sedimentology 20: 47-64.

Bacon, M.P., D.W. Spencer, and P.G. Brewer (1976). $^{210}Pb/^{226}Ra$ and $^{210}Po/^{210}Pb$ disequilibrium in seawater and suspended particulate matter, Earth Planet. Sci. Lett. 32: 277-296.

Bacon, M.P., C.A. Huh, A.P. Fleer, and W.G. Deuser (1985). Seasonality in the flux of natural radionuclides and plutonium in the deep Sargasso Sea, Deep Sea Res. 32: 273-286.

Barnes, D.J. (1973). Growth in colonial scleractinians, Bull. Mar. Sci. 23: 280-298.

Baumgartner, A. and E. Reichel (1975). The World Water Balance, Elsevier: Amsterdam.

Benninger, L.K. and R.E. Dodge (1983). Fallout Pu in annual bands from the coral Montastrea annularis, St. Croix, U.S.V.I., EOS Trans. AGU 64: 1031.

Biggins, P.D.E. and R.M. Harrison (1979). Atmospheric chemistry of automotive lead, Environ. Sci. Technol. 13: 558-565.

Boyle, E.A. (1986). Paired carbon isotope and cadmium data from benthic foraminifera: Implications for changes in oceanic phosphorus, oceanic circulation, and atmospheric carbon dioxide, Geochim. Cosmochim. Acta 50: 265-276.

Boyle, E.A., F. Sclater, and J.M. Edmond (1976). On the marine geochemistry of cadmium, Nature 263: 42-44.

Boyle, E.A. and S. Huested (1983). Aspects of the surface distributions of copper, nickel, cadmium, and lead in the North Atlantic and North Pacific. In: Trace Metals in Seawater. C.S. Wong, E.A. Boyle, K. Bruland, D. Burton and E.D. Goldberg, eds., pp. 379-394. Plenum, New York.

Boyle, E.A., S.D. Chapnick, G.T. Shen, and M.P. Bacon (1986). Temporal variability of lead in the western North Atlantic Ocean, Geochim. Cosmochim. Acta 91: 8573-8593.

Broecker, W.S. and T.H. Peng (1982). Tracers in the Sea. Lamont-Doherty Geological Observatory: Palisades, N.Y.

Bruland, K.W., K. Bertine, M. Koide, and E.D. Goldberg (1974). History of metal pollution in Southern California Coastal Zone, Environ. Sci. Technol. 8: 425-432.

Bruland, K.W. and R.P. Franks (1983). Mn, Ni, Cn, Zn and Cd in the western North Atlantic. In: Trace Metals in Seawater. C.S. Wong, E.A. Boyle, K. Bruland, D. Burton and E.D. Goldberg, eds., pp. 395-414. Plenum, New York, N.Y.

Buddemeier, R.W. (1974). Environmental controls over annual and lunar monthly cycles in hermatypic coral calcification. In: Proc. 2nd Int. Coral Reef Symposium, Brisbane, Vol. 2: 259-267.

Buddemeier, R.W., J.E. Maragos, and D.W. Knutson (1974). Radiographic studies of reef coral exoskeletons: rates and patterns of coral growth, J. Exp. Mar. Biol. Ecol. 14: 177-200.

Buddemeier, R.W. and R.A. Kinzie (1975). The chronometric reliability of contemporary corals. In: Growth Rhythms and the History of the Earth's Rotation. G.D. Rosenberg and S.K. Runcorn, eds. pp. 135-147. John Wiley and Sons, London.

Bureau of the Census of the U.S. Department of Commerce. The Statistical History of the United States from Colonial Times to the Present, Vol. 1965 - 1984, Fairfield Publishers, Inc., Stanford, Conn.

Chow, T.J. and C.C. Patterson (1962). The occurrence and significance of lead isotopes in pelagic sediments, Geochim. Coshim. Acta 26: 263-308.

Chow, T.J. and J.L. Earl (1970). Lead aerosols in the atmosphere: Increasing concentrations, Science 169: 577-580.

Chow, T.J., K.W. Bruland, K. Bertine, A. Soutar, M. Koide, and E.D. Goldberg (1973). Lead pollution: Records in Southern California coastal sediments, Science 181: 551-580.

Church, T.M., J.M. Tramontano, J.R. Scudlark, T.D. Jickells, J.J. Tokos, A.H. Knap, and J.N. Galloway (1984). The wet deposition of trace metals to the coastal and western Atlantic Ocean, Atmos. Environ. 18: 2657-2664.

Craig, H., S. Krishnaswami, and B.L.K. Somayajulu (1973). ^{210}Pb - ^{226}Ra: Radioactive disequilibrium in the Deep Sea, Earth Planet. Sci. Lett. 17: 295-305.

Cross, T.S. and B.W. Cross, (1983). U, Sr and Mg in Holocene and Pleistocene corals, J. Sed. Petr. 53: 587-594.

Dodge, R.E. and J. Thomson (1974). The natural radiochemical and growth records in contemporary hermatypic corals from the Atlantic and Caribbean, Earth Planet. Sci. Lett. 23: 313-322.

Dodge, R.E. and J.C. Lang (1983). Environmental correlates of hermatypic coral (Montastrea annularis) growth on the East Flower Gardens Bank, northwest Gulf of Mexico, Limnol. Oceanogr. 28: 228-240.

Dodge, R.E. and T.R. Gilbert (1984). Chronology of lead pollution contained in banded coral skeletons, Mar. Biol. 82: 9-13.

Druffel, E.M. and H.E. Suess (1983). On the radiocarbon record in banded corals: Exchange parameters and net transport of $^{14}CO_2$ between atmosphere and surface ocean, J. Geophys. Res. 88: 1271-1280.

Druffel, E.M. and T.W. Linick (1978). Radiocarbon in annual coral rings of Florida, Geophys. Res. Lett. 5: 913-916.

Emiliani, C., J.H. Hudson, B. Lidz, E.A. Shinn, and R.Y. George (1978). Oxygen and carbon isotopic record of growth in a reef coral from the Florida Keys and a deep-sea coral from Blake Plateau, Science 202: 627-629.

Flegal, A.R. and C.C. Patterson (1983). Vertical concentration profiles of lead in the central Pacific at 15°N and 20°S, Earth Planet. Sci. Lett. 64: 19-32.

Flegal, A.R., B.K. Schaule, and C.C. Patterson (1984). Stable isotope ratios of lead in surface waters of the central Pacific, Mar. Chem. 14: 281-287.

Flegal, A.R., K. Itoh, C.C. Patterson and C.S. Wong (1986). Vertical profile of lead isotopic compositions in the north-east Pacific, Nature 321: 689-690.

Flor, T.H. and W.S. Moore (1977). Radium/calcium and uranium/ calcium determinations for western Atlantic reef corals. Pro. 3rd Int. Coral Reef Symposium, Miami 2: 555-561.

Francis, C.W., G. Chesters and L.A. Haskin (1970). Determination of ^{210}Pb mean residence time in the atmosphere, Environ. Sci. Technol. 4: 586-589.

Goreau, T.F. (1963). Calcium carbonate deposition by coralline algae and corals in relation to their roles as reef-builders, Ann. N.Y. Acad. Sci. 109: 127-167.

Goreau, T.F. (1977). Coral skeletal chemistry: Physiological and environmental regulation of stable isotopes and trace metals in Montastrea annularis, Proc. R. Soc. Lond. B 196: 291-315.

Houck, J.E., R.W. Buddemeier, and K.E. Chave (1975). Skeletal low-magnesium calcite in living scleractinian corals, Science 189: 997-999.

Hudson, J.H. (1981). Growth rates in Montastrea annularis: A record of environmental change in Key Largo Coral Reef Marine Sanctuary, Florida, Bull. of Mar. Sci. 31: 444-457.

Hudson, J.H., E.A. Shinn, R.B. Halley, and B. Lidz (1976). Sclerochronology: A tool for interpreting past environments, Geology 4: 361-364.

Jickells, T.D., A.H. Knap, and T.M. Church (1984). Trace metals in Bermuda rainwater, J. Geophys. Res. 89: 1423-1428.

Jickells, T.D., W.G. Deuser, and A.H. Knap (1984). The sedimentation rates of trace elements in the Sargasso Sea measured by sediment trap, Deep Sea Res. 31: 1169-1178.

Kinsman, D.J.J. (1964). Reef coral tolerance of high temperatures and salinities, Nature 202: 1280-1283.

Knutson, D.W., R.W. Buddemeier, and S.V. Smith (1972). Coral chronometers: Seasonal growth bands in reef corals, Science 177: 270-271.

Livingston, H.D. and G. Thompson (1971). Trace element concentrations in some modern corals, Limnol. and Oceanogr. 16: 786-796.

Lorens, R.B. (1981). Cadmium, manganese, and cobalt distribution coefficients in calcite as a function of calcite precipitation rate, Geochim. Cosmochim. Acta 45: 553-561.

Mart, L., H.W. Nurnberg, and D. Dryssen (1983). Low-level determination of trace metals in Arctic seawater and snow by differential pulse anodic stripping voltammetry. In: Trace Metals in Seawater. C.S. Wong, E.A. Boyle, K.W. Bruland, J.D. Burton, and E.D. Goldberg, eds., pp. 113-130. Plenum Press: New York.

Moore, W.S. and S. Krishnaswami (1972). Coral growth rates using ^{228}Ra and ^{210}Pb, Earth Planet. Sci. Lett. 15: 187-190.

Murozumi, M., T.J. Chow, and C.C. Patterson (1969). Chemical concentrations of pollutant lead aerosols, terrestrial dusts, and sea salts in Greenland and Antarctic snow strata, Geochim. Cosmochim. Acta 33, 1247-1294.

Ng, A. and C.C. Patterson (1982). Changes of lead and barium with time in California off-shore basin sediments, Geochim. Cosmochim. Acta 46: 2307-2321.

Nozaki, Y., J. Thomson, and K.K. Turekian (1976). The distribution of ^{210}Pb and ^{210}Po in the surface waters of the Pacific Ocean, Earth Planet. Sci. Lett. 32, 304-312.

Nozaki, Y., K.K. Turekian, and K. Von Damm (1980). ^{210}Pb in GEOSECS water profiles from the North Pacific, Earth Planet. Sci. Lett. 49: 393-400.

Nozaki, Y. and S. Tsunogai (1976). ^{226}Ra, ^{210}Pb, ^{210}Po disequilibria in the Western North Pacific, Earth Planet. Sci. Lett. 32: 313-321.

Nozaki, Y., D.M. Rye, K.K. Turekian, and R.E. Dodge (1978). A 200 year record of carbon-13 and carbon-14 variations in a Bermuda coral, Geophys. Res. Lett. 5: 825-828.

Nriagu, J.O. (1978). Lead in the atmosphere. In: The Biogeochemistry of Lead in the Environment - Part A. J.O. Nriagu, ed. Elsevier/North Holland Biomedical Press: Amsterdam.

Nriagu, J.O. (1979). Global inventory of natural and anthropogenic emissions of trace metals to the atmosphere, Nature 279: 409-411.

Oomori, T., K. Kaneshima, Y. Nakamura, and Y. Kitano (1986). Seasonal variation of minor elements in coral skeletons, Galaxea.

Schaule, B. and C.C. Patterson (1980). The occurrence of lead in the northeast Pacific and the effects of anthropogenic inputs. In: Lead in the Marine Environment. M. Branika and Z. Konrad, eds., pp. 31-43. Proc. Int. Experts Discussion, Rovinj, 1977, Pergamon Press: Oxford.

Schaule, B.K. and C.C. Patterson (1981). Lead concentrations in the Northeast Pacific: Evidence for global anthropogenic perturbations, Earth Planet. Sci. Lett. 54: 97-116.

Schaule, B.K. and C.C. Patterson (1983). Perturbations of the natural lead depth profile in the Sargasso Sea by industrial lead. In: Trace Elements in Seawater. C.S. Wong, E.A. Boyle, K. Bruland, D. Burton and E.D. Goldberg, eds., pp. 487-503. Plenum, New York.

Scherer, M. and H. Seitz (1980). Rare earth element distribution in Holocene and Pleistocene corals and their redistribution during diagenesis, Chem. Geol. 28: 279-289.

Schott, G. (1944). Geographie des Atlantischen Ozean.

Schuhmacher, H. and H. Zibrowius (1985). What is hermatypic? A redefinition of ecological groups in corals and other organisms, Coral Reefs 4: 1-9.

Settle, D.M. and C.C. Patterson (1982). Magnitudes and sources of precipitation and dry deposition fluxes of industrial and natural leads to the North Pacific at Eniwetak, J. Geophys. Res. 87: 8857-8869.

Shannon, R.D. (1976). Revised effective ionic radii and systematic studies of interatomic distances in Halides and Chalocogenides, Acta Crystallogr A32: 751-767.

Shaw, H.F. and G.J. Wasserburg (1985). Sm-Nd in marine carbonates and phosphates: Implications for Nd isotopes in seawater and crustal ages, Geochim. Cosmochim. Acta 49: 503-518.

Smith, S.V., R.W. Buddemeier, R.C. Redalje, and J.E. Houck (1979). Strontium-calcium thermometry in coral skeletons, Science 204: 404-407.

Speer, J.A. (1983). Crystal chemistry and phase relations of orthorhombic carbonates. In: Carbonates: Mineralogy and Chemistry, pp. 145-189. Mineralogical Society of America, Chelsea: Michigan.

Stukas, V.J. and C.S. Wong (1981). Stable lead isotopes as a tracer in coastal waters, Science 211: 1424-1427.

Swart, P.K. (1981). The strontium, magnesium and sodium composition of recent scleractinian coral skeletons as standards for paleoenvironmental analysis, Paleogeog., Paleoclim., Paleoecol. 34: 115-136.

Swart, P.K. (1983). Carbon and oxygen isotope fractionation in scleractinian corals: A review, Earth Sci. Rev. 19: 51-80.

Swart, P.K., and J.A.E.B. Hubbard (1982). Uranium in scleractinian coral skeletons, Coral Reefs 1: 13-19.

Talbot, R.W. and A.W. Andren (1983). Relationships between Pb and ^{210}Pb in aerosol and precipitation at a semiremote site in northern Wisconsin, J. Geophys. Res. 88: 6752-6760.

Tchernia, P. (1980). Descriptive Regional Oceanography, Pergamon, New York.

Toggweiler, J.R. and S. Trumbore (1985). Bomb-test ^{90}Sr in Pacific and Indian Ocean surface water as recorded by banded corals, Earth Planet. Sci. Lett. 74: 306-314.

Thomson, J. and K.K. Turekian (1976). ^{210}Po and ^{210}Pb distributions in ocean water profiles from the eastern South Pacific, Earth Planet. Sci. Lett. 32: 297-303.

Trefry, J.H., S. Metz, R.P. Trocine, and T.A. Nelsen (1985). A decline in lead transport by the Mississippi River, Science 230: 439-441.

Turner, P.R., M. Whitfield, and A.G. Dickson (1981). The equilibrium speciation of dissolved components in freshwater and seawater at 25°C and 1 atm pressure, Geochim. Cosmochim. Acta 45: 855-881.

Veeh, H.H. and K.K. Turekian (1968). Cobalt, silver and uranium concentrations of reef-building corals in the Pacific Ocean, Limnol. Oceanogr. 13: 304-308.

Veeh, H.H. and D.C. Green (1977). Radiometric geochronology of coral reefs. In: Biology and Geology of Coral Reefs, Vol. IV, Academic Press, New York.

Von Damm, K.L. (1983). Chemistry of submarine hydrothermal solutions at 21°N, East Pacific Rise and Guaymas Basin, Gulf of California. Ph.D. Thesis. Massachusetts Institute of Technology-Woods Hole Oceanographic Institution Joint Program in Oceanography, Woods Hole, Massachusetts, WHOI-84-3.

Weber, J.N. and P.M.J. Woodhead (1972). Temperature dependence of oxygen-18 concentration in reef coral carbonates, J. Geophys. Res. 77: 463-473.

Weber, J.N. (1974). Skeletal chemistry of scleractinian reef corals: Uptake of magnesium from seawater, Am. J. Sci. 274: 84-93.

Wells, J.W. (1956). Scleractinia, In: Treatise on Invertebrate Paleontology. R.C. Moore, ed. pp. F328-F444. Geol. Soc. Am. and University of Kansas Press, Lawrence: Kansas.

Wolff, E.W. and D.A. Peel (1985). The record of global pollution in polar snow and ice, Nature 313: 535-540.

Zirino, A. and S. Yamamoto (1972). A pH dependent model for the chemical speciation of copper, zinc, cadmium and lead in seawater, Limnol. Oceanogr. 17: 661-671.

CHAPTER 2

METHODS

2.1 Introduction

Corals have proven useful in numerous efforts to reconstruct changes in modern and ancient surface ocean composition. Chemical studies have traced isotopic variations resulting from natural processes (^{18}O, ^{13}C, ^{14}C, ^{210}Pb) and bomb radionuclide release to the atmosphere (^{14}C, ^{90}Sr, $^{239,240}Pu$). Elemental analyses have focused primarily on alkali and alkaline earth metals to understand environmental effects (temperature, light intensity, etc.) on distribution coefficients. With the exception of uranium (Cross and Cross, 1983), chronological studies of trace metals have not been reported until very recently for lead (Dodge and Gilbert, 1984).

In contrast to isotopic and minor element determinations in corals, however, trace elements are highly susceptible both to pre-existing surface contamination (detrital and organic), and contamination introduced during sample recovery and preparation. A sampling of typical lattice-bound mole ratios expressed relative to calcium includes: $Pb/Ca = 10 \times 10^{-9}$; $Cd/Ca = 0.5 \times 10^{-9}$; $Zn/Ca = 6 \times 10^{-9}$; and $V/Ca = 100 \times 10^{-9}$. This chapter presents a detailed methodology which enabled circumvention of these contamination problems in six of eight coral specimens studied. The corals investigated, like most reported in the literature, are among the dominant reef builders; order Scleractinia and class Anthozoa. Owing to great differences in coral morphology, growth environment, and handling practices, the range of possible analytical difficulties is very broad. Therefore, the techniques described represent a culmination of "worst case" strategies. The method was designed specifically for lead and lead isotopic analysis, but has proven equally well suited to other transition metals. Interpretation of coral Pb measurements also relies upon accurate

determinations of dissolved Pb distributions. Thus, the techniques used for concentration and stable isotope analysis in seawater are also described in this chapter.

2.2 Coral Methods

2.2.1 Sample preparation

While trace element clean practices cannot be adopted throughout the earliest stages of preparation, it is worth prefacing these discussions with a cautionary recommendation to avoid unnecessary contamination wherever possible. Minor attention to details early on can result in major savings of time and effort during final sample cleaning.

Fig. 2.1 depicts the general preparation sequence. Normally, coral samples are recovered as individual heads or cores cut by diver-operated rotary hydraulic or pneumatic drills. Sampling guidelines which address Pb concentration anomalies associated with near-shore environments are given in section 3.7.1. An outline of drilling techniques with attention to reef conservation can be found in Hudson et al. (1981). Samples are bleached in hypochlorite and slabbed on a clean rock saw to obtain slices of approximately 5-8 mm thickness. Clean water should be used as a cutting lubricant. Thicker slabs may result in poor-quality x-radiographs, especially if coring or slabbing is off-axis from corallite growth. X-ray exposure and film recommendations are discussed in Buddemeier et al. (1974) and Hudson (1981). In the event of ambiguous coral banding frequency, ^{210}Pb ($t_{1/2}$ = 22.5 yrs) dating can be used to distinguish annual from subannual banding in specimens younger than 100 years (see section 2.2.5). Companion measurements of ^{18}O or bomb radionuclides (^{14}C, $^{239,240}Pu$, ^{90}Sr, ^{241}Am) can be as useful. Transporting and storage of corals in plastic bags will minimize contamination. Care should be taken to avoid

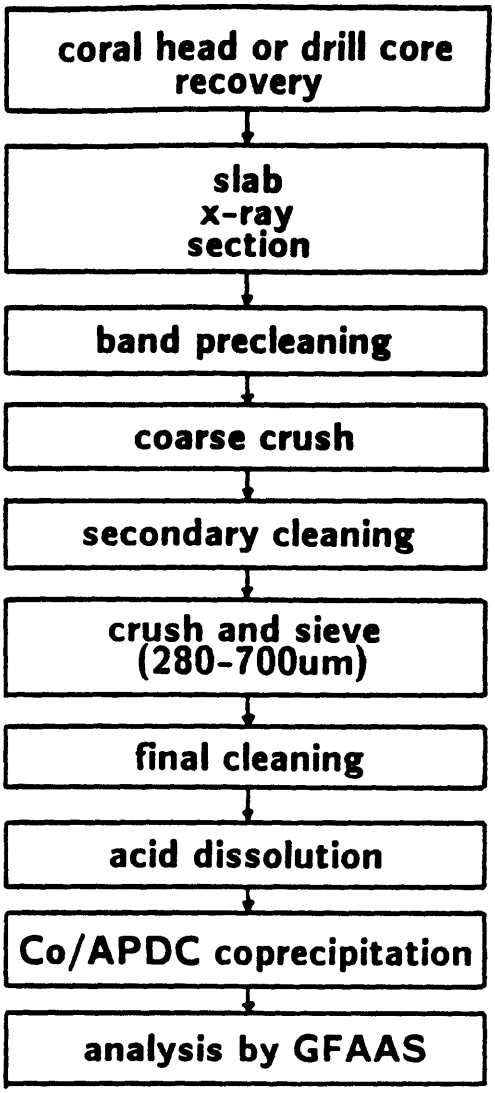

Figure 2.1 Overall preparative sequence for trace element analysis of coral.

exposure to gasoline engine exhausts which will contaminate samples for Pb.

At this juncture, frequency of sampling must be decided. This will depend both on interest in recovering seasonal information as well as annual band thickness for a given coral. Tropical corals which exhibit rapid growth (>1 cm/yr) can often be sectioned subannually with relative ease. Lunar growth response such as that observed by Buddemeier and Kinzie (1975) in specimens of Porites lobata, may even provide monthly sectioning guides. Temperate corals such as those found in Bermuda, however, accrete bands only several millimeters wide. In anticipating sample needs for analysis by graphite furnace atomic absorption spectrophotometry (GFAAS), one should generally plan on triplicate samples of 100 mg of cleaned coral per designated band. Allowing for cutting, sieving and cleaning losses, this means a minimum of about 1.5 g of intact coral per sample band.

If possible, slab sectors containing relatively straight banding should be isolated. This will allow precise sectioning with a circular low-speed rock saw (e.g. Buehler - Isomet; 0.3 mm diamond wafering blade). If the sample has been cored, the circumference should be avoided due to probable contamination from the coring device. A cutting template should be produced from the original x-radiograph on clear drafting film and taped to the corresponding coral subslab. If band irregularities preclude use of this type of saw, a normal band saw can be used. Cutting losses will be appreciable, but a 0.35 mm thick blade will minimize waste. Sample loss can be further minimized and particularly distorted banding resolved through the use of a jeweler's saw with a 0.15 mm blade.

2.2.2 Sample cleaning

Individual cuttings stored in clean glass or plastic vials are next cleaned of freshly emplaced residues from saw blades, cutting fluid, and

handling. This is accomplished by repeated washing in distilled water in an ultrasonic bath. Several final washes in clean 0.2N HNO_3 will help to remove persistent metal contamination from exterior sample surfaces.

A secondary cleaning sequence ensues on coarsely crushed (<5 mm) fragments of each cut band. This involves 10 minutes of ultrasonic cleaning in water, 3 minutes in 0.15N HNO_3, 20 minutes in a 50%/50% oxidizing mixture of 30% H_2O_2 and 0.2N NaOH with alternating heating in a water bath, and a final 3 minutes in 0.15N HNO_3. This sequence is repeated for samples which are still visibly discolored. The samples should be dried thoroughly before continuing.

The purpose of these pre-cleanings is to remove as much surface contamination as possible before sample crushing. Contaminants become difficult to isolate after they are homogenized in smaller particles. The purpose of crushing is to gain access to coral-included detritus and organic matter. The strategy is to expose as many surfaces as possible, while segregating pure coral fragments from contaminant-laden fines. Morphological considerations may intervene here. Straightforward crushing of precleaned coarse fragments in an agate mortar and pestle followed by sieving through polypropylene screens to retain the 280-700 μm fraction, has yielded good results for Pavona clavus, Hydnophora micrococonos, and Platygyra rustica (sampled from the Pacific and Indian Oceans). In section, these corals are marked by a very homogeneous framework in which it is difficult to distinguish individual trabeculae (termed a fenestrate septum). In contrast, Diploria strigosa, Diploria labyrinthiformis, Montastrea annularis and Favia speciosa form laminar septa. In cross-section, centers of calcification are plainly evident as they radiate outward from an axis of divergence. In these corals (with exception of M. annularis), the consolidated trabeculae (high density) must be separated from the intervening network of septal trabeculae and synapticula (low density). These void-filling constituents appear to harbor more extraneous matter which often results

in contaminated analyses. Successful trace element chronologies have been recovered from two Diploria species from Bermuda and M. annularis from the Florida Straits. F. speciosa (Eniwetak), however, appeared heavily contaminated, even after fragment discrimination. A final example warranting mention is Porites lobata which exhibits a relatively homogeneous, extremely fine-grained morphology. Sections of this important Pacific reef builder resemble finely fritted glass. As a consequence, crushing results in generation of a fine dust, and cleaning of intact bands cannot penetrate the fine network of interstices. Thirty-six analyses of a Porites lobata from Lisianski Island, Hawaii failed to yield a credible Pb value.

Following crushing and sieving, samples are ready for final cleaning. Sample size may vary depending on expected trace element contents and previously experienced cleaning losses. For typical Pb determinations by GFAAS, 60-120 mg are usually adequate to yield final sample aliquots of 500 μl. Additional sample is recommended for Cd determinations in corals from oligotrophic waters, unless smaller final dilution volumes are used. Sample weights should be consistent to within 2 mgs in order to achieve uniform solution pH's for subsequent coprecipitation. All suceeding steps are carried out in acid-leached 1.5 ml polyethylene centrifuge vials with hinged closures. Hand made polycarbonate or acrylic racks which can be immersed in ultrasonic and boiling water baths are useful. The final cleaning sequence is an extension of the reductive/complexing treatment of Boyle (1981). The steps are as follows:

1) The samples are cleaned in distilled water with ultrasonic agitation for 10 minutes.
2) The samples are cleaned in 0.15N HNO_3 for 2 minutes with ultrasonic agitation and repeated inversion.
3) The samples are cleaned in a 50%/50% mixture of 30% H_2O_2 and 0.2N NaOH to hydrolyze and oxidize organic residues. Samples are

immersed in a boiling water bath and subjected to ultrasonic agitation at 2-minute intervals for a total of 20 minutes.

4) The samples are rinsed twice with distilled water.

5) The samples are subjected to reductive cleaning to remove any oxide coatings. The medium consists of a mixture of 1 part hydrazine (H_2NNH_2; anhydrous 97%), 6 parts concentrated NH_4OH, and 3 parts 0.3M solution of citric acid in 7N NH_4OH. The samples are secured in a rack designed to hold the vials closed while heating to 80°C in a water bath for 30 minutes. The samples are agitated ultrasonically every 2 minutes.

6) The samples are rinsed twice with distilled water.

7) Steps 2 and 3 are repeated, followed by a distilled water wash.

8) From this point, samples should be handled under clean conditions only (see Bruland, 1983 and refs. therein). The samples are rinsed for 2 minutes, three consecutive times with 0.15N HNO_3 and ultrasonic agitation. Longer exposure should be avoided to prevent metal readsorption as the wash solution pH increases.

9) Samples are transferred in a laminar flow bench to acid-leached polypropylene AA autosampler cups for dissolution. Just prior to dissolution, two final 0.15N HNO_3 washes are performed.

Wash solution volumes for the above protocol are generally 250-500 μl, depending on sample size. Spent solutions are removed by siphoning through a fine pipette tip. Throughout the cleaning sequence, attempts should be made to eliminate all fines. Initial problems with contamination resulting from methanol rinsing led to purification of all cleaning reagents. Although the need for this is not fully established, the techniques used are offered as a useful precaution. NaOH was purified by LaOH coprecipitation and filtration. Citric acid was purified by addition of 25 mls of Chelex 100 slurry (NH_4^+ form) to a neutral 0.5M solution, followed by overnight shaking and filtration. Selected bottles of Ultrex H_2O_2 (Baker) and analytical grade NH_4OH (Mallinckrodt) giving GFAAS lead absorbances at the detection limit (350

pM) were identified and reserved for trace analysis. Hydrazine (Matheson, Coleman and Bell) reliably contained Pb concentrations below the detection limit.

2.2.3 Coprecipitation and analysis

Ideally, the samples at this point are ready for analysis, and indeed, a constituent such as barium (several umoles/mole Ca) can be injected for analysis by GFAAS directly after dissolution (a far less exacting cleaning protocol would also suffice). Lesser abundances of trace elements such as Pb, Cd, and V, however, would require sample matrices of close to 1M Ca in order to obtain adequate absorbances. This concentration of calcium reduces graphite tube life and results in poor reproducibility over even short series of injections. Thus, for any kind of survey requiring more than a few samples, the metals of interest are chemically separated from calcium.

The flowchart of Fig. 2.2 depicts the chemical procedure which is based upon the seawater technique of Boyle and Edmond (1975). Example volumes are provided to illustrate aliquot partitioning for the various supporting and final analyses. The samples are dissolved in a slight excess of 2.0N HNO_3. After the sample is completely dissolved, a 10 μl subsample is removed for later calcium normalization by flame atomic absorption spectrophotometry. An exact transfer of the residual (preferably a round, constant volume to simplify calculations) is pipetted to a new acid-leached vial. To this, 100 μl of 6N ammonium acetate buffer (pKa = 4.7), 250 μl of aqueous 2.5 mM $CoCl_2$, and 250 μl of aqueous 1% APDC (ammonium pyrrolidine dithiocarbamate) are added. The samples are shaken briefly, and allowed to precipitate for 1 hour. Pb and Cd (and in all likelihood, Zn, V and a host of other transition metals) are coprecipitated quantitatively between pH 2-8. This contrasts with pH-variable coprecipitation observed in preconcentrating elements such as Cd and Zn from seawater (Boyle and Edmond, 1975). Since the APDC chelate coprecipitation technique is used here more as a

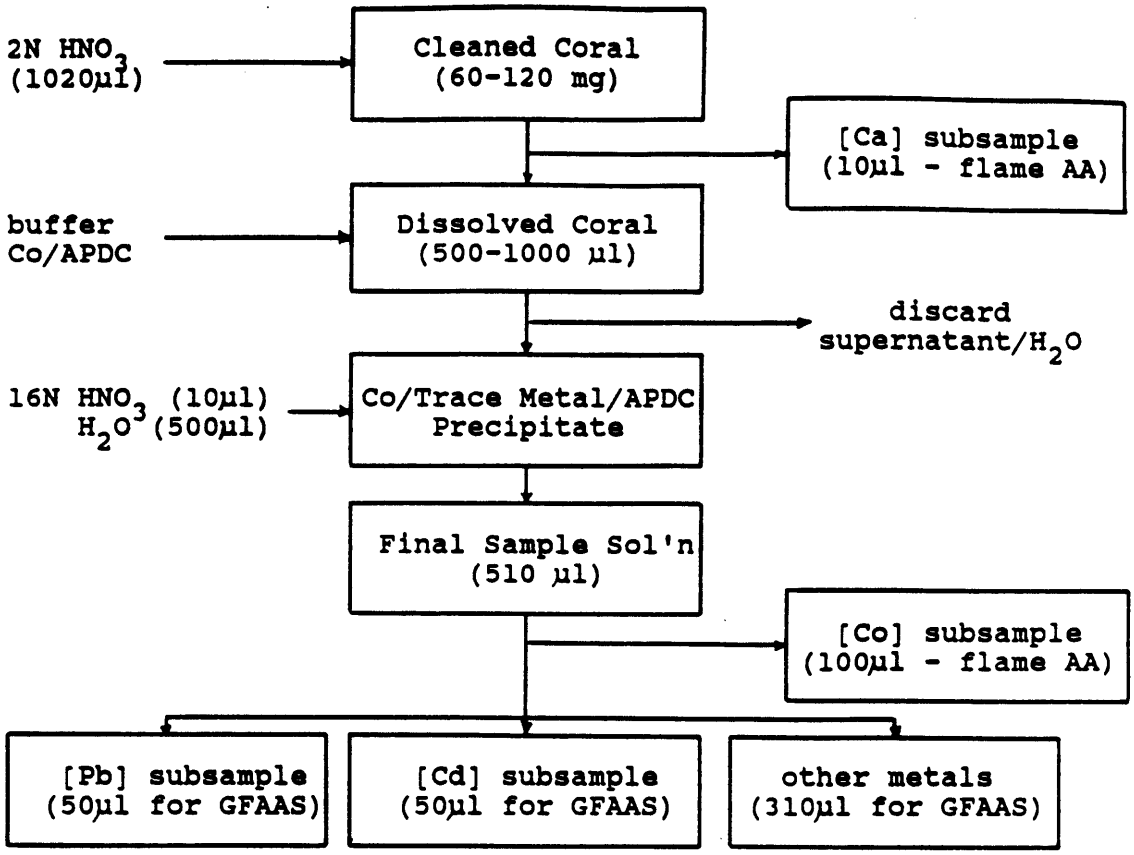

Figure 2.2 Flow diagram of chemical procedures used to isolate trace metals from coral matrix for final analysis by GFAAS.

means of purification than preconcentration, cobalt and APDC concentrations in the small samples are over one-hundred times greater than those used in typical seawater analyses. Below pH 2, recovery losses can become significant, due to increased competition from H^+ ions or decomposition of the dithiocarbamate anion. Spot checks of sample pH's can be performed to reveal whether acid or buffer use should be adjusted. At the end of the hour, the samples should be shaken to homogenize the precipitates and centrifuged (11,500 rpm) for 5 minutes. The supernatant is siphoned-off and the precipitate dispersed in 1.0 ml of distilled water to remove residual Ca. Following a second centrifugation and removal of the wash water, the precipitate is digested in 10 μl of 16N HNO_3. Within 20 minutes, the samples can be diluted with distilled water to final volume, normally 500 μl.

The reagents used throughout the coprecipitation treatment should of course, be as pure as possible. Nitric acid was vycor-distilled at full strength repeatedly until the blank was imperceptible by direct injection GFAAS. The acetate buffer was cleaned by Chelexing in the same manner as citric acid. APDC was extracted 6 times in carbon tetrachloride or until its blank (measured as a digested and diluted cobalt precipitate) was also negligible. Cobalt solution was purified either by cation exchange of the chloride salt on Dowex 50W-X8 or by retention of Pb and Cd bromide anions on a Biorad AG1-X8 column.

Bulk standards with matrices matched to samples yield more consistent results over the long term as compared with in-run matrix preparation and spiking. Additionally, several bulk consistency standards resembling dissolved coral in their Ca and metal contents were prepared. Reagent $CaCO_3$ can be purified for this purpose by cation exchange chromatography or Chelexing. Coprecipitation and analysis of a set of these consistency standards within each sample run provided a continuous measure of absolute recovery efficiency. Lastly, inclusion of 4-6 reagent blanks per run allowed close monitoring of contaminant sources. Simple reagent blanks, however, do not address the coral

preparation portion of the method. If a well characterized source of coral fragments is available, this can be used to measure contamination incurred during the cleaning sequence. In preparing reagent blanks, the nitric acid normally used for dissolution was partially neutralized before coprecipitation. This was accomplished by addition of 150 μl of 5.1N sub-boiling distilled NH_4OH.

Samples were analyzed by atomic absorption spectrophotometry on a Perkin Elmer Model 5000 spectrometer with HGA 400 graphite furnace. Continuum background correction was employed for all analyses. Determinations were based on duplicate 20 μl injections of each sample and standard. For Pb analysis, a L'vov platform enhanced sample absorbances by about 70%. A 1% ascorbic acid modifier improved reproducibility of Ba measurements. Program conditions for several successfully analyzed elements are shown in Table 2.1.

Mechanical losses of Pb during coprecipitation were assumed proportional to cobalt losses, and corrections were made accordingly. Cobalt concentrations were determined by flame atomic absorption analysis (Perkin Elmer Model 403 spectrophotometer; air/acetylene flame through triple slot burner head). Coprecipitation recoveries were always > 90%. Ultimate Pb recoveries based on consistency standards were 100% ($\pm$4-10% depending on standard Pb concentration - Table 2.2). Final trace metal normalization to calcium is accomplished by flame AA analysis of 10 μl subsamples of dissolved coral removed earlier (diluted 10,000-fold).

Measurement precision varied with coral species and band age. In general, replicate analyses of trace metals in older bands (up to several hundred years) were better than those in younger bands (1-10 years), especially for Pb. Dissolved organic carbon measurements on old and recent bands (cleaned and dissolved D. labyrinthiformis from North Rock, Bermuda) showed residual organic carbon levels of only 0-2 ppm. In the worst possible case, assuming an oceanic particulate Pb concentration of 70 ppm Pb (Jickells et al., 1984), organically-bound Pb

Table 2.1 HGA 400 program conditions.

Element	Wavelength	Dry	Char	Atomize	Clean	Tube
Pb	283.1 nm	140-200, 25 s 200, 15 s	200-800, 15 s 800, 10 s	2500, MPH	2700, 6 s	non-pyro (w/platform)
Cd	228.8 nm	100-120, 15 s 120, 10 s	120-450, 15 s 450, 10 s	450-2400, 1 s 2400, 4 s	2700, 5 s	non-pyro
V	318.4 nm	110-250, 25 s 250, 15 s	250-1200, 15 s 1200, 10 s	2950, MPH	3000, 8 s	pyro
Zn	213.9 nm	100-120, 15 s 120, 10 s	120-500, 15 s 500, 10 s	500-2200, 1 s 2200, 4 s	2700, 5 s	non-pyro
Ba	553.3 nm	110-150, 20 s 150, 15 s	150-1650, 25 s 1650, 10 s	2850, MPH	3 { 20, 5 s 2800, 8 s }	pyro

Table 2.2 Lead recovery efficiencies as determined by analysis of spiked consistency standards.

[Pb] in Standard* (nM)	[Pb] Measured (nM)
3.9	3.7 ± 0.5 (n=10)
7.9	8.0 ± 0.8 (")
19.5	19.3 ± 1.3 (")
38.7	38.7 ± 1.7 (")

*all standards prepared in purified 0.84M $CaCO_3$ solution

could account for only 0.1 nmol Pb/mol Ca -- 2% of the lowest coral Pb measurement yet made. Maximum organically-bound contributions of Cd, Zn, and V are also small: 2 pmol Cd/mol Ca, 0.9 nmol Zn/mol Ca, and 0.2 nmol V/mol Ca. Furthermore, organic carbon levels showed no evidence of any age dependence over the last 50 years in this specimen (see Table B.10). Scanning electron microscopy also failed to show any differences between old and young samples which might explain the age-contamination relationship. Attainable 1-sigma errors for triplicate analyses are: $\pm$1 nmol Pb/mol Ca, $\pm$0.10 nmol Cd/mol Ca, $\pm$1 nmol Zn/mol Ca, and $\pm$ 2 nmol V/mol Ca. These errors constituted 2-25% of total encountered signals for Pb and Cd, 20% for Zn, and about 2% for V which exhibited high concentrations and milder contamination problems. Blanks improved continually as better reagent purification and procedural techniques were devised. Present blank concentrations within final 500 μl sample aliquots are near or at detection limits for three of the elements attempted; i.e. 0.4 nM Pb (0.0010 absorbance units), 0.1 nM Cd (.0015 absorbance units), and undetectable for V. Contamination control proved most difficult for Zn (blank concentrations of 2-3 nM), however, this may have been an artifact of method development since Pb analysis was the foremost concern.

2.2.4 Stable lead isotopic analysis

Sample cleaning is at least as critical for Pb isotopic analysis as it is for determination of Pb concentrations. While a contaminant level of 5% may be hard to distinguish in terms of total Pb in a sample, unusual contaminant isotopic ratios may impart large biases to mass spectrometric determinations of isotopic composition. Experience also shows that one cannot assume non-lattice Pb to bear the same isotopic ratio as the lattice-bound fraction. Thus, all the treatments described in section 2.2.2 also apply to isotopic analysis. Sample sizes for the Pb isotope measurements reported in this thesis ranged from 300 - 3000 mgs of crushed coral, giving final yields of 20-30 ngs purified Pb. Due

to these comparatively large sample requirements, partitioning of samples is necessary to ensure effective cleaning.

Unlike the Pb concentration method, sample purification for isotopic analysis is not based on cobalt-APDC chelate coprecipitation. Large organic residues are not amenable to sample loading on rhenium filaments used for thermal ionization. Instead, dissolved coral samples are purified by anion exchange chromatography following the procedure of Manhes et al. (1978). Cleaned samples are dissolved in vycor-distilled concentrated HBr (8.9N) and diluted with enough distilled water to yield a solution Br^- concentration of 0.75N. A subsample may be removed for Pb/Ca determination as a check on cleaning efficacy. Columns are prepared from 2.5 ml acid-leached pipette tips fitted with supports made from porous polyethylene (Bel-Art). Resin beds consist of 100 ul Biorad AG1-X8 (200-400 mesh) slurry which has been preconditioned in aqua-regia for 24 hours and washed 10 times with 0.2N HNO_3. Once the columns are prepared, additional washing with clean 0.5N HNO_3 is recommended to remove any traces of Pb from the resin and column walls. Finally, the resin is put into Br^- form by addition of 3.0 ml of 0.75N HBr.

The dissolved coral samples are loaded onto the columns (multiple columns for voluminous samples) and washed 4 times with 2.0 ml additions of 0.75N HBr. Lead is eluted with 2.0 ml 0.5N HNO_3 in clean 10 ml Teflon beakers. At this point, the samples usually contain unacceptable levels of residual calcium resulting from the coral matrix which is 40% Ca. As Ca begins to ionize within the upper range of Pb ionization temperatures , it is desirable to remove as much of this interferent as possible. Signal suppression, instability, and fractionation may result without additional purification. Higher sample purity is accomplished simply by repeated anion exchange on fresh columns. Before reprocessing samples, however, all traces of HNO_3 must be removed by evaporation in a clean environment. Combined infrared/hotplate heating within a glass enclosure fed with a filtered airstream (to minimize condensation) has given acceptable results. The entire operation should be carried out in

a laminar flow bench. Samples should be taken to dryness gently and then redissolved in 0.75N HBr. One or two additional passes through the anion exchange columns is usually sufficient to reduce Ca to acceptable levels. Frequently, one must trade off higher sample purity against increased handling and reagent use which contribute additional picograms of Pb blank. Estimated total blank levels achieved for coral isotope determinations were 50-100 pg.

At the completion of sample purification, small aliquots of eluted sample (25 μl) can be measured for Pb concentration by GFAAS in order to assess a net ion exchange recovery (should be greater than 80%). 20 μls of high-purity 0.1N H_3PO_4 are added to the remainder, and the samples are concentrated by evaporation to tiny drops suitable for filament loading. Using a Teflon capillary, samples are deposited on small beds of silica gel which have been dried on rhenium filaments. The use of phosphoric acid and a fused silica support has been found to increase the ionization efficiency of Pb over thermal production from PbS (Cameron et al., 1969). Samples are carefully dried and then flashed by increasing the filament current stepwise from 1.5 amp (5 min.) to 2.0 amps (5 min.) to 2.5 amps (2 min.) to 3.0 amps (1 min.) to 3.5 amps (5 sec.) to 3.8 amps (20 sec.).

Lead isotopic ratios were determined on a 12" magnetic sector, solid source mass spectrometer (M.I.T. Department of Earth, Atmospheric, and Planetary Sciences; S.R. Hart). Filament currents generally ranged from 2.7-3.0 amps. Whenever signal strength permitted, 60 - 100 sets of 204,206,207 and 208Pb ratios were collected. Measurement error (95% confidence limits) is conservatively estimated at $\pm$0.0010 for the reported $^{206/207}$Pb ratios to allow for variable mass fractionation. In

2.2.5 ^{210}Pb analysis

Analysis of ^{210}Pb ($t_{1/2}$ = 22.5 yrs) in corals to corroborate sample ages and Pb distribution coefficients was adapted from the ^{210}Po ($t_{1/2}$ = 138.4 days) method of Flynn (1968). Corals analyzed were all at least 2

years old, so ^{210}Pb - ^{210}Po secular equilibrium was well established. In retrospect, sample cleaning is recommended to be as vigorous as for stable Pb analysis (see section 3.5). This recommendation stems from the finding that non-lattice ^{210}Pb (or ^{210}Po) accumulated by corals in the reef environment represents a potentially large contaminant reservoir. It was initially assumed that in the expected absence of any handling contamination for ^{210}Pb, naturally emplaced contaminants would be removed by a less stringent cleaning protocol.

Cleaned samples were weighed to the nearest 0.01 g and dissolved in 12N HCl. Approximately 2 dpm of ^{208}Po ($t_{1/2}$ = 2.93 yr) was added as a yield monitor followed by 5 ml 20% hydroxylamine HCl, 2 ml 25% sodium citrate, and 10 mg Bi carrier (in solution). Samples were diluted to 50 $\pm$ 5 mls and adjusted to pH 2. Plating of ^{210}Po and ^{208}Po was by autodeposition on silver disks at 85-90°C. One hour platings with vigorous stirring generally resulted in $\geq$90% deposition.

Alpha counting of ^{210}Po and ^{208}Po was performed on EG & G Ortec Model 576 alpha spectrometers fitted with 450 mm^2 low-background detectors. Whenever possible, samples were sized to provide at least 500 counts over 72 hours. For a recently collected coral with an initial ^{210}Pb activity of 0.4 dpm/g, this means about 1 g of cleaned coral (assuming a detector efficiency of 30%). This enabled errors due to counting statistics to be held below 5%.

2.2.6 Efficacy of sample preparation and cleaning

Results and discussion of Pb and Cd measurements on corals sampled from the North Atlantic, Pacific, and Indian Oceans are given in Chapters 3 and 4. Analytical trials which led to the final data, however, serve to illustrate the importance of various aspects of the method.

Fig. 2.3 compares the historical lead records obtained from two corals inhabiting North Rock, Bermuda (a reef 14 km north of Bermuda).

Figure 2.3 Historic skeletal Pb/Ca mole ratios in D. strigosa and D. labyrinthiformis, North Rock, Bermuda. D. strigosa analyses were performed on high-density trabecular structures only; D. labyrinthiformis analyses were performed on whole coral. In most cases, annual determinations were performed in triplicate or more. Error bars represent 1σ deviation from means.

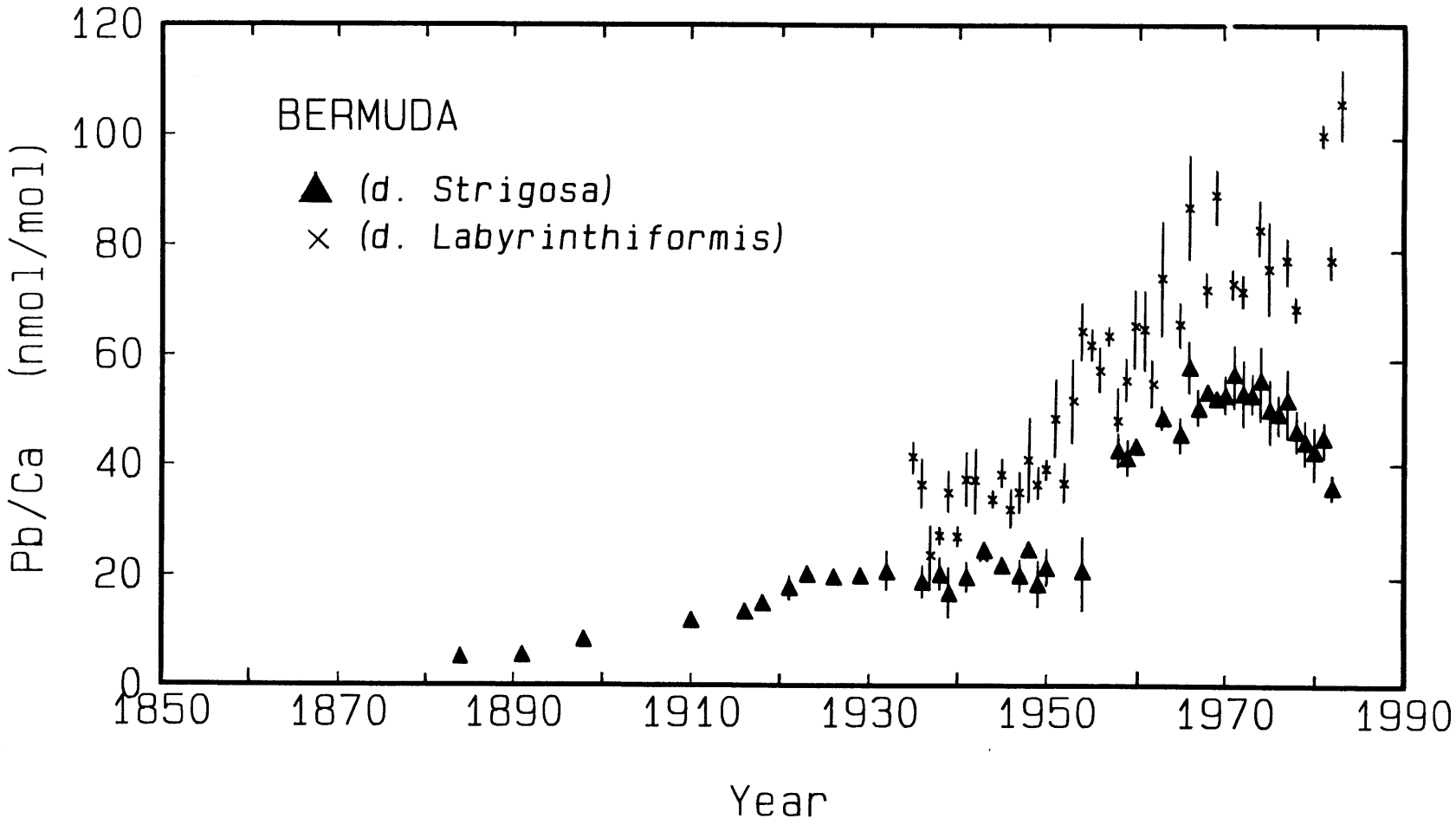
BERMUDA
▲ (d. Strigosa)
× (d. Labyrinthiformis)
Pb/Ca (nmol/mol)
120
100
80
60
40
20
0
1850
1870
1890
1910
1930
1950
1970
1990
Year

Late 19th and 20th century North American industrialization is responsible for the temporal changes recorded in the corals. The techniques used for each of the two species, Diploria labyrinthiformis and Diploria strigosa, were the same except for discrimination between structural parts in preparing samples of D. strigosa. While only dense trabecular fragments were isolated for D. strigosa, whole coral aliquots were prepared for D. labyrinthiformis. Higher levels of contamination and resultant poorer reproducibility are immediately evident in the D. labyrinthiformis data, especially in younger bands. A distribution coefficient of 2.3 for Pb in D. strigosa is obtained by comparing the 1983-84 skeletal Pb concentration (30 nmol Pb/mol Ca) to the seasonally-averaged surface water concentration for the same time period (128 pM Pb or 13 nmol Pb/mole Ca). (See Table 3.1.) Applying this value of K_D to the oldest coral measurements implies a pre-industrial surface water concentration of less than 20 pM Pb. The plausibility of this temporal response by D. strigosa over the last century suggests that all of the Pb being measured in this coral is lattice-bound.

Additional evidence that the present technique is adequate for purposes of removing extraneous Pb from Diploria corals is seen in Fig. 2.4. Analyses of a third coral (another D. strigosa) from the southern reef preserve of Bermuda (sampled 0.5 km offshore) show attainment of a constant skeletal Pb concentration, regardless of additional cleaning (bands analyzed were from 1936-1939). Normal sample losses are targeted at 25-35%. The higher Pb level measured in this specimen compared to that at North Rock is a result of enhanced dissolved Pb concentrations caused by coastal resuspension.

It is difficult to assess the relative importance of the various cleaning steps since much depends on the coral in question. Corals with higher organic content will respond to an oxidizing treatment more than corals with noticeable detrital inclusions which are better removed by reductive cleaning and acid leaching. Rapidly growing corals from relatively calm transparent waters may only require ultrasonic cleaning

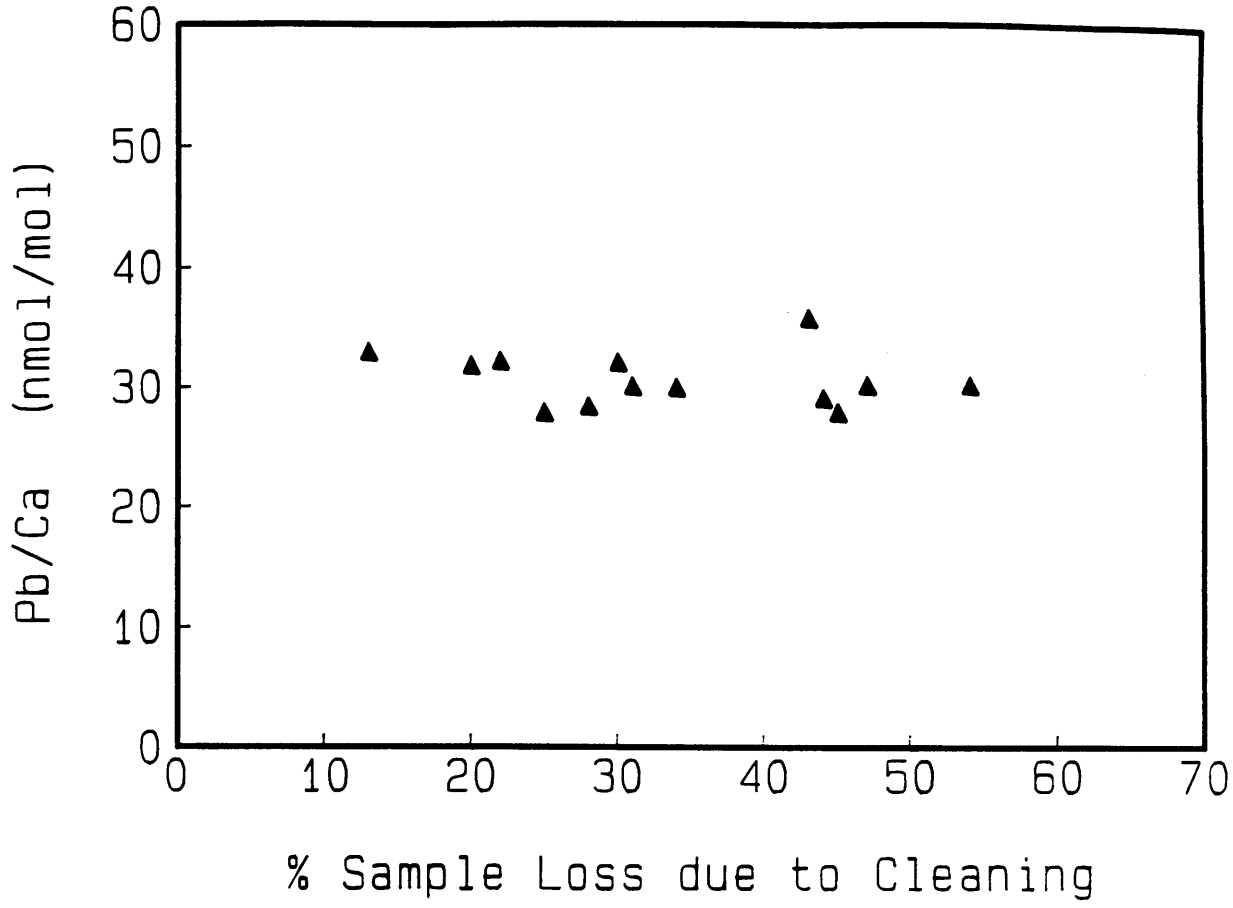

Figure 2.4 Effects of intensified cleaning on Pb concentrations in D. strigosa, Southern Reef Preserve, Bermuda. Bands selected for analysis, 1936-1939, do not differ in industrial Pb content.

in weak HNO_3; many instances of this have been observed. In the case of Montastrea annularis (Florida Straits), it is apparent that each cleaning phase can be important in removing contaminant trace metals (Table 2.3). Reductions in total Pb, Cd, and Zn in progressing from crushed pre-cleaned coral through the full cleaning treatment are approximately 3, 4 and 6-fold, respectively. The problem of removing contaminants from pulverized coral (<280 μm) is also illustrated in Table 2.3. To achieve maximum consistency, the same cleaning strategy was employed throughout this thesis research. In the event of a net blank addition caused by cleaning (for which there is no evidence), this would also enable intercomparison of results.

2.3 Seawater Methods

2.3.1 Lead concentration analysis

Determination of seawater Pb concentrations followed the technique outlined in Boyle et al., (1986). Preconcentration of Pb in acidified seawater samples was accomplished by cobalt-APDC coprecipitation in 40 ml acid-leached Teflon centrifuge tubes. Cobalt (500 μl 0.005M $CoCl_2$) was added before APDC (800 μl 2% solution) to ensure a well-dispersed precipitate. Ultrasonication (10 min) of the freshly formed precipitate improved Pb recoveries. Samples were allowed to stand for 1 hour and then centrifuged at 2,500 rpm for 40 minutes. Precipitates were washed with distilled water and re-centrifuged in order to remove residual sea salts. Final precipitates were digested with 8N HNO_3 and evaporated by water bath/infrared heating in a laminar flow bench. Residues were redissolved in 100 μl 0.1N HNO_3 immediately prior to analysis by GFAAS. Cobalt recoveries were measured by flame AAS as per the coral trace element technique.

Table 2.3 Cleaning treatment efficacy on Montastrea annularis, Florida Straits, (1984)

Sample cleaned thru stage:	Size Distribution	Pb/Ca (nmol/mol)	Cd/Ca (nmol/mol)	Zn/Ca (nmol/mol)
0 (precleaned only)	280-700 μm	96	8.0	121
1 (distilled water)	"	72	3.9	85
2 (0.15N HNO_3)	"	66	3.3	71
4 (oxidative wash)	"	66	3.3	42
6 (reductive wash)	"	56	3.0	22
6 (red. wash + 2 x HNO_3 rinse)	"	45	2.6	21
6 (red. wash + 2 x HNO_3 rinse)	< 280 μm	67	3.7	28
9 (entire treatment)	280-700 μm	38	2.3	

2.3.2 Stable lead isotopic analysis

Analysis of stable Pb isotopes in seawater has in the past been impeded by contamination problems associated with sampling and analysis. Surface seawater measurements have been reported by Flegal et al. (1984) for the central Pacific, and a single N. Atlantic determination is given in Schaule and Patterson (1983). To date, the vertical distribution of stable Pb isotopes has been reported for one only one station (4 points) in the Northeast Pacific (Flegal et al., 1986).

The main difficulty lies in sampling of subsurface waters. Lead contamination is easily introduced by leaching of samplers and/or hydrowire corrosion. Patterson and coworkers have overcome this problem with a single use-per cast 10-liter sampler which is mounted at the very end of a hydrowire (Schaule and Patterson, 1981). Using Go-Flo samplers and Kevlar hydrowire, Martin et al. (1986) have recently determined Pb concentrations in the Northeast Pacific which are consistent with earlier C.I.T. data. Subsurface seawater analyzed in this thesis consisted of pooled unused portions of samples collected by the "vane sampler" of Boyle et al. (1986). Larger volume (1-liter) samples collected with vanes designed specifically for Pb isotopes (Fig. 2.5) exhibited small offsets in $^{206/207}Pb$ (+0.0060 units) relative to the Boyle samples. These isotopic shifts were probably due to small amounts of contamination introduced during sampler turnaround. Surface waters used for isotope analysis were recovered by pole sampling and underway pumping.

Preconcentration of Pb from liter-sized seawater samples was performed by ion exchange chromatography on Chelex 100. Chelex resin (200-400 mesh) was pretreated in alternating 0.5N HNO_3 and 0.5N NH_4 OH (20 times) and stored in NH_4^+ form. One ml of Chelex slurry was added to acid-leached 10 ml polyethylene Econo-Columns and conditioned as follows:

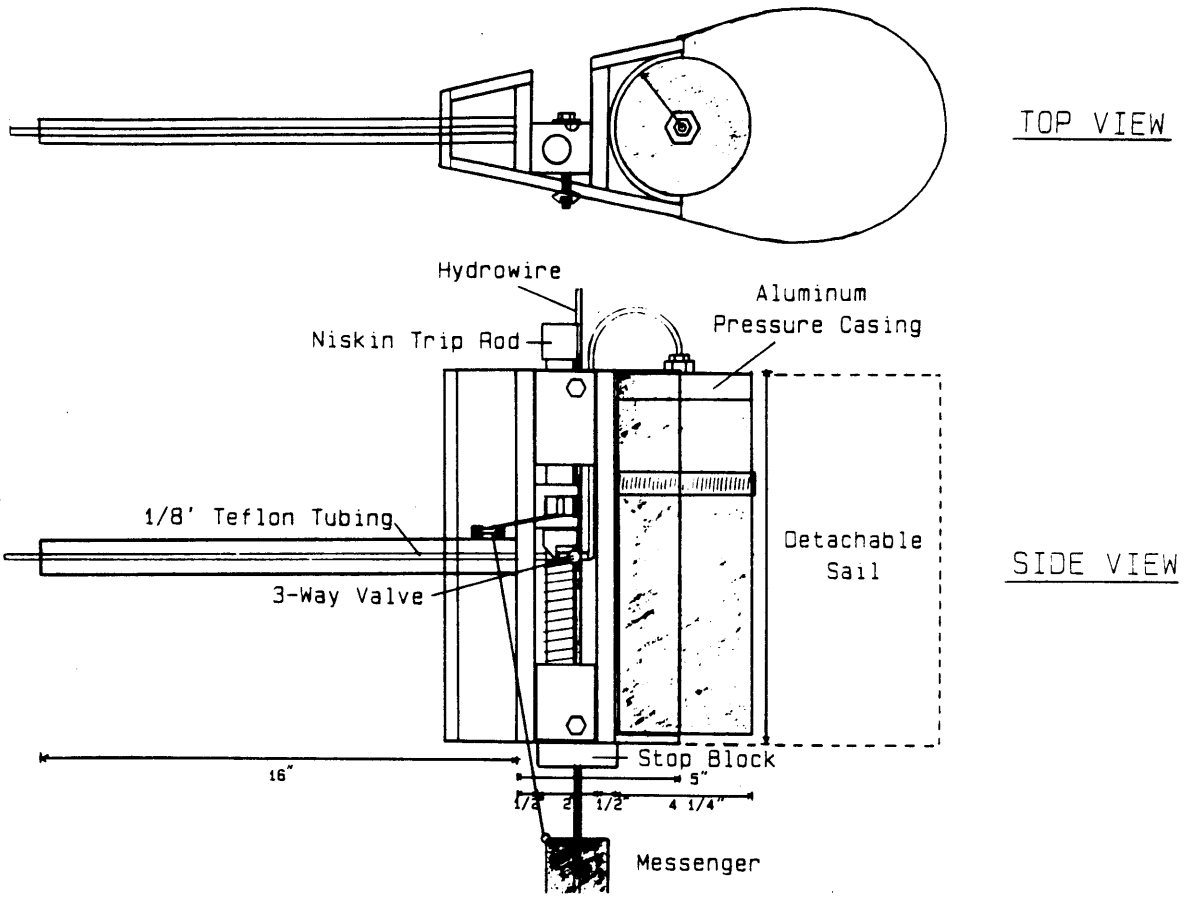

1-LITER TRACE ELEMENT SAMPLER

Figure 2.5 1-liter trace element sampler for subsurface seawater. All components in contact with sample are Teflon or polyethylene (1-liter narrow mouth LDPE bottle inside pressure casing). Sampler is submerged empty @ 1 atm. pressure. Sampler is tripped by messenger impact on three-way valve and filled by pressure differential.

1) 5 ml 2N HNO_3
2) 10 ml 0.2N HNO_3
3) 2 ml 0.5N HNO_3
4) 2 ml 2.0N NH_4OH
5) 2 ml dist.H_2O

Samples were neutralized to pH 7-8 immediately before Chelexing using concentrated NH_4OH. Columns were directly attached to sample bottles (1-liter or 500 ml narrow-mouth CPE) by means of machined Teflon adapters. Thus, samples and columns formed closed systems protected from external contaminants. Processing was carried out in laminar clean benches for added protection. Liter-sized samples were usually exhanged within 12 hours.

Lead and other cations exchanged by Chelex were eluted by adding 5 ml 0.5N HNO_3. Recovery was usually near-quantitative, demonstrating that wall adsorption of Pb from neutral seawater was not a problem over 12 hours. Seawater cation levels in the eluted Pb fractions at this point, however, were too high to allow filament loading and mass spectrometry. Additional purification was effected via anion exchange chromatography of $PbBr_x^-$ species (see section 2.2.4). Owing to sample limitations in all but western N. Atlantic surface waters, care must be taken throughout this entire procedure to achieve maximum Pb recovery and minimal contamination. One liter of seawater containing 50 pM Pb represents only 10 ng of Pb if recovery and loading are 100% efficient. Actual final ion exchange recoveries ranged from 70-90%. Correction for reagent and loading blanks where sample size was limiting is described in Appendix Table E. 2.

Sample loading and mass spectrometry of stable Pb in seawater are the same as described for coral Pb isotopes (section 2.2.4).

2.4 Trace Element Sediment Trapping

In order to evaluate Pb isotopic exchange via particle interactions, an array of miniature free-drifting sediment traps was deployed on several cruises to and from Bermuda. Traps consisted of 18" x 3" O.D. (2 13/16" I.D.) polycarbonate (Lexan) cylinders solvent bonded to Millipore filtration funnels (24 mm filter size). Baffles were constructed from 3" x 5/8" O.D. polycarbonate tubes bonded together to form a honeycomb arrangement. Traps were deployed at three depths (100, 400, 860 m), supported by Lexan crossframes (4-ft. span) designed to hold four traps each. Normally, one trap per crossframe was used as a blank, leaving a capture area of 3 x 37 cm^2 or 112 cm^2 per depth. The trap array was connected with 1/2" polypropylene line and weighted with 125 lbs of anchor chain. Flotation was provided by two 16"-diameter glass spheres (Benthos). A 25 m string of fisherman's floats terminated by a spar buoy, radar reflector, and strobe enabled visual/radar tracking of the array over several days of station work.

In spite of extreme precautions including acid-leaching of traps and deployment of the traps covered and filled with distilled water (covers held by dissolvable links except for blank traps; distilled water to prevent entry of Pb-rich surface water), filter blanks averaged 5 ng Pb. Since total capture masses ranged only from 2-20 ng Pb, the high blank prohibited total filter digestions. Instead, filters were shaken to release captured particles into clean Teflon beakers. Particles were then digested in concentrated HBr and purified as per the coral Pb isotope procedure (section 2.2.4).

2.5 Conclusions

Retrieval of historic chemical information from corals has in the past been largely limited to radioisotopic studies. The methods presented here extend this capability to trace elements which are incorporated into coral aragonite. Detrital, organic, and

handling/storage associated contaminants can be completely removed from most coral genera by an intense series of oxidative, reductive and leaching treatments. Owing to differences in coral morphology and growth habitat, however, optimum cleaning strategies may differ from individual to individual. Sample matrix purification by dithiocarbamate coprecipitation with a cobalt carrier and subsequent analysis by GFAAS is applicable to a host of transition metals. In the case of Pb, historic stable isotope distributions recorded by corals are also recoverable.

As will be seen in subsequent chapters, these methods have been applied to reconstruct relatively recent temporal changes in the surface ocean prompted by anthropogenic activity (Pb, Cd), as well as natural perturbations in circulation (Cd). Older paleo-reconstructions should be possible provided samples have not recrystallized. Based on size, charge and coordination constraints, a variety of other metals are predicted to demonstrate aragonite lattice compatibility. Expected low abundances (e.g. rare earths; Shaw and Wasserburg, 1985) and susceptibility to contamination (e.g. Fe, Hg, Mn), however, may make these analyses difficult. The usefulness of measurements of these untested elements remains to be seen.

References

Boyle, E.A. (1981). Cadmium, zinc, copper, and barium in foraminifera tests, Earth Planet. Sci. Lett. 53: 11-35.

Boyle, E.A. and J.M. Edmond (1975). Determination of trace metals in aqueous solution by APDC chelate co-precipitation. In: Advances in Chemistry, Vol. 147. American Chemical Society, Washington, D.C., pp. 44-55.

Boyle, E.A., S.D. Chapnick, G.T. Shen, and M.P. Bacon (1986). Temporal variability of lead in the western North Atlantic Ocean, Geochim. Cosmochim. Acta 91: 8573-8593.

Bruland, K.W. (1983). Trace elements in sea-water. In: Chemical Oceanography, Vol. 8, J.P. Riley, ed., pp. 157-220. Academic Press, New York, N.Y.

Buddemeier, R.W., J.E. Maragos, and D.W. Knutson (1974). Radiographic studies of reef coral exoskeletons: Rates and patterns of coral growth, J. Exp. Mar. Biol. Ecol. 14: 177-200.

Buddemeier, R.W. and R.A. Kinzie (1975). The chronometric reliability of contemporary corals. In: Growth Rhythms and the History of the Earth's Rotation. G.D. Rosenberg and S.K. Runcorn, eds., pp. 135-147. John Wiley and Sons, London.

Cameron, A.E., D.H. Smith and R.L. Walker (1969). Mass spectrometry of nanogram-size samples of lead, Anal. Chem. 41: 525-526.

Cross, T.S. and B.W. Cross (1983). U, Sr and Mg in Holocene and Pleistocene corals, J. Sed. Petr. 53: 587-594.

Dodge, R.E. and T.R. Gilbert (1984). Chronology of lead pollution contained in banded coral skeletons, Mar. Biol. 82: 9-13.

Flegal, A.R., B.K. Schaule and C.C. Patterson (1984). Stable isotope ratios of lead in surface waters of the central Pacific, Mar. Chem. 14: 281-287.

Flegal, A.R., K. Itoh, C.C. Patterson and C.S. Wong (1986). Vertical profile of lead isotopic compositions in the north-east Pacific, Nature 321: 689-690.

Flynn, W.W. (1968). The determination of low levels of Polonium-210 in environmental materials, Anal. Chim. Acta 43: 221-227.

Hudson, J.H. (1981). Growth rates in Montastrea annularis: a record of environmental change in Key Largo Coral Reef Marine Sanctuary, Florida. Bull. of Mar. Sci 31: 444-457.

Jickells, T.D., W.G. Deuser, and A.H. Knap (1984). The sedimentation rates of trace elements in the Sargasso Sea as measured by sediment trap, Deep Sea Res. 31: 304-312.

Manhes, G., J.F. Minster and C.J. Allegre (1978). Comparative uranium-thorium-lead and rubidium-strontium study of the Saint-Severin amphoterite: Consequences for early solar system chronology, Earth Planet. Sci. Lett. 39: 14-24.

Martin, J.H., G.A. Knauer and W.W. Broenkow (1985). Vertex: The lateral transport of manganese in the northeast Pacific, Deep Sea Res. 32: 1405-1427.

Schaule, B.K. and C.C. Patterson (1981). Lead concentrations in the Northeast Pacific: Evidence for global anthropogenic perturbations, Earth Planet. Sci. Lett. 54: 97-116, 1981.

Schaule, B.K. and C.C. Patterson (1983). Perturbations of the natural lead depth profile in the Sargasso Sea by industrial lead, in: Trace Elements in Seawater, C.S. Wong, E. Boyle, K. Bruland, D. Burton and E.D. Goldberg, eds., pp. 487-503. Plenum, New York, N.Y.

Shaw, H.F. and G.J. Wasserburg (1985). Sm-Nd in marine carbonates and phosphates: Implications for Nd isotopes in seawater and crustal ages, Geochim. Cosmochim. Acta 49: 503-518.

CHAPTER 3

LEAD IN CORALS
RECONSTRUCTION OF GLOBAL INDUSTRIAL PERTURBATIONS

3.1 Introduction

Over the past two decades, evidence of global environmental contamination by industrial lead has accumulated. Murozumi and coworkers (1969) documented historic increases of lead in snow strata cored in Greenland and Antarctica in 1969. More recent snow and ice core determinations from both hemispheres have confirmed their original findings (see review by Wolff and Peel (1985)). In these most pristine of locations, however, contamination continues to hamper measurement efforts, particularly in the case of ancient samples.

Extension of anthropogenic lead mapping to the oceans succeeded more recently when Schaule and Patterson (1981) overcame attendant new sampling difficulties in 1976. Together with newer oceanic data (Flegal and Patterson, 1983; Schaule and Patterson, 1983; Flegal et al., 1984; Boyle et al. 1986), and atmospheric flux measurements (Settle and Patterson, 1982; Settle et al., 1982; Jickells et al., 1984; Church et al., 1984), expected key influences of industrial proximity and meteorology have been ascertained. It is now clear that aeolian delivery of stable lead parallels that of ^{210}Pb (Boyle et al., 1986; Talbot and Andren, 1983; Turekian et al., 1977) but the stable Pb source function is independent and has been evolving over time. The transient nature of this flux suggests application of stable Pb as an oceanic chemical tracer to complement findings based on chloroflourocarbons and bomb-produced radionuclides. As discussed by Boyle et al. (1986) in a preliminary modeling attempt, however, the success of such an application hinges on construction or recovery of accurate regional source deposition records. At present, the longest Pb measurement time series (now beginning its fourth year) is that of Boyle and coworkers in

the Sargasso Sea. Continued tracking of anthropogenic Pb in the ocean is planned.

This chapter describes the reconstruction of past surface ocean Pb concentrations and Pb isotopic distributions using the skeletal lead content of annually-banded corals. Measurements on corals from the western North Atlantic, Florida Straits, Pacific, and Indian Oceans reconfirm the pervasive nature of industrial Pb aerosols and provide detailed chronologies of 20th century worldwide industrialization.

3.2 Bermuda

Positioned in the southern portion of the North American Westerly flow path (see Fig. 1.1), Bermuda is a prime site for recording historic industrial lead fallout to the Sargasso Sea. Fig. 3.1 contains two such depositional records in corals. The lower record reflects the Pb transient in the open ocean, and the upper incorporates additional near-shore perturbations to dissolved Pb due to resuspension. The conspicuous gap (1955-1957) in the North Rock data is due to an attenuation of dense structural parts (trabeculae) which are isolated for analysis in this particular species of brain coral. Apparently, this coral suffered from some unknown stress during this 3-year period while the more southerly coral did not. The major features of the record are: (1) a gradual increase in skeletal Pb levels near the end of the 19th century; (2) a second more pronounced increase beginning in the 1950's, and (3) a dramatic decline initiated in the early 1970's. This progression of events very closely parallels the development of American industries tied to possible lead emissions, as can be seen in Fig. 3.2. The Pb source responsible for the turn of the century rise cannot be exactly specified, since early growth patterns for most large-scale industries are virtually identical. Nevertheless, the early perturbation must be a direct consequence of the American industrial revolution. The striking resemblance between the subsequent portion of the coral record and U.S. alkyl lead consumption suggests that this

Figure 3.1 Skeletal Pb concentrations in two colonies of D. strigosa cored near Bermuda: (+) Southern Reef Preserve; (▲) North Rock). In most cases, data points represent triplicate analyses or better. Error bars are 1 standard deviation. Error bars for the Southern Reef chronology have been omitted for clarity (magnitudes comparable to N.Rock). Four contaminated bands (1955-57, 1983) in the N.Rock record ranging from 45-65 nmol Pb/mol Ca (27 analyses; see Table A.1) are not shown (see text).

Figure 3.2 Historical U.S. production of (a) primary lead (b) iron ore (c) coal (d) alkyl lead (consumption) (Sources: Bureau of the Census of the U.S. Department of Commerce; testimony by Ethyl Corp. to EPA public hearing on proposed regulations on the lead content of gasoline, Aug. 31, 1984)

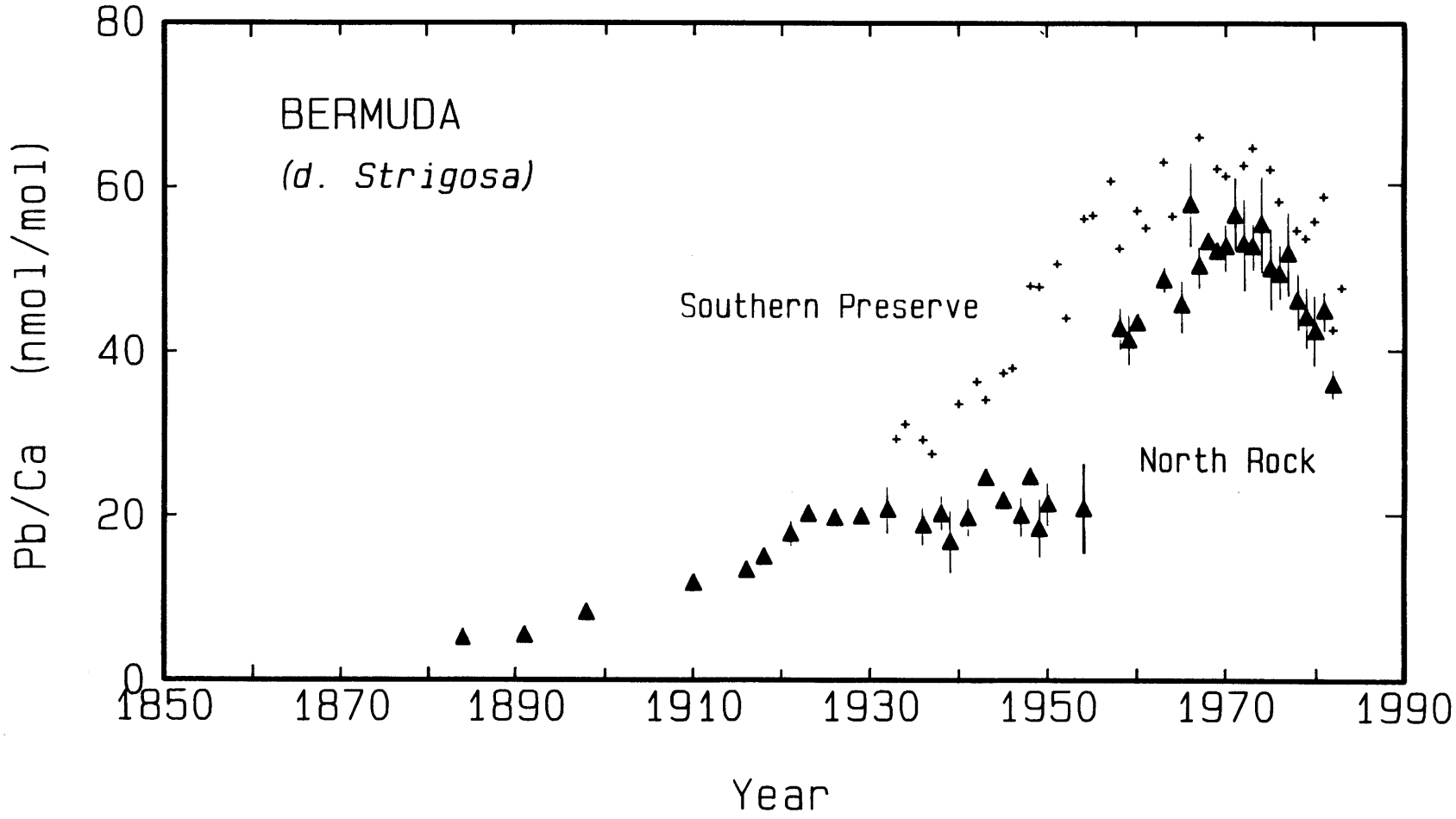
BERMUDA
(d. Strigosa)
Southern Preserve
North Rock
Pb/Ca (nmol/mol)
Year
0
20
40
60
80
1850
1870
1890
1910
1930
1950
1970
1990

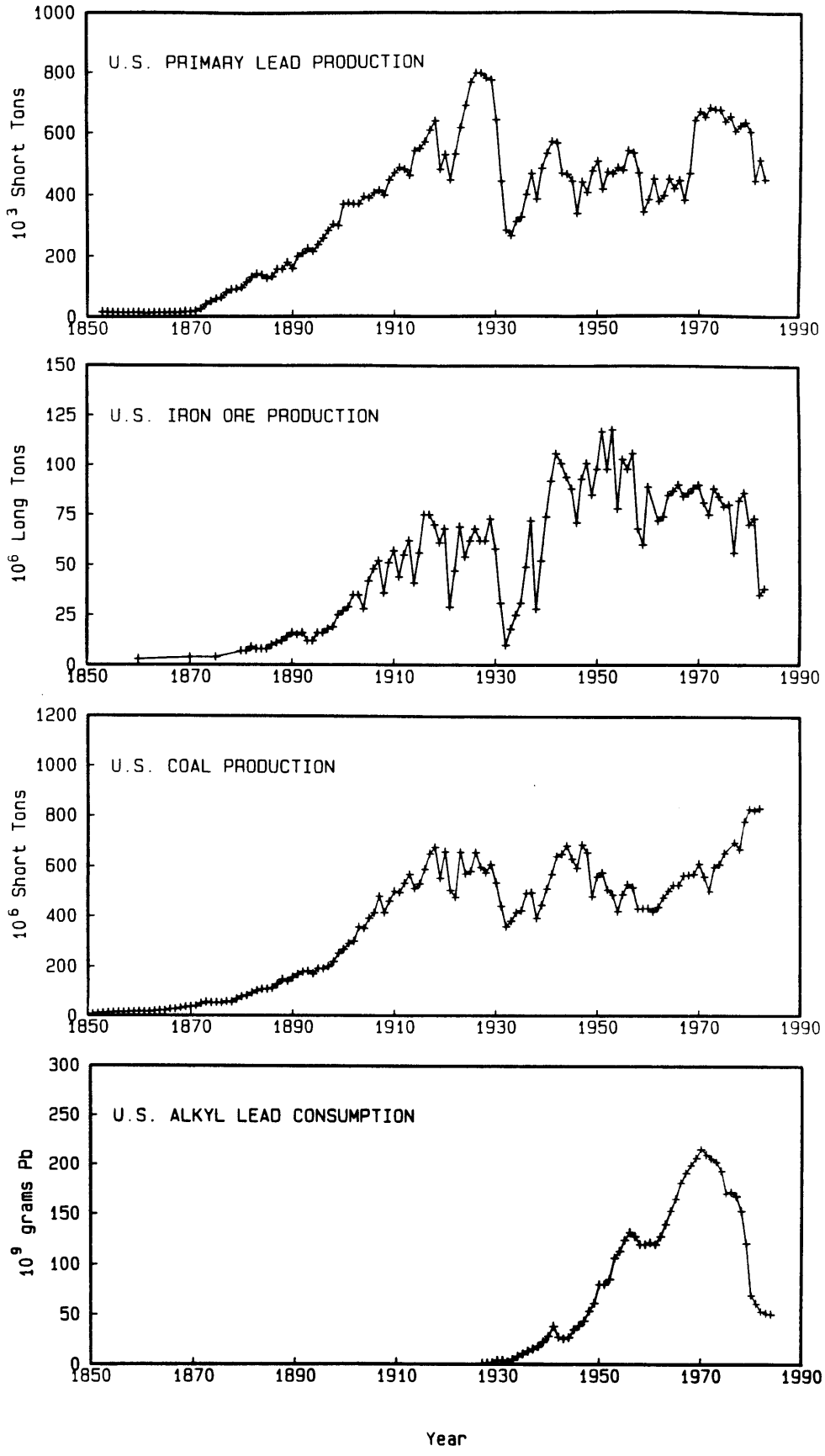
U.S. PRIMARY LEAD PRODUCTION
10^3 Short Tons
0
200
400
600
800
1000
1850
1870
1890
1910
1930
1950
1970
1990
U.S. IRON ORE PRODUCTION
10^6 Long Tons
0
25
50
75
100
125
150
U.S. COAL PRODUCTION
10^6 Short Tons
0
200
400
600
800
1000
1200
U.S. ALKYL LEAD CONSUMPTION
10^9 grams Pb
0
50
100
150
200
250
300
Year

source gained prominence with the rise of the automobile. Because competing sources appear to have levelled-off later in the century, the alkyl lead pattern is accurately superimposed on the earlier coral record. This is true even to the extent that the contemporary coral Pb value appears to have receded close to the 1920's-30's value. A 1-year time lag between the coral and alkyl Pb source history is consistent with estimates of ^{210}Pb mixed layer residence times of 1.7-2.5 years (Bacon et al., 1976; Nozaki et al., 1976).

The surface ocean Pb decline of 1.5-fold recorded by the Bermuda corals between 1979 and 1984 is in agreement with the earliest time series data available for dissolved Pb and ^{210}Pb. The ratio of Schaule and Patterson's July 1979 surface water Pb measurement to our own in June 1984 is 164 pM/103 pM or 1.6, however, extreme seasonality in surface ocean Pb places a high degree of uncertainty on this value (Boyle et al., 1986). Since Pb and ^{210}Pb fluxes have exhibited a close coupling over Bermuda, one could also compare a ^{210}Pb-normalized ratio over time: $(Pb/^{210}Pb)_{July\ '79}/(Pb/^{210}Pb)_{1984\ avg.(n=4)} = 1.9$. A closer comparison might result if the coral Pb decrease from 1980-1985 were known. The absolute flux of Pb to the surface and deep ocean has been estimated by three independent rain and sediment trap measurements by Jickells et al. (1984a, 1984b) and Church et al. (1984) for the period 1981-1983. These results all fall within the range 0.88-1.18 $mg/m^2/yr$. Settle and Patterson's (1982) mean flux of 1.7 $mg/m^2/yr$ is higher, but corresponds to surface water, rain and dry deposition measurements from 1979 when the industrial flux was higher. Integrating an annual flux of 1.0 $mg/m^2/yr$ over the western North Atlantic between 30°N and 50°N (latitudes over which U.S. westerlies prevail) gives a rough total Pb flux of 10×10^{10} g/yr for 1982. This represents about 20% of the total Pb consumed as alkyl Pb in the U.S. that year. However, it can be estimated (see Fig. 3.3) that alkyl lead was responsible for only about 35% of the total industrial Pb flux in 1982 (based on the 1983 estimated contribution to the coral which allows for a one-year surface water lag time). Thus, a gasoline-derived Pb flux of approximately 3.5×10^{10} g

Figure 3.3 Reconstructed contributions of natural and anthropogenic Pb to the Sargasso Sea based on the North Rock coral chronology of Fig. 3.1. Industrial (non-alkyl Pb) inputs are assumed constant after 1923 with alkyl Pb presumed responsible for subsequent perturbations. Note that real time breakdowns probably anticipate the coral-based curves by 1-2 years due to surface ocean integration of lead inputs.

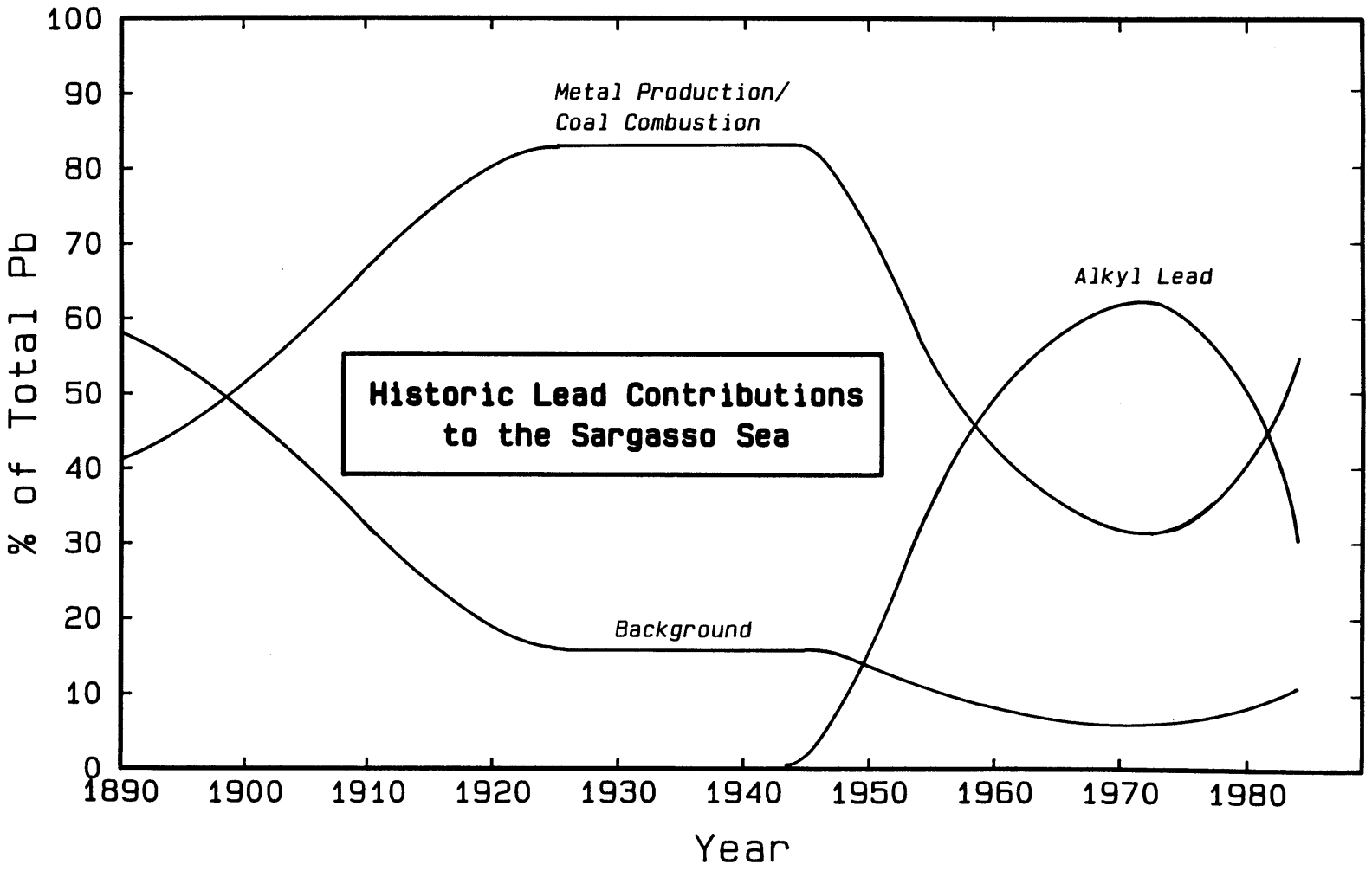
Historic Lead Contributions
to the Sargasso Sea
Metal Production/
Coal Combustion
Alkyl Lead
Background
% of Total Pb
Year
100
90
80
70
60
50
40
30
20
10
0
1890
1900
1910
1920
1930
1940
1950
1960
1970
1980

(7% of the raw additive usage) was delivered to the western North Atlantic in 1982.

The coral-based Pb source breakdown of Fig. 3.3 is surprisingly consistent with Nriagu's (1979) global Pb emission summary for 1975. His estimated contributions for anti-knock additives (58%), all other anthropogenic sources (37%), and background (5%) compare favorably to our own 1978 estimates (again allowing for a brief time lag) of 56%, 37%, and 7% for these same respective sources. As far as the relative roles of key industries and their Pb emissions, Nriagu's contemporary analysis suggests that iron/steel production is about 1.5 times as important as lead production, twice as important as copper production, and 3 times as important as coal combustion or zinc production.

At the opposite end of the time scale, the question of pre-industrial environmental Pb levels arises. Before addressing this question, it would be useful to translate skeletal Pb concentrations to a more meaningful measure, namely, ambient Pb concentrations in seawater. This can be accomplished by means of a distribution coefficient (K_D) for Pb in corals relative to surface water (see Appendix - Table 5.2). Based on 1983-84 seasonally-averaged surface water dissolved Pb concentrations, the North Rock and Southern Reef Preserve coral records (both Diploria strigosa) extrapolate to K_D = 2.1 - 2.3 (Table 3.1). Thus, D. strigosa discriminates in favor of Pb over Ca during skeletal accretion.

Applying K_D = 2.3 to the coral record reveals that as of 1890, surface waters of the western North Atlantic contained 24 pM Pb. However, production of iron ore, coal, lead, and other primary metals had been steadily increasing the previous 20-30 years. If one carefully examines the relative growth rate of each possible source industry between 1890-1920, primary Pb production matches the coral record most closely (both experienced 3.5-fold increases versus 6-fold increases in the steel, copper and coal industries). This comparison, however, leads to the expectation that surface water Pb fell very close to 0 pM by

Table 3.1 Lead distribution coefficients for two Bermuda corals

	Southern Reef Preserve (D. strigosa)	North Rock (D. strigosa)
Bermuda Coral [Pb]/[Ca] (nmol/mol)		
1983-84 est.	42×10^{-9}	30×10^{-9}
Seawater [Pb] (pM)		
6/83	200 (filt.)	100
9/83	197 (filt.)	153
1/84	180 (filt.)	119
4/84		140
6/84	216 (filt.)	101
9/84		157
12/84		95
1983-84 Avg.	198 ± 15	128 ± 26
K_D	2.1	2.3

1870. There are several reasons to believe this unrealistic. 1) The Pb decline in D. strigosa over the previous 7 years to the equivalent of 22 pM Pb in 1884 is too mild to extrapolate to 0 pM at 1870. 2) Pb isotopes (see subsequent paragraphs) show identical $^{206/207}Pb$ ratios in 1887 and 1895 which already fall within the background envelope. 3) A 1920 Fiji coral determination suggests a pre-industrial surface ocean Pb concentration of 16-19 pM in the S. Pacific. Although this determination may contain a resuspended Pb component, it is probably not more than 50% of the total (see Appendix 3.7.1). Thus, it is unlikely that the North Atlantic, with its higher fluvial and aerosol inputs, could have supported a concentration much lower than 10 pM. If, on the other hand, control of the early portion of the coral record was by one or a combination of the iron ore, copper, or coal industries, the projected pre-Industrial Revolution surface water value would be approximately 15 pM. Flegal and Patterson (1983) suggest a comparable value in estimating that 1979 North Atlantic surface waters (160 pM) were enriched by 10-fold over pre-historic concentrations. Their estimate, however, was conceived to span over two centuries of anthropogenic activity as justified by the Greenland snow strata record of Murozumi et al. (1969). This poses the question of the importance of anthropogenic Pb prior to 1850. Simple scaling of our own 1850 surface water estimate to the snow record results in a prehistoric extrapolation of close to 0 pM, which again appears unrealistic for the reasons cited earlier. Such an extrapolation is unwarranted, however, if one considers that a) prehistoric aerosol fluxes to Camp Century, Greenland were very small relative to those reaching the Sargasso Sea; and b) the Sargasso Sea may have received substantial fluvial inputs of Pb, whereas Greenland ice did not. Thus, an estimated Sargasso Sea surface water value of 15-20 pM Pb for the year 1850 is probably also a good prehistoric approximation.

Industrial leads are isotopically very heterogeneous due to radiogenic production (from ^{238}U, ^{235}U, and ^{232}Th) and a multiplicity of lead ore genesis pathways (Brown, 1965). The range of Bermuda coral

ratios exhibited in Fig. 3.4 represents only a few percent of the range bounded by the anomalously radiogenic Mississippi Valley-type ores of the U.S. ($^{206/207}Pb \approx 1.30$) and the nonradiogenic ores of Australia's Broken Hill Mine ($^{206/207}Pb \approx 1.00$). Yet, there is sufficient analytical precision within the range of historic American emissions to monitor changes in corals and seawater. Fig. 3.4 is the isotopic complement to the North Rock, Bermuda concentration record of Fig. 3.1. Eighty-five years ago, the $^{206/207}Pb$ isotopic signature of the surface ocean, 1.2147, was indistinguishable from the background value (Chow and Patterson, 1962), suggesting that an anthropogenic component was nonexistent or coincidentally bore a background signature. Industrial growth then prompted a migration toward less radiogenic values until the 1940's. None of the possible source industries discussed earlier can be dismissed on the basis of Pb isotopes since isotopic data for iron and copper ores are not available, and coal and lead ore signatures can both be found in the required 1.18-1.19 $^{206/207}Pb$ range (Chow and Earl, 1972; Doe, 1970). Subsequently, due to changing feedstocks for alkyl lead and efficient Pb dispersal from internal combustion engines, the isotopic progression was reversed. Introduction of more radiogenic Pb's, possibly by admixture of Mississippi Valley ores, is implicated. In the mid-1970's, a second reversal occurred, roughly in parallel with the U.S. phase-out of leaded gasoline. As in the case of the Pb concentration record, the present-day isotopic value appears to have reached the pre-alkyl lead (ca. 1930-1940) value. A single cross-check is afforded by an isotopic Pb measurement of 1979 Sargasso Sea surface water by Ng et al. (in Schaule and Patterson, 1983). Their reported ratios of 1.199 ($^{206/207}Pb$) and 0.492 ($^{206/208}Pb$) agree closely with ratios measured in the 1980 band of D. strigosa: 1.203 and 0.492.

3.3 Florida Straits

The general pattern of Pb increase in the Florida Straits over time (Fig. 3.5) is depressed relative to the Bermuda records. In addition, subtle distinctions suggest a modified source term from that affecting

Figure 3.4 Lead isotopic history of Sargasso Sea surface waters as recorded by D. strigosa -- North Rock, Bermuda. Background field is based on Chow and Patterson (1962). 1984 and 1985 determinations are seasonally-averaged surface seawater analyses (5 in 1984; 4 in 1985).

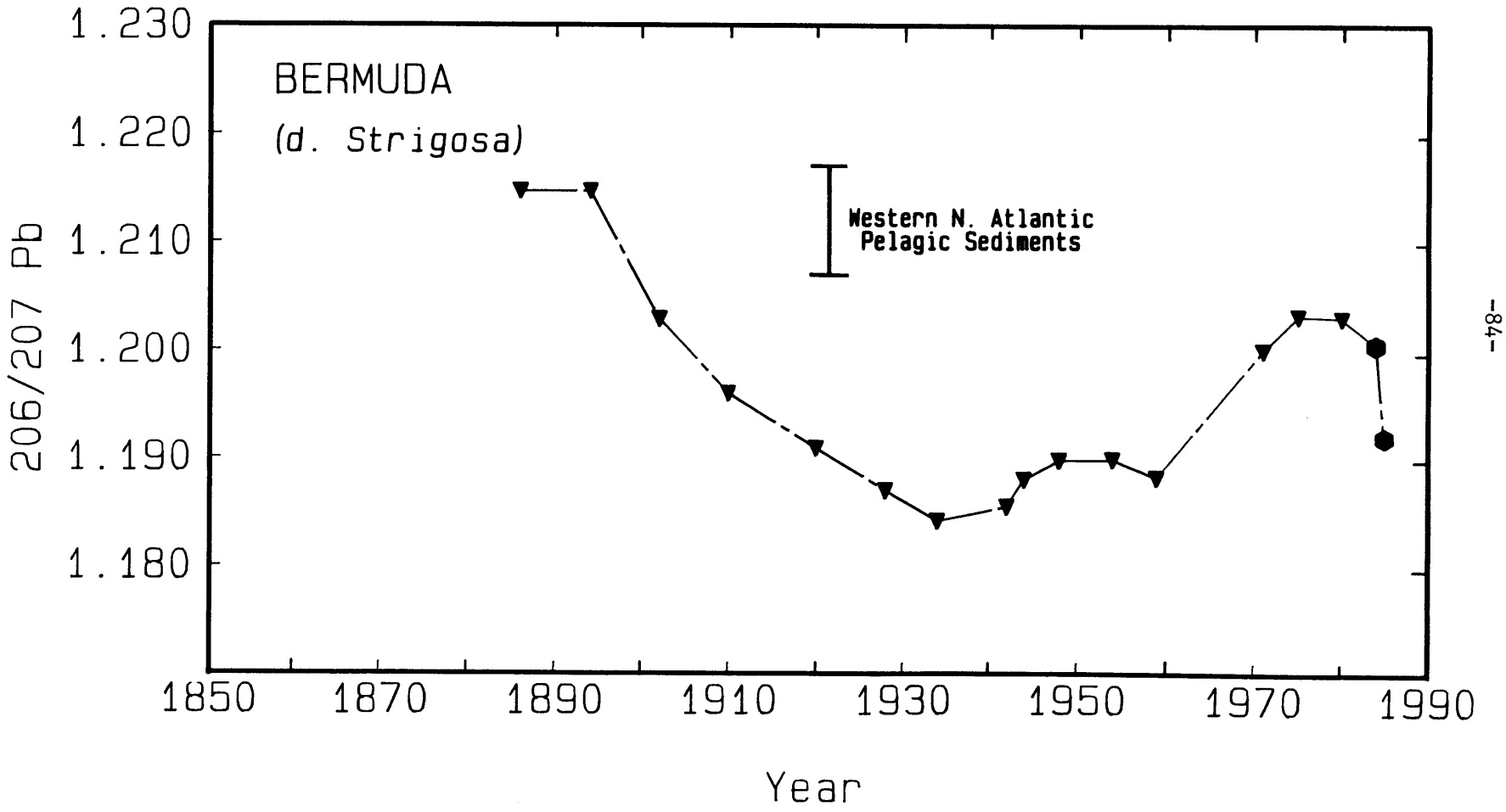
BERMUDA
(d. Strigosa)
Western N. Atlantic
Pelagic Sediments
206/207 Pb
1.230
1.220
1.210
1.200
1.190
1.180
1850
1870
1890
1910
1930
1950
1970
1990
Year

Figure 3.5 Skeletal Pb concentrations in M. annularis, Florida Straits. Annual determinations are in most cases, based on triplicate analyses or better. Error bars are 1σ.

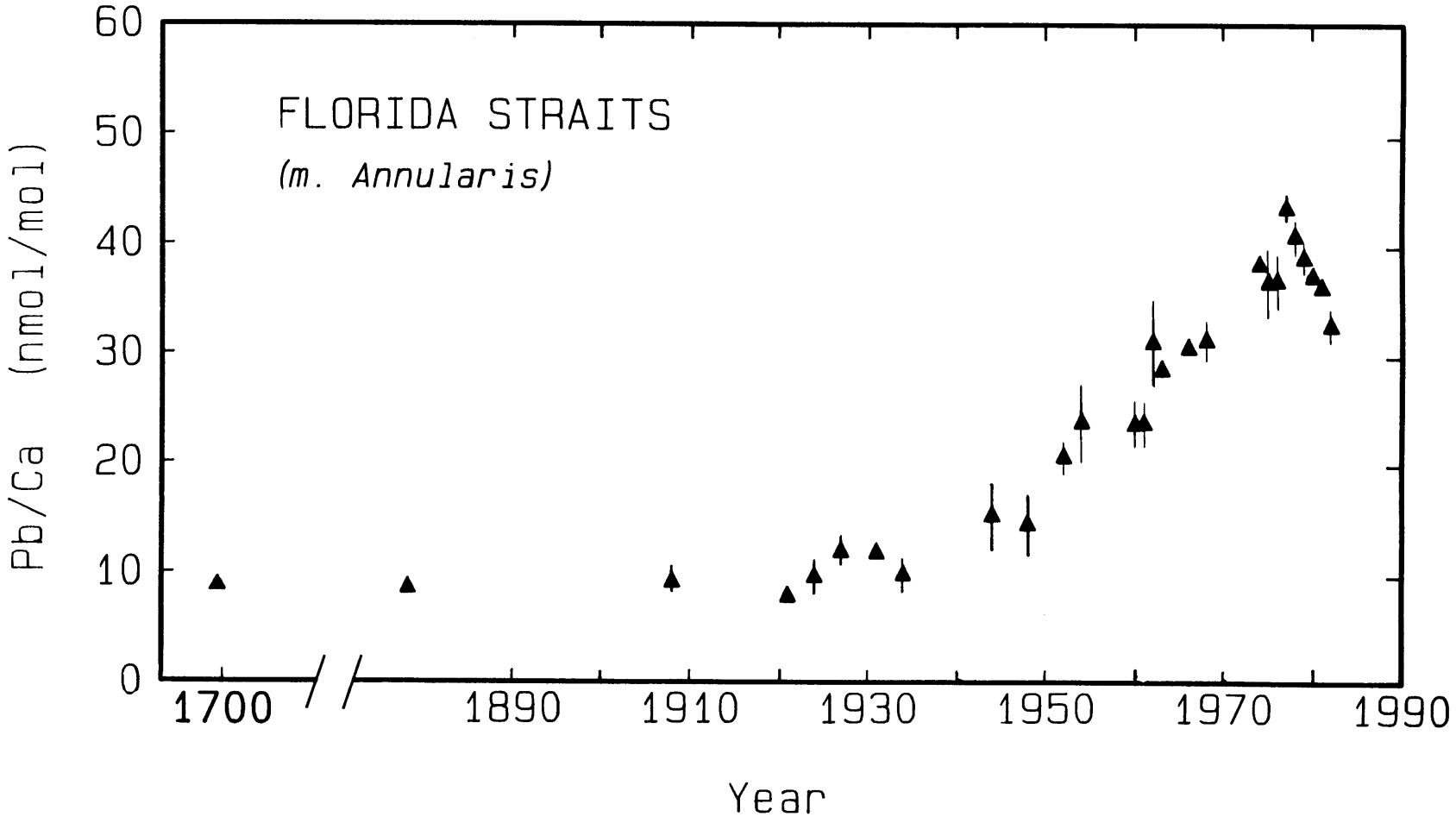
FLORIDA STRAITS
(m. Annularis)
Pb/Ca (nmol/mol)
60
50
40
30
20
10
0
1700
1890
1910
1930
1950
1970
1990
Year

Bermuda. For example, the turn of the century rise is absent as levels appear to have remained fixed at 10 nmol Pb/mol Ca back to the year 1698. Also, the post-World War II increase is moderated and the 1970's peak occurs several years later. Since Pb sources to the Florida Straits are borne by easterly winds and surface waters which have transited the Caribbean Sea, dissimilarities between records are expected. Heavy industrial emissions originating in the northeastern U.S. may play a lesser role in the Florida Straits, with greater representation of Pb aerosols from the southern U.S. and perhaps nations encircling the Caribbean. The existence of a peak in the coral record at 1977 has important implications. This maximum identifies the presence of U.S. emissions in the area since use of octane-boosting alkyl leads in Latin America and Caribbean nations has not been curtailed to the extent legislated in the U.S. More importantly, though, the timing of this maximum is 6 years delayed relative to the signal at Bermuda. If horizontal transport of a N. Atlantic source is responsible for this delay, this implies an average surface ocean recirculation velocity (assuming a 6000 km travel path from Bermuda, through the Antilles, and around the Caribbean) of 3.2 cm/sec. This is comparable to surface Ekman transport estimates and wind drift speeds observed in the center of the subtropical gyre (Sarmiento and Bryan, (32)). There are some qualifications to this interpretation, however. Pb is stripped from oligotrophic surface waters within three years, so a mixed layer source originating from northerly latitudes may be unrealistic. In addition, while subsurface waters (> 100 m) complete an anti-cyclonic trajectory through the Caribbean, the northern branch of the North Equatorial Current hinders southward passage of surface waters flowing from the north. Thus, if a portion of the Florida Straits signal is derived from long range horizontal transport, it must include Pb which has been mixed from deeper in the thermocline. The sill depths of the Anegada and Jungfern Passages separating the Caribbean from North Atlantic are sufficiently deep (1500-2000 m) to permit passage of thermocline waters containing longer-lived Pb (Dietrich, 1939).

Re-enrichment of surface waters may occur by mixing through the narrow passages of the Yucatan Channel and Florida Straits (sill depths shoal from 1600 to 800 m). Dilution of North Atlantic Pb by waters originating from the South Atlantic is probably of order 20-25% as estimated by Iselin (1936) based on T-S distributions in source waters and the Yucatan Channel. Additional insight can be drawn from data published by Dodge and Gilbert (1984) for a coral (also M. annularis) collected 1850 km southeast of Florida at St. Croix, U.S. Virgin Islands. Their 26-year record (1954-1980) at Buck Island (Fig. 3.6) shows a gradual rise from 10.3 nmol Pb/mol Ca in 1954 to a maximum of 24.5 nmol Pb/mol Ca in 1976; the Round Reef record is heavily influenced by sewage inputs and dredging activity. This maximum, which occurs between those recorded at Bermuda and the Florida Straits, appears to accord with a horizontally transported U.S. Pb source. The oldest concentration approaches the pre-industrial value measured in the Florida Straits. However, 1954 is relatively recent as far as industrial emissions are concerned, so an even lower pre-industrial value is likely for this location.

Since M. annularis from the Florida Straits was the first coral studied in this research program, supplementary chemical analyses were performed to ensure the validity of the Pb record. A detailed ^{210}Pb chronology (Fig. 3.7) affirmed that coral growth was continuous over at least the last century. More to the point, however, the uniform exponential disappearance of ^{210}Pb over time ($t_{1/2}$ = 24.3 yrs) indicates that ^{210}Pb uptake (and by analogy, stable Pb uptake) remained proportional to ambient dissolved concentrations of ^{210}Pb (and stable Pb). The weighted least squares intercept for 1982 (the collection year) of 14.7 dpm/100 g coral translates to a dissolved ^{210}Pb concentration of only 6.4 dpm/100, assuming K_D = 2.3. This is 2-3 times lower than typical western North Atlantic surface values. Evidently, advected ^{210}Pb must be scavenged en route to the Florida Straits.

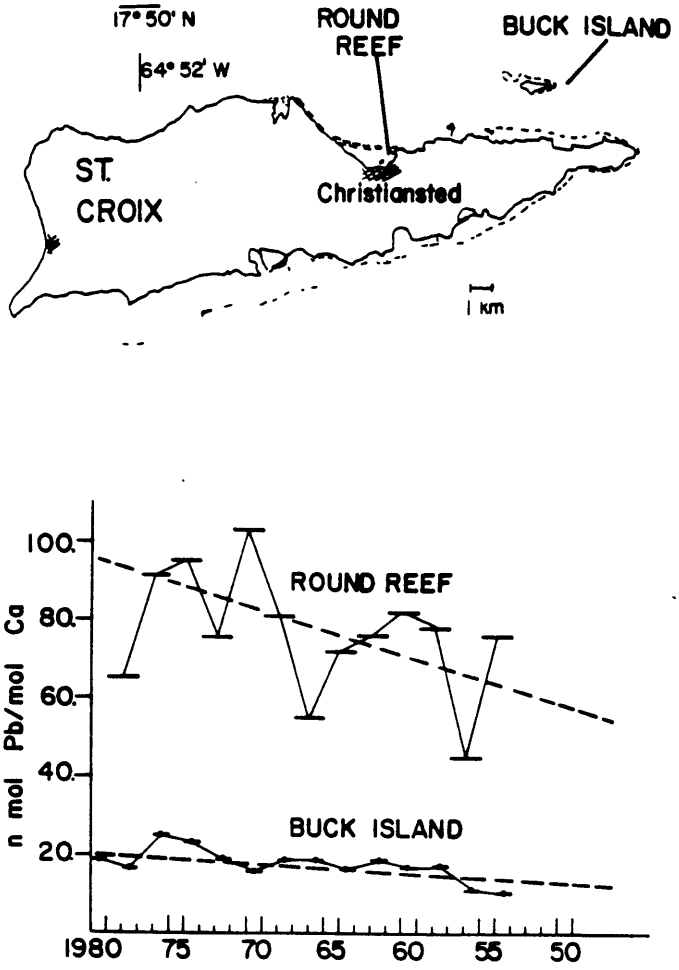

Figure 3.6 Skeletal Pb concentrations in two specimens of M. annularis from St.Croix, U.S. Virgin Islands (from Dodge and Gilbert, 1984).

Figure 3.7 Skeletal ^{210}Pb concentrations in M. annularis, Florida Straits. (unsupported ^{210}Pb in dpm/100 g coral)

Figure 3.8 Partial Pb isotopic histories for other sample sites. Left margin background ranges estimated from Chow and Patterson, 1962 and Sun, 1980. Right margin industrial emission data are from Flegal et al., 1984; Doe, 1970; and Fig. 3.4

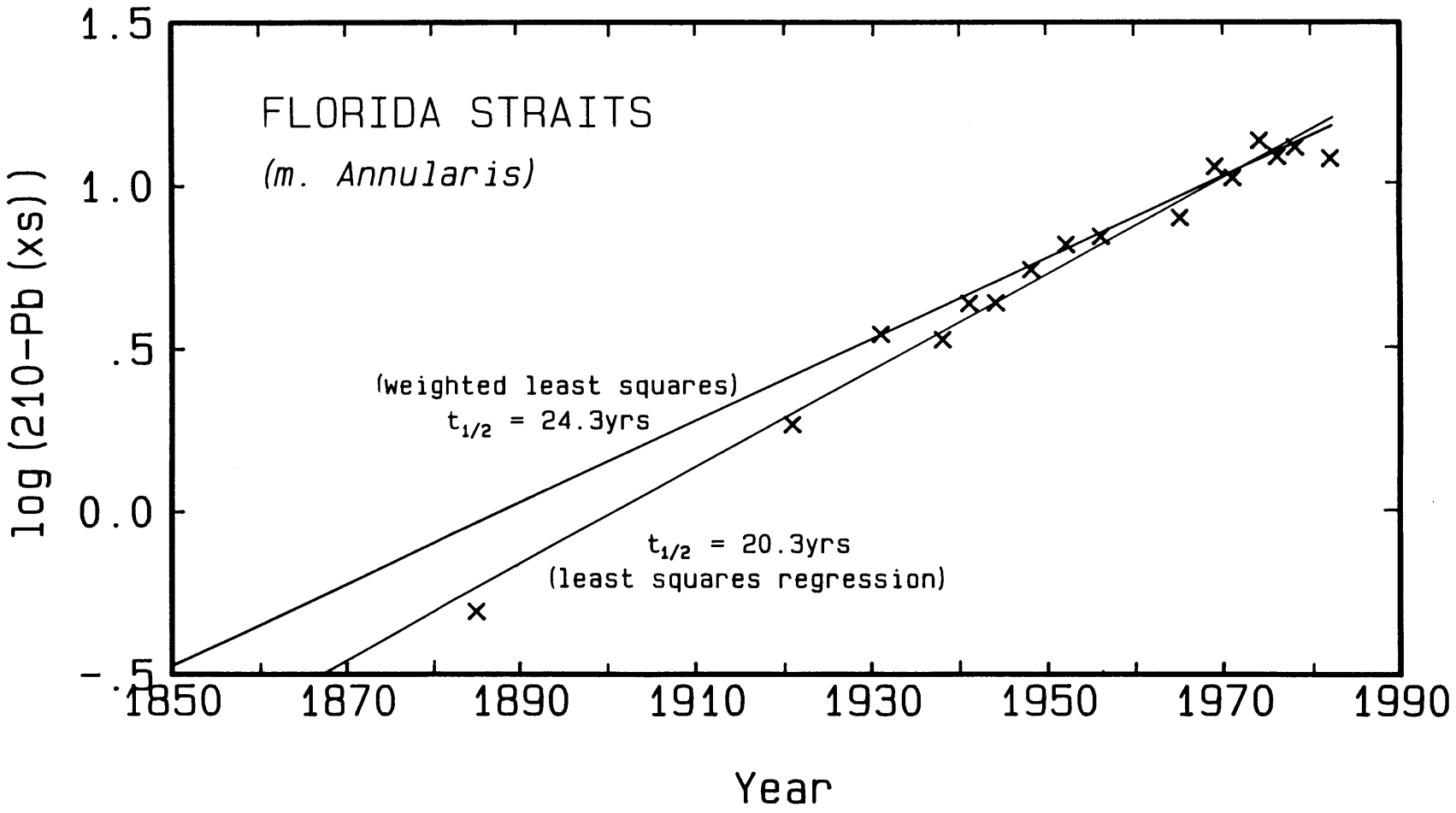
FLORIDA STRAITS
(m. Annularis)
log (210-Pb (xs))
1.5
1.0
.5
0.0
-.5
1850
1870
1890
1910
1930
1950
1970
1990
Year
(weighted least squares)
t1/2 = 24.3yrs
t1/2 = 20.3yrs
(least squares regression)

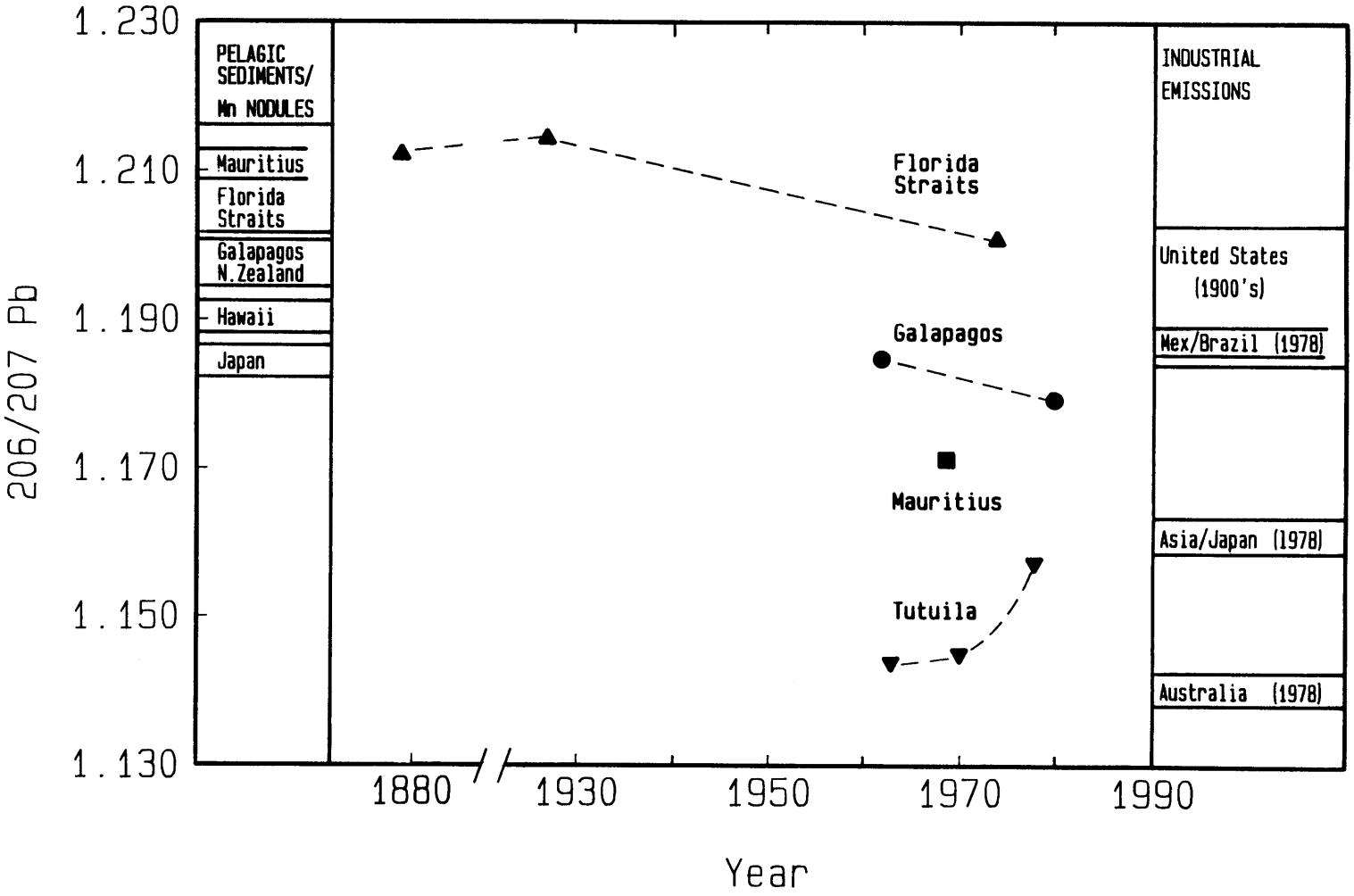
1.230
1.210
1.190
1.170
1.150
1.130
206/207 Pb
PELAGIC SEDIMENTS/ Mn NODULES
Mauritius
Florida Straits
Galapagos N.Zealand
Hawaii
Japan
Florida Straits
Galapagos
Mauritius
Tutuila
INDUSTRIAL EMISSIONS
United States (1900's)
Mex/Brazil (1978)
Asia/Japan (1978)
Australia (1978)
1880
1930
1950
1970
1990
Year

Additional uptake records of cadmium and a biochemical analogue of lead, barium, are described in Chapter 4.

Due to the difficulty of the measurement, only a partial stable Pb isotopic record has been completed for the Florida Straits (Fig. 3.8). The data suggest that as late as 1929, inputs of industrial Pb to these waters was minimal. This was also the turning point in the concentration record after which levels began to increase. The subsequent isotopic shift as indicated by the lone measurement at 1974 resembles that which occurred at Bermuda.

3.4 South Pacific and Indian Ocean

In comparing the above data with coral measurements from the more remote locations of Galapagos, Tutuila, Fiji, and Mauritius (Figs. 3.9 and 3.10), the tremendous influence of the United States as an industrial source can be appreciated. Skeletal Pb levels here do not exceed 15 nmol Pb/mol Ca. As a consequence of these lower levels, it is more difficult to ascertain historic patterns. This problem is compounded by the scarcity of old sample cores from these outlying regions. The single determination from Fiji (4.1 ± 0.4 nmol Pb/mol Ca) points out a possible tripling or more of Pb between 1920 and 1960 in tropical reef waters of the central South Pacific. Despite the overall low levels of Pb encountered, however, concerns regarding island influences on these remotely situated corals are addressed in the next section. The Indian Ocean specimen from Mauritius was too young to furnish a useful time series, but contemporary concentrations are roughly half those found in the South Pacific. Occasional unusually high values, particularly among recent coral bands (e.g. Mauritius, Galapagos, Bermuda (see Appendix - Table A.1)), are probably a result of a refractory contaminant Pb phase as described earlier.

As for the Florida Straits, only partial stable Pb isotopic records are presented for the Pacific and Indian Ocean corals (Fig. 3.8). The results thus far concur with a global blanketing of industrial Pb.

Figure 3.9 Skeletal Pb concentrations in P. clavus from the Galapagos Islands. Annual determinations are based on triplicate analyses. Error bars are 1σ.

Figure 3.10 Skeletal Pb concentrations in corals from Tutuila (H. microconos), Mauritius (P. rustica), and Fiji (P. rustica). Annual determinations are based on triplicate analyses. Error bars are 1σ.

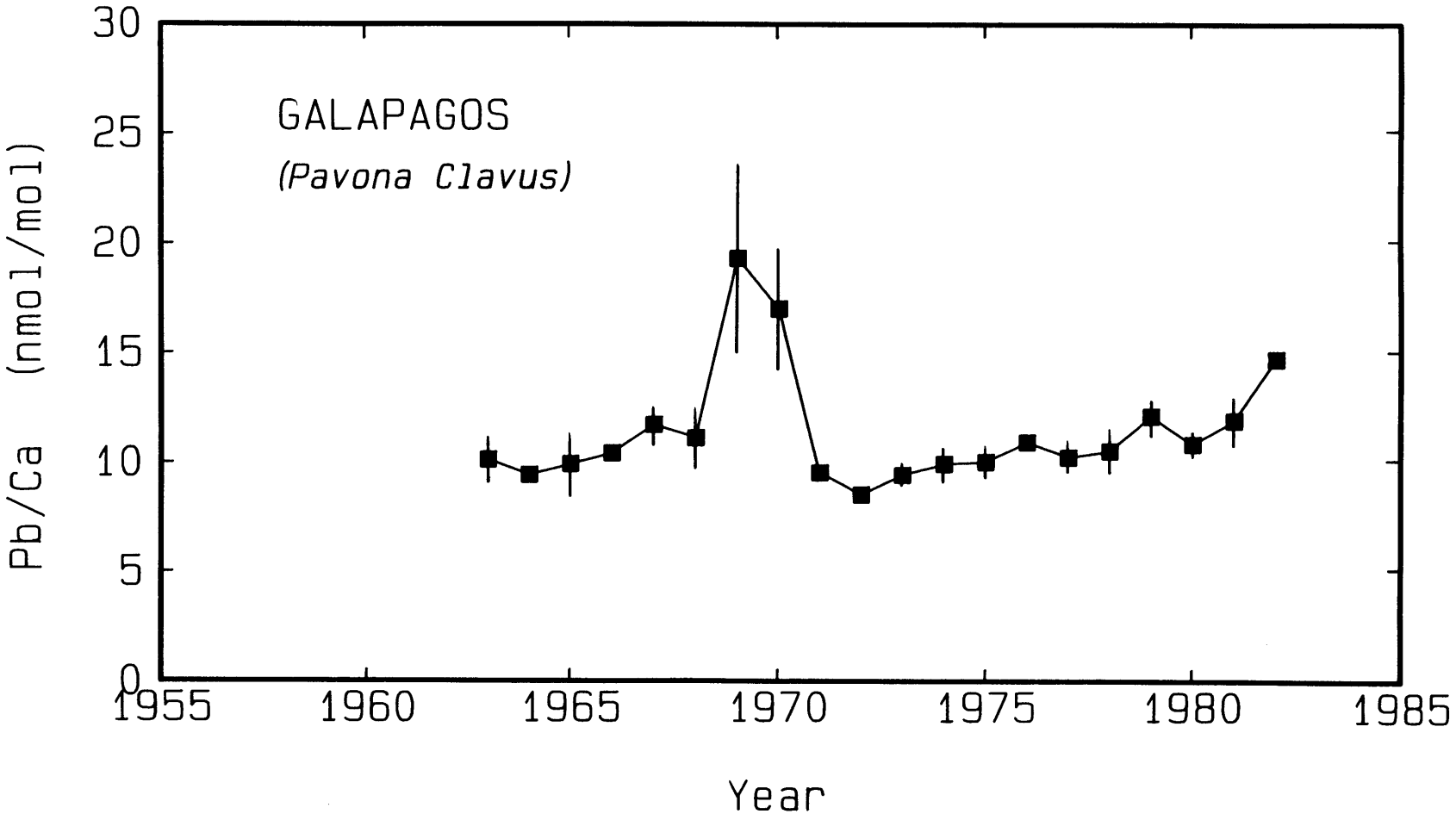
GALAPAGOS
(Pavona Clavus)
Pb/Ca (nmol/mol)
30
25
20
15
10
5
0
1955
1960
1965
1970
1975
1980
1985
Year

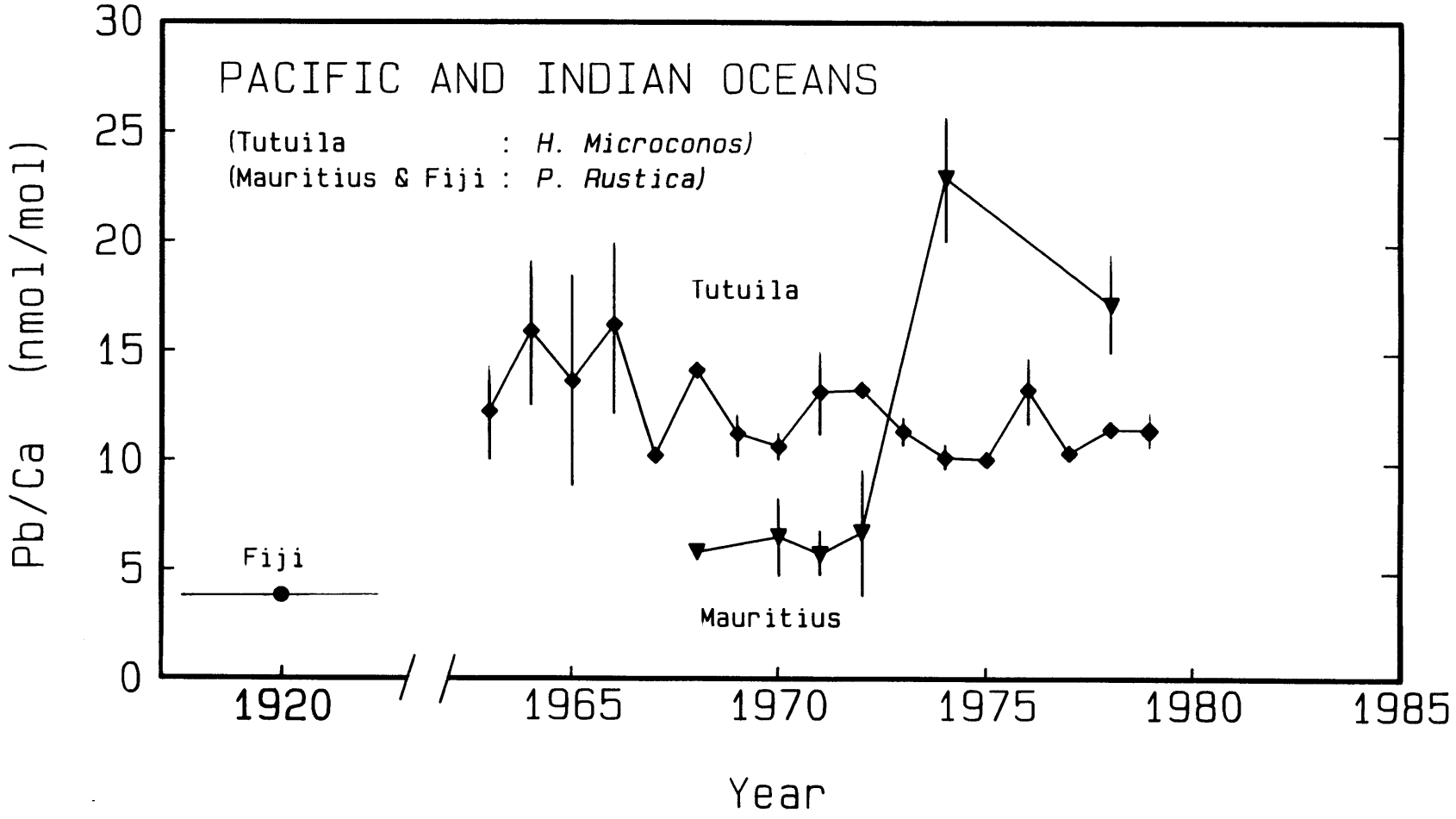
PACIFIC AND INDIAN OCEANS
(Tutuila : H. Microconos)
(Mauritius & Fiji : P. Rustica)
Tutuila
Fiji
Mauritius
Pb/Ca (nmol/mol)
Year
0
5
10
15
20
25
30
1920
1965
1970
1975
1980
1985

Anthropogenic influence in these remote regions is more reliably identified via isotopic shifts than by concentration anomalies because exact pre-anthropogenic concentrations are as yet unknown. For example, the waters around Mauritius are clearly industrially influenced, despite very low skeletal lead levels in P. rustica. The magnitude of these perturbations cannot be assessed from Pb isotopes until historic source signatures have been better characterized. Point determinations in time of industrial emission signatures shown in the right margin of Fig. 3.8 only indicate that the measured departures from background are in the expected directions. The Tutuila record displays a curious trend away from Broken Hill-type (Australian) Pb in recent years, which appears to be supported by a single surface water measurement ($^{206/207}$Pb=1.176) by Flegal and Patterson (1984) at 15°0'S, 150°0'W in January, 1980. Introduction of unleaded fuels in Australia over the last several years, however, has been too recent to account for the isotopic shift. Also, the coral Pb concentration record from Tutuila (Fig. 3.10) shows no concomitant change. A large-scale conversion in ore useage either regionally or locally may be responsible.

3.5 A Survey of ^{210}Pb in Corals

Though a shortage of site-specific dissolved Pb measurements precludes additional estimates of stable Pb distribution coefficients for the above corals, amassed ^{210}Pb data are more plentiful. Citing open ocean values from the literature, a suite of ^{210}Pb-based estimates of K_D is reported in Table 3.2. It is immediately evident that these estimates are consistently higher than the value based on stable Pb in Bermuda (K_D = 2.3). This is true even for several specimens from North Rock, Bermuda (including the one analyzed in Fig. 3.1) for which an accurate dissolved ^{210}Pb concentration can be deduced from seasonal measurements. Most of these inconsistencies are explainable.

Table 3.2 Estimated lead distribution coefficients for various corals based on ^{210}Pb

Location	Genus/Species	Initial Unsupported ^{210}Pb (dpm/100 g coral)	Observed Surface ^{210}Pb (dpm/100 l)	Reference	Implied K_D
North Atlantic					
Bermuda	D. strigosa	56	19.7 ± 3.4 (n = 5)	(a)	2.8
Bermuda	D. labyrinthiformis	63	"		3.2
Bermuda	M. annularis	65	"		3.3
Florida Straits	M. annularis	15	?		?
North Pacific					
Eniwetak	F. speciosa	75	13	(b)	5.8
Lisianski	P. lobata	69	20	(c)	3.4
Equatorial Pacific					
Galapagos	P. clavus	33	9	(d)	3.7
South Pacific					
Tutuila	H. microconos	30	10-11	(e)	2.8
Heron Island	P. lobata	18	7.6	(e)	2.4
Indian					
Mauritius	P. rustica	32	9-11	(f)	3.2

References:

(a) Boyle et al., 1986 (b) Nozaki and Tsunogai, 1973 (c) Nozaki et al, 1976 (d) Thomson and Turekian, 1976 (e) Tsunogai and Nozaki, 1971 (f) Cochran et al, 1984

In the case of the Bermuda corals where convergence with the stable Pb result is most expected, the discrepancy is likely due to two factors. First, ^{210}Pb was determined from whole coral crushings while stable Pb analyses were performed only on the consolidated trabeculae of the Diploria corals. Attempts to determine stable Pb on coral fragments which included smaller septal trabeculae and synapticula (low-density, high surface area structures), resulted in a +10-20 nmol Pb/mol Ca offset marked by very poor reproducibility (section 2.2.6). This extraneous Pb amounts to approximately 30% of the true lattice-bound Pb pool. If ^{210}Pb is distributed similarly to stable Pb as one might expect, this would effectively explain the difference in calculated distribution coefficients. The second explanation is the less stringent cleaning protocol adopted for ^{210}Pb assay compared with the stable Pb procedure (the initial assumption having been that in the absence of handling contamination for ^{210}Pb, natural contaminants would constitute a small easily removed component). Coupled with a sample bias toward very young bands (which are often difficult to clean), these natural contaminants are probably also responsible for part of the K_D inconsistency. M. annularis would have been especially susceptible to a cleaning/age bias since only two bands were analyzed, and these were only 2.5 and 6.5 years old.

As far as any of the Pacific and Indian Ocean K_D estimates are concerned, it is first necessary to point out that the cited dissolved ^{210}Pb measurements represent single season determinations of waters in the general vicinity of the sampled coral reefs. Sargasso Sea surface ^{210}Pb concentrations have been observed to change by as much as 50% in three months, depending on rainfall and mixed layer integrity (Boyle et al., 1986). A small bias may actually be transmitted to the coral record through the interplay of seasonal surface water variation and skeletal mass accumulation. However, since coral growth is known to be continuous (Buddemeier, 1974) and seasonal band width and density generally vary inversely (Dodge and Brass, 1984; Dodge and Thomson,

1974), the effect of seasonally-dependent accretion is probably limited to only a few percent. Apart from the possibility of applying a non-representative surface water ^{210}Pb concentration in calculating K_D, it should also be noted that neither of the two North Pacific corals in Table 3.2 produced useable stable Pb data. If this was a consequence of unfavorable morphology rather than poor sample storage, (a strong possibility in the cases of Porites and Favia speciosa), the ^{210}Pb results may also be suspect and should be considered as upper limits. In the Galapagos Islands case, the coral measurements are probably not so much at fault as the choice of a surface water ^{210}Pb value. Eastern Equatorial Pacific waters are distinguished by variable upwelling and associated high and low productivity and scavenging regimes. The only surface water ^{210}Pb measurements available in the area are from the Peru Basin at 11°S (9.1 dpm/100 kg) and 19°S (3.0 dpm/100 kg), non-upwelling and upwelling locations, respectively (Thomson and Turekian, 1976). Although coral cadmium measurements indicate that the Galapagos site at San Cristobal Island is nutrient enriched by upwelling (section 4.2), a relatively high dissolved ^{210}Pb concentration (>11 dpm/100 kg) is required to yield $K_D < 3.0$. This condition would depart from the conclusion reached by Thomson and Turekian that high productivity zones exhibit depleted ^{210}Pb relative to parent ^{226}Ra, particularly in surface waters. With regard to the remaining cases, discrepancies between ^{210}Pb and stable Pb K_D's appear small or attributable to mechanisms previously discussed.

In view of the above discussion, the actual range of Pb distribution coefficients exhibited by eight species (seven genera) is probably very small, perhaps 2.3 - 3.0. This is a desirable outcome in that coral Pb measurements can be interpreted directly, without the need to normalize according to genus as in the case of ^{18}O coral paleothermometers (Weber and Woodhead, 1972).

If one accepts, tentatively, a minor K_D dependence on genus, plots such as those depicted in Fig. 3.11 can be constructed giving surface ocean Pb concentrations at any site, at any time in the past. The 1984 reconstructions appear reasonable in light of SEAREX and WATOX atmospheric fluxes (Settle and Patterson, 1982; Church et al., 1984), but a pair of surface water measurements near American Samoa of 17 and 21 pM by Flegal and Patterson (1983) suggests that the Tutuila coral may have been subject to island influences. On the 'pre-industrial' plot, the 1920±5 Fiji coral determination (4.1 ± 0.4 nmol Pb/mol Ca) translates to a surface water dissolved Pb value of 16-19 pM (12-15 pM if K_D = 3.0), which may be slightly high if one accepts the South Pacific seawater data and a strong anthropogenic invasion to this region since 1920. Mass spectrometric measurements of the same coral sample (acid leached to 40% of initial mass) have yielded a Pb concentration of 4.4 nmol/mol Ca, confirming our own results (J. Chen - C.I.T., personal communication). If Flegal and Patterson are indeed correct in arguing a maximum pre-industrial Pacific surface water concentration of about 10 pM, then nearshore resuspended Pb must be invoked as the source of the coral offset. By analogy to Bermuda, however, dissolved Pb anomalies 2.5 kilometers away from Fiji are expected to be small. Therefore, the South Pacific prehistoric surface water Pb concentration was probably not much lower than 10 pM.

In contrast to the South Pacific, surface waters of the Florida Straits remained near 38 pM throughout the 18th and 19th centuries. Presumably, this is a reflection of the importance of shelf and/or resuspended Pb in the waters overlying this coral reef.

3.6 Conclusions

(1) This survey of stable Pb and Pb isotopes in corals from four major ocean basins confirms by independent means, the anthropogenic

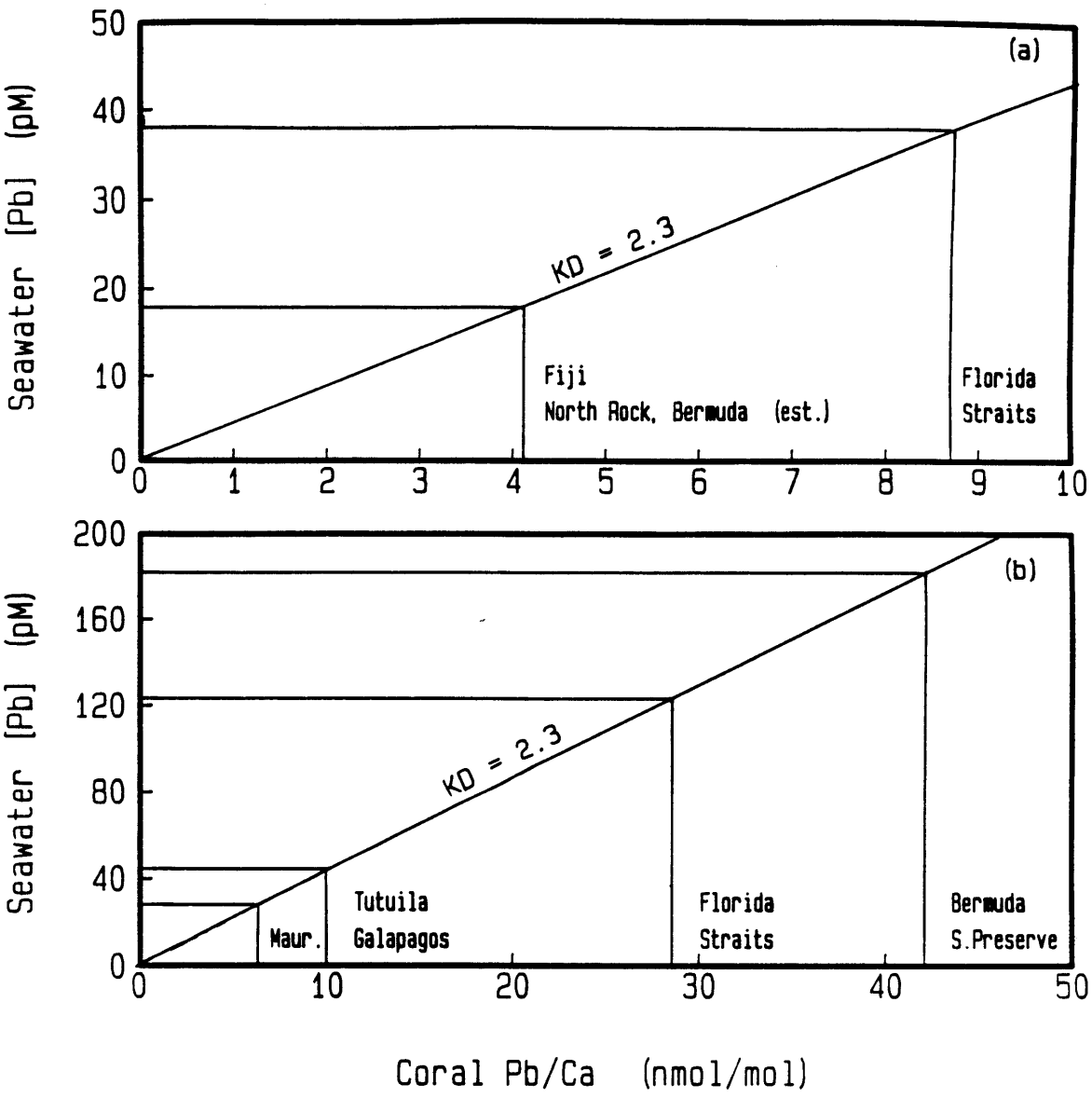

Figure 3.11 Reconstructed dissolved lead concentrations in surface seawater corresponding to various coral sampling sites based on K_D = 2.3 for (a) pre-industrial time and (b) 1984.

nature of Pb found throughout the surface ocean today, and over the past century.

(2) Constancy of replicate measurements, consistency of temporal and regional response to industrial fluxes, low background concentrations, and comparison to other trace substituents of aragonite, support direct lattice substitution of Pb. A Bermuda-based coral:seawater Pb distribution coefficient of 2.3 is estimated for the species, Diploria strigosa. K_D dependence on species and genus is estimated to be small (estimated range = 2.3-3.0) based on similarity of ^{210}Pb-based K_D estimates and plausibility of inferred seawater dissolved Pb concentrations.

(3) In view of the above conclusions, historic surface ocean conditions may be reconstructed as follows:

In Sargasso Sea surface waters, the pre-anthropogenic dissolved Pb concentration was probably between 15-20 pM ($^{206/207}Pb$=1.215). This value rose to near 90 pM in the 1920's as a result of the American industrial revolution ($^{206/207}Pb$=1.184-1.190). Subsequent combustion of alkyl leads pushed the surface value to a maximum of 240 pM in 1971 ($^{206/207}Pb$=1.202). A one-year time lag between this maximum and peak U.S. alkyl Pb combustion in 1970 is a reflection of the brief mixed layer residence time of Pb. Since then, phasing-out of leaded gasoline has caused a precipitous return to near post-industrial revolution levels ($^{206/207}Pb$=1.186)

The Florida Straits maintained a fluvial/shelf supported surface water concentration of 38 pM Pb until about 1930. Levels grew gradually to a peak of near 190 pM in 1977, followed by a decline to 142 pM in 1982. Relative to the Bermuda records, the Florida coral lacks a strong industrial revolution signal, and exhibits a moderated post-WW II Pb increase and later maximum. These patterns reflect dilution of U.S. Pb sources and delayed response due to long-range horizontal transport.

In the South Pacific, a single coral measurement from Fiji (1920±5 yrs) suggests a pre-industrial surface water Pb concentration of 16-19 pM (12-15 pM if K_D = 3.0). Although coastal resuspended Pb may have biased this result, such a contribution is expected to be small. Therefore, South Pacific pre-industrial waters were probably not much lower than 12 pM Pb. Recent corals from Tutuila and Galapagos imply higher concentrations of 40-50 pM resulting from regional industrial influence and possible local effects.

The coral from Mauritius was too young to furnish historical perspective, but contemporary surface water Pb values are estimated at 25-29 pM. The Pb isotopic signature of this coral is clearly indicative of anthropogenic perturbation.

(4) A survey of near and inshore waters around Bermuda suggests the following general trace-element sampling strategies for remotely situated islands. Unless local pollutant signals are the study object, enclosed and partially enclosed waterways must always be avoided. Coastal sampling is prone to resuspension effects which cause elevated dissolved and particulate concentrations of Pb. The limits of these anomalies will vary from island to island, but the Bermuda results suggest that 2.5 km is probably a safe minimum sampling distance with respect to dissolved Pb concentrations.

(5) The paleo-chemical recording capability of corals offers a sensitive means of reconstructing historic Pb fluxes and isotopic labels to the temperate/tropical ocean. Future transport modeling of Pb in the ocean can be based on such reconstructions of regional Pb transients.

3.7 Appendices

3.7.1 Island influences

Lead of local origin may influence coral-based reconstructions via habitat pollution or dissolved-particulate interactions in waters overlying reefs. Coastal Pb pollution resulting from urban effluents and mine tailings run-off has been documented by Patterson et al. (1976), Stukas and Wong (1981), and Bruland et al. (1974) among others. A survey of Bermudian waterways (Fig. 3.12) reveals that neither large populations nor heavy industries are required to grossly contaminate inshore surface waters. The progression in dissolved Pb concentrations from well-flushed coastal zones to urban Hamilton Harbor yields values 1.5 to 20 times open ocean concentrations. A similar situation can be inferred for St. Croix, U.S. Virgin Islands from coral analyses of Dodge and Gilbert (1984). Particulate Pb in nearshore waters can also be observed in Fig. 3.12 to account for up to 85% of the total measured Pb. This contrasts with levels of 10% or less encountered in the open ocean (Flegal and Patterson, 1983; Bacon et al., 1976).

In the coastal zone of Bermuda, an interesting phenomenon is revealed by seasonal seawater measurements and comparison of the two Bermuda coral Pb records. Point "A" on Fig. 3.12 represents four separate water samplings accumulated over three different seasons from 6/83 - 6/84. The average dissolved Pb concentration here shows little seasonal variation and amounts to 198 $\pm$ 15 pM as compared to a seasonally-averaged oceanic value of 128 pM for 1984. The Southern Reef Preserve coral of Fig. 3.1 was captured only two km east of Point "A" in similar waters. The constant skeletal Pb offset (approx. 10 nmol Pb/mol Ca) exhibited relative to the North Rock specimen suggests that the elevated dissolved Pb concentration is sustained by the high particulate Pb burden in nearshore waters. Additionally, absence of seasonality in the dissolved Pb measurements at Point A suggests that the suspended Pb

Figure 3.12 Total and dissolved (<0.4 um) lead in waterways and coastal areas around Bermuda, (April, 1984). Four samplings at Point 'A' spanned 6/83 - 6/84; see Table 3.1.

Figure 3.13 Local transect seawater Pb data heading from Bermuda toward:

(a) North Rock (April 13,1984)
(b) Station 'S' (Panulirus Station)(0-3 miles: June 12, 1984; 3-7 miles: December 11, 1984)

Dashed lines depict dissolved Pb concentrations measured at Station 'S' (50 km southeast of Bermuda) during the same time periods.

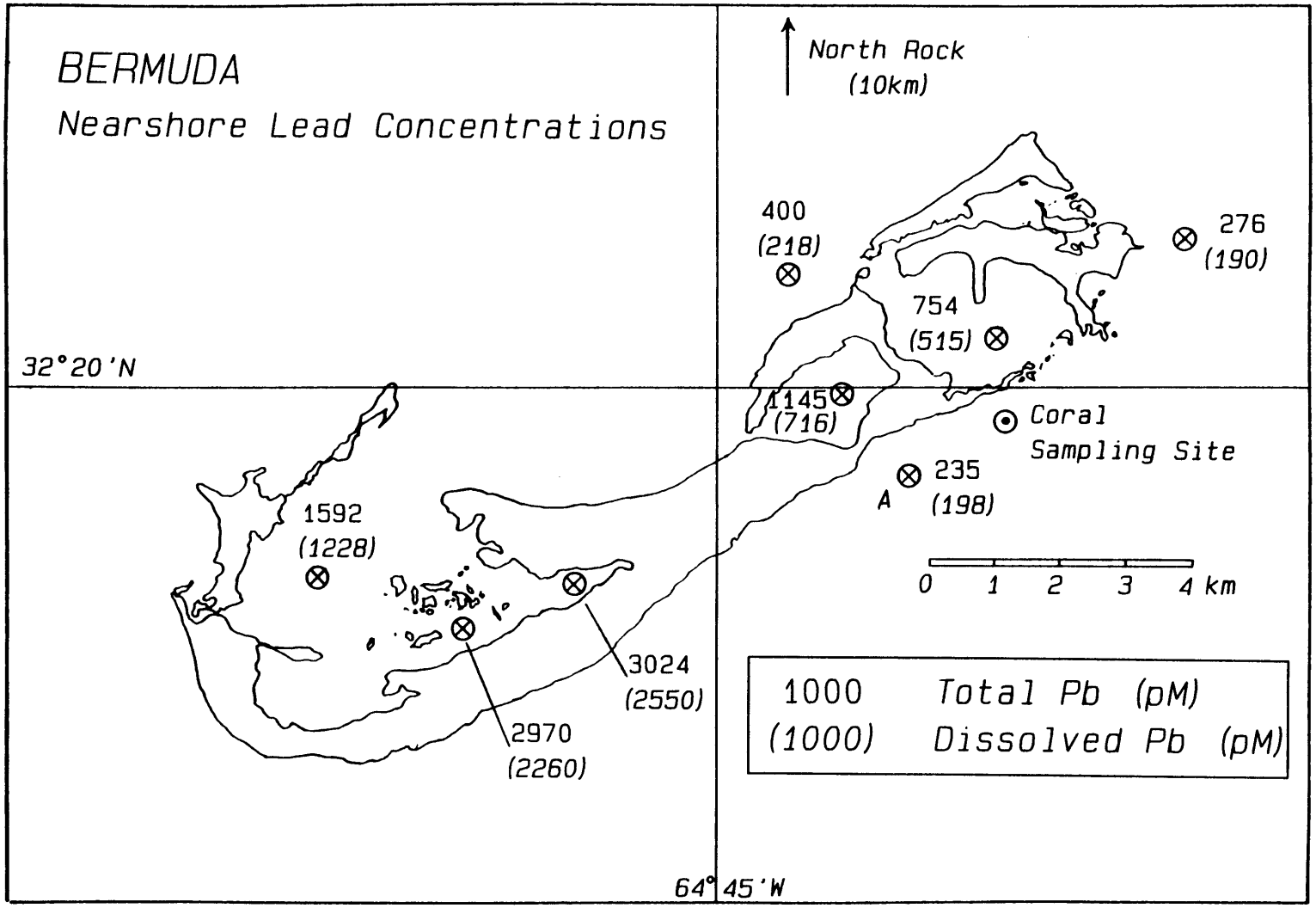
BERMUDA
Nearshore Lead Concentrations
North Rock
(10km)
400
(218)
276
(190)
754
(515)
32°20'N
1145
(716)
Coral
Sampling Site
235
(198)
A
1592
(1228)
0 1 2 3 4 km
3024
(2550)
2970
(2260)
1000 Total Pb (pM)
(1000) Dissolved Pb (pM)
64°45'W

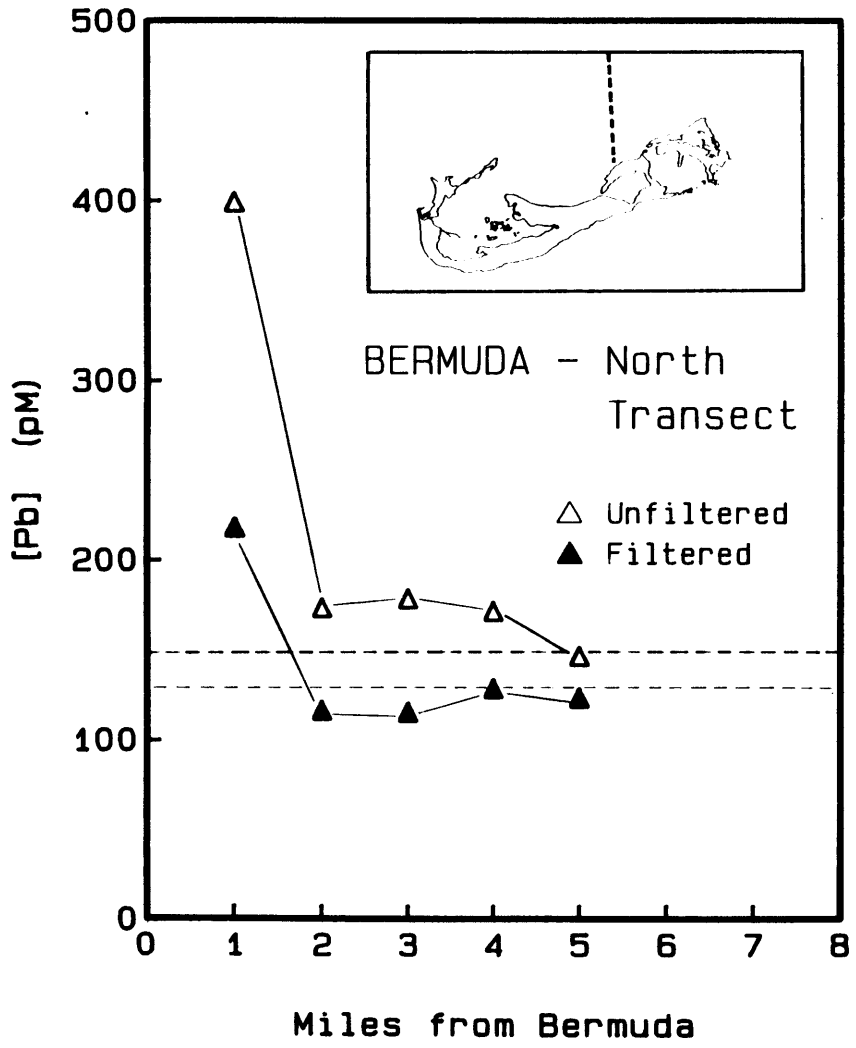
500
400
300
200
100
0
[Pb] (pM)
0 1 2 3 4 5 6 7 8
Miles from Bermuda
BERMUDA - North
Transect
Unfiltered
Filtered

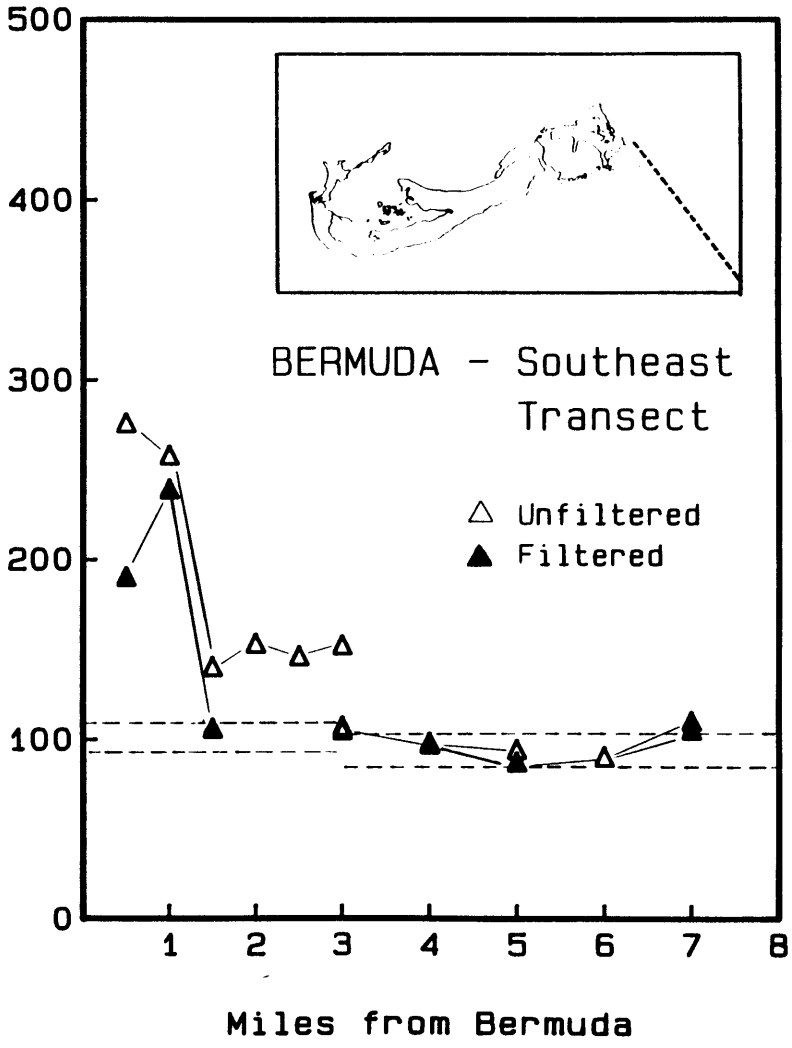
500
400
300
200
100
0
1 2 3 4 5 6 7 8
Miles from Bermuda
BERMUDA - Southeast
Transect
Unfiltered
Filtered

inventory acts to buffer the dissolved Pb concentration. The extent of this coastal effect was assessed in two transects heading away from Bermuda (Fig. 3.13). The first transect was directed toward North Rock, 9 miles north of the island. The second transect headed southeast toward Station 'S' (formerly known as the Panulirus Station), 20 miles away, where the bulk of our hydrographic work is done (Boyle et al., 1986). The results show convergence of total Pb concentrations to prevailing ocean values within 5 miles from shore. Dissolved Pb, the more relevant measure in terms of coral Pb uptake, appears to stabilize within 1.5 miles from the island. Given that Bermuda is well-populated by remote island standards, a 1.5 mile coral sampling boundary seems a reasonable rule for future collections targeted for trace elements. Seawater samples collected within 5 miles must be filtered before analysis in order to assess ambient dissolved Pb concentrations.

3.7.2 The lead distribution coefficient in aragonite

The standard means of expressing an enrichment or depletion of a lattice-bound element relative to seawater is embodied in the distribution coefficient K_D:

$$K_D = \frac{([M]/[Ca])_{lattice}}{([M]/[Ca])_{seawater}} \qquad (1)$$

Earlier, it was established by means of stable lead and ^{210}Pb-based distribution coefficients that corals discriminate mildly in favor of Pb over Ca during skeletogenesis. A thermodynamic basis for this preference can be invoked if the solid solution behavior of $PbCO_3$ (cerrusite) and aragonite are examined. Both of these mineral phases generally occur in near end-member composition, but limited solid solution of $PbCO_3$ with $CaCO_3$ (up to 3 mole %) has been reported (Speer, 1983). The equilibrium constant for Pb substitution in aragonite

$$CaCO_3(s) + Pb^{2+} \longleftrightarrow PbCO_3(s) + Ca^{2+} \quad (2)$$

$$K = \frac{X_{PbCO3}\ f_{PbCO3}}{X_{CaCO3}\ f_{CaCO3}} \cdot \frac{[Ca^{2+}]\ f_{Ca^{2+}}}{[Pb^{2+}]\ f_{Pb^{2+}}} \quad (3)$$

is equivalent to equation (1) if the ratios of solid and aqueous phase total activity coefficients (including species complexing) are equal to unity. In this case, K_D is given simply by the ratio of $CaCO_3$ (aragonite) and $PbCO_3$ solubility products in surface seawater. Since K_{sp} (aragonite) in surface seawater (25°C) is reported by Morse et al. (1980) as $10^{-6.18}$ mol^2/kg^2, and K_{sp} ($PbCO_3$) ($10^{-13.1}$ mol^2/kg^2 @ 25°C - Smith and Martell, 1976) can be corrected for seawater ionic strength by the Davies equation to give $10^{-11.8}$ mol^2/kg^2, a theoretical K_D of 4 x 10^5 results. While Ca^{2+} and Pb^{2+} activity coefficients are expected to be similar ($\approx$ 0.23), however, species complexing for the two elements are very different. Garrels and Thompson (1962) calculated that 91% of dissolved Ca in seawater exists as the free Ca^{+2} ion. In contrast, CO_3^{2-} and Cl^- complexing of Pb reduces the free Pb^{2+} concentration to only about 3% of the total Pb (Turner et al., 1983). Thus, the effect of differential ion-association is to decrease K_D to about 10^4. This value, nearly 6,000 times higher than the observed K_D resulting from biogenic precipitation of aragonite, suggests that the activity coefficient of the solid solute, f_{PbCO3} must be very high -- i.e. near 6,000. A simple laboratory experiment demonstrated that inorganic precipitation of aragonite gives results similar to coral-mediated precipitation. Clean seawater was spiked to a Pb concentration of 8.2 nM, seeded with a few clean coral crystals, and allowed to precipitate at 60°C for one month. Two such solutions were then filtered and the precipitates immersed in 0.1N HNO_3 to dissolve only the new crystal growth surrounding the coral seeds. Due to uncertainties stemming from adsorption of Pb onto container walls, the experimental K_D ranged from

20 - 35; about an order of magnitude higher than the coral-based K_D. Part of the enhanced discrimination for Pb is likely due to increased precipitation rate induced by the higher temperature and presence of seed crystals, as described by Lorens (1981) for Sr precipitation in calcite. The experimental result, nonetheless, generally supports preferential uptake of Pb over Ca during aragonite precipitation.

References

Bacon, M.P., D.W. Spencer, and P.G. Brewer (1976). $^{210}Pb/^{226}Ra$ and $^{210}Po/^{210}Pb$ disequilibrium in seawater and suspended particulate matter, Earth Planet. Sci. Lett. 32: 277-296.

Boyle, E.A. and J.M. Edmond (1975). Determination of trace metals in aqueous solution by APDC chelate co-precipitation. In: Advances in Chemistry, Vol. 147, pp. 44-55, American Chemical Society, Washington, D.C.

Boyle, E.A. and J.M. Edmond (1977). Determination of copper, nickel and cadmium in seawater by APDC chelate coprecipitation and flameless atomic absorption spectrometry, Anal. Chim. Acta 91: 189-197.

Boyle, E.A., S.D. Chapnick, G.T. Shen and M.P. Bacon (1986). Temporal variability of lead in the western North Atlantic Ocean, Geochim. Cosmochim. Acta. 91: 8573-8593.

Brown, J.S. (1965). Oceanic lead isotopes and ore genesis, Econ. Geol. 66: 47-68.

Bruland, K.W., K. Bertine, M. Koide, and E.D. Goldberg (1974). History of metal pollution in southern California coastal zone, Environ. Sci. Technol. 8: 425-432.

Buddemeier, R.W. (1974). Environmental controls over annual and lunar monthly cycles in hermatypic coral calcification, In: Proc. 2nd Int. Coral Reef Symposium, Vol. 2, pp. 259-267, Brisbane.

Buddemeier, R.W., J.E. Maragos, and D.W. Knutson (1974). Radiographic studies of reef coral exoskeletons: rates and patterns of coral growth, J. Exp. Mar. Biol. Ecol. 14: 177-200.

Bureau of the Census of the U.S. Department of Commerce. The Statistical History of the United States from Colonial Times to the Present, Vol. 1965 - 1984, Fairfield Publishers, Inc., Stanford, Conn.

Chow, T.J. and C.C. Patterson (1962). The occurrence and significance of lead isotopes in pelagic sediments, Geochim. Cosmochim. Acta 26: 263-308.

Chow, T.J. and J.L. Earl (1972). Lead isotopes in North American coals, Science 176: 510-511.

Church, T.M., J.M. Tramontano, J.R. Scudlark, T.D. Jickells, J.J. Tokos, A.H. Knap, and J.N. Galloway (1984). The wet deposition of trace metals to the coastal and western Atlantic Ocean, Atmos. Environ. 18: 2657-2664.

Cochran, J.K., M.P. Bacon, S. Krishnaswami, and K.K. Turekian (1984). ^{210}Po and ^{210}Pb distributions in the central and eastern Indian Ocean, Earth Planet. Sci. Lett. 65: 433-452.

Dietrich, G. (1939). Das Amerikanische Mittelmeer, Gesellsch.f.Erdkunde zu Berlin, Zeitschr., p.108-130.

Dodge, R.E. and J. Thompson (1974). The natural radiochemical and growth records in contemporary hermatypic corals from the Atlantic and Caribbean, Earth Planet. Sci. Lett. 23: 313-322.

Dodge, R.E. and G.W. Brass (1984). Skeletal extension, density and calcification of the reef coral, Montastrea annularis: St. Croix, U.S. Virgin Islands, Bull. Mar. Sci. 34: 288-307.

Dodge, R.E. and T.R. Gilbert (1984). Chronology of lead pollution contained in banded coral skeletons, Mar. Biol. 82: 9-13.

Doe, B.R. (1970). Lead Isotopes, Springer Verlag, New York.

Druffel, E.M. and T.W. Linick (1978). Radiocarbon in annual coral rings of Florida, Geophys. Res. Lett. 5: 913-916.

Emiliani, C., J.H. Hudson, B. Lidz, E.A. Shinn, and R.Y. George (1978). Oxygen and carbon isotopic record of growth in a reef coral from the Florida Keys and a deep-sea coral from Blake Plateau, Science 202: 627-629.

Flegal, A.R. and C.C. Patterson (1983). Vertical concentration profiles of lead in the central Pacific at 15°N and 20°S, Earth Planet. Sci. Lett. 64: 19-32.

Flegal, A.R., B.K. Schaule, and C.C. Patterson (1984). Stable isotope ratios of lead in surface waters of the central Pacific, Mar. Chem. 14: 281-287.

Flynn, W.W. (1968). The determination of low levels of Polonium-210 in environmental materials, Analytic. Chimica. Acta 43: 221-227.

Garrels, R.M. and M.E. Thompson (1962). A chemical model for sea water at 25°C and one atmosphere total pressure, Am. J. Sci. 260: 57-66.

Hudson, J.H. (1981). Growth rates in Montastrea annularis: a record of environmental change in Key Largo Coral Reef Marine Sanctuary, Florida, Bull. of Mar. Sci. 31: 444-457.

Iselin, C.O'D. (1936). A study of the circulation of the western North Atlantic, Papers in Physical Oceanogr. and Meteorol., vol.4.

Jickells, T.D., W.G. Deuser, and A.H. Knap (1984). The sedimentation rates of trace elements in the Sargasso Sea measured by sediment trap, Deep Sea Res. 31: 1169-1178.

Jickells, T.D., A.H. Knap, and T.M. Church (1984). Trace metals in Bermuda rainwater, J. Geophys. Res. 89: 1423-1428.

Lorens, R.B. (1981). Sr, Cd, Mn and Co distribution coefficients in calcite as a function of calcite precipitation rate, Geochim. Cosmochim. Acta 45: 553-561.

Manhes, G., J.F. Minster, and C.J. Allegre (1978). Comparative uranium-thorium-lead and rubidium-strontium study of the Saint Severin Amphoterite: Consequences for early solar system chronology, Earth Planet. Sci. Lett. 39: 14-24.

Morse, J.W., A. Mucci, and F.J. Millero (1980). The solubility of calcite and aragonite in seawater at 35‰ salinity at 25°C and atmospheric pressure, Geochim. Cosmochim. Acta 44: 85-94.

Murozumi, M., T.J. Chow, and C. Patterson (1969). Chemical concentrations of pollutant lead aerosols, terrestrial dusts, and sea salts in Greenland and Antarctic snow strata, Geochim. Cosmochim. Acta 33: 1247-1294.

Nozaki Y. and S. Tsunogai (1973). Lead-210 in the North Pacific and the transport of terrestrial material through the atmosphere, Earth Planet. Sci. Lett. 20: 88-92.

Nozaki, Y., J. Thomson, and K.K. Turekian (1976). The distribution of ^{210}Pb and ^{210}Po in the surface waters of the Pacific Ocean, Earth Planet. Sci. Lett. 32: 304-312.

Nriagu, J.O. (1979). Global inventory of natural and anthropogenic emissions of trace metals to the atmosphere, Nature 279: 409-411.

Patterson, C.C., D. Settle, and B. Glover (1976). Analysis of lead in polluted coastal seawater, Mar. Chem. 4: 305-319.

Sarmiento, J.L. and K. Bryan (1982). An ocean transport model for the North Atlantic, J. Geophys. Res. 87: 394-408.

Schaule, B.K. and C.C. Patterson (1981). Lead concentrations in the northeast Pacific: evidence for global anthropogenic perturbations, Earth Planet. Sci. Lett. 54: 97-116.

Schaule, B.K. and C.C. Patterson (1983). Perturbations of the natural lead depth profile in the Sargasso Sea by industrial lead. In: Trace Elements in Seawater, C.S. Wong, E. Boyle, K. Bruland, D. Burton, and E.D. Goldberg, eds., pp. 487-503, Plenum, New York: N.Y.

Schott, G. (1944). Geographie des Atlantischen Ozean.

Schuhmacher, H. and H. Zibrowius (1985). What is hermatypic? A redefinition of ecological groups in corals and other organisms, Coral Reefs 4: 1-9.

Settle, D.M. and C.C. Patterson (1982). Magnitudes and sources of precipitation and dry deposition fluxes of industrial and natural leads to the North Pacific at Eniwetak, J. Geophys. Res. 87: 8857-8869.

Settle, D.M., C.C. Patterson, K.K. Turekian, and J.K. Cochran (1982). Lead precipitation fluxes at tropical ocean sites determined from ^{210}Pb measurements, J. Geophys. Res. 87: 1239-1245.

Smith, R.M. and A.E. Martell (1976). Critical Stability Constants, Vol. 4. Plenum, New York: N.Y.

Speer, J.A. (1983). Crystal chemistry and phase relations of orthorhombic carbonates. In: Carbonates: Mineralogy and Chemistry, pp. 145-189, Mineralogical Society of America, Chelsea: Michigan.

Stukas, V.J. and C.S. Wong (1981). Stable lead isotopes as a tracer in coastal waters, Science 211: 1424-1427.

Sun, S.S. (1980). Lead isotopic study of young volcanic rocks from mid-ocean ridges, ocean islands and island arcs, Phil. Trans. R. Soc. Lond. A 297: 409-445.

Talbot, R.W. and A.W. Andren (1983). Relationships between Pb and ^{210}Pb in aerosol and precipitation at a semiremote site in northern Wisconsin, J. Geophys. Res. 88: 6752-6760.

Thomson, J. and K.K. Turekian (1976). ^{210}Po and ^{210}Pb distributions in ocean water profiles from the eastern South Pacific, Earth Planet. Sci. Lett. 32: 297-303.

Tsunogai, S. and Y. Nozaki (1971). Lead-210 and polonium-210 in the surface water of the Pacific, Geochem. J. 5: 165-173.

Turekian, K.K., Y. Nozaki, and L.K. Benninger (1977). Geochemistry of atmospheric radon and radon products, Ann. Rev. Earth Planet. Sci. 5: 227-255.

Weber, J.N. and P.M.J. Woodhead (1982). Temperature dependence of oxygen-18 concentration in reef coral carbonates, J. Geophys. Res. 77: 463-473.

Wolff, E.W. and D.A. Peel (1985). The record of global pollution in polar snow and ice, Nature 313: 535-540.

Zirino, A. and S. Yamamoto (1972). A pH dependent model for the chemical speciation of copper, zinc, cadmium, and lead in seawater, Limnol. Oceanogr. 17: 661-671.

CHAPTER 4

CADMIUM, BARIUM, ZINC AND VANADIUM IN CORALS

4.1 Introduction

The cleaning, coprecipitation, and analytical (AAS) techniques employed for coral Pb analysis are suited to a host of transition metals. As a consequence, all coral preparations were sized for potential multi-element determination. The questions remained as to which elements would demonstrate incorporation in aragonite and what might be learned from historical records of these elements in the surface ocean.

This chapter describes 20th century distributions of Cd, Ba, Zn, and V in corals from a variety of locations. Cd is proposed as a useful tracer of both natural and anthropogenic perturbations to surface waters. This biologically-mediated element is particularly sensitive to natural fluctuations in surface levels due to upwelling, since it exhibits a very steep phosphate-like gradient over the upper several hundred meters. Gradients in Ba, a silicate analogue, are not nearly so strong, else, this element might prove as useful as Cd. Depletion of Cd in the mixed layer also enables recognition of relatively faint industrial Cd signals, as shall be seen for the Sargasso Sea. Industrial V might also be discernable in recent corals were it not for a surface ocean concentration of 40 nM (Huizenga and Kester, 1982) - a level 2000 times higher than that of Cd. Perturbations to the natural distribution of Zn are not obvious, despite heavy industrial emissions and a depleted mixed layer concentration. Due to scatter in the data, however, small changes over the last century (less than a factor of two) cannot be ruled out.

4.2 Cadmium in a Galapagos Coral - Surface Ocean Paleofertility

Non-seasonal short term chemical variations occur naturally in the surface ocean in several types of locations: (1) areas adjacent to boundary currents (meander flow paths, warm and cold core eddies, warm outbreaks), (2) coastal areas subject to terrestrial influence (variable river discharge, resuspension, etc.), and (3) areas affected by upwelling. The third domain is of special interest, particularly with regard to large-scale ocean-atmosphere perturbations in the Pacific, known collectively as El Nino - Southern Oscillation (ENSO) phenomena. Manifestations of ENSO activity such as warmer sea surface temperature (SST) and changes in biota, sea level, and rainfall are most dramatic in the eastern tropical Pacific. Surface ocean transitions are especially sharp near the coast of South America because waters here are unusually cold and productive due to coastal upwelling driven by the southeast trade winds. Thus, in reconstructing historic patterns of ENSO activity, the eastern Equatorial Pacific is the location of choice in terms of large amplitude signals. Although regions of intense upwelling are normally too cold to support scleractinian coral growth, warmer adjoining areas can be more hospitable and yet experience similar chemical anomalies. The Galapagos islands, lying directly on the equator, are a good example.

A 20-year coral Cd record from San Cristobal Island on the eastern flank of the Galapagos Island chain is depicted in Fig. 4.1. Cd/Ca mole ratios in Pavona clavus vary from about 1.5 to 6.4 nmol Cd/mole Ca. On a San Diego-to-Panama transect through this same area, Boyle and Huested (1983) observed surface water Cd concentrations varying from about 15 to 75 pM in traversing non-upwelling and upwelling regions, respectively. If one assumes that the Galapagos coral inhabited a zone of variable upwelling, a similar range of surface water Cd concentrations (15-64 pM) is implied by a coral:seawater distribution coefficient (K_D) of 1.0. This inferred K_D is noteworthy in that $CdCO_3$ is more commonly known as

Figure 4.1 Skeletal Cd concentrations in P. clavus from San Cristobal Island, Galapagos Islands. Annual determinations are based on triplicate analyses with resulting 1σ errors.

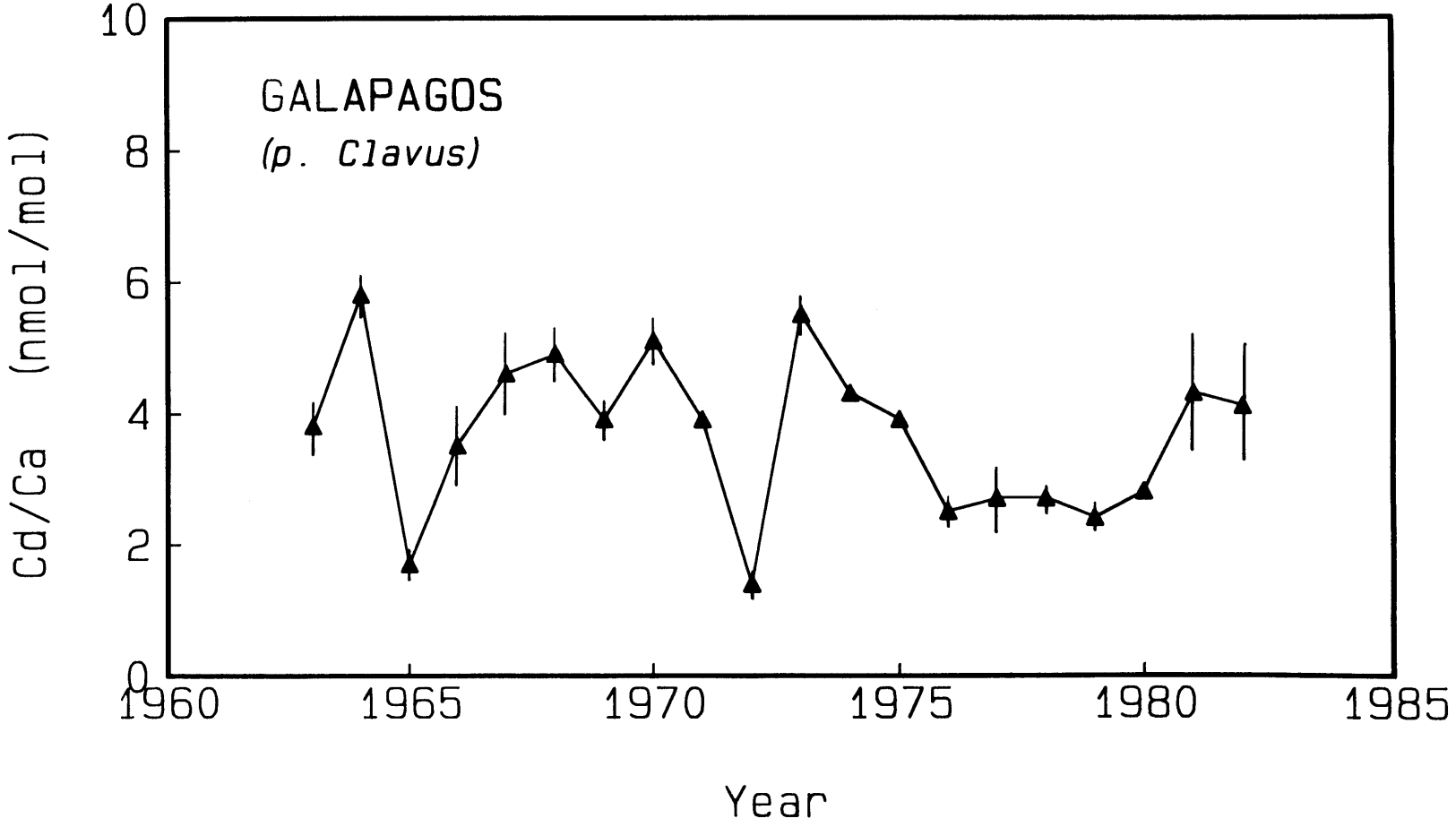
GALAPAGOS
(p. Clavus)
Cd/Ca (nmol/mol)
Year
0
2
4
6
8
10
1960
1965
1970
1975
1980
1985

the 6-coordinated rhombohedral calcite structure. Apparently, due to excellent size compatibility with Ca^{2+} (effective ionic radii of 1.12 Å and 1.10 Å for Ca^{2+} and Cd^{2+}, respectively (Shannon, 1976)) and similarity of electron configuration ($4s^2$ vs. $4d^{10}$ $5s^2$), Cd also conforms to an aragonitic structure in nature.

That the variable upwelling experienced by Pavona clavus was not random is suggested by comparison to records of sea surface temperature anomaly and southern oscillation index (SOI) (Fig. 4.2). Dips in the Cd record reflecting nutrient-depleted conditions appear to correlate with warm water temperatures (recorded at Puerto Chicama, Peru) and negative surface pressure differential (Tahiti minus Darwin). Correspondence is readily apparent for the two most intense El Nino events of 1965 and 1972. The record-breaking 1982-83 episode is not visible because the coral was cored in 1982 before the full impact of El Nino was felt. Lesser events (1963, 1969, 1976) and periods of intense upwelling (1964, 1973) also appear to follow expected trends. The mechanism by which surface nutrient depletion occurs stems not so much from curtailed upwelling (Enfield, 1981), as from vertical displacement of source waters. As equatorial easterlies weaken during ENSO episodes (Barnett, 1981), the difference in sea level between the eastern and western equatorial Pacific is diminished (Wyrtki, 1975), causing an eastward migration of warm surface waters and Kelvin waves along the equatorial wave guide. This basin-wide perturbation is recorded in the form of $\delta^{18}O$ anomalies in corals as far away as Fanning and Canton Islands (Druffel, 1985). It also leads to a depression of colder, nutrient-rich thermocline waters in the Peru - Galapagos Islands region. Since upwelled waters originate from less than 160 m depth (Quay et al., 1983; Fine et al., 1985; Bryden and Brady, 1985), and upper thermocline gradients for Cd, phosphate, and nitrate are very steep (on the order of 5 pM/m, 0.016 uM/m, and 0.3 uM/m, respectively - Boyle and Huested, 1983; Collier, 1984), a relatively wide range of surface Cd or nutrient concentrations may result, depending on the intensity of vertical restructuring . The range of surface water Cd concentrations inferred

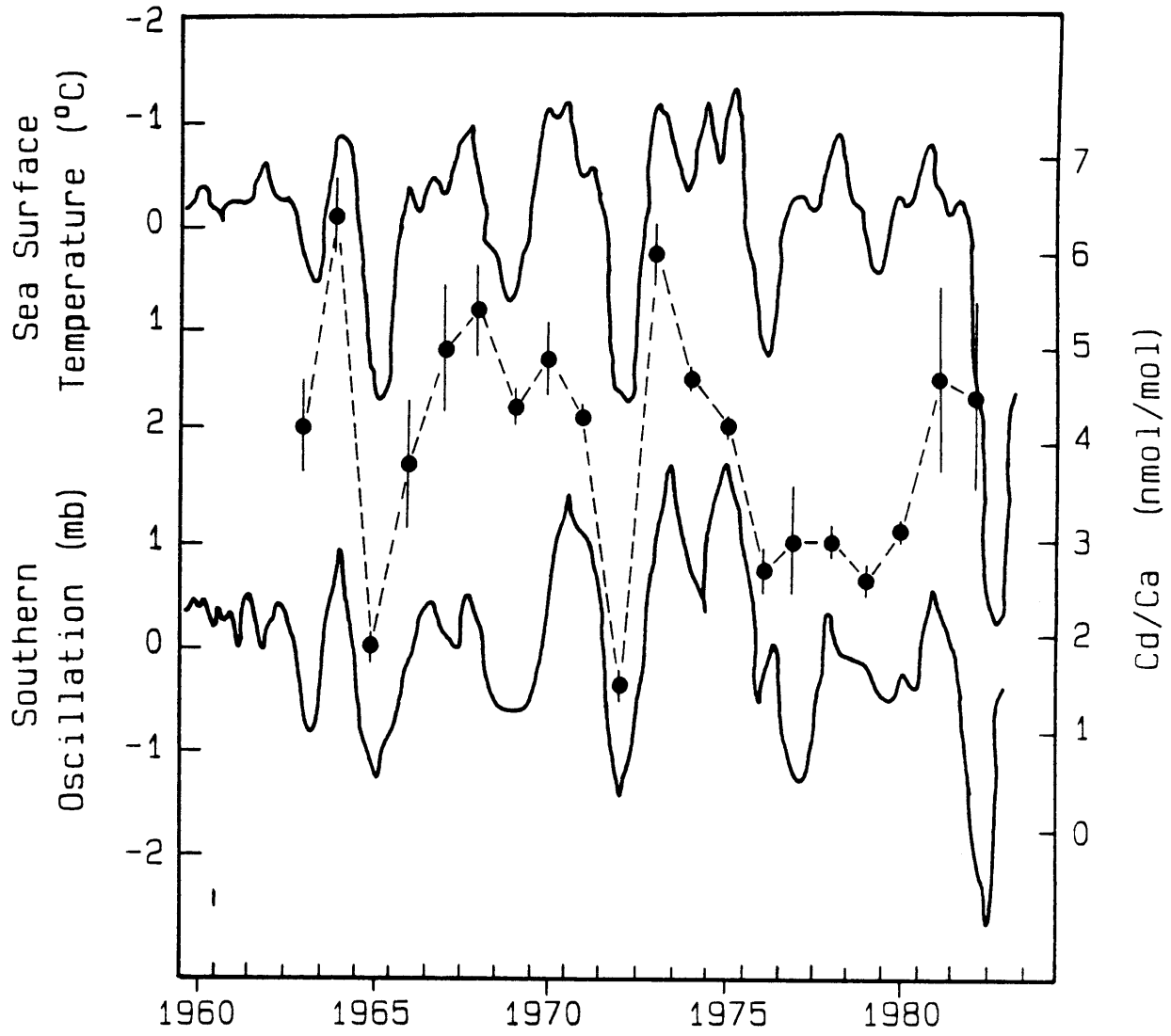

Figure 4.2 Historic sea surface temperature at Puerto Chicama, Peru and Southern Oscillation Index (Tahiti minus Darwin) compared to Cd in P. clavus (Source: Rasmusson, 1984)

from Pavona clavus at San Cristobal Island (15-64 pM) suggests a source water deepening of only 10 meters (discounting changes in productivity) in changing from normal to ENSO conditions in this area.

4.3 Cadmium in a Bermuda Coral: Another Industrial Marker

At North Rock, Bermuda in the Sargasso Sea, there is no significant upwelling. This is evident in the very low skeletal Cd levels found in Diploria strigosa (Fig. 4.3), the highest of which only approach depleted conditions in the eastern Equatorial Pacific. If we assume K_D = 1.0 as in the Galapagos Islands case, surface waters near Bermuda take on values of 3-12 pM. Bruland and Franks (1983) reported values close to 2 pM for 1979 Sargasso Sea surface waters. The coral-inferred seawater value at 1979 is about 7 pM, but is obscured by poor analytical precision (a general characteristic of recent coral bands for several trace metals). Regardless of this possible offset, anomalously high Cd values appear to have existed between 1916-1932 and 1942-present. A two-phase industrial lead rise was observed in the same coral over the periods 1884-1923 and 1942-1972, followed by a sharp decline (see Fig. 3.1). The more recent Cd trend is reminiscent of the industrial Pb trend and in fact, resembles both U.S. zinc and cadmium metal production (Fig. 1.5). The older Cd rise centered on 1916-17, however, does not follow the pattern of early American industrialization in as predictable a manner as Pb.

Historically, cadmium has been recovered primarily as a by-product of zinc smelting and to a lesser extent, lead and copper-zinc smelting. Typical Cd/Zn ratios range from 0.3-0.7 weight % in various Pb-Zn and Cu-Zn deposits, with particularly high ratios in the Joplin Pb-Zn deposits (0.63%) of Missouri (Nriagu, 1980). Initial Cd recovery normally follows either a hydro- or pyrometallurgical procedure, both of which involve Cd collection as flue dust. Comparison of the U.S. cadmium recovery curve with U.S. primary production of Zn in Fig. 1.5 reveals the origin of the unexpectedly high concentrations in the early

Figure 4.3 Skeletal Cd concentrations in D. strigosa from North Rock, Bermuda. In most cases, data points represent triplicate analyses or better. Error bars are 1σ.

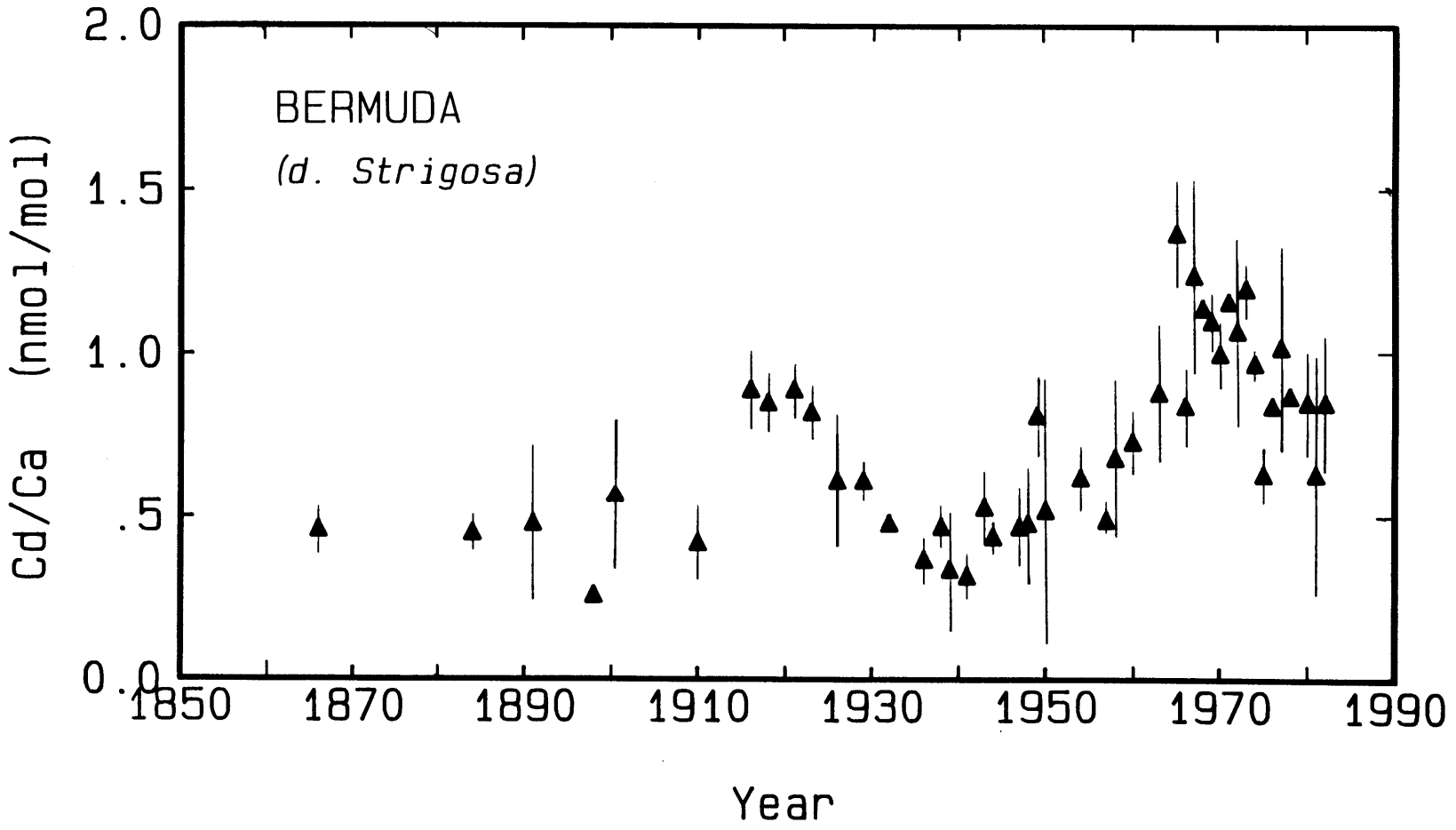
BERMUDA
(d. Strigosa)
Cd/Ca (nmol/mol)
2.0
1.5
1.0
.5
0.0
1850
1870
1890
1910
1930
1950
1970
1990
Year

coral record. The production of Zn waned between 1916 and 1932 (as did Pb and Fe ore production), though somewhat more irregularly than recorded by the coral. More importantly, however, Cd production, which began in 1906, only reached significant levels in the mid-1920's. Thus, the coral Cd peak at 1916-17 is a result of a zinc production maximum which occurred at a time when flue dust recovery was negligible. The subsequent Cd decrease in the coral record reflects a combination of declining Zn production and industrial exploitation of Cd-rich smelting exhausts. Ambient Cd concentrations in surface water appear to have regained a 1916-like value fairly recently (≈1970) as Zn production reached its zenith of approximately 10^6 metric tons/year. A doubling of Zn production between 1916 and 1970, however, implies that about 1/2 of the flue dust capable of long range transport was still escaping to the environment during ore smelting in 1970. This is surprising in view of technological advances in dust recovery (Wedow, 1973; Athanassiadis, 1969). The explanation lies in decreased contributions of Cd emissions by Zn processing in recent years, relative to other sources (e.g. Cu smelting and waste incineration). Nriagu (1979) estimates that on a global basis, Zn operations accounted for only 40% of total Cd emissions in 1975

The absolute flux of industrial Cd to the Sargasso Sea can be estimated in a number of ways. Assumption of a mixed layer depth of 100 m, a Cd concentration of 3 pM, and a surface residence time of 5 yrs (by analogy to phosphate), yields a steady state background flux of 7 ug/m^2/yr. Alternatively, Jickells et al. (1984a) and Church et al. (1984) estimated an annual flux of 90 ug/m^2/yr to Bermuda (1981-82) based on wet deposition measurements. Subsequent sediment trap measurements suggesting a maximum flux of 10 ug/m^2/yr @ 3200 m (1980-82), however, led Jickells et al. (1984b) to conclude that rain must contain a large Cd component resulting from recycled sea salt. The relative proportions of surface water industrial Cd, background Cd, and PVC trap-derived Cd comprising this 10 ug/m^2/yr are unknown, precluding further refinement of the surface Cd flux estimate. If we integrate a

peak industrial flux of 20 ug/m^2/yr (three times the calculated background flux as suggested by the coral record) over the western North Atlantic Ocean, a total Cd flux of approximately 2 x 10^9 g/yr results for the period around 1970. This agrees well with estimates of U.S. emissions from 1970-1975 from various published sources (1.5-2.4 x 10^9 g/yr; see Nriagu, 1980). It also represents a 0.8 g Cd/kg Zn emission factor for U.S. primary Zn production. Nriagu (1979) assumed a factor of 0.5 g Cd/kg Zn in his survey of worldwide anthropogenic Cd emissions for 1975-76.

In an attempt to determine whether the observed Sargasso Sea Cd chronology might be a natural phenomenon, nutrient data collected since 1954 at the Panulirus Station (50 km southeast of Bermuda) were examined. Unfortunately, surface water values for both phosphate and nitrate are near the respective detection limits of 0.03 uM and 0.5 uM for the standard colorimetric methods. Thus, no historical nutrient patterns can be discerned.

It is interesting to consider the implications of a Cd excess above natural levels in oligotrophic surface waters. Though dissolved Cd is removed by plankton as though it were a nutrient, its biochemical utility, if any, is unknown. The amplitude of the coral Cd record and its rough concordance with emissions estimates suggest that biological uptake of Cd has not increased in the Sargasso Sea. Thus, nitrate limitation or an inherently low nutritive value of Cd have precluded biological exploitation of the 20th century anthropogenic enrichment.

4.4 Barium and Cadmium in the Florida Straits

In section 3.3, a comparison of skeletal Pb and ^{210}Pb was drawn as a means of validating the stable Pb record in M. annularis from the Florida Straits. Here, the uptake histories of barium, another biochemical analogue of Pb, (Elias et al., 1982; Burnett et al., 1980), and Cd are described for the same specimen. Within analytical uncertainty, barium and cadmium show little change over time (Figs. 4.4

Figure 4.4 Skeletal Ba concentrations in M. annularis from the Florida Straits. Annual determinations are based on duplicate GFAAS measurements with resulting 1σ errors.

Figure 4.5 Skeletal Cd concentrations in M. annularis from the Florida Straits. In most cases, data points represent triplicate analyses. Error bars are 1σ.

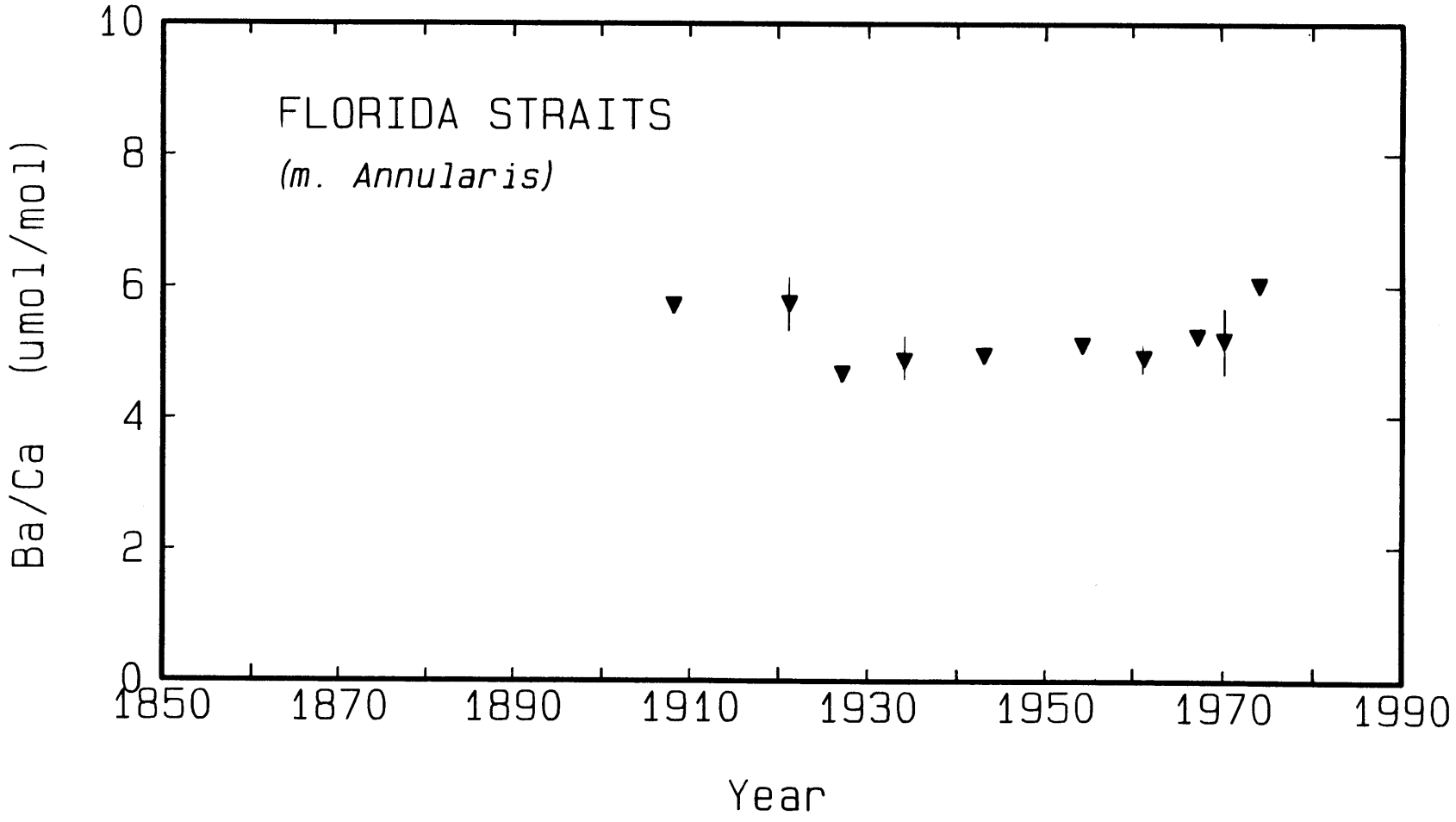
FLORIDA STRAITS
(m. Annularis)
Ba/Ca (umol/mol)
Year
0
2
4
6
8
10
1850
1870
1890
1910
1930
1950
1970
1990

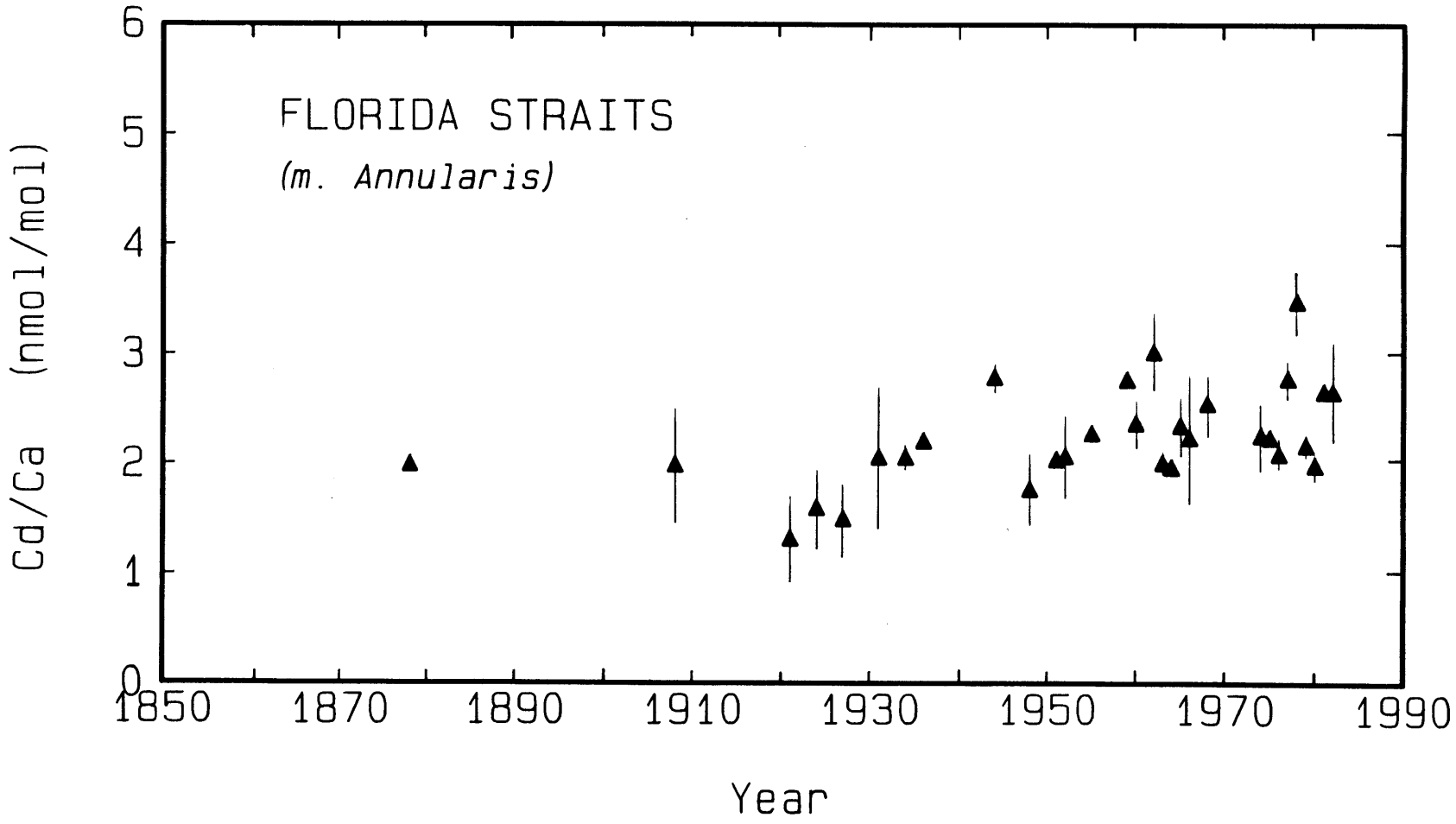
FLORIDA STRAITS
(m. Annularis)
Cd/Ca (nmol/mol)
0
1
2
3
4
5
6
1850
1870
1890
1910
1930
1950
1970
1990
Year

and 4.5) which is the expected result assuming unchanged seawater levels of these elements. If K_D = 1.0 for Cd in corals as suggested by the chronologies from Galapagos and Bermuda (sections 4.2 and 4.3), a Florida Straits surface water value of 20 nM Cd can be inferred. Anthropogenic Cd perturbations of about 0.8 nmol/mol Ca detected in D. strigosa in Bermuda are probably muted in the Florida Straits (as were Pb perturbations) and effectively masked by the apparent high background concentration. Similarly, if K_D = 1.0 for Ba in corals as supported by studies by Buddemeier et al. (1981) and Livingston and Thompson (1971), surface water Ba would be about 52 nM. Both inferred values for Cd and Ba are high relative to open ocean surface conditions and suggest upwelling, fluvial, continental shelf, or resuspension influence. The fact that pre-industrial Pb also appears high based on analyses of M. annularis (Figs. 3.5 and 3.10), argues against an upwelling source. Riverine fluxes of dissolved Pb appear to be insignificant (see section 1.2.2), but Boyle et al. (1984) determined that excess copper in the Florida Straits could be accounted for by Amazon, Mississippi, and Orinoco inputs. although, significant shelf fluxes could not be ruled out. Measured concentrations of Cd along the South Florida Shelf were generally low, but small anomalies approaching 20 pM were evident along the transect.

Based on Ba, Cd, Pb, and ^{210}Pb reconstructions in M. annularis, it may be concluded that lattice-compatible trace element uptake occurs in a regular predictable manner. If this behavior is universal among reef-building corals, trace element reconstructions should be immune from vital effects which cause temporally variable discrimination.

4.5 Other Cadmium Records

A few measurements of Cd in corals from other locations were made in order to test for inter-genera variability in Cd uptake. Assuming K_D = 1.0, measurements on P. rustica from Mauritius (Fig. 4.6) suggest a surface water Cd concentration of 5-6 pM for the western Indian Ocean.

Figure 4.6 Skeletal Cd concentrations in corals from Eniwetak, Lisianski Island, and Mauritius. Annual determinations are in most cases based on duplicate or triplicate analyses. Error bars are 1σ.

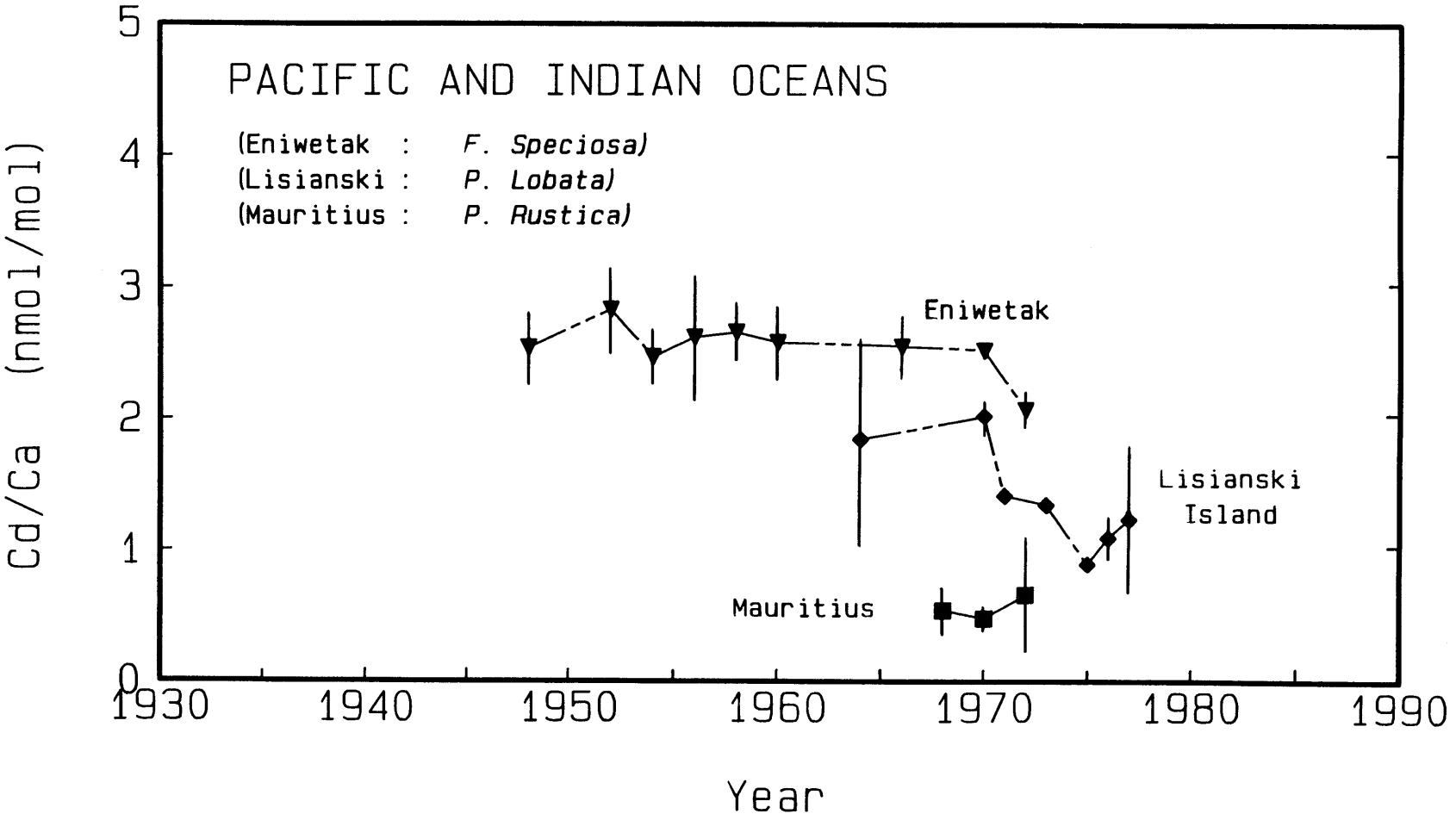
PACIFIC AND INDIAN OCEANS
(Eniwetak : F. Speciosa)
(Lisianski : P. Lobata)
(Mauritius : P. Rustica)
Eniwetak
Lisianski
Island
Mauritius
Cd/Ca (nmol/mol)
Year
0
1
2
3
4
5
1930
1940
1950
1960
1970
1980
1990

In view of dissolved Cd measurements from the North Atlantic and North Pacific Oceans (Bruland and Franks, 1983; Boyle and Huested, 1983), this value appears reasonable. The data from Eniwetak (F. speciosa) and Lisianski Island (P. lobata) should be interpreted with more caution since these corals were heavily contaminated for Pb (section 3.5). Inferred surface water values adjacent to Eniwetak Atoll and Lisianski Island are 25 pM and 9-20 pM, respectively. Relative to the North Pacific central gyre (2 pM), these concentrations are high -- possibly due to residual contamination. Natural causes such as upwelling and resuspension, however, could also easily account for offsets of 10 to 20 pM.

4.6 Zinc and Vanadium in a Bermuda Coral

While $PbCO_3$ (cerrusite) and $BaCO_3$ (witherite) are known to form limited solid solutions with aragonite (Speer, 1983), and Cd^{2+} possesses an ionic radius similar to that of Ca^{2+}, Zn^{2+} (ionic radius = 0.90 Å) incorporation by corals is less certain. Fig. 4.7 represents an attempt to trace possible industrial perturbations to surface water Zn in the Sargasso Sea from the coral record. Parallel reconstructions for Cd and Pb have revealed approximate 4 and 15-fold maximum increases of these respective trace metals (Figs. 3.1 and 4.3). Since Pb, Cd, and Zn are all (a) relatively volatile metals, (b) largely co-produced from the same ores, and (c) relatively depleted in surface waters, an anthropogenic oceanic Zn signal seems likely. But while such a perturbation in the coral record cannot be entirely ruled out on the basis of Fig. 4.7, the scatter does rule out any historic change of greater than 2-fold. Interestingly, the data appear to center on approximately 6 nmol Zn/mol Ca which suggests $K_D = 1.0$ since Bruland and Franks (1983) determined dissolved Zn in Sargasso Sea surface waters to be 60 $\pm$ 20 pM (or 6 nmol Zn/mol Ca in seawater). Thus, despite having an ionic radius 20% smaller than Ca^{2+}, Zn^{2+} appears to be indiscriminately precipitated with respect to its seawater distribution. The same conclusion can be reached for cobalt which shares an identical

Figure 4.7 Skeletal Zn concentrations in D. strigosa from North Rock, Bermuda. Annual determinations are based on triplicate analyses in most cases. Error bars are 1σ.

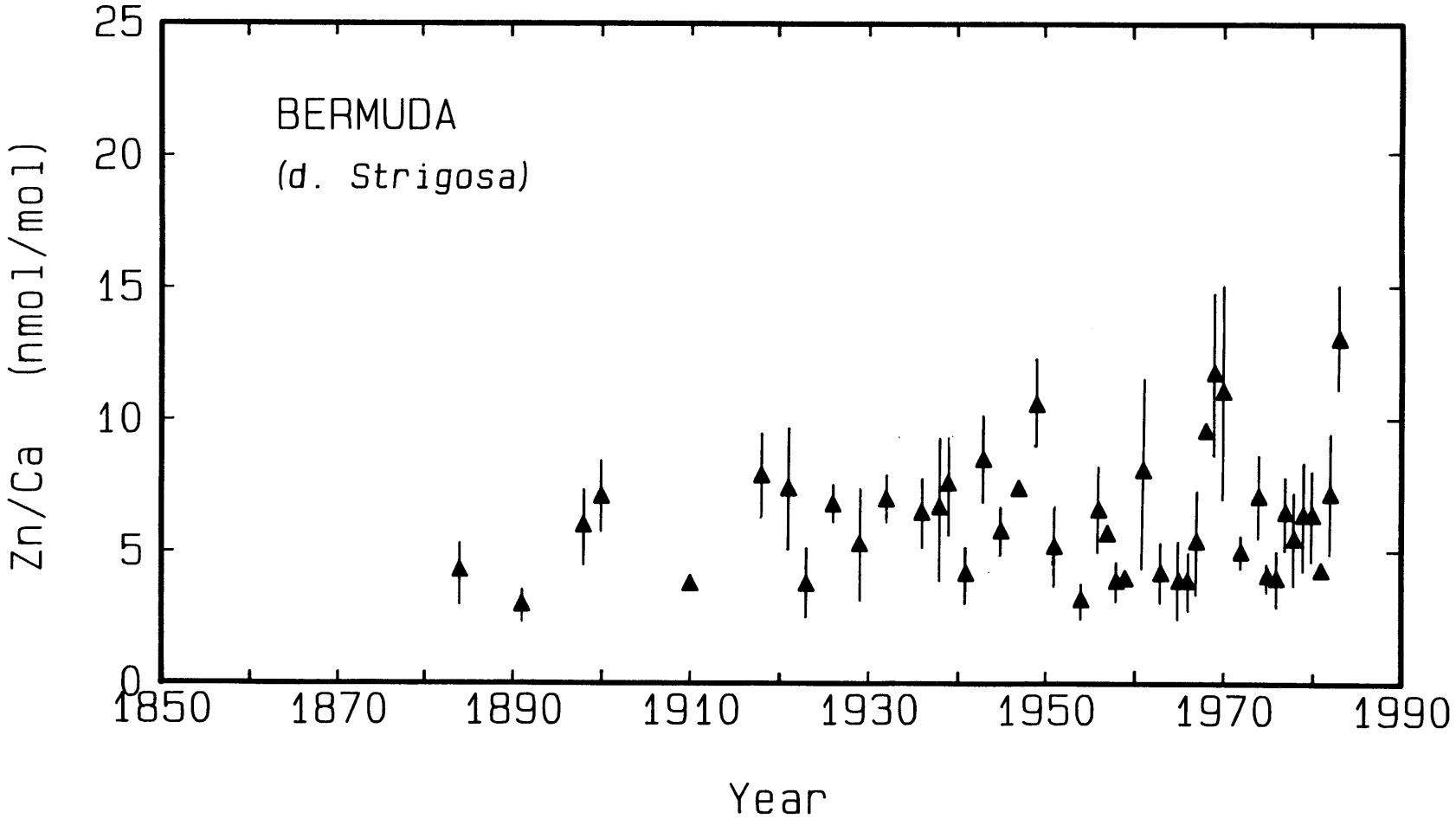
BERMUDA
(d. Strigosa)
Zn/Ca (nmol/mol)
25
20
15
10
5
0
1850
1870
1890
1910
1930
1950
1970
1990
Year

effective ionic radius (Veeh and Turekian, 1968). This brings the known total to seven elements in Table 4.1 (Ra, Ba, Nd, Sr, Cd, Co, Zn) with +2 ionic radii ranging from 0.90-1.48 Å, which are incorporated by corals in much the same ratio as they are found in seawater. (Table 4.1 is an updated version of Table 1.4). This result is particularly intriguing in the case of neodymium since rare earth elements occur principally in the +3 oxidation state in seawater. If Nd is actually substituted as the Nd^{2+} cation, then it must be reduced from its seawater +3 state in the coral ectoderm. Photosynthesis is known to produce localized centers of highly negative pe (conversion of CO_2 to glucose requires pe = -7.2), so fixation of CO_2 by coral zooxanthellae may provide a possible mechanism. Only Pb and perhaps Sm demonstrate preferential uptake in coral aragonite. In the exceptional case of Mg, its high concentration in seawater would require corals to consist predominantly of $MgCO_3$ if K_D were equal to 1.0. Clearly, this is not the case (K_D on the order of 0.001), although a substantial amount of Mg does appear to be substituted (Amiel et al., 1973).

Beyond direct substitution, it is also known that uranium can be skeletally incorporated (K_D = 0.6-1.0) despite its existence as a negatively charged complex in seawater (Cross and Cross, 1983; Veeh and Turekian, 1968). Swart and Hubbard (1982) calculated that dissolved U exists as $UO_2(CO_3)_2^{2-}$ (68%) and $UO_2(CO_3)_3^{4-}$ (32%). The incorporation mechanism in corals is not understood, however, it seems possible that the uranyl carbonate complex actually replaces several $CaCO_3$ groups in the aragonite lattice. Fig. 4.8 depicts the skeletal uptake of a second metal which exists in seawater as an anionic complex, vanadium. Although the mechanism by which vanadium is skeletally fixed from seawater vanadate ($VO_2(OH)_3^{2-}$ is even less clear, incorporation by <u>D. strigosa</u> of 100 nmol V/mol Ca appears constant in time. Assuming surface waters near North Rock, Bermuda contain 39 nM V (Huizenga and Kester, 1982), this suggests K_D = 0.026. As expected from its incompatibility with an aragonite structure (+5 valence, small ionic radius), vanadium is heavily discriminated against. It may be that

Table 4.1 $^{+2}$ cations exhibiting octahedral coordination with effective ionic radii and abundances in corals.

Cation	Effective Ionic Radius (A) (1)	Measured Abundance in Coral*	Predicted Abundance in Coral* (K_D=1)
Ra^{2+}	1.48	6 dpm ^{226}Ra/100g (2)	7.4 dpm ^{226}Ra/100g
Ba^{2+}	1.42	4-6 x 10^{-6} (Fig.4.4)	3.6-4.4 x 10^{-6}
Pb^{2+}	1.29	4-60 x 10^{-9} (Fig.3.1) (Table 3.1)	(K_D = 2.3)
Nd^{2+}	1.29	0.3-6.6 x 10^{-9} (3)	0.3-3.4 x 10^{-9}
Sm^{2+}	1.27	13-130 x 10^{-9} (4)	0.06-0.6 x 10^{-9}
Sr^{2+}	1.26	7.5-8.5 x 10^{-3} (5)	8.4 x 10^{-3}
Am^{2+}	1.26		0.01 dpm ^{241}Am/100g
Eu^{2+}	1.25		0.02-.08 x 10^{-9}
Hg^{2+}	1.14		1.5 x 10^{-9}
Yb^{2+}	1.14		0.08-.43 x 10^{-9}
Ca^{2+}	1.12	0.40	0.40
Cd^{2+}	1.10	0.4-6.5 x 10^{-9} (Figs.4.1, 4.3, 4,5)	0.2-6.5 x 10^{-9}
Mn^{2+}	0.96		0.6-3.0 x 10^{-8}
Fe^{2+}	0.92		15 x 10^{-9}
Co^{2+}	0.90	1-10 x 10^{-9} (6)	0.5-10 x 10^{-9}
Zn^{2+}	0.90	3-9 x 10^{-9} (Fig.4.7)	4-8 x 10^{-9}
Mg^{2+}	0.89	3-8 x 10^{-3} (7)	5.3

* Expressed as mole ratios relative to Ca. Seawater abundances used are simply predicted coral abundances multiplied by $[Ca]_{sw}$ or 0.0104.

Refs. (1) Shannon, 1976 (2) Dodge and Thomson, 1974 (3) Shaw and Wasserburg, 1985 (4) Scherer and Seitz, 1980 (5) Cross and Cross, 1983 (6) Veeh and Turekian, 1968 (7) Weber, 1974

Figure 4.8 Skeletal V concentrations in D. strigosa from North Rock, Bermuda. Annual determinations are based on triplicate analyses in most cases. Error bars are 1σ.

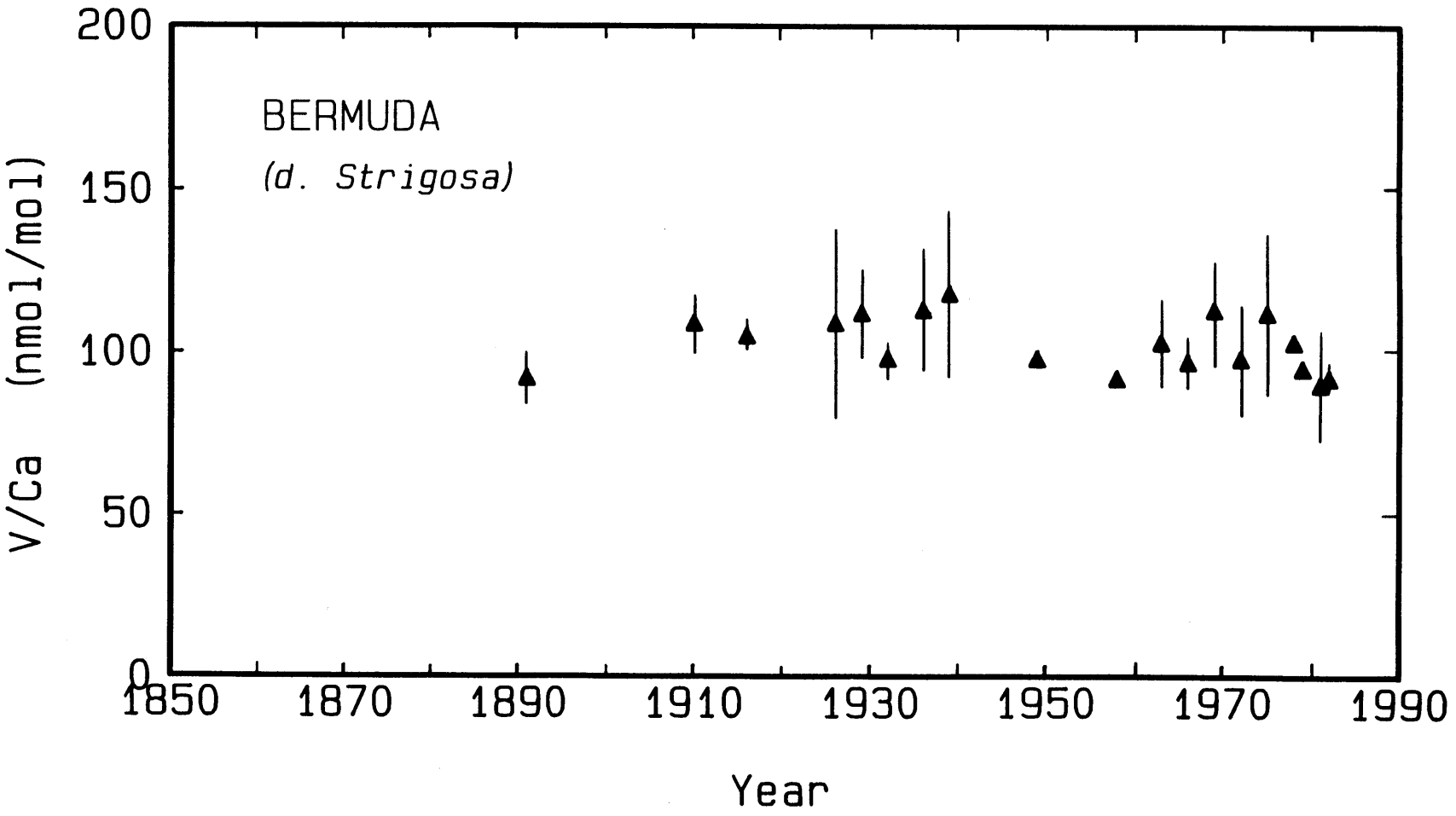
BERMUDA
(d. Strigosa)
V/Ca (nmol/mol)
200
150
100
50
0
1850
1870
1890
1910
1930
1950
1970
1990
Year

regular amounts of V are substituted interstitially within the relatively open aragonite framework.

It also happens that V in the contemporary environment has a strong industrial source. Duce and Hoffman (1976) estimated a net flux of 3-5 $ng/cm^2/yr$ to the western North Atlantic, some 20 times the natural weathering flux. The principal sources of anthropogenic V are fossil fuels, particularly fuel oils; thus the geographic source distribution for V is probably comparable to North American Pb. The reason for the absence of an oceanic response is the unusually high concentration of V in seawater -- 300 and 2000 times higher than the corresponding present day Pb and Cd concentrations in the Sargasso Sea. At 1975 fallout rates, Duce and Hoffman calculated that the mixed layer V inventory changed by only 0.01% per year. The coral results confirm that anthropogenic V is indeed swamped by the background inventory of V in the surface ocean.

4.7 Conclusions

While contemporary industrial perturbation of Pb in the western North Atlantic is of sufficient scale to allow transport modeling, the industrial Cd signal is prohibitively small to enable a parallel study. Likewise, the natural distributions of Zn and V in Sargasso Sea surface waters appear to have undergone little or no change over the past century. This result is surprising in the case of Zn since recent and all-time anthropogenic emission estimates are comparable to those of Pb (see Tables 1.2 and 1.3). Contemporary concentrations in surface waters are also roughly comparable (Pb $\approx$ 100 pM vs. Zn $\approx$ 70 pM), unlike the case for V where industrial fluxes are obscured by a high mixed layer concentration of 40 nM. Long-range transport of Zn aerosols has been shown to be similar to that of Pb (Jickells et al., 1984; Church et al., 1984), and surface ocean Zn is largely dissolved; an explanation for the lack of a strong industrial perturbation is not apparent.

Corals in the eastern Equatorial Pacific (Galapagos Islands) display Cd perturbations driven by a natural phenomenon known as the El Nino - Southern Oscillation. These perturbations arise as a result of upwelling of anomalously warm waters which displace colder, nutrient-rich source waters during ENSO events. Application of Cd in corals as a paleo-upwelling tracer offers great promise. Since existing sea surface temperature, pressure, and marine wind measurements go back only to 1841 (Quinn et al., 1978), an extended coral Cd record would augment our historical perspective of ENSO activity. For example, although the existing record indicates that ENSO events occur aperiodically, an extended record might reveal superimposed longer period cycles which are presently not obvious. These may in turn implicate forcing mechanisms which are poorly understood at present. Comparison of the Cd record with SST or ^{18}O measurements in corals may also distinguish between physical mechanisms governing changes in SST (i.e. the role of thermocline migration and upwelling versus surface heat flux -- Cd measures only the former while ^{18}O integrates both). Since historical records of climate on the continents (air temperatures, precipitation, surface pressure, ice-cover) are generally older and more reliable than comparable records over the Pacific Ocean, a variety of unforeseen ENSO teleconnections might become apparent in light of the reconstructed record. Further, by performing subannual coral measurements of Cd, onset/termination timing patterns over many additional ENSO cycles can be evaluated in relation to the "canonical El Nino" of the past century (Cane, 1983).

The addition of Cd and Zn to the growing list of trace element substituents in corals points out an important general phenomenon. It is increasingly apparent that lattice-compatible metals are incorporated into coral aragonite in much the same ratios to calcium as exist in seawater. Distribution coefficients for Ra, Ba, Nd, Sr, Cd, Co and Zn are all surprisingly close to unity, despite expected varying degrees of ion association. Model calculations by Turner et al. (1981), for example, suggest that proportions of free Cd^{2+}, Zn^{2+}, and Ba^{2+} in

seawater are 3, 46, and 86%, respectively. While this uptake pattern bespeaks simplicity, a thermodynamic basis is not obvious. One possibility is that in the supersaturated and possibly reducing environment of the coral ectoderm, carbonate complexes prevail, and these are indiscriminately coprecipitated with $CaCO_3$ in a kinetically controlled non-equilibrium process. The preference manifested toward Pb is a matter of speculation.

References

Amiel, A.J., G.M. Friedman, and D.S. Miller (1973). Distribution and nature of incorporation of trace elements in modern aragonitic corals, Sedimentology 20: 47-64.

Athanassiadis, Y.C. (1969). Air pollution aspects of cadmium and its compounds, U.S. Department of Commerce, PB 188 086.

Barnett, T.P. (1981). Statistical relations between ocean/atmosphere fluctuations in the Tropical Pacific, J. Phys. Oceanogr. 11: 1043-1058.

Boyle, E.A. and S. Huested (1983). Aspects of the surface distributions of copper, nickel, cadmium, and lead in the North Atlantic and North Pacific. In: Trace Metals in Seawater. C.S. Wong, E.A. Boyle, K. Bruland, D. Burton and E.D. Goldberg, eds., pp. 379-394. Plenum, New York.

Boyle, E.A., D.F. Reid, S.S. Huested and J. Hering (1984). Trace metals and radium in the Gulf of Mexico: an evaluation of river and continental shelf sources, Earth Planet. Sci. Lett. 69: 69-87.

Broecker, W.S. and T.H. Peng (1982). Tracers in the Sea. Lamont-Doherty Geological Observatory: Palisades, N.Y.

Bruland, K.W. and R.P. Franks (1983). Mn, Ni, Cn, Zn and Cd in the western North Atlantic. In: Trace Metals in Seawater. C.S. Wong, E.A. Boyle, K. Bruland, D. Burton and E.D. Goldberg, eds., pp. 395-414. Plenum, New York, N.Y.

Bryden, H.L. and E.C. Brady (1985). Diagnostic model of the three-dimensional circulation in the upper equatorial Pacific Ocean, J. Phys. Oceanogr. 15: 1255-1273.

Buddemeier, R.W., R.C. Schneider and S.V. Smith (1981). The alkaline earth chemistry of corals. Proc. 4th Int. Coral Reef Symposium, Manila. 2: 81-85.

Bureau of the Census of the U.S. Department of Commerce. The Statistical History of the United States from Colonial Times to the Present, Vol. 1965 - 1984, Fairfield Publishers, Inc., Stanford, Conn.

Burnett, M.W. and C.C. Patterson (1982). Perturbation of natural lead transport in nutrient calcium pathways of marine ecosystems by industrial lead. In: Isotope Marine Chemistry. Y. Horibe and K. Saruhashi, eds., pp. 413-438. Uchida Rokakuho Publ. Co., Tokyo.

Cane, M.A. (1983). Oceanographic events during El Nino, Science 222: 11819-1194.

Church, T.M., J.M. Tramontano, J.R. Scudlark, T.D. Jickells, J.J. Tokos, A.H. Knap, and J.N. Galloway (1984). The wet deposition of trace metals to the coastal and western Atlantic Ocean, Atmos. Environ. 18: 2657-2664.

Collier, R.W. (1984). Particulate and dissolved vanadium in the North Pacific Ocean, Nature 309: 441-444.

Cross, T.S. and B.W. Cross, (1983). U, Sr and Mg in Holocene and Pleistocene corals, J. Sed. Petr. 53: 587-594.

Dodge, R.E. and J. Thomson (1974). The natural radiochemical and growth records in contemporary hermatypic corals from the Atlantic and Caribbean, Earth Planet. Sci. Lett. 23: 313-322.

Druffel, E.M. (1985). Detection of El Nino and decade time scale variations of sea surface temperature from banded coral records: implications for the carbon dioxide cycle. In The Carbon Cycle and Atmospheric CO_2: Natural Variations Archean to Present. E.T. Sundquist and W.S. Broecker, eds., pp. 111-122. American Geophysical Union: Washington, D.C.

Duce, R.A. and G.L. Hoffman (1976). Atmospheric vanadium transport to the ocean, Atmos. Environ. 10: 989-996.

Elias, R.W., Y. Hirao and C.C. Patterson (1980). The circumvention of the natural biopurification of calcium along nutrient pathways by atmospheric inputs of industrial lead, Geochim. Cosmochim. Acta.46:2561-2580.

Enfield, D.B. (1981). Thermally driven wind variability in the planetary boundary layer above Lima, Peru, J. Geophys. Res. 86: 2005-2016.

Fine, R.A., W.H. Peterson and H. Ostlund (1986). Penetration of tritium into the tropical Pacific, (submitted to J. Phys. Oceanogr).

Huizenga, D.L. and D.R. Kester (1982). The distribution of vanadium in the Northwestern Atlantic Ocean, EOS Trans. AGU 63:990.

Jickells, T.D., A.H. Knap, and T.M. Church (1984). Trace metals in Bermuda rainwater, J. Geophys. Res. 89: 1423-1428.

Jickells, T.D., W.G. Deuser, and A.H. Knap (1984). The sedimentation rates of trace elements in the Sargasso Sea measured by sediment trap, Deep Sea Res. 31: 1169-1178.

Livingston, H.D. and G. Thompson (1971). Trace element concentrations in some modern corals, Limnol. and Oceanogr. 16: 786-796.

Nriagu, J.O. (1979). Global inventory of natural and anthropogenic emissions of trace metals to the atmosphere, Nature 279: 409-411.

Nriagu, J.O. (1980). Production, Uses, and Properties of Cadmium. In: Cadmium in the Environment - Part I. J.O. Nriagu, ed. John Wiley and Sons: New York, N.Y.

Quay, P.D., M. Stuiver and W.S. Broecker (1983). Upwelling rates for the equatorial Pacific derived from the bomb ^{14}C distribution, J. Mar. Res. 41: 769-792.

Quinn, W.H., D.O. Zopf, K.S. Short, and R.T.W. Yang (1978). Historical trends and statistics of the Southern Oscillation, El Nino, and Indonesian Droughts, Fish. Bull. 76: 663-678.

Rasmusson, E.M. (1984). El Nino: the ocean/atmosphere connection, Oceanus 27: 4-12.

Scherer, M. and H. Seitz (1980). Rare earth element distribution in Holocene and Pleistocene corals and their redistribution during diagenesis, Chem. Geol. 28: 279-289.

Shannon, R.D. (1976). Revised effective ionic radii and systematic studies of interatomic distances in Halides and Chalocogenides, Acta Crystallogr A32: 751-767.

Shaw, H.F. and G.J. Wasserburg (1985). Sm-Nd in marine carbonates and phosphates: Implications for Nd isotopes in seawater and crustal ages, Geochim. Cosmochim. Acta 49: 503-518.

Smith, R.L. (1983). Peru coastal currents during El Nino: 1976 and 1982, Science 221: 1397-1399.

Speer, J.A. (1983). Crystal chemistry and phase relations of orthorhombic carbonates. In: Carbonates: Mineralogy and Chemistry, pp. 145-189. Mineralogical Society of America, Chelsea: Michigan.

Swart, P.K., and J.A.E.B. Hubbard (1982). Uranium in scleractinian coral skeletons, Coral Reefs 1: 13-19.

Turner, P.R., M. Whitfield, and A.G. Dickson (1981). The equilibrium speciation of dissolved components in freshwater and seawater ar 25°C and 1 atm pressure, Geochim. Cosmochim. Acta 45: 855-881.

Veeh, H.H. and K.K. Turekian (1968). Cobalt, silver and uranium concentrations of reef-building corals in the Pacific Ocean, Limnol. Oceanogr. 13: 304-308.

Weber, J.N. (1974). Skeletal chemistry of scleractinian reef corals: Uptake of magnesium from seawater, Am. J. Sci. 274: 84-93.

Wedow, H. (1873). Improved cadmium recovery from flue dust, U.S.G.S. Prof. Paper 820, pp. 105-109.

Wyrtki, K. (1975). El Nino - the dynamic response of the equatorial Pacific Ocean to atmospheric forcing, J. Phy. Oceanogr. 5: 572-584.

CHAPTER 5

THERMOCLINE VENTILATION MODELS AND THE LEAD TRANSIENT IN THE WESTERN NORTH ATLANTIC

5.1 Introduction

The concentration and isotopic record of Pb in corals has revealed a 100-year history of anthropogenic perturbation in the western North Atlantic. Presently, this transient is decaying rapidly in the surface ocean, but continues to penetrate the thermocline and deep ocean. Because of the extended history and intensity of North American Pb emissions, the Sargasso Sea gyre is well suited as a location in which to model the vertical distribution of Pb. Time series measurements of Pb and ^{210}Pb near Bermuda by Boyle, Bacon and coworkers are in their fourth year; thus, a number of high quality concentration profiles are available. Additionally, the first stable Pb isotopic profile for the Atlantic Ocean is presented in this chapter.

Boyle et al. (1986) attempted to reconstruct the buildup and decline of industrial Pb in the Sargasso Sea via an adaptation of the ventilated thermocline model of Jenkins (1980). The Pb source function was assumed proportional to U.S. alkyl lead consumption, and penetration was governed by tritium and ^{3}He-modeled ventilation rates. The steady state vertical distribution of ^{210}Pb imposed an additional constraint. In successfully reproducing the general features of measured Pb concentration profiles, Boyle et al. reconfirmed the importance of lateral transport along isopycnal surfaces. However, refinements incorporating scavenging and regeneration could not be uniquely specified. This was due to uncertainties in the assumed Pb input history and expected geographic variability in Pb fluxes over outcropping winter source waters.

This chapter is an attempt to refine the conclusions of Boyle et al. by incorporating additional model constraints. Among these are the actual depositional history of industrial Pb near Bermuda as recorded by

D. strigosa, and complementary tracer systematics made possible by measurements of stable Pb isotopic ratios.

5.2 A Ventilated Thermocline Model for Stable Lead

The model selected calls exclusively on lateral transport of Pb rather than vertical exchange, except via scavenging or regeneration. Jenkins (1980) demonstrated that a vertical model incorporating either fixed or depth-dependent diffusivities could not generate observed oceanic distributions of ^{3}He and tritium simultaneously. Required vertical diffusivities of 1-10 cm^2/sec were over an order of magnitude greater than normally encountered. This suggests that transport of a conservative tracer within the thermocline by cross-isopycnal exchange is probably less than 10% of the total transport. In estimating isopycnal ventilation rates, Jenkins employed an open-ended box model in which injected tracers mix instantaneously. This is a valid approximation in the upper thermocline, however, for $\sigma_\theta > 26.8$, lateral gradients in tritium may become significant, resulting in spatially variable ventilation rates (Sarmiento, 1982).

In applying the continuum box model concept and ^{3}H-^{3}He ventilation rates to Pb, a number of simplifying assumptions can be made: (1) Pb and ^{210}Pb deposition are coupled geographically; (2) scavenging is first-order with respect to concentration; (3) ^{210}Pb regeneration is proportional to the apparent oxygen utilization rate (AOUR), and consequently, Pb regeneration is proportional to the product of the ^{210}Pb regeneration rate and the surface water $Pb/^{210}Pb$ ratio; (4) regenerated Pb bears a mixed layer isotopic signature. Assumption (1) is discussed in Chapter 1 and in Boyle et al. (1986). Assumptions (2) and (3) are not strictly necessary, but simplify the model equations. The validity of assumption (4) has not been strictly tested, but the very brief residence time and high concentrations of Pb in the mixed layer suggest this is a good approximation. The mechanisms responsible for Pb transport must

therefore satisfy three chemical tracer distributions simultaneously: ^{210}Pb, stable Pb, and stable Pb isotopes. The governing expressions are:

$$\frac{\partial C}{\partial t} = \frac{C_o(z,t) - C(z,t)}{\tau(z)} - k_1 C(z,t) + k_2 R \frac{C_o(0,t)}{A_o(0)} \quad (1)$$

$$\frac{\partial A}{\partial t} = \frac{A_o(z) - A(z,t)}{\tau(z)} - k_1 A(z,t) + k_2 R(z) + \lambda[A_{226}(z) - A(z,t)] \quad (2)$$

$$\frac{\partial I}{\partial t} = \left\{ \left(\frac{[C_o(z,t) I_o(t) + C(z,t) I(z,t)]}{[C_o(z,t) + C(z,t)]} - I(z,t) \right) / \tau(z) \quad x \right. \quad (3)$$

$$\left. \left(C(z,t) - k_2 R \frac{C_o(0,t)}{A_o(0)} \right) + \left(I_o(t) k_2 R \frac{C_o(0,t)}{A_o(0)} \right) \right\} / \quad C(z,t)$$

where:

$C(z,t)$ is the concentration of stable Pb at depth z and time t (pM)

$C_o(z,t)$ is the concentration of stable Pb in winter source waters for depth z at time t (pM)

$A(z,t)$ is the activity of ^{210}Pb at depth z and time t (dpm/100kg)

$A_o(z)$ is the activity of ^{210}Pb in winter source waters for depth z (dpm/100kg)

$A_{226}(z)$ is the activity of ^{226}Ra at depth z (dpm/100kg)

$I(z,t)$ is the isotopic composition of Pb at depth z and time t (dimensionless)

$I_o(t)$ is the isotopic composition of Pb in winter source waters at time t (dimensionless)

$\tau(z)$	is the helium-tritium ventilation age for depth z (yr)
k_1	is the first-order scavenging constant (yr^{-1})
k_2	is the ^{210}Pb regeneration rate multiplier (dpm/100kg/ml/l)
R(z)	is the apparent oxygen utilization rate (AOUR) at depth z (ml/l/yr)
λ	is the ^{210}Pb decay constant (yr^{-1})

The principal adjustable parameters are the scavenging and regeneration rate constants, k_1 and k_2. Adjustment of winter source water ^{210}Pb and Pb concentrations ($A_o(z)$ and $C_o(z)$) to allow for latitudinal variability, provides a third free parameter. Changes in $A_o(z)$ and $C_o(z)$, though, are coupled as required by assumption (1). No provision is made for geographic variability in stable Pb isotopes. ^{226}Ra concentrations are estimated from silicate measurements as per Boyle et al. (1986) using the correlation of Broecker et al. (1976). The steady state mixed layer ^{210}Pb concentration is assumed equal to the measured value, 15.46 dpm/100 kg (omitting highly variable measurements in the extreme surface layer). This value corresponds to a steady state atmospheric flux of 0.76 $dpm/cm^2/yr$ assuming a mixed layer thickness of 100 m and a residence time of 2 years. Turekian et al. (1983) estimated an average flux of 0.69 $dpm/cm^2/yr$ based on monthly rain measurements at Bermuda. Apparent oxygen utilization rates used are those of Jenkins (1980). Values of adopted model parameters are summarized in Table 5.1.

Input functions for stable Pb and Pb isotopes (C_o and I_o) consist of polynomial fits to the corresponding records recovered from D. strigosa at North Rock, Bermuda (Figures 3.1 and 3.4). Very recent Pb isotopic source signatures (1983-1986) are based on eleven measurements of surface waters at Station "S" as shown in Fig. 5.1. Seasonal isotopic variability in the surface layer is very pronounced as has been observed for Pb concentrations (Boyle et al., 1986). Interpretation of the temporal pattern, however, is not straightforward. One might expect, for example, that late summer surface Pb should strongly reflect an aeolian Pb isotopic

Table 5.1 Model parameter values

Depth (m)	σ_θ	τ* (yr)	AOUR* (ml/l/yr)	^{226}Ra** (dpm/100kg)
300	26.4	1	.459	7.5
400	26.5	8	.094	7.5
500	26.65	12	.103	8.1
600	26.8	16.5	.087	8.2
750	27.1	39	.057	8.4
950	27.5	73	.036	8.7
1100	27.68	53	.033	8.6
1400	27.79	65	.021	8.6
1700	27.82	150	.0078	8.5

* from Jenkins, 1980
**from Boyle et al., 1986

Figure 5.1 $^{206/207}Pb$ ratios in Sargasso Sea surface waters (Station "S": June 1983 - January 1986) and Bermuda rain samples (rain samples furnished by T.M. Church).

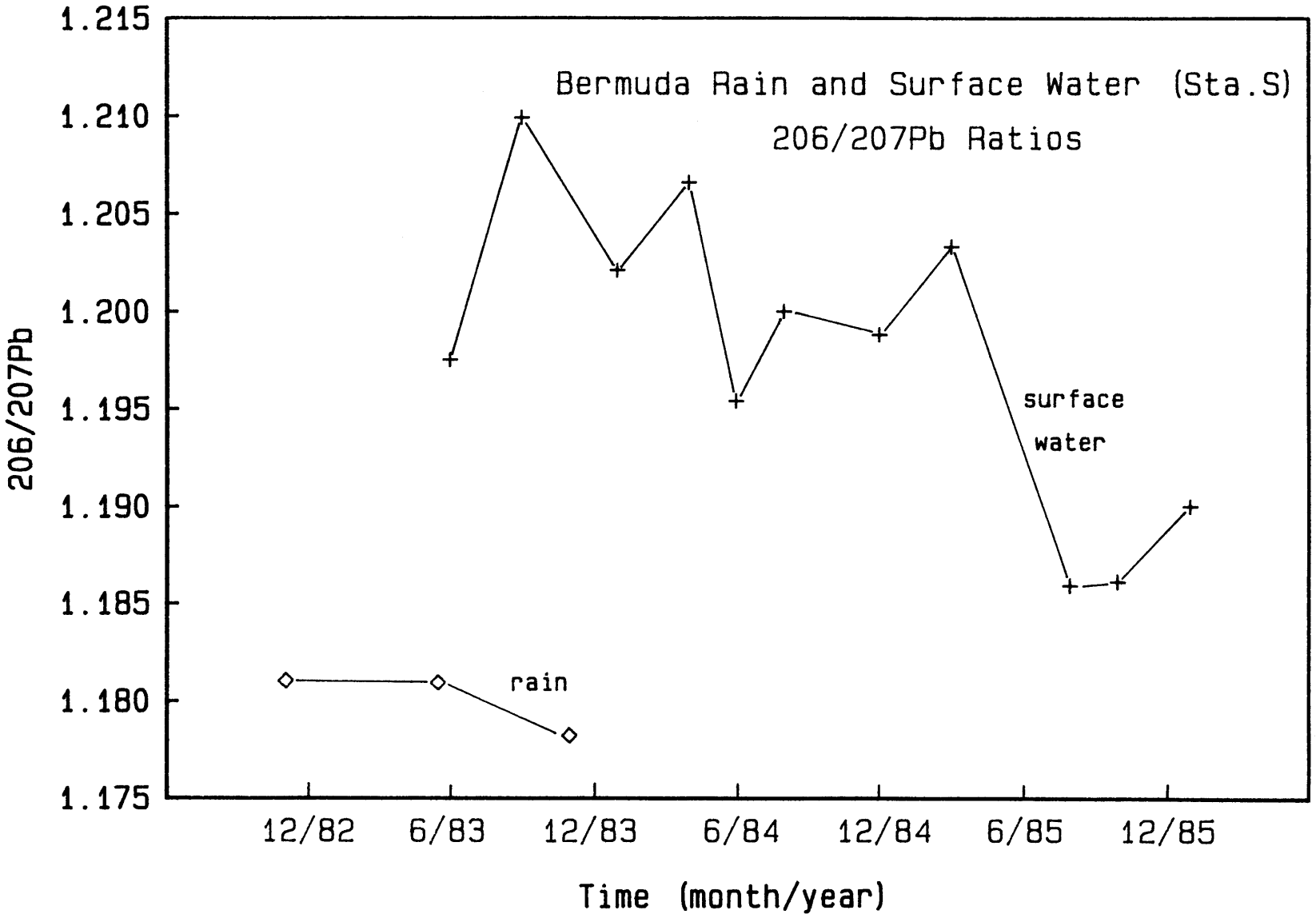
Bermuda Rain and Surface Water (Sta.S)
206/207Pb Ratios
206/207Pb
1.215
1.210
1.205
1.200
1.195
1.190
1.185
1.180
1.175
surface
water
rain
12/82
6/83
12/83
6/84
12/84
6/85
12/85
Time (month/year)

signature, since aerosols accumulate in the thin mixed layer during the summer. Conversely, winter surface waters might be expected to exhibit a slightly older signature arising from breakdown of the summer mixed layer and mixing with deeper waters. If the isotopic rain measurements included in Fig. 5.1 (samples collected in Bermuda by T.M. Church and coworkers) are indicative of the industrial Pb signature reaching the Sargasso Sea in 1983, then the surface water progression is the reverse of our expectations. Although the rain data fall significantly below concurrent surface water $^{206/207}Pb$ values, they are consistent with the observed decline in surface $^{206/207}Pb$ over 1983-1986. If one assumes: (a) surface ocean $^{206/207}Pb = 1.205$ in July 1983, (b) a 2-year Pb residence time in surface waters, (c) a constant rain $^{206/207}Pb = 1.180$, and (d) steady state conditions (a rough calculation only), projected $^{206/207}Pb$ ratios for 7/84, 7/85, and 7/86 are 1.197, 1.191, and 1.186, respectively. These values fall very close to the observed trend. The counter-intuitive isotopic changes observed in the surface layer may reflect seasonal changes in Pb source intensity. For example, gasoline Pb emissions are probably higher in summer than winter since more gasoline is consumed during summer, and since the Pb content of summer gasoline has historically been increased by 10-20% over winter usage (Shelton et al., 1982). Alternatively, high frequency alteration of surface Pb signatures may arise via storms which have travelled over different routes, thus acquiring unique Pb isotopic signatures. Storm related surface salinity changes documented by Stommel et al. (1969) and Boyle et al. (1986) are of sufficient magnitude to cause isotopic and concentration pulses in surface Pb over periods of days. Over the course of a year, these are averaged sufficiently to allow smooth annual progressions as witnessed by the coral record.

To facilitate model computations incorporating a wide variety of constraints, a finite difference scheme was used rather than exact solutions to the differential equations (Boyle et al., 1986). The model is initiated in the year 1880 assuming a negligible background Pb concentration at all depths except the surface (background surface

concentration = 15-20 pM as discussed in section 3.2). The model is stepped through time to 1986 in 0.1-year increments.

The vertical profiles against which model comparisons are drawn are given in Figs. 5.2-5.4. The stable Pb and ^{210}Pb and concentration data were accumulated over 4-6 occupations of Station "S" between 1983-1984 (Boyle et al., 1986). The isotopic data represent single mass spectrometric determinations of Boyle's "trace element vane" samples which were collected in 1984 and pooled to yield sufficient volumes. Depth ranges over which isotopic samples were combined are illustrated in Fig. 5.3 along with weighted mean depths. Plotted data points are the actual $^{206/207}Pb$ ratios determined by mass spectrometry. The error bars are back-calculated maximum offsets attributable to reagent and sample loading blanks.

5.2.1 Conservative evolution

In the simplest possible model, Pb is conservative (no scavenging or particulate regeneration) and winter source waters are assigned the same ^{210}Pb and Pb concentrations as those measured at Station "S". The results are shown in Fig. 5.5. First apparent is an overestimation of ^{210}Pb in waters below 300 m, relative to the measured distribution (Fig. 5.5a). This result implies that the assumption of uniform source water concentrations is likely to be inaccurate. The model predictions for stable Pb (Fig. 5.5c) show excesses throughout the same depth range, suggesting that adjustment of source water concentrations should improve the model fits to ^{210}Pb and Pb simultaneously. Fig. 5.5b depicts the historic evolution of Pb concentrations in the Sargasso Sea according to this simple conservative model. Note that the American phase-out of leaded gasoline has caused a rapid reversal in the concentration profile in the upper water column since 1972. While the shape of the 1984 model distribution (Fig. 5.5c) is similar to that derived by Boyle et al. assuming an alkyl Pb source function, the entire profile is offset toward higher values. This is a consequence of a substantial anthropogenic Pb

Figure 5.2 Sargasso Sea Pb concentrations (unfiltered samples) (Station "S" : April 1984, June 1984, and September 1984; from Boyle et al., 1986).

Figure 5.3 Sargasso Sea $^{206/207}Pb$ ratios (Station "S": samples pooled from 4 station occupations in 1984). Data points represent actual $^{206/207}Pb$ values determined by mass spectrometry (see Table E.2). Error bars represent maximum possible offsets due to reagent + loading blanks.

Figure 5.4 Sargasso Sea ^{210}Pb concentrations (Station "S": June 1983 - September 1984; from Boyle et al., 1986).

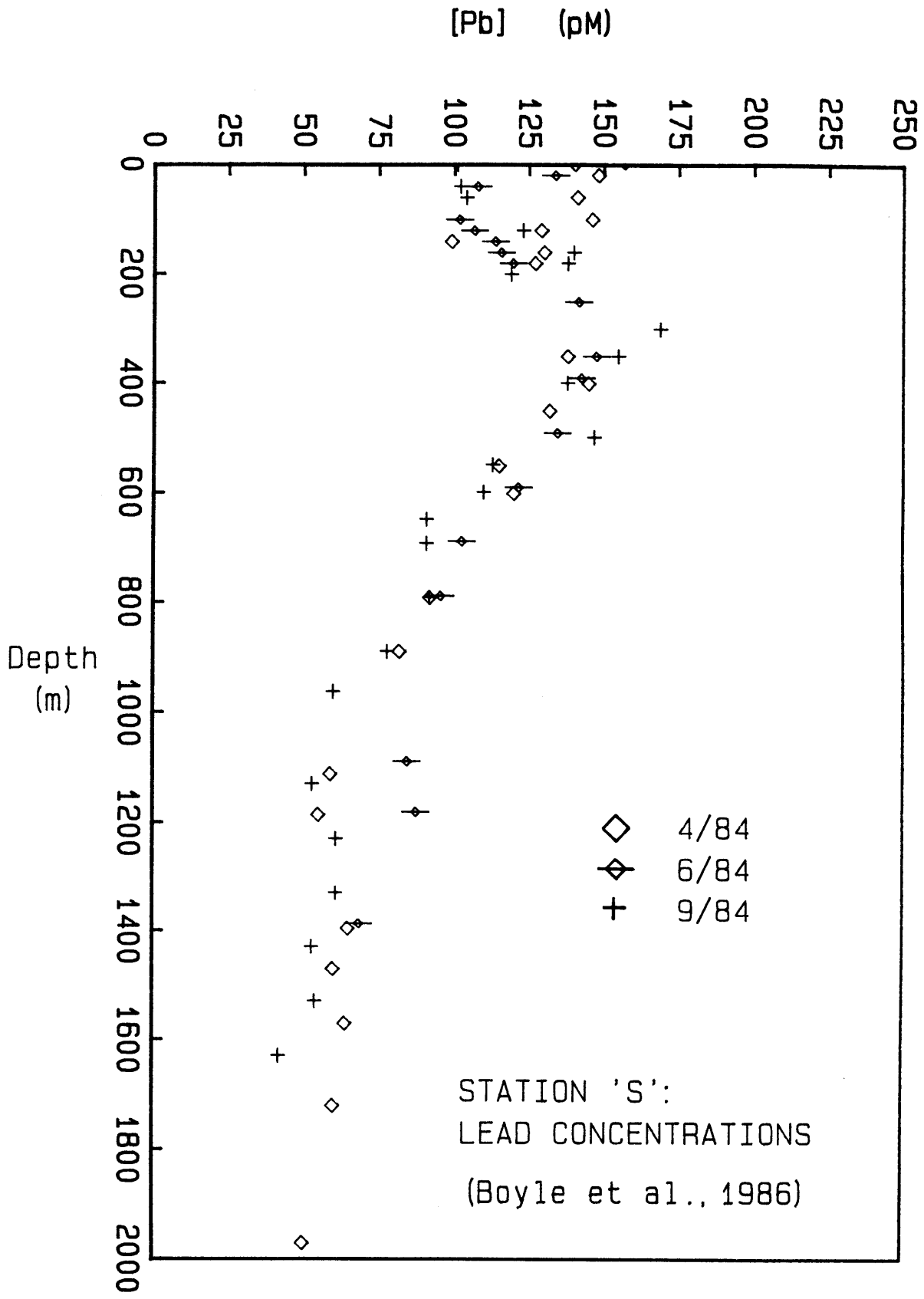
[Pb] (pM)
0
25
50
75
100
125
150
175
200
225
250
Depth (m)
0
200
400
600
800
1000
1200
1400
1600
1800
2000
4/84
6/84
9/84
STATION 'S':
LEAD CONCENTRATIONS
(Boyle et al., 1986)

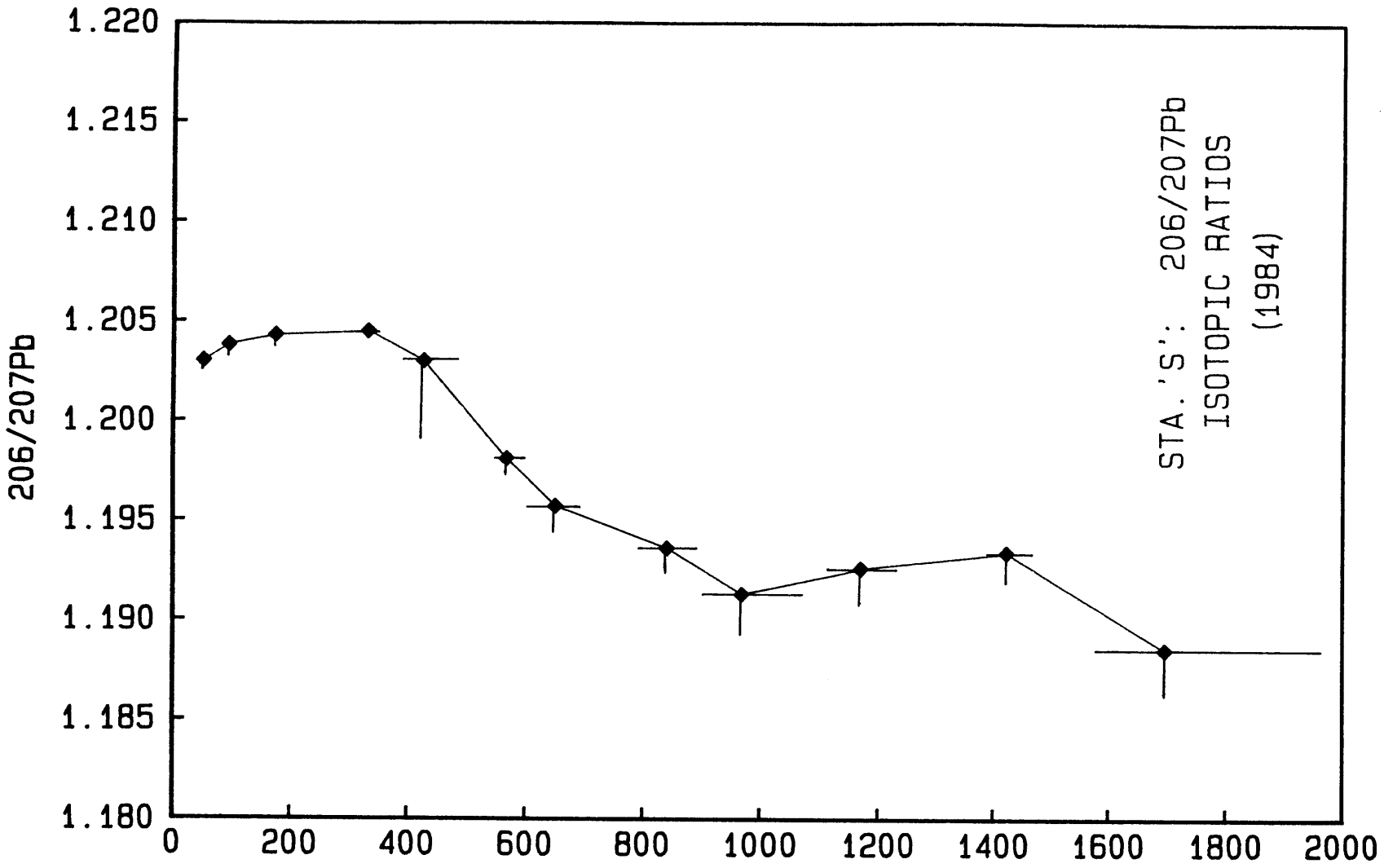
1.220
1.215
1.210
1.205
1.200
1.195
1.190
1.185
1.180
206/207Pb
0
200
400
600
800
1000
1200
1400
1600
1800
2000
STA. 'S': 206/207Pb
ISOTOPIC RATIOS
(1984)

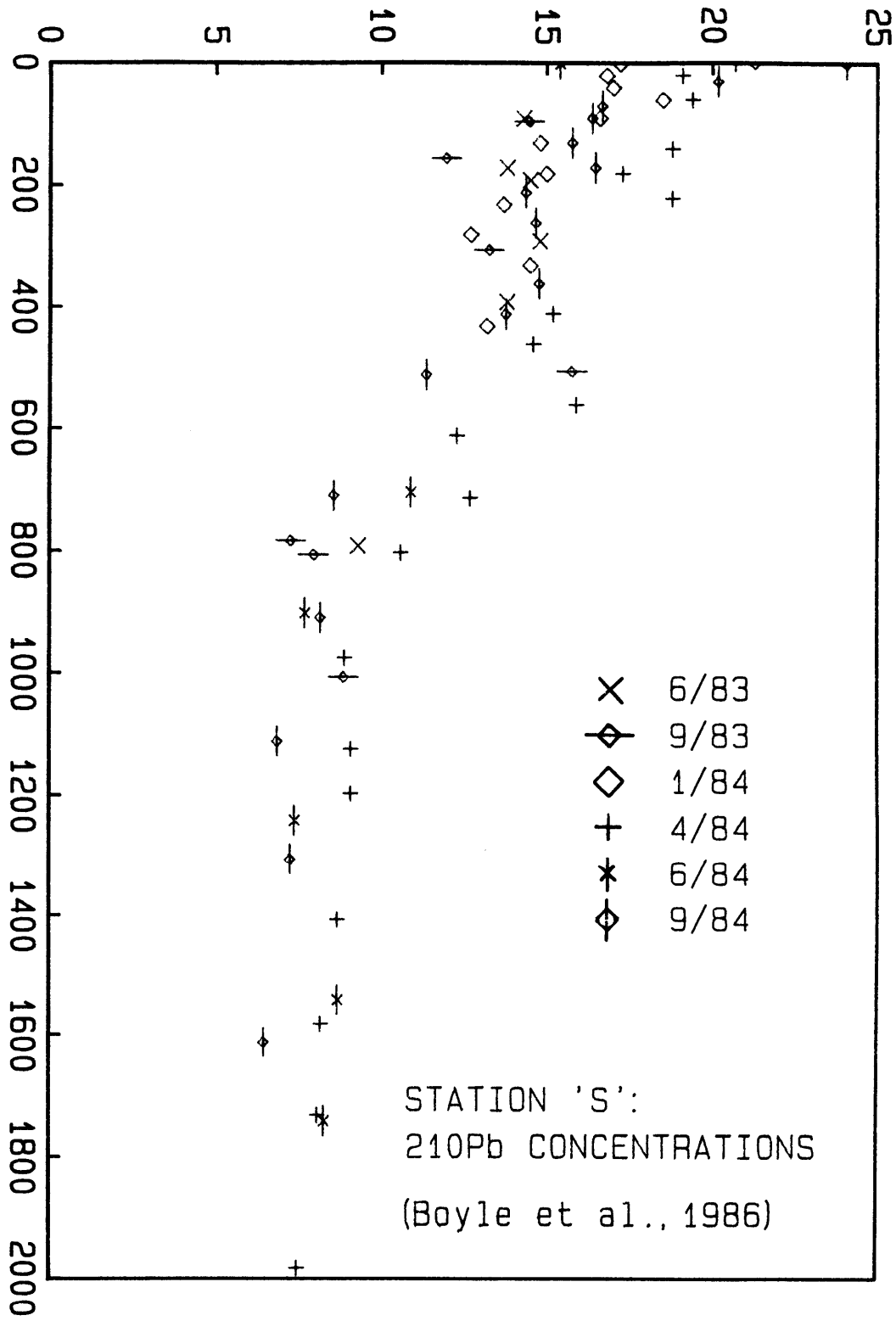
[210Pb] (dpm/100kg)
0
5
10
15
20
25
0
200
400
600
800
1000
1200
1400
1600
1800
2000
6/83
9/83
1/84
4/84
6/84
9/84
STATION 'S':
210Pb CONCENTRATIONS
(Boyle et al., 1986)

Conservative Evolution

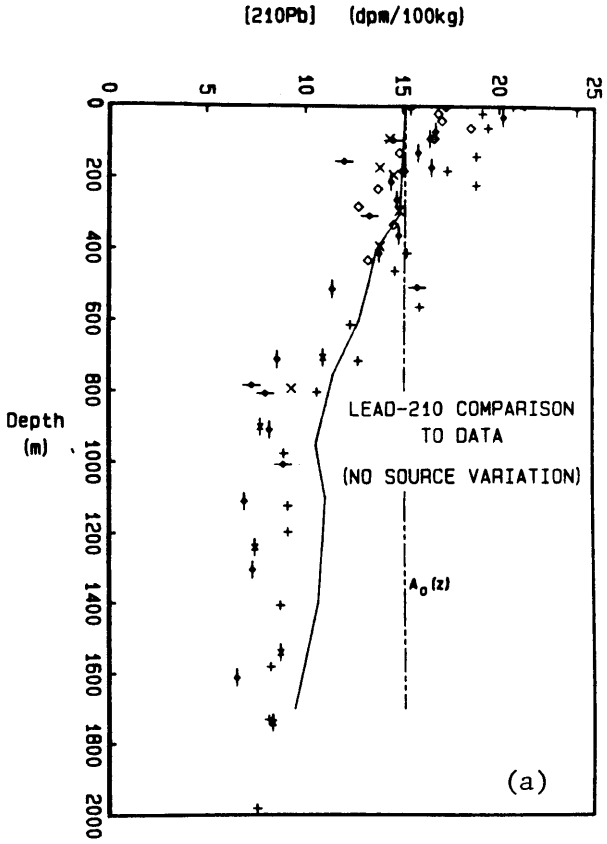

Figure 5.5 Conservative evolution model results:

(a) Model ^{210}Pb profile assuming pure physical ventilation with no source water ^{210}Pb concentration adjustment.
(b) 20th century model time evolution of stable Pb concentrations.
(c) Model 1984 Pb concentration distribution compared to data of Figure 5.2.
(d) 20th century model time evolution of stable Pb isotope ($^{206/207}Pb$) distributions.
(e) Model 1984 $^{206/207}Pb$ distribution compared to data of Fig. 5.3.

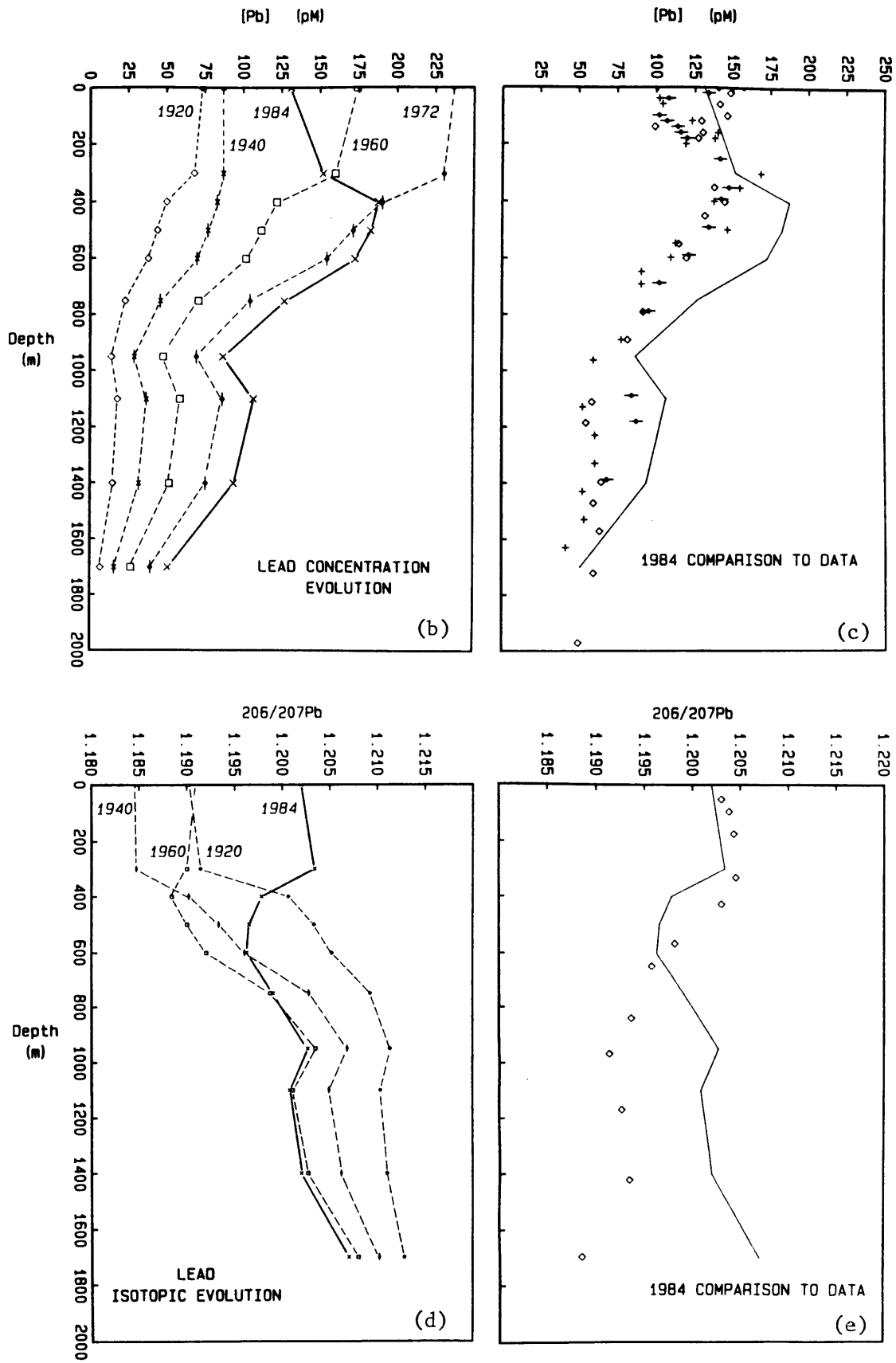
[Pb] (pM)
1920
1940
1984
1960
1972
Depth (m)
LEAD CONCENTRATION EVOLUTION
(b)
[Pb] (pM)
1984 COMPARISON TO DATA
(c)
206/207Pb
1940
1960
1920
1984
Depth (m)
LEAD ISOTOPIC EVOLUTION
(d)
206/207Pb
1984 COMPARISON TO DATA
(e)

flux which originated prior to the advent of leaded gasoline in 1923, and continues today (iron, steel, non-ferrous metals prodouction, coal combustion, etc.). More problematic than the concentration discrepancies between model and data, however, are the isotopic differences which appear to grow with increasing depth. The isotopic data below 600 m (Fig. 5.5e) indicate the presence of substantial amounts of Pb bearing low $^{206/207}Pb$ signatures ($\approx$ 1.190-1.195). Upon consulting the historical record in D. strigosa (Fig. 3.4), this implicates Pb of 1920's-to-1950's vintage. The question is how to transport Pb of relatively recent origin to waters which ventilate over 40-100 year time scales. Additionally, the quantities transported must be sufficient to erase the signature of older (including background) more radiogenic Pb.

5.2.2 Conservative evolution with source tuning

Remaining within a conservative framework, ^{210}Pb concentrations in winter source waters are next adjusted so as to achieve a better fit to the steady state ^{210}Pb distribution. Actual variations likely occur as a result of flux dependence on latitude (σ_θ = 26.4-27.8 isopycnals outcrop between 38° and 65°N) and variable surface water residence times, however, these have not been documented in the western North Atlantic. ^{210}Pb in western North Pacific surface waters exhibits strong latitudinal dependence in declining from 20-25 dpm/100 kg at 30°N to less than 15 dpm/100 kg north of 45°N (Nozaki et al., 1976). Wind patterns, however, are very different between the North Pacific and North Atlantic (Figs. 1.1 and 1.2). North American westerlies appear capable of delivering a more latitudinally-uniform ^{210}Pb flux than that observed over the western N. Pacific. In the absence of actual wintertime measurements, source water "tuning" in all subsequent scenarios will be based upon the steady state ^{210}Pb distribution at Station "S".

The results of the best-fit ^{210}Pb source variation model are shown in Figure 5.6. Required surface ocean ^{210}Pb boundary conditions (Fig. 5.5a) remain near 15 dpm/100 kg down to 600 m, but fall off to near 5 dpm/100 kg

at 1700 m. When applied to the stable Pb model (Figs. 5.6b & c), these severe source corrections overcompensate for the excesses observed in the simple conservative model and result in a predicted Pb deficiency between 800 - 1700 m. At the same time, relatively minor positive adjustments (1-10%) at 400, 500, and 600 m cause a pronounced subsurface maximum to appear in the stable Pb profile. The source tuning effect is amplified in this portion of the water column because Pb concentrations here are highest. Since the model is initiated with no Pb below the mixed layer, the isotopic evolution (Figs. 5.6d & e) reflects a pure coral-dictated end-member and therefore remains unchanged. Before considering chemical mechanisms which would alter the isotopic fit, it is useful to explore in greater detail the sensitivity of the concentration model to additional refinements.

The model represented by Fig. 5.7 slightly relaxes the ^{210}Pb fit at 400-600 m since the stable Pb response is highly sensitive to source adjustment in this interval, and the profile is not well constrained throughout. The subsurface maximum remains (Figs. 5.7b and c), but is greatly moderated. The isotopic progression is as before.

Though the general features of the Pb concentration model are clearly correct, discrepancies below 800 m and discordant isotopic predictions reveal that a conservative model cannot satisfactorily account for all three Pb distributions. Even removal of the Pb-^{210}Pb coupling assumption would do nothing to affect the Pb isotope model predictions unless a vertical exchange mechanism were introduced.

5.2.3 Scavenging with source tuning

Inclusion of a scavenging term in the model significantly alters the source corrections required to fit the ^{210}Pb profile (Fig. 5.8a). If $k_1 = 0.01\ yr^{-1}$ (corresponding to a Pb residence time of 100 years with respect to scavenging removal), surface ^{210}Pb boundary conditions for the deepest isopycnals approximate 12 dpm/100 kg. This is close to the average value of 11.2 dpm/100 kg (n=4) reported by Bacon et al. (1978) for

Conservative Evolution + Source Tuning to Pb-210 (Model I)

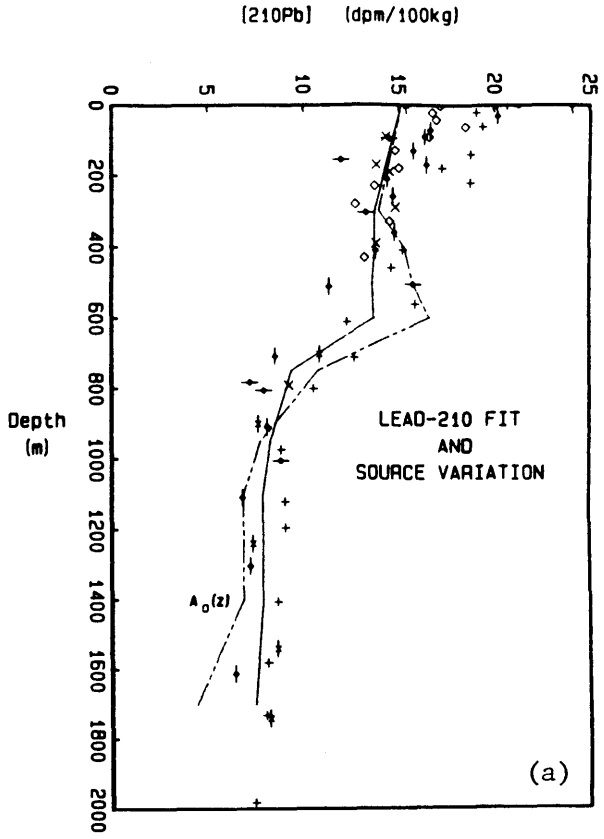

Figure 5.6 Conservative evolution + source tuning model I results:

(a) Model ^{210}Pb profile assuming pure physical ventilation with source water concentration adjustments to fit steady state ^{210}Pb profile.
(b) 20th century model time evolution of stable Pb concentrations.
(c) Model 1984 Pb concentration distribution compared to data of Figure 5.2.
(d) 20th century model time evolution of stable Pb isotope ($^{206/207}Pb$) distributions.
(e) Model 1984 $^{206/207}Pb$ distribution compared to data of Fig. 5.3.

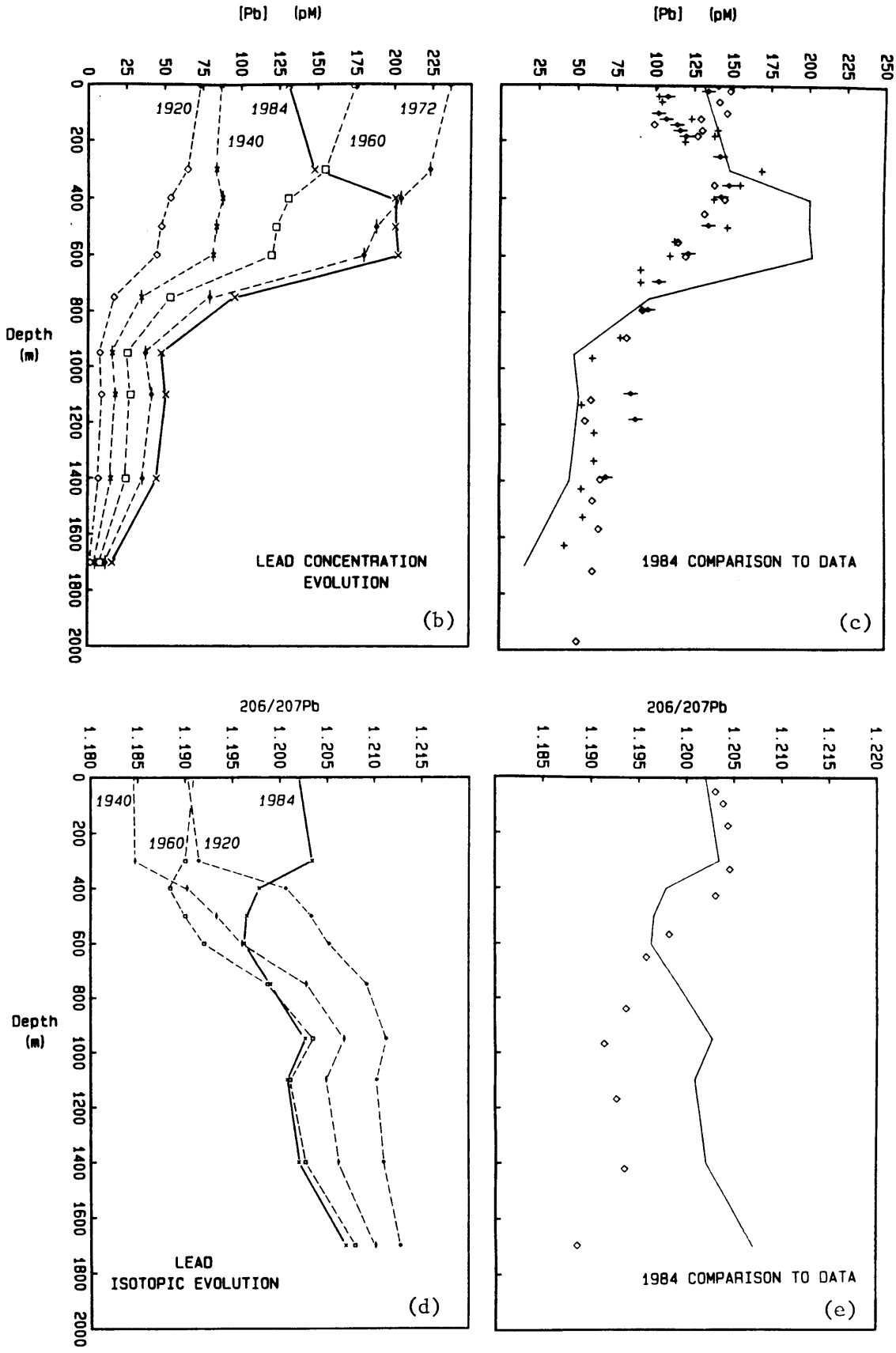
[Pb] (pM)
Depth (m)
1920
1940
1984
1960
1972
LEAD CONCENTRATION EVOLUTION
(b)
[Pb] (pM)
1984 COMPARISON TO DATA
(c)
206/207Pb
1940
1960
1920
1984
LEAD ISOTOPIC EVOLUTION
(d)
206/207Pb
1984 COMPARISON TO DATA
(e)

Conservative Evolution + Source Tuning to Pb-210 (Model II)

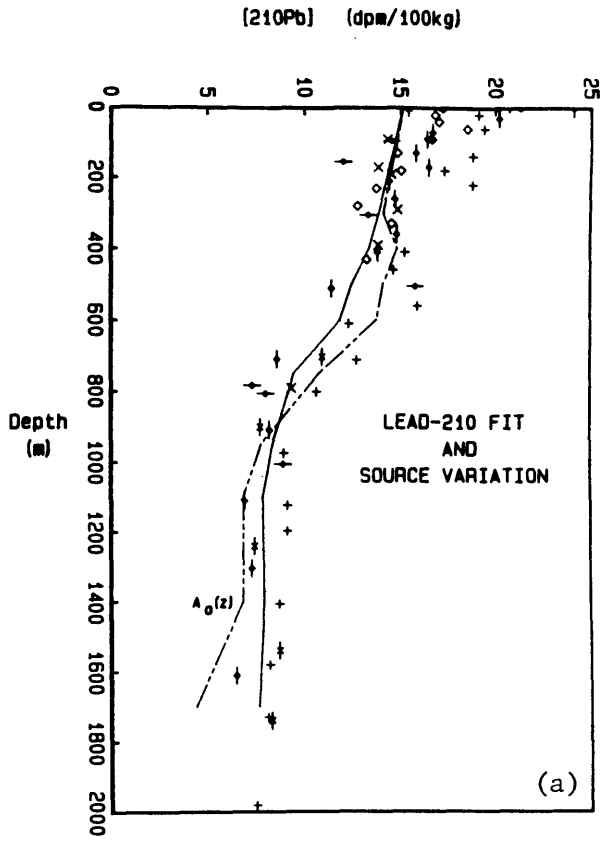

Figure 5.7 Conservative evolution + source tuning model II results:

(a) Model ^{210}Pb profile assuming pure physical ventilation with source water concentration adjustments to fit steady state ^{210}Pb profile. Fit between 400-600 m is relaxed slightly to improve stable Pb model fit.
(b) 20th century model time evolution of stable Pb concentrations.
(c) Model 1984 Pb concentration distribution compared to data of Figure 5.2.
(d) 20th century model time evolution of stable Pb isotope ($^{206/207}Pb$) distributions.
(e) Model 1984 $^{206/207}Pb$ distribution compared to data of Fig. 5.3.

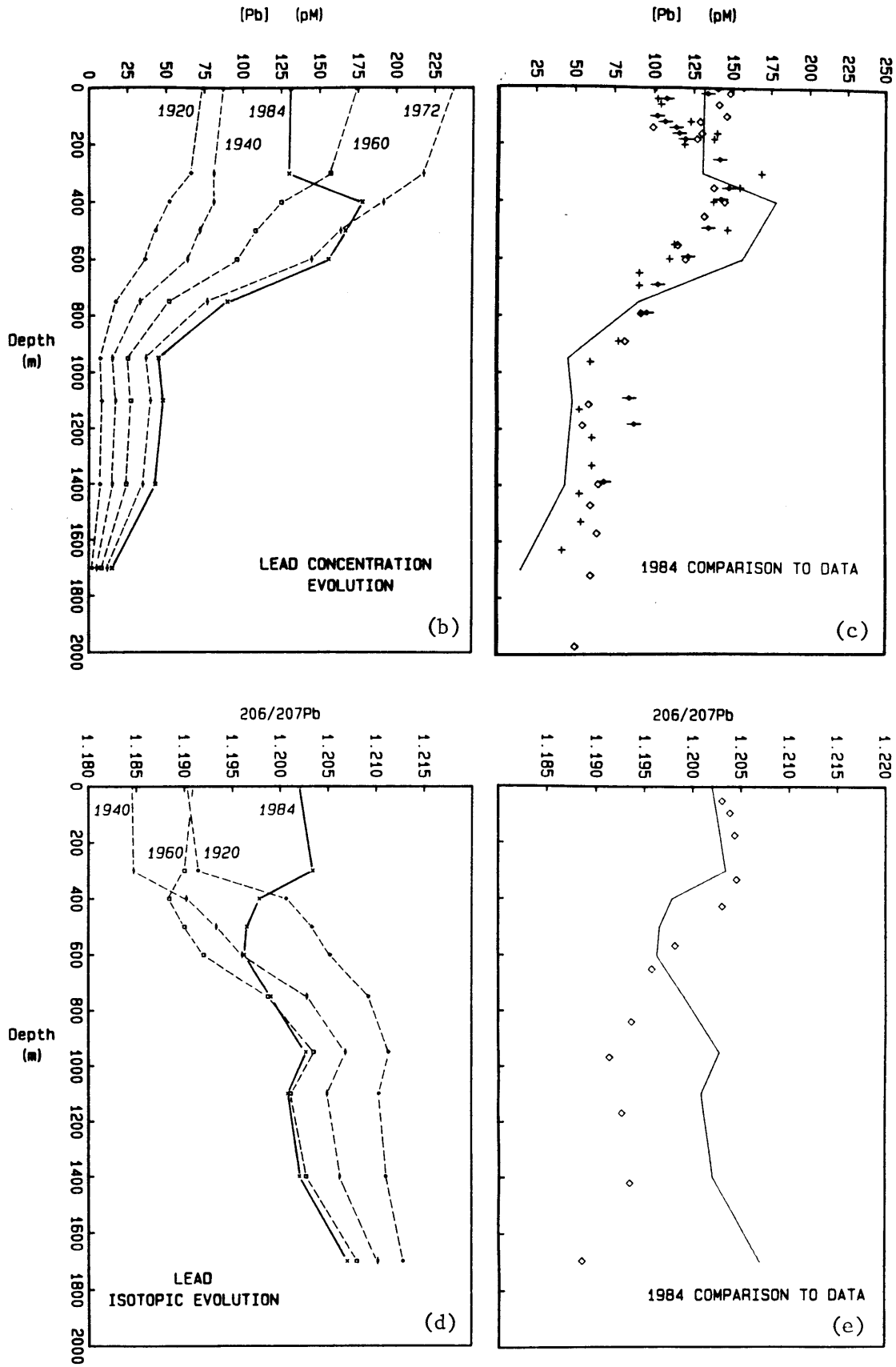
[Pb] (pM)
Depth (m)
1920
1940
1984
1960
1972
LEAD CONCENTRATION EVOLUTION
(b)
[Pb] (pM)
1984 COMPARISON TO DATA
(c)
206/207Pb
1940
1960
1920
1984
LEAD ISOTOPIC EVOLUTION
(d)
206/207Pb
1984 COMPARISON TO DATA
(e)

Scavenging

+

Source Tuning
to Pb-210

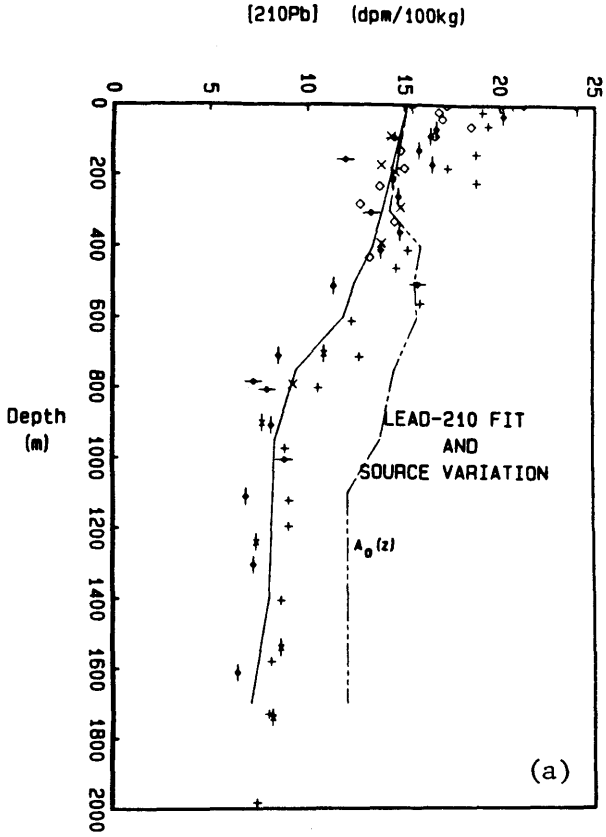

Figure 5.8 Scavenging + source tuning model results:

(a) Model ^{210}Pb profile assuming scavenging constant k1 = 0.01 (corresponding to 100-yr residence time) with source water concentration adjustments to fit steady state ^{210}Pb profile.
(b) 20th century model time evolution of stable Pb concentrations.
(c) Model 1984 Pb concentration distribution compared to data of Figure 5.2.
(d) 20th century model time evolution of stable Pb isotope ($^{206/207}Pb$) distributions. Note that there is no change from the earlier conservative models as a result of simple scavenging.
(e) Model 1984 $^{206/207}Pb$ distribution compared to data of Fig. 5.3. Again, there is no change from Figs. 5.6 (e) or 5.7 (e).

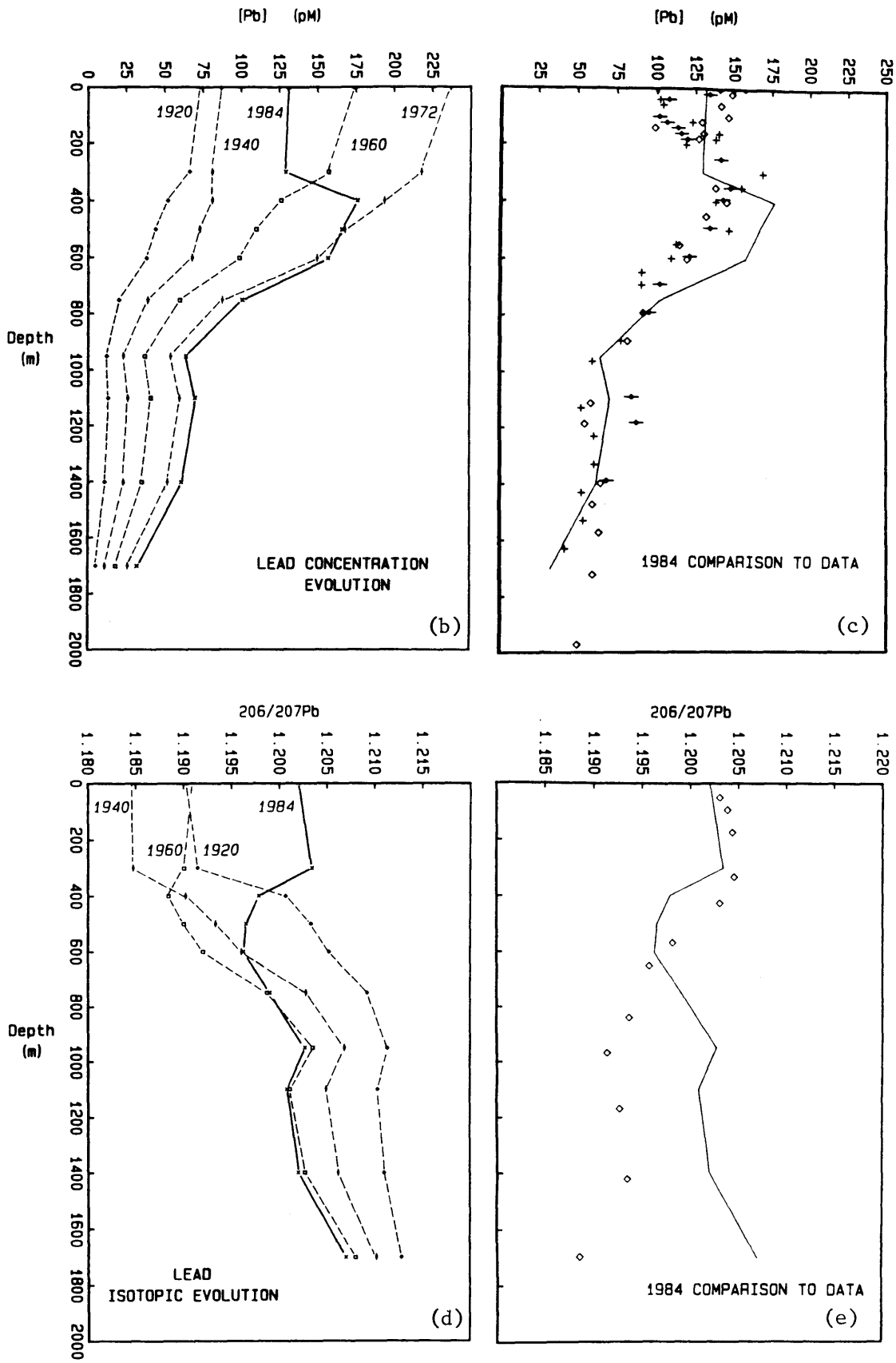
[Pb] (pM)
0 25 50 75 100 125 150 175 200 225
1920
1940
1984
1960
1972
Depth (m)
0 200 400 600 800 1000 1200 1400 1600 1800 2000
LEAD CONCENTRATION EVOLUTION
(b)
[Pb] (pM)
25 50 75 100 125 150 175 200 225 250
1984 COMPARISON TO DATA
(c)
206/207Pb
1.180 1.185 1.190 1.195 1.200 1.205 1.210 1.215
1940
1984
1960
1920
Depth (m)
0 200 400 600 800 1000 1200 1400 1600 1800 2000
LEAD ISOTOPIC EVOLUTION
(d)
206/207Pb
1.185 1.190 1.195 1.200 1.205 1.210 1.215 1.220
1984 COMPARISON TO DATA
(e)

Labrador Sea waters at 90-100 m depth. One-hundred years is also consistent with the range of reported deep water ^{210}Pb residence times (50-100 yrs; see section 1.2.1). This refinement shifts the 1984 model Pb profile (Fig. 5.8c) very nearly within the range of measured values. Departures remain at 400-600 m (predicted excess) and 1700 (predicted deficit). In the absence of endmember mixing (no pre-existing Pb at depth), simple scavenging does not result in a redistribution of Pb isotopes; thus, the isotopic evolution (Figs. 5.8d & e) again remains unchanged from previous schemes. The enhanced concentration and isotopic deviations from data at 1700 m appear to be associated with the very long ^{3}H-^{3}He ventilation age (150 yrs) modeled by Jenkins (1980). The estimated error in age at this depth is $\pm$25 yrs. Substitution of τ = 125 yrs at 1700 m results in more uniform behavior at depth, but a yet smaller τ would benefit the predicted distributions even more.

5.2.4 Scavenging, regeneration, and source tuning

In order to influence the conservative isotopic distribution of Pb in the Sargasso Sea, a means of vertical exchange or non-uniform mixing of Pb along isopycnal surfaces is necessary. The most obvious mechanism which accomplishes this is particulate Pb regeneration.

In Model I (Fig. 5.9), a ^{210}Pb regeneration rate multiplier of 2 dpm/100 kg/ml O_2/l is selected, which corresponds to a net regeneration efficiency of 12% throughout the water column to 1700 m. On the basis of ^{210}Pb profiles from the North Equatorial Atlantic, Bacon et al. (1976) estimated a recycling efficiency of about 8% for ^{210}Pb between 50-400 m depth. To offset deep water increases in Pb concentration due to regenerated Pb, k_1 is increased to 0.015 yr^{-1} (corresponding to a 67-year Pb residence time). Adjustments to source water ^{210}Pb concentrations (Fig. 5.9a) are more severe than in the simple scavenging model, however, they are still within reason. A large correction at 1700 m is again apparent as a consequence of the 150-year ventilation rate assumed at this depth.

The direction of the resultant shift in deep water isotopic signatures (Fig. 5.9e) is as desired, although the magnitude of the shift is not large enough to accord with the data. Displacement of deep waters toward lower $^{206/207}Pb$ ratios as a result of regeneration could have been anticipated on the basis of the historical coral record (Fig. 3.4). Since flushing times for waters below 900 m are greater than 50 years, Pb in these waters would be expected to possess a relatively old isotopic signature in the absence of regeneration ($^{206/207}Pb \approx 1.200$-$1.205$). By introducing a regeneration term at all depths in the model, more recent source signatures ($^{206/207}Pb \approx 1.190$ between 1920-1960) act to drive the deep water ratios toward lower values. The effect, however, is reversed after 1960 as fallout $^{206/207}Pb$ ratios climb back toward higher more radiogenic values. This explains why the model curve for the year 1960 (Fig. 5.9d) falls toward lower $^{206/207}Pb$ relative to 1984 in deep waters. Although a dramatic redistribution of Pb isotopes is achieved, the stable Pb concentration profile changes very little as a result of regeneration. The reason is that Pb added by regeneration at a given depth is compensated by reduced Pb introduced by ventilation (as dictated by ^{210}Pb tuning). Both of these fluxes are first order with respect to the source water concentration, $C_o(z,t)$ as seen in equation (1).

If a 12% net Pb recycling efficiency improves the isotopic fit so substantially, an even greater degree of regeneration might be expected to yield a very close fit to the data. Model II (Fig. 5.10) shows that this is not the case. In this scheme, the proportion of regenerated Pb is nearly doubled ($k_2 = 3.5$; equivalent to 20% Pb recycling efficiency to 1700 m) and scavenging is adjusted ($k_1 = 0.025$; corresponding to a residence time of 40 years) to moderate necessary source water adjustments to ^{210}Pb and Pb. Once again, the stable Pb profile is largely unaltered, but the same holds for the 1984 $^{206/207}Pb$ profile. The isotopic improvement over Model I (12% net regeneration) is only about 0.0004 units toward lower $^{206/207}Pb$. Apparently, a point of diminishing returns has been reached insofar as adjusting subsurface isotopic signatures through

Scavenging

+

Regeneration

+

Source Tuning
to Pb-210

(Model I)

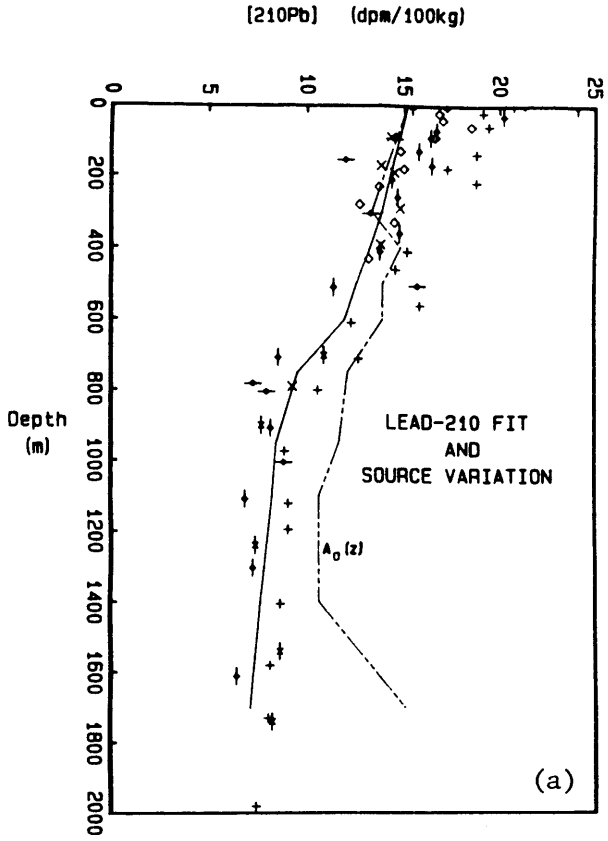

Figure 5.9 Scavenging + regeneration + source tuning model I results:

(a) Model ^{210}Pb profile assuming regeneration rate multiplier k2 = 2 dpm/100 kg/ml/l (equivalent to net recycling efficiency of 12% through upper 1700 m). Scavenging constant is enhanced slightly to k1 = 0.015 (corresponding to 67-yr residence time) in order to moderate necessary source water concentration adjustments based on steady state ^{210}Pb profile.

(b) 20th century model time evolution of stable Pb concentrations.

(c) Model 1984 Pb concentration distribution compared to data of Figure 5.2.

(d) 20th century model time evolution of stable Pb isotope ($^{206/207}Pb$) distributions.

(e) Model 1984 $^{206/207}Pb$ distribution compared to data of Fig. 5.3. Note the improved model agreement with data resulting from moderate scavenging.

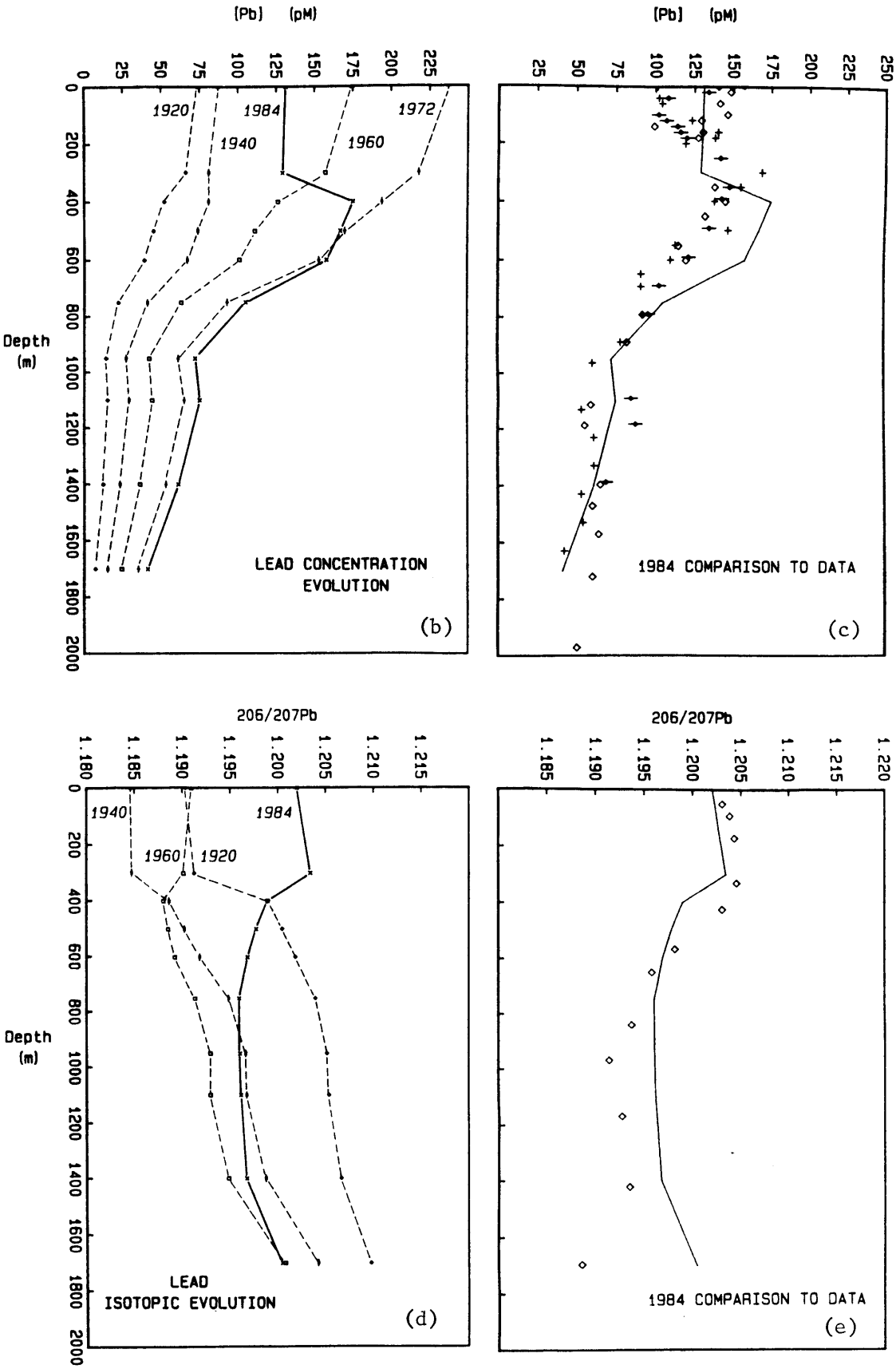
[Pb] (pM)
0 25 50 75 100 125 150 175 200 225
Depth (m)
0 200 400 600 800 1000 1200 1400 1600 1800 2000
1920
1940
1984
1960
1972
LEAD CONCENTRATION EVOLUTION
(b)
[Pb] (pM)
25 50 75 100 125 150 175 200 225 250
1984 COMPARISON TO DATA
(c)
206/207Pb
1.180 1.185 1.190 1.195 1.200 1.205 1.210 1.215
Depth (m)
0 200 400 600 800 1000 1200 1400 1600 1800 2000
1940
1984
1960
1920
LEAD ISOTOPIC EVOLUTION
(d)
206/207Pb
1.185 1.190 1.195 1.200 1.205 1.210 1.215 1.220
1984 COMPARISON TO DATA
(e)

Scavenging

+

Regeneration

+

Source Tuning
to Pb-210

(Model II)

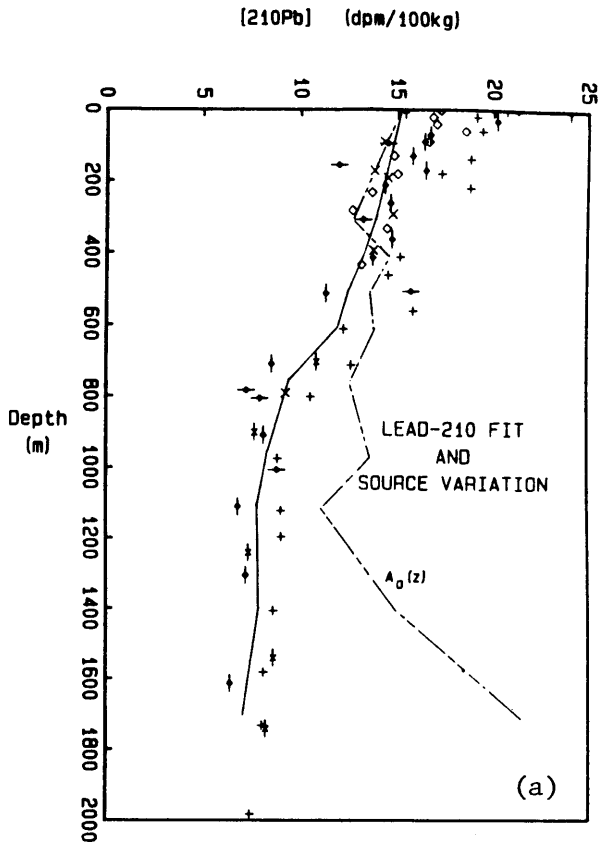

Figure 5.10 Scavenging + regeneration + source tuning model II results:

(a) Model ^{210}Pb profile assuming regeneration rate multiplier k2 = 3.5 dpm/100 kg/ml/l (equivalent to net recycling efficiency of 20% through upper 1700 m). Scavenging constant is increased to k1 = 0.025 (corresponding to 40-yr residence time) in order to moderate necessary source water concentration adjustments based on steady state ^{210}Pb profile.

(b) 20th century model time evolution of stable Pb concentrations.

(c) Model 1984 Pb concentration distribution compared to data of Figure 5.2.

(d) 20th century model time evolution of stable Pb isotope ($^{206/207}Pb$) distributions.

(e) Model 1984 $^{206/207}Pb$ distribution compared to data of Fig. 5.3. Note that enhanced scavenging over Model I (12% recycling efficiency) does not further improve model fit to data. See text for discussion of possible alternative mechanisms.

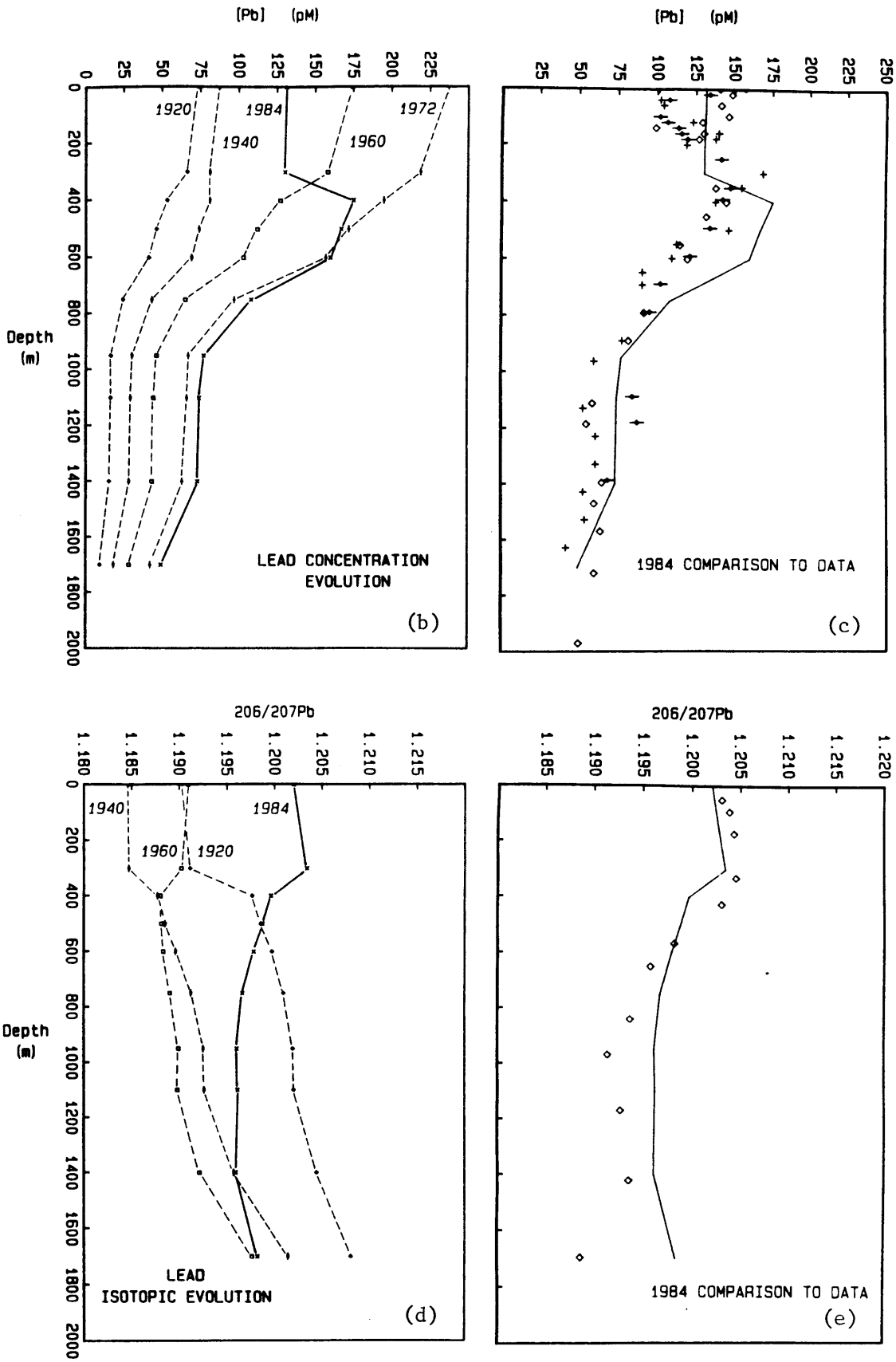
[Pb] (pM)
Depth (m)
1920
1940
1984
1960
1972
LEAD CONCENTRATION EVOLUTION
(b)
[Pb] (pM)
1984 COMPARISON TO DATA
(c)
206/207Pb
1940
1960
1920
1984
LEAD ISOTOPIC EVOLUTION
(d)
206/207Pb
1984 COMPARISON TO DATA
(e)

addition of surface Pb. Further enhanced regeneration is useless; besides, Model II is already near the limit of credibility with respect to observed scavenging and regeneration behavior for ^{210}Pb.

Evidence of a particulate transfer mechanism was sought directly via isotopic measurements of particles collected in trace element-clean, free-drifting sediment traps. Samples collected on two deployments (August 1984 and March 1985) were barely abundant enough to allow measurement of Pb isotopic ratios at 100, 400, and 860 m (Fig. 5.11). Curiously, the data from the two deployments are contradictory. The August 1984 sample from 860 m possesses the same $^{206/207}Pb$ ratio as particles collected at 100 m. This suggests that particles do not continuously accumulate Pb as they transit the water column. Loss of original Pb picked up from the mixed layer, though, may occur without altering the isotopic state of the particles. Thus, the August 1984 particulate isotope distribution is consistent with the requirements of a regeneration model. Analyses of the March 1985 samples, on the other hand, suggest the complete opposite situation. From these data, one would conclude that falling particles exchange Pb rapidly and continuously so as to maintain isotopic equilibrium with surrounding waters, throughout the water column. Such a continuous exchange process would also shift model $^{206/207}Pb$ ratios in the desired direction, but the net effect would be very small. Additional measurements are needed to characterize the particulate Pb exchange process more clearly. Standard large-scale trap deployments, however, will probably not serve unless careful attention is directed toward contamination control. Three measurements of material from Deuser's PARFLUX Bermuda time series resulted in anomalously low $^{206/207}Pb$ ratios which have never before existed in surface waters of the western North Atlantic (see Table F.1).

The residual discrepancy between the observed and modeled Pb isotopic distribution with depth may be attributable to a variety of factors. (1) Foremost is the possibility of spatially variable isotopic fluxes. Unlike Pb concentration boundary conditions which can be tuned against the

Figure 5.11 $^{206/207}Pb$ ratios of particulate material captured by free-drifting trace element sediment traps at 100, 400, and 860 m depths. Data points are mass spectrometric values (see Table F.1). Error bars represent maximum possible offsets due to reagent + loading blank. August 1984 deployment was at 33° 40'N, 57° 37'W (400 miles northeast of Bermuda). March 1985 traps were deployed at Station "S".

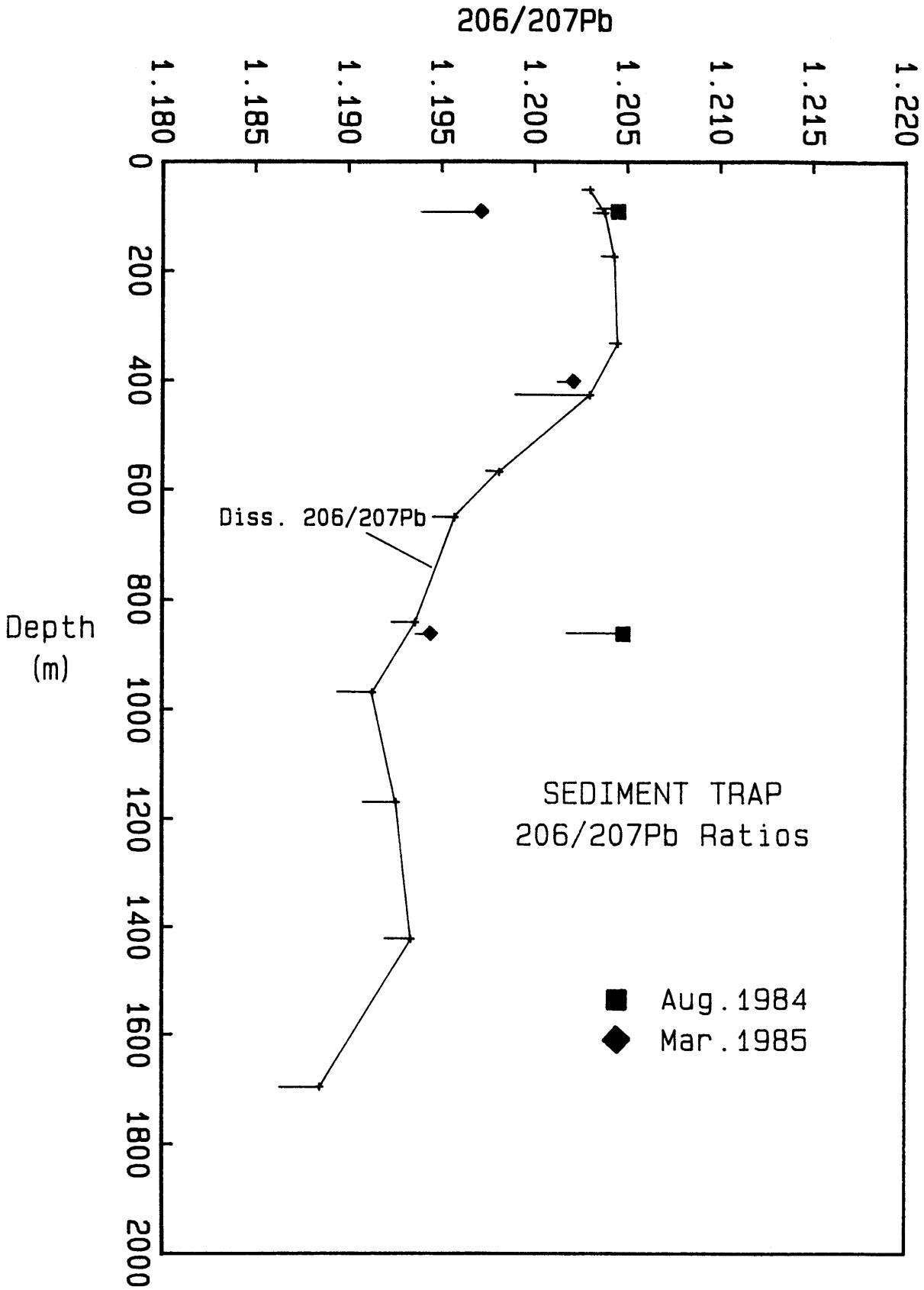
206/207Pb
1.180
1.185
1.190
1.195
1.200
1.205
1.210
1.215
1.220
0
200
400
600
800
1000
1200
1400
1600
1800
2000
Depth
(m)
Diss. 206/207Pb
SEDIMENT TRAP
206/207Pb Ratios
Aug.1984
Mar.1985

steady state ^{210}Pb profile, no constraints exist for tuning of isotopic boundary conditions. Boyle et al. (1986) have proposed mapping the distribution of source water concentrations of Pb and ^{210}Pb along winter isopycnal outcrops. This will provide a critical new constraint on the Pb concentration tracer. Mapping of Pb isotope distributions should be performed concurrently, but corrections may prove more difficult to extrapolate backwards in time. (2) A second mechanism not incorporated into the ventilated thermocline model is diapycnal mixing. This model basis would call for lateral advective/diffusive transport and acknowledge the existence of concentration and isotopic gradients along isopycnals, particularly in deeper waters ($\sigma_\theta > 26.8$). In a general sense, this type of model should reduce the role of newer inputs to the surface boundary since these will require a finite time to travel laterally. In Jenkins' "continuum box model", new inputs are instantaneously and uniformly absorbed along the entire length of an isopycnal surface. In terms of the stable Pb isotope problem, a de-emphasis of very recent Pb inputs ($^{206/207}Pb$ from 1965-1984 $\approx$ 1.195-1.205) should allow a model scheme incorporating regeneration to match the measured Pb isotopic distribution more closely. (3) A third possible variation of the thermocline ventilation model might introduce time dependency for ventilation rates. Jenkins (1983) demonstrated decadal variations in water mass renewal rates in examining historic records of salinity in the Sargasso Sea. Reconstructed renewal rates along shallow isopycnals (<500 m) near Bermuda show 2-fold variations over the past 30 years. In the deeper water column where the modeled Pb isotopic distribution is in question, however, temporal variations in ventilation rates are probably small. At best, we might adjust Jenkins' ^{3}H-^{3}He ventilation rates, but varying these rates over time for $\sigma_\theta > 26.7$ would be arbitrary. Simple hastening or slowing of ventilation rates will affect water column Pb concentrations and ^{210}Pb and Pb source water corrections, but proportions of old versus new isotopic ratios will remain the same. (4) A final possible modification of the model emphasizing deep water isotopic change would be incorporation of background Pb at depth. Although deep waters (600-2000 m) could hardly

be expected to support more than 15 pM Pb (the background surface value estimate based on D. strigosa), this would be sufficient to modify the contemporary isotopic signature in these waters which contain only 50-75 pM total Pb. In adopting a background Pb isotopic signature, the obvious approach is to estimate a value from Chow and Patterson's (1962) survey of pelagic sediments and manganese nodules ($^{206/207}Pb \approx 1.208 - 1.218$). However, since we are concerned with intermediate water and not surface water (from which most sedimented Pb is presumably derived), it may be advisable to seek out a particular weathering source signature -- continental leads supplying the Labrador Sea might be more appropriate. Lead from the Canadian shield, however, is probably at least as radiogenic as Pb in pelagic sediments (Doe, 1970). We require a relatively non-radiogenic background signature in order to shift the model isotopic profile toward lower $^{206/207}Pb$. Thus, assumption of a significant background Pb inventory in the lower depth regime of the model would only worsen the fit to the observed isotopic distribution. This result can be looked upon as indirect evidence of low stable Pb concentrations in pre-industrial intermediate and deep waters.

5.3 Conclusions

Among the results presented in Chapter 3 of this thesis, two records are particularly relevant to our understanding of the transport and geochemical behavior of Pb in the oceans. The Pb concentration and isotopic records in the coral D. strigosa accurately characterize the input history of industrial lead to the Sargasso Sea near Bermuda. Coupled with nearby vertical distributions of Pb, Pb isotopes, and ^{210}Pb (Boyle et al., 1986 and this thesis), models can be generated to deduce probable transport mechanisms.

Extension of the thermocline ventilation model of Boyle et al. (1986) which is based on ^{3}H-^{3}He ventilation rates (Jenkins, 1980), has revealed a number of new insights:

1. Simple conservative models based on ^{3}H-^{3}He ventilation rates cannot account simultaneously, for observed profiles of stable Pb, ^{210}Pb, and $^{206/207}Pb$. At best, only one concentration distribution can be satisfied at a time through coupled adjustment of ^{210}Pb and Pb winter source water concentrations.

2. Inclusion of particulate scavenging in the model enables reasonably close fits to observed Pb and ^{210}Pb distributions, but does not improve the Pb isotopic model fit. The model isotopic distribution reflects inadequate supply of more recent Pb (post-1920) to depths greater than 600 m. In the absence of vertical mixing of Pb or local gradients along isopycnal surfaces, the observed Pb isotopic distribution cannot be reproduced.

3. Regeneration of particulate Pb of surface origin (assumed proportional to AOUR) improves the isotopic fit, while preserving realistic Pb and ^{210}Pb distributions with depth. Isotopic ratios measured on sediment trap particles collected in August 1984 are consistent with the assumption that falling particles retain a surface signature. March 1985 trap collections, however, suggest rapid exchange of Pb between particles and the water column. Additional particulate isotopic analyses are needed to resolve the actual exchange process. The regeneration mechanism is deficient in that it can only correct the modeled isotopic profile part of the way toward the measured $^{206/207}Pb$ distribution. Diapycnal mixing may constitute a secondary mechanism which would drive deep water $^{206/207}Pb$ toward observed lower values by diminishing the influence of very recent Pb inputs (post-1965 inputs are characterized by more radiogenic ratios). Alternatively, two unconstrained mechanisms exist which could potentially cause a modified isotopic distribution at depth. The first and more likely possibility is a spatially variable flux of Pb isotopes to winter source waters. The extent of such variability can be evaluated in the near future by appropriate sampling. The second mechanism would require faster ventilation rates during periods of low $^{206/207}Pb$ surface input (i.e. 1920-1960). Two-fold variations in renewal

rates have been observed by Jenkins (1983) at shallow depths, however, coincidental rate variations at depths > 600 m are doubtful.

References

Bacon, M.P., D.W. Spencer and P.G. Brewer (1976). $^{210}Pb/^{226}Ra$ and $^{210}Po/^{210}Pb$ disequilibrium in seawater and suspended particulate matter, Earth Planet. Sci. Lett. 32: 277-296.

Bacon, M.P., D.W. Spencer and P.G. Brewer (1978). Lead-210 and Polonium-210 as marine geochemical tracers: Review and discussion of results from the Labrador Sea. In: Natural Radiation Environment III, Vol. 1., T.F. Gesell and W.F. Lowder, eds., pp. 473-501, U.S. Department of Energy report: CONF-780422, Washington, D.C.

Boyle, E.A., S.D. Chapnick, G.T. Shen and M.P. Bacon (1986). Temporal variability of lead in the western North Atlantic Ocean, Geochim. Cosmochim. Acta 91: 8573-8593.

Broecker, W.S., J. Goddard and J. Sarmiento (1976). The distribution of ^{226}Ra in the Atlantic Ocean, Earth Planet. Sci. Lett., 32:220-235.

Chow, T.J. and C.C. Patterson (1962). The occurrence and significance of lead isotopes in pelagic sediments, Geochim. Cosmochim. Acta 26: 263-308.

Doe, B.R. (1970). Lead Isotopes, Springer Verlag, New York.

Jenkins, W.J. (1980). Tritium and ^{3}He in the Sargasso Sea, J. Mar. Res. 38: 533-569.

Jenkins, W.J. (1982). On the climate of a subtropical ocean gyre: Decade timescale variations in water mass renewal in the Sargasso Sea, J. Mar. Res. 40 (suppl.): 265-290.

Jenkins, W.J. and J.C. Goldman (1985). Seasonal oxygen cycling and primary production in the Sargasso Sea, J. Mar. Res. 43: 465-491.

Nozaki, Y., J. Thomson and K.K. Turekian (1976). The distribution of ^{210}Pb and ^{210}Po in the surface waters of the Pacific Ocean, Earth Planet. Sci. Lett. 32:304-312.

Sarmiento, J.L. (1983). A tritium box model of the North Atlantic Thermocline, J. Phys. Oceanogr. 13: 1269-1274.

Shelton, E.M., M.L. Whisman and P.W. Woodward (1982). Long-term trends in gasoline properties are charted, Oil and Gas J., Aug. 2, 1982, 95-99.

Stommel, H., K. Saunders, W. Simmons and J. Cooper (1969). Observations of the duiurnal thermocline, Deep Sea Res. 16 (Suppl.): 269-284.

Turekian, K.K., L.K. Benninger and E.P. Dion (1983). ^{7}Be and ^{210}Pb total deposition fluxes at New Haven, Connecticut and at Bermuda, J. Geophys. Res. 88: 5411-5415.

Worthington, L.V. (1959). The 18^{o} water in the Sargasso Sea, Deep Sea Res. 5: 297-305.

CHAPTER 6

GENERAL SUMMARY

6.1 Lead

Studies of lead in the contemporary environment are of particular significance for several reasons. More so than for any other trace metal, Pb exhibits a global distribution which is clearly governed by non-nuclear anthropogenic activities. Reconstructed historical records of Pb encompassing remote regions are therefore useful in elucidating atmospheric/oceanic transport mechanisms for aeolian particles of industrial origin. Environmental Pb signals are particularly informative due to the existence of four stable Pb isotopes. Industrial sources and extents of observed perturbations over background can, in principle, be assessed via Pb isotope ratios. Thus, in terms of a chemical tracer, Pb is doubly-tagged. In the modern ocean, Pb distributions have been continuously evolving over the past century as a result of changing industrial fluxes. Peak inputs to the western North Atlantic are already 15 years behind. Since Pb is redistributed in the upper ocean over decadal time scales, the time is favorable for careful documentation of the anthropogenic Pb transient.

Concentration and isotopic measurements of Pb in corals from the western North Atlantic, Florida Straits, central South Pacific, eastern Equatorial Pacific, and southwestern Indian Ocean confirm that anthropogenic Pb in the modern environment is ubiquitous. While the contemporary record is consistent with recent oceanic and atmospheric measurements of Pb, coral-based reconstructions reveal historical details which were hitherto unavailable.

(a) Sargasso Sea

In prehistoric times, Pb levels in Sargasso Sea surface waters were probably 15-20 pM. Pre-industrial Pb isotope ratios near

Bermuda ($^{206/207}Pb$ = 1.215) resemble values reported for pelagic sediments and manganese nodules by Chow and Patterson (1962). As a result of the American industrial revolution, surface concentrations rose to near 90 pM in the 1920's, and the Pb isotopic composition of surface waters changed to a less radiogenic state ($^{206/207}Pb$ = 1.184-1.190). The advent of alkyl leads (anti-knock gasoline additives) dramatically increased Pb aerosol emissions and pushed the surface ocean Pb concentration to a maximum of 240 pM in 1971. Alkyl leads were evidently relatively radiogenic since $^{206/207}Pb$ returned to 1.202 in 1971. A one-year time lag between the 1971 concentration maximum and peak U.S. alkyl Pb combustion is due to short-term accumulation of Pb in the mixed layer in accord with a 2-year residence time. Since the perturbation maximum in 1971, surface water Pb concentrations and isotopic ratios have reversed rapidly toward post-industrial revolution values ([Pb] in 1984 = 130 pM; $^{206/207}Pb$ in 1985 = 1.186) as a consequence of phasing-out of leaded gasoline in the U.S.

(b) Florida Straits

Pre-anthropogenic Pb concentrations in the Florida Straits are estimated to have been approximately 38 pM, or roughly double the Sargasso Sea background concentration. Continental shelf and/or resuspended inputs of Pb are assumed responsible for the excess. The industrial revolution signal seen in the Bermuda coral record is absent, and the post-World War II increase is moderated, culminating in a peak concentration of 190 pM in 1977. These patterns appear to reflect a diluted American Pb flux resulting from long-range horizontal transport from the subtropical gyre. Pb of U.S. origin is implicated by virtue of the 1977 maximum, since Latin American and Caribbean lead emissions have probably not declined. The six-year time delay from the Bermuda Pb concentration peak implies an average

surface ocean recirculation velocity of 3-4 cm/sec which is comparable to surface Ekman transport estimates and observed wind drift speeds.

(c) South and Equatorial Pacific

The coral-inferred pre-industrial Pb concentration in surface waters of the South Pacific is 16-19 pM, however, coastal resuspension near Fiji may have biased this result. Based on nearshore dissolved Pb measurements at Bermuda, such a bias is expected to be small (less than 30%). Therefore, the pre-industrial surface Pb concentration in the South Pacific was probably not lower than 10 pM. Contemporary concentration and isotopic analyses in corals from the Galapagos Islands and Tutuila imply industrially-perturbed concentrations of 40-50 pM. These elevated levels and their isotopic signatures are consistent with regional industrial influence, although island-associated artifacts caused by sampling within 1 km from shore cannot be ruled out.

The Bermuda coral Pb concentration and isotopic records are particularly relevant to our understanding of the evolution of the industrial Pb transient in the Sargasso Sea. Coupled with vertical distributions of Pb, Pb isotopes, and ^{210}Pb, models can be generated to deduce physical and chemical transport mechanisms. The ventilated thermocline model of Jenkins (1980) as adapted by Boyle and coworkers (1986) has been extended to place important new constraints on the geochemical behavior of Pb in the oceans. Conservative models driven purely by lateral ventilation on ^{3}H-^{3}He time scales cannot account for observed distributions of Pb and ^{210}Pb simultaneously. More compelling, however, are model inconsistencies from the measured vertical distribution of stable Pb isotopes. The observed $^{206/207}Pb$ profile below 600 m clearly requires mixing of ventilated Pb (ventilation time scales

below 600 m are > 50 years) with Pb of more recent origin (ca. 1920-1965). Regeneration of particulate Pb of surface origin in proportion to apparent oxygen utilization rates improves the model fit considerably. Beyond a 12% net recycling efficiency, however, the fit to the data cannot be further improved. Diapycnal mixing constitutes a second possible mechanism which would force deep water $^{206/207}Pb$ ratios toward observed values by diminishing the influence of very recent (post-1965) Pb inputs. Alternatively, it is possible that industrial Pb fluxes to outcropping winter source waters exhibit mild spatial variability in their isotopic ratios. Quantification of such variability along with source water Pb and ^{210}Pb concentration gradients will comprise the next step in future model refinement.

6.2 Cadmium and other Trace Metals

Besides Pb, only Cd has unequivocally demonstrated temporal variability associated with industrialization and/or natural perturbations in circulation. The extent of coral-inferred surface ocean perturbations by industrial Cd observed in the Sargasso Sea was unanticipated. Relative to Pb, anthropogenic Cd fluxes are small (7% of U.S. Pb flux in 1975; Nriagu, 1979). Owing to biological depletion of Cd in surface waters, however, industrial fluxes are very visible. Three to four-fold increases over background are evident over the periods 1915-1920 and 1960-1980. These can be traced to historic U.S. Cd and Zn production trends and other more recent sources. The nutrient-like distribution of Cd, however, renders the industrial signal invisible everywhere but in the mixed layer, which limits the usefulness of Cd as a chemical tracer. This element is ideally suited, however, for chemical reconstructions in upwelling zones.

Corals in the eastern Equatorial Pacific display Cd perturbations driven by natural phenomena known collectively as the El Nino-Southern Oscillation. These variations arise as a result of upwelling of anomalously warm, nutrient-depleted waters ([Cd] $\geq$ 15 pM) which displace

colder, fertile source waters ([Cd] $\leq$ 70 pM) during ENSO events. Close correlation to sea surface temperature and Southern Oscillation indices suggests that the coral Cd record is an accurate index of surface ocean paleo-fertility. Since existing records of SST, surface pressure, and surface marine wind go back only to 1841, an extended coral Cd record would greatly augment our historical perspective of ENSO activity.

The natural distributions of Zn and V in Sargasso Sea surface waters appear to have undergone little change over the past century. This result is surprising in the case of Zn since surface ocean concentrations and industrial emissions are roughly comparable to Pb. In the case of V, large industrial fluxes are obscured by a mixed layer concentration of 40 nM -- a level some 2,500 times higher than the pre-industrial surface concentration of Pb.

Cadmium and zinc constitute the sixth and seventh trace elements which appear to be indiscriminately precipitated by corals relative to their seawater distributions; i.e. their K_D's are close to unity. These aragonite compatible elements (Ra, Ba, Nd, Sr, Cd, Zn, and Co) all possess +2 effective ionic radii approaching or exceeding that of Ca^{2+}, suggesting direct lattice substitution. Lead also appears to be skeletally substituted, though it is precipitated preferentially to calcium (K_D = 2.3). A thermodynamic basis for such uniform solid solution behavior is not evident, since differences in chemical speciation favor widely varying K_D's. Model calculations of Turner et al. (1981) suggest, for example, that the proportions of free Cd^{2+}, Zn^{2+}, and Ba^{2+} in seawater are 3, 46 and 86%, respectively. In addition, rare earth elements (e.g. Nd) and uranium exhibit oxidation states and anionic complexing in seawater which are unsuited for one-to-one substitution for Ca^{2+}. Clearly, the chemical microenvironment of the coral ectoderm must differ substantially from seawater. Supersaturation with respect to aragonite precipitation and reducing conditions brought about by zooxanthellate photosynthesis are conceivable mechanisms which may contribute toward the observed precipitation behavior of corals.

APPENDIX A

Coral Lead Concentrations

Table A.1 Pb/Ca mole ratios in Diploria strigosa
North Rock, Bermuda

YEAR	[Pb]/[Ca]x10^{-9}	Standard Deviation	n	Comments
1865-68	17.2	1.8	6/6	100 mg/cont.
1883-85	7.8	1.7	3/3	55 mg sample
1883-85	5.2	0.3	4/4	100 mg sample
1890-93	5.5	0.6	3/3	"
1898-99	8.3	1.0	4/5	"
1900-01	12.3	1.2	3/3	55 mg sample
1910-11	11.9	1.2	3/3	100 mg sample
1916-17	13.5	0.4	3/3	"
1918-19	15.1	1.1	3/3	"
1921	17.9	1.5	2/2	"
1923	20.3	0.2	3/3	"
1926	19.8	0.6	2/3	55 mg sample
1929	20.0	1.2	3/3	
1932	20.8	2.8	3/3	
1936	18.9	2.0	3/3	
1938	20.3	2.0	3/3	
1939	16.9	3.8	3/3	
1941	19.8	2.2	2/2	
1943	24.7	1.3	3/3	
1944	28.1	2.8	3/3	tot. crush-cont.
1945	21.9		1/4	
1947	20.1	2.3	3/3	
1948-49	24.8	1.2	3/3	
1949	18.5	3.3	3/3	low Ca
1950-51	21.5	2.5	7/7	
1954	20.9	5.8	4/4	
1955	58.9	9.6	3/3	cont.
1955	52.1	2.2	4/4	cont.
1956	45.4	1.2	2/2	cont.
1956	52.8	3.0	2/3	cont.
1956	47.3	1.6	3/4	cont.
1957	50.3	0.6	3/3	cont.
1957	59.4	13.8	2/2	cont.
1958	42.9	2.4	3/3	
1959	41.5	2.8	2/2	
1960-61	43.6	0.4	3/3	
1963	48.8	1.5	3/3	
1965	45.8	3.1	3/3	
1966	58.0	5.0	3/3	
1967	50.5	2.4	3/3	
1968	53.5	1.2	3/3	
1969	52.3	0.3	3/3	

Table A.1 continued

YEAR	[Pb]/[Ca]x10^{-9}	Standard Deviation	n	Comments
1970	52.9	2.8	3/3	
1971	56.7	4.5	3/3	
1972	53.2	5.6	4/7	
1973	52.9	2.7	3/3	
1974	55.6	5.9	3/3	
1975	50.2	5.3	3/3	
1976	49.5	3.2	3/3	
1977	52.0	5.3	3/3	
1978	46.3	3.3	3/3	
1979	44.3	3.5	3/3	
1980	42.6	4.4	2/3	
1981	45.1	2.4	3/3	
1982	36.1	1.7	3/3	
1983	58.0	2.2	3/5	cont.
1983	64.7	18.9	4/4	cont.
1983	64.9		1/3	cont.

Table A.2 Pb/Ca mole ratios in Diploria strigosa Southern Coral Reef Preserve, Bermuda

YEAR	$[Pb]/[Ca]x10^{-9}$	Standard Deviation	n	Comments
1933	29.6	0.7	2/3	
1934	31.4	4.2	3/3	
1936	29.5	0.5	3/3	
1937	27.8	0.7	3/3	
1940	33.9	1.8	3/3	
1942	36.6	1.4	3/3	
1943	34.4	3.7	3/3	
1945	37.7	2.4	3/3	
1946	38.3	2.6	3/3	
1948	48.3	9.0	3/3	
1949	48.2	3.7	3/3	
1951	51.0	0.5	3/3	
1952	44.4	4.0	3/3	
1954	56.5	4.1	3/3	
1955	56.9	0.9	3/3	
1957	61.1	6.2	3/3	
1958	52.9	2.7	3/3	
1960	57.5	6.8	3/3	
1961	55.4	3.1	3/3	
1963	63.4	0.9	3/3	
1964	56.8	1.3	3/3	
1966	58.3	2.3	3/3	
1967	66.4	3.9	3/3	
1969	62.6	2.1	3/3	
1970	61.7	7.0	3/3	
1972	63.0	5.8	3/3	
1973	65.1	5.2	3/3	
1975	62.5	1.3	3/3	
1976	58.6	1.4	3/3	
1978	55.1	5.1	3/3	
1979	54.1	3.9	3/3	
1980	56.2	1.6	3/3	
1981	59.2	4.5	3/3	
1982	43.0	4.0	2/3	
1983	48.1	2.3	2/3	

Table A.3 Pb/Ca mole ratios in Diploria labyrinthiformis North Rock, Bermuda

YEAR	[Pb]/[Ca]x10^{-9}	Standard Deviation	n	Comments
1935	41.5	3.0	2/3	Run I
1938	27.2	1.6	2/3	(whole fragment analyses)
1941	37.4	4.8	2/3	
1944	33.8	1.1	3/3	
1947	35.1	3.5	2/3	
1950	39.3	1.4	3/3	
1953	51.8	7.2	3/3	
1956	57.3	2.8	3/3	
1959	55.5	3.6	3/3	
1962	54.9	4.0	3/3	
1965	65.7	4.2	3/3	
1968	72.0	3.2	3/3	
1971	73.1	2.8	3/3	
1974	82.9	5.0	3/3	
1977	77.3	4.3	3/3	
1980	122.6	7.9	3/3	
1983	105.7	6.6	2/3	
1937	23.6	5.3	3/3	Run II
1940	27.0	1.6	3/3	(whole fragment analyses)
1943	23.3	1.0	3/3	
1949	36.5	2.4	3/3	
1952	36.7	3.6	3/3	
1958	48.2	6.6	3/3	
1961	64.8	7.1	2/3	
1964	62.2	5.5	3/3	
1967	57.7	6.6	3/3	
1970	60.9	2.1	3/3	
1973	58.6	5.2	2/3	
1976	59.0	3.4	3/3	
1979	60.6	18.2	2/3	
1982	77.3	3.1	2/3	
1936	36.4	4.8	3/3	Run III
1939	35.0	3.5	3/3	(whole fragment analyses)
1942	37.3	6.4	3/3	
1945	38.3	2.9	3/3	
1946	31.9	3.4	3/3	
1948	41.0	8.1	3/3	
1951	48.5	7.2	3/3	
1954	64.4	5.3	3/3	
1955	61.9	1.9	3/3	
1957	63.6	1.2	3/3	
1960	65.4	6.8	2/3	

Table A.3 continued

YEAR	[Pb]/[Ca]x10^{-9}	Standard Deviation	n	Comments
1963	74.1	10.5	3/3	
1966	87.0	9.5	3/3	
1969	89.2	4.8	3/3	
1972	71.6	3.4	3/3	
1975	75.7	9.2	2/3	
1978	68.5	2.4	3/3	
1981	100.0	2.0	3/3	

Table A.4 Pb/Ca mole ratios in Montastrea annularis Florida Straits (full data set)

YEAR	[Pb]/[Ca]x10^{-9}	Standard Deviation	n	Comments
1645-55	9.5		1/3	Run I & II Composite
1906-10	9.3	1.5	5/6	
1920-22	8.0	0.6	3/3	
1923-25	9.8	1.7	3/3	
1926-29	12.4	1.3	3/6	
1930-32	12.0		1/3	
1933-35	10.0	1.5	3/3	
1936-37	26.7		1/3	cont.
1944	22.7		1/3	cont.
1948	14.6	2.7	5/6	
1951	25.7	0.1	2/3	cont.
1952	20.7	1.5	6/6	
1954	23.9	3.6	3/6	
1955	36.2		1/3	cont.
1959	35.3		1/6	cont.
1961	23.8	2.0	3/5	
1963	28.7	1.0	2/3	
1965	37.6	3.8	2/6	cont.
1967	40.8	3.6	3/3	cont.
1969	43.3	3.0	2/3	cont.
1972	46.3	2.9	3/6	cont.
1974	48.9	1.6	5/10	cont.
1974	54.3	1.4	2/3	RunIII, cont.
1975	40.6	5.3	3/3	
1976	52.7	7.5	3/3	cont.
1977	57.1	0.9	3/3	cont.
1978	52.3	1.4	3/3	cont.
1979	41.3	2.5	2/3	
1980	54.2	4.8	3/3	cont.
1981	49.4	3.6	3/3	cont.
1982	40.8	1.6	3/3	cont.
1974	39.2	1.3	3/3	Run IV
1975	37.3	5.0	2/2	
1975-76	35.4	1.9	2/2	
1976	39.5		1/1	
1976-77	40.6	1.2	2/2	
1977	44.9	1.2	2/2	
1978	40.9	1.4	3/3	
1979	38.6	1.7	2/3	
1980	37.2	0.9	3/3	
1981	36.2	0.8	3/3	
1982	32.7	1.6	3/3	

Table A.4 continued

YEAR	[Pb]/[Ca]x10^{-9}	Standard Deviation	n	Comments
1944	15.4	3.0	3/3	Follow-up runs
1960	23.7	2.2	3/3	
1962	31.2	4.0	3/3	
1964	49.4	2.7	3/3	cont.
1966	30.7	0.6	3/3	
1968	31.4	1.8	3/3	
1974	45.3	0.7	3/3	cont.
1698-99	8.9	0.6	3/3	
1876-80	8.7	0.6	2/2	
1926-29	12.3		1/2	
1956	30.7	0.4	2/2	
1965	51.2	2.9	2/2	cont.
1974	41.3	3.1	3/3	cont.

Table A.5 Pb/Ca mole ratios in Montastrea annularis Florida Straits (final data composite)

YEAR	[Pb]/[Ca]x10^{-9}	Standard Deviation	n	Comments
1645-55	9.5		1	
1698-99	8.9	0.6	3	
1876-80	8.7	0.6	2	
1906-10	9.3	1.5	5	
1920-22	8.0	0.6	3	
1923-25	9.8	1.7	3	
1926-29	12.1	1.3	4	
1930-32	12.0		1	
1933-35	10.0	1.5	3	
1944	15.4	3.0	3	
1948	14.6	2.7	5	
1952	20.7	1.5	6	
1954	23.9	3.6	3	
1960	23.7	2.2	3	
1961	23.8	2.0	3	
1962	31.2	4.0	3	
1963	28.7	1.0	2	
1966	30.7	0.6	3	
1968	31.4	1.8	3	
1974	38.3	0.5	3	
1975	36.7	3.1	5	
1975-76	35.4	1.9	2	
1976	39.5		1	
1976-77	40.6	1.2	2	
1977	44.9	1.2	2	
1978	40.9	1.4	3	
1979	38.9	1.4	3	
1980	37.2	0.9	3	
1981	36.2	0.8	3	
1982	32.7	1.6	3	

Table A.6 Pb/Ca mole ratios in Pavona clavus
San Cristobal Island, Galapagos Islands

YEAR	$[Pb]/[Ca]x10^{-9}$	Standard Deviation	n	Comments
1963	10.1	1.1	3/3	
1964	9.4	0.5	3/3	
1965	9.9	1.5	2/3	
1966	10.4	0.4	3/3	
1967	11.7	0.9	3/3	
1968	11.1	1.4	3/3	
1969	19.3	4.4	6/6	cont. (?)
1970	17.0	2.8	3/3	cont. (?)
1971	9.5	0.2	2/3	
1972	8.5	0.3	3/3	
1973	9.4	0.6	3/3	
1974	9.9	0.9	3/3	
1975	10.0	0.7	3/3	
1976	10.9	0.5	3/3	
1977	10.2	0.7	3/3	
1978	10.5	1.0	6/6	
1979	12.1	0.8	3/3	
1980	10.8	0.6	3/3	
1981	11.9	1.1	3/3	
1982	14.7	0.5	3/3	cont.(?)

Table A.7 Pb/Ca mole ratios in Hydnophora microconos Aunuu, Tutuila

YEAR	[Pb]/[Ca]x10^{-9}	Standard Deviation	n	Comments
1962	32.1	5.2	3/3	cont.
1963	12.2	2.2	3/3	
1964	15.9	3.4	3/3	
1965	13.6	4.8	3/3	
1966	16.2	3.9	3/3	
1967	10.2	0.5	3/3	
1968	14.1	0.4	3/3	
1969	11.2	0.9	3/3	
1970	10.6	0.6	3/3	
1971	13.1	1.9	3/3	
1972	13.2	0.5	3/3	
1973	11.3	0.6	3/3	
1974	10.1	0.6	3/3	
1975	10.0	0.5	3/3	
1976	13.2	1.5	3/3	
1977	10.3	0.2	3/3	
1978	11.4	0.4	3/3	
1979	11.4	0.9	3	

Table A.8 Pb/Ca mole ratios in Platygyra rustica Suva, Fiji

YEAR	[Pb]/[Ca]x10^{-9}	Standard Deviation	n	Comments
1920(±5)	4.1	0.4	4	

Table A.9 Pb/Ca mole ratios in Platygyra rustica Mauritius

YEAR	$[Pb]/[Ca]x10^{-9}$	Standard Deviation	n	Comments
1968	5.8	0.5	3/3	
1970	6.5	1.8	3/3	
1971	5.7	1.0	2/2	
1972	6.7	2.9	3/3	
1974	22.9	2.9	3/3	cont. (?)
1976	55.2	4.3	4/6	cont. (?)
1978	17.1	2.3	3/3	cont. (?)

APPENDIX B

Coral Cadmium, Barium, Zinc, Vanadium, and Organic Carbon Concentrations

Table B.1 Cd/Ca mole ratios in Diploria strigosa
North Rock, Bermuda

YEAR	[Cd]/[Ca]x10^{-9}	Standard Deviation	n	Comments
1865-68	.46	.07	5/6	100 mg sample
1883-85	.39	.08	3/3	55 mg sample
1883-85	.46	.02	2/3	55 mg/whole fragment
1883-85	.45	.12	4/4	100 mg sample
1890-93	.48	.24	3/3	"
1898-99	.26	.04	4/5	"
1900-01	.57	.22	3/3	"
1910-11	.42	.11	3/3	"
1916-17	.89	.12	3/3	"
1918-19	.85	.09	3/3	"
1921	.89	.08	2/2	"
1923	.82	.08	3/3	"
1926	.61	.20	3/3	55 mg sample
1929	.61	.06	2/3	
1932	.48	.02	3/3	
1936	.37	.07	3/3	
1938	.47	.09	3/3	
1939	.34	.18	3/3	
1941	.32	.07	2/2	
1943	.53	.11	3/3	
1944	.80	.17	3/3	whole fragment; cont.
1944-45	.44	.05	4/4	
1947	.47	.12	3/3	
1948-49	.48	.17	3/3	
1949	.81	.12	2/3	
1950-51	.52	.41	7/7	(?)
1954	.62	.10	4/4	
1955	1.40	.35	3/3	cont.
1955	3.13	1.14	4/4	cont.
1956	1.20	.46	2/2	cont.
1956	1.15	.15	3/3	cont.
1956	.89	.02	3/4	cont.
1957	.49	.04	3/3	
1957	.80		1/2	cont.
1958	.68	.24	3/3	
1959	2.54		1/2	cont.
1960-61	.73	.10	3/3	
1963	.88	.21	3/3	
1965	1.37	.16	3/3	
1966	.84	.12	3/3	
1967	1.24	.30	3/3	

Table B.1 continued

YEAR	[Cd]/[Ca]x10^{-9}	Standard Deviation	n	Comments
1968	1.14	.03	2/3	
1969	1.10	.09	3/3	
1970	1.00	.10	2/3	
1971	1.16		1/3	
1972	1.07	.29	7/7	
1973	1.20	.08	2/3	
1974	.97	.04	3/3	
1975	.63	.08	3/3	
1976	.84	.03	2/3	
1977	1.02	.31	2/3	
1978	.87		1/3	
1979	2.75	.84	3/3	cont.
1980	.85	.16	3/3	
1981	.63	.37	3/3	
1982	.85	.21	3/3	
1983	1.41	.08	3/3	cont.
1983	1.26	.12	4/4	cont.

Table B.2 Cd/Ca mole ratios in Montastrea annularis Florida Straits

YEAR	[Cd]/[Ca]x10^{-9}	Standard Deviation	n	Comments
1876-80	1.99	.03	2/2	
1906-10	1.99	.50	3/3	
1920-22	1.32	.37	3/3	
1923-25	1.60	.34	3/3	
1926-29	1.50	.31	2/3	
1930-32	2.06	.64	3/3	
1933-35	2.06	.11	3/3	
1936-37	2.21	.09	2/3	
1944	2.79	.12	3/3	
1948	1.77	.32	2/3	
1951	2.04		1/3	
1952	2.07	.35	3/3	
1955	2.28		1/3	
1959	2.77	.08	2/3	
1960	2.37	.21	3/3	
1962	3.02	.33	3/3	
1963	2.01	.11	3/3	
1964	1.97	.06	3/3	
1965	2.35	.25	2/3	
1966	2.24	.57	3/3	
1968	2.55	.26	3/3	
1974	2.26	.29	3/3	
1975	2.32	.01	2/2	
1975-76	2.08	.00	2/2	
1976	1.96		1/1	
1976-77	2.41	.25	2/2	
1977	2.87	.16	2/2	
1978	3.48	.28	3/3	
1979	2.17	.11	3/3	
1980	1.99	.10	3/3	
1981	2.66	.09	2/2	
1982	2.66	.45	3/3	

Table B.3 Cd/Ca mole ratios in Pavona clavus
San Cristobal Island, Galapagos Islands

YEAR	[Cd]/[Ca]x10^{-9}	Standard Deviation	n	Comments
1963	3.8	0.4	3/3	
1964	5.8	0.3	3/3	
1965	1.7	0.2	3/3	
1966	3.5	0.6	3/3	
1967	4.6	0.6	3/3	
1968	4.9	0.4	3/3	
1969	3.9	0.3	6/6	
1970	5.1	0.35	3/3	
1971	3.9	0.15	3/3	
1972	1.4	0.2	3/3	
1973	5.5	0.3	3/3	
1974	4.3	0.15	3/3	
1975	3.9	0.13	3/3	
1976	2.5	0.2	3/3	
1977	2.7	0.5	3/3	
1978	2.7	0.2	3/3	
1979	2.4	0.2	3/3	
1980	2.8	0.15	3/3	
1981	4.3	0.9	3/3	
1982	4.1	0.9	3/3	

Table B.4 Cd/Ca mole ratios in Favia speciosa
Eniwetak Atoll

YEAR	[Cd]/[Ca]x10^{-9}	Standard Deviation	n	Comments
1948	2.54	.28	3/3	
1950	4.18	.63	2/2	cont.
1952	2.83	.32	3/3	
1954	2.47	.21	3/3	
1956	2.62	.49	3/3	
1958	2.66	.22	3/3	
1960	2.58	.29	3/3	
1962	7.91	.54	3/3	cont.
1963	5.18		1/4	cont.
1964	3.63	.30	3/3	cont.
1966	2.55	.24	2/3	
1968	7.19	.22	3/3	cont.
1970	2.52	.03	3/3	
1972	2.07	.14	3/3	

Table B.5 Cd/Ca mole ratios in Porites lobata
Lisianski Island (N.W. Hawaiian chain)

YEAR	[Cd]/[Ca]x10^{-9}	Standard Deviation	n	Comments
1964	1.84	.84	2/2	
1970	2.02	.12	2/2	
1971	1.41		1/2	
1973	1.34		1/2	
1975	0.89		1/2	
1976	1.09	.18	2/2	
1977	1.23	.56	2/2	
1979	2.3		1/1	

Table B.6 Cd/Ca mole ratios in Platygyra rustica Mauritius

YEAR	[Cd]/[Ca]x10^{-9}	Standard Deviation	n	Comments
1968	0.54	.17	3/3	
1970	0.48	.09	2/3	
1972	0.66	.44	2/3	
1974	0.96		1/3	cont.
1976	0.93		1/3	cont.
1978	>8		0/3	cont.

Table B.7 Ba/Ca mole ratios in *Montastrea annularis* Florida Straits

YEAR	[Ba]/[Ca]x10^{-6}	Standard Deviation	n	Comments
1646	4.70	.11	2/2	
1906-10	5.72	.07	2/2	
1920-22	5.75	.40	2/2	
1926-29	4.68	.07	2/2	
1933-35	4.88	.35	2/2	
1943	4.96	.04	2/2	
1954	5.12	.07	2/2	
1961	4.92	.20	2/2	
1967	5.25	.05	2/2	
1970	5.19	.57	2/2	
1974	6.03		1/1	

Table B.8 Zn/Ca mole ratios in Diploria strigosa North Rock, Bermuda

Year	[Zn]/[Ca]x10-9	Standard Deviation	n	Comments
1883-85	4.3	1.2	7/7	55 & 100 gm samples
1890-93	3.0	0.6	3/3	100 mg samples
1898-99	6.0	1.5	4/4	"
1900-01	7.1	1.3	2/3	"
1910-11	3.8	0.1	3/3	"
1916-17	7.4	1.0	3/3	"
1918-19	7.9	1.6	3/3	"
1921	7.4	2.3	2/2	"
1923	3.8	1.3	3/3	"
1926	6.8	0.7	3/3	55 mg samples
1929	5.3	2.1	2/3	
1932	7.0	0.9	3/3	
1936	6.5	0.9	2/3	
1938	6.7	2.7	3/3	
1939	7.6	1.9	3/3	
1941	4.2	1.1	2/2	
1943	8.5	1.6	3/3	
1944-45	5.8	0.9	3/4	
1947	7.4	0.1	2/2	
1949	10.6	1.7	2/3	
1950-51	5.2	1.5	4/4	
1954	3.2	0.8	3/4	
1955	39.4	9.9	4/4	cont.
1956	6.6	1.6	2/2	
1957	5.7	0.2	2/2	
1958	3.9	0.8	3/3	
1959	4.0		1/2	
1960-61	8.1	3.7	2/3	
1963	4.2	1.2	3/3	
1965	3.9	1.5	3/3	
1966	3.9	1.2	3/3	
1967	5.4	2.0	3/3	
1968	9.6	0.1	2/3	
1969	11.8	3.1	3/3	
1970	11.1	4.2	2/3	
1971	34.1	20.1	3/3	cont.
1972	5.0	0.9	3/4	
1972	18.5	4.2	2/3	cont.
1974	7.1	1.6	3/3	
1975	4.1	0.6	2/2	
1976	4.0	1.1	3/3	
1977	6.5	1.4	3/3	

Table B.8 continued

Year	[Zn]/[Ca]x10-9	Standard Deviation	n	Comments
1978	5.5	1.8	3/3	
1979	6.4	2.1	3/4	
1980	6.4	1.7	3/3	
1981	4.3	0.0	2/3	
1982	7.2	2.3	3/3	
1983	12.1	2.2	6/12	cont.

Table B.9 V/Ca mole ratios in Diploria strigosa
North Rock, Bermuda

YEAR	[Cd]/[Ca]x10^{-9}	Standard Deviation	n	Comments
1890-93	92	8	3/3	
1910-11	109	9	3/3	
1916-17	105	4	3/3	
1923	60	3	3/3	(?)
1926	109	29	3/3	
1929	112	14	2/3	
1932	98	6	3/3	
1936	113	19	2/3	
1939	118	26	2/3	
1949	98		1/3	
1958	92	2	3/3	
1963	103	14	3/3	
1966	97	8	3/3	
1969	113	16	3/3	
1972	98	17	2/3	
1975	112	25	3/3	
1978	103	2	2/3	
1979	95	3	3/3	
1981	90	17	3/3	
1982	92	4	3/3	

Table B.10 Organic C/Ca ratio in Diploria labyrinthiformis after cleaning. North Rock, Bermuda

Year	[Org. C]/[Ca] (μmol/mol)	Comments
1935	det.lim.	whole coral analysis
1937	10.5	"
1940	13.7	"
1943	d.l.	"
1946	13.4	"
1948	13.6	"
1949	12.4	"
1952	0.3	"
1956	14.1	"
1958	d.l.	"
1959	11.2	"
1962	13.4	"
1964	24.9	"
1967	11.5	"
1970	14.3	"
1972	12.1	"
1973	0.7	"
1976	d.l.	"
1979	8.5	"
1981	10.2	"
1982	9.9	"

10 μmole C/mol Ca = 1.2 ppm
≈ 3 ppm adsorbed "organic matter"

if "organic matter" contains 70 ppm Pb (upper limit estimate based on sediment trap data - Jickells et al., 1984)

10 μmol C/mol Ca would carry 0.2 ppb Pb
= 0.1 nmol Pb/mol Ca

this represents only 2.5% of lowest skeletal Pb content measured

APPENDIX C

Coral ^{210}Pb Concentrations

Table C.1 Unsupported ^{210}Pb in Montastrea annularis
Florida Straits

YEAR	Age	Unsupported ^{210}Pb* (dpm/100 g)	log(^{210}Pb)	($\sqrt{(c)}/c$)%
1982	0	12.13	1.084	7.7
1978	4	13.12	1.118	5.3
1976	6	12.30	1.090	4.8
1974	8	13.74	1.138	5.6
1971	11	10.59	1.025	6.4
1969	13	11.45	1.059	5.8
1965	17	7.98	0.902	6.4
1962	19	(12.02)	(1.080)	17.4**
1956	26	6.99	.845	5.7
1952	30	6.60	.819	5.2
1948	34	5.53	.743	5.3
1944	38	3.35	.641	4.4
1941	41	4.35	.639	4.2
1938	44	4.37	.528	3.9
1930-32	51	3.51	.545	3.3
1920-22	61	1.85	.267	2.9
1885	97	0.005	-.307	3.3

*all samples corrected to year of collection assuming skeletal [^{226}Ra] = 7.40 dpm/100 g coral

**small sample (0.36 g coral)

Unweighted least squares regression yields:

R^2 = .978
intercept = 1.2033 (15.97 dpm/100 g)
half-life = 20.3 years

Weighted least squares regression yields:

R^2 = .891
intercept = 1.1679 (14.72 dpm/100 g)
half-life = 24.3 years

Table C.2 Unsupported ^{210}Pb in Bermudian Corals

CORAL	Year	Age	Unsupported ^{210}Pb* (dpm/100 g)	log(^{210}Pb)	$(\sqrt{(c)}/c)\%$	Correlation Coeff. r^2**	$t_{1/2}$** (years)	Initial Unsupported 210Pb** (dpm/100 g)
D. strigosa								
(North Rock, 1983)	1980-81	2.5	45.43	1.657	3.7			
	1972-74	10	44.04	1.644	3.0			
	1964-65	18.5	28.59	1.456	2.9	0.84	18.4	55.6
	1956	27	17.20	1.236	4.7	(n=6/6)		
	1945-46	37.5	8.88	.948	4.4			
	1912-15	69.5	2.02	.305	4.7			
D. labyrinthiformis								
(North Rock, 1983)	1980-81	2.5	54.45	1.736	3.2			
	1976-77	6.5	57.19	1.757	4.0	0.71	22.8	63.2
	1967-69	15	37.22	1.571	4.0	(n=3/3)		
M. annularis								
(North Rock, 1983)	1980-81	2.5	62.32	1.795	3.2			
	1976-77	6.5	58.47	1.767	3.2	(n=2/2)	43.5	64.9
D. strigosa								
(North Rock, 1982)	1980-82	1	(39.04)	(1.592)	3.9			
	1976-77	5.5	46.66	1.669	4.0			
	1973-74	8.5	37.90	1.579	4.6	(n=2/3)	10.0	68.2

*All samples corrected to year of collection assuming skeletal [^{226}Ra] = 7.40 dpm/100 g coral.

**As determined by weighted least squares regression

Table C.3 Unsupported ^{210}Pb in Pacific and Indian Ocean Corals

CORAL	Year	age	Unsupported ^{210}Pb* (dpm/100 g)	log(^{210}Pb)	$(\sqrt{(c)}/c)$%	Correlation Coeff. r^2**	$t_{1/2}$** (years)	Initial Unsupported ^{210}Pb** (dpm/100 g)
Galapagos	1980	2	30.31	1.482	4.4			
(P. clavus, 1982)	1975	7	29.12	1.464	4.1			
	1970	12	22.95	1.361	4.5	0.87	23.7	33.2
	1965	17	21.55	1.333	4.2	(n=5/5)		
	1961	21	19.38	1.287	4.0			
Tutuila	1978	1	28.93	1.461	4.8			
(H. microconos,	1977	2	28.32	1.452	4.0			
1979)	1974	5	21.57	1.334	3.6	0.96	12.6	30.3
	1972	7	19.61	1.292	4.0	(n=6/6)		
	1967	12	14.91	1.173	3.7			
	1962	17	13.33	1.125	4.8			
Lisianski	1977	2	62.27	1.794	3.4			
(P. lobata, 1979)	1972	7	54.64	1.737	3.7	0.97	17.7	68.8
	1963-64	15.5	36.16	1.558	3.2	(n=3/3)		
Heron Island	1977	6	17.09	1.233	4.0			
(P. lobata, 1983)	1965	18	9.93	.997	4.6			
	1948-50	34	9.59	.982	4.1	0.89	33.0	18.4
	1937-38	45	(10.60)	(1.025)	3.5	(n=4/5)		
	1920-22	62	5.37	.730	3.6			
Mauritius	1977	1	32.07	1.506	4.2			
(P. rustica, 1978)	1975	3	28.33	1.452	3.1	0.86	21.3	32.5
	1972	6	27.22	1.435	4.9	(n=3/4)		
	1968	10	(26.81)	(1.428)	4.5			
Eniwetak	1971	1	74.80	1.874	1.8			
(F. speciosa,	1968	4	54.34	1.735	1.8	0.95	11.5	75.3
1972)	1964	8	43.56	1.639	1.8	(n=5/5)		
	1958	16	26.54	1.424	2.8			
	1954-55	19.5	27.53	1.440	2.7			

*All samples corrected to year of collection assuming skeletal [^{226}Ra] = 7.40 dpm/100 g coral.

**As determined by weighted least squares regression

APPENDIX D

Coral Stable Lead Isotope Ratios

Table D.1 Lead isotopic composition of various corals.

Sample	ngs Pb	Current (amps)	# Ratios	Fractionation Factor	206/207 (95% CFL)	208/206 (95% CFL)	206/204 (95% CFL)	207/204 (95% CFL)	208/204 (95% CFL)
Florida Straits (M.annularis)									
1876-80	14	2.8	120	1.0007	1.2122	2.0379	18.972	15.650	38.663
					(.011%)	(.011%)	(.081%)	(.081%)	(.081%)
1926-29	11.2	3.0	60	0.9994	1.2141	2.0313	18.958	15.620	38.512
					(.029)	(.068)	(.165)	(.162)	(.167)
1974	27.3	2.9	66	1.0002	1.2006	2.0401	18.828	15.682	38.416
Galapagos (P. clavus)									
1962	25.4	2.8	24		1.1844	2.0639	18.502	15.621	38.187
					(.019)	(.026)	(.177)	(.177)	(.176)
1980	17.4	2.8	78	0.9993	1.1788	2.0708	18.373	15.586	38.045
					(.010)	(.011)	(.078)	(.079)	(.077)
Mauritius (P. rustica)									
1968	19.9	2.9	42	1.0000	1.1710	2.0779	18.206	15.548	37.836
					(.035)	(.048)	(.234)	(.221)	(.230)
Tutuila (H. microconos)									
1963	27.9	2.8	78	0.9996	1.1441	2.1108	17.748	15.512	37.461
					(.020)	(.018)	(.125)	(.122)	(.124)
1970	19.8	2.9	72	0.9998	1.1452	2.1076	17.769	15.519	37.451
					(.016)	(.029)	(.125)	(.125)	(.122)
1978	17	2.8-2.9	66	0.9996	1.1569	2.0929	18.006	15.564	37.682

Table D.2 Lead isotopic composition of Diploria strigosa
North Rock, Bermuda

Year	ngs/Pb	Current	# Ratios	Fractionation Factor	206/207 (95% CFL)	208/206 (95% CFL)	206/204 (95% CFL)	207/204 (95% CFL)	208/204 (95% CFL)
1886-87	14.0	2.9-3.0	33	1.0012	1.2147	2.0395	19.276	15.834	39.225
					(.081)	(.090)	(.916)	(.894)	(.864)
1894-95	3.9	3.1-3.2	42	0.9990	1.2147	2.0441	19.748	16.247	40.225
					(.082)	(.070)	(1.69)	(1.68)	(1.54)
1902-03	22.4	2.6-2.9	72	1.0001	1.2029	2.0557	18.603	15.656	18.613
					(.013)	(.011)	(.129)	(.129)	(.130)
1910-11	3.4	3.2	25	1.0000	1.1955	2.0639	19.331	16.118	39.737
					(.146)	(.146)	(2.284)	(2.264)	(2.197)
1920	26.7	2.7-2.9	78	1.0000	1.1909	2.0674	18.588	15.610	38.430
					(.011)	(.007)	(.084)	(.086)	(.085)
1928-29	6.6	3.1-3.2	34	1.0006	1.1875	2.0692	18.514	15.615	38.399
					(.130)	(.063)	(1.218)	(1.180)	(1.170)
1934-35	15.1	2.8-2.9	78	0.9996	1.1842	2.0701	18.417	15.553	38.126
					(.012)	(.010)	(.119)	(.112)	(.116)
1942	36.2	2.6-2.7	96	1.0001	1.1855	2.0696	18.511	15.614	38.310
					(.007)	(.006)	(.082)	(.082)	(.081)
1944	16.6	3.0	44	0.9993	1.1880	2.0674	18.603	15.656	38.458
					(.045)	(.066)	(.255)	(.254)	(.247)
1948	22.4	3.0	60	0.9994	1.1898	2.0629	18.580	15.617	38.331
					(.012)	(.010)	(.144)	(.145)	(.145)
1954	8.5	3.0	66	0.9991	1.1889	2.0635	18.554	15.606	38.284
					(.017)	(.017)	(.094)	(.094)	(.096)
1959	48	2.7-2.9	72	0.9994	1.1882	2.0586	18.557	15.617	38.201
					(.005)	(.009)	(.049)	(.051)	(.052)
1971	41.9	2.8-2.9	66	1.0008	1.2000	2.0391	18.743	15.618	38.217
					(.008)	(.009)	(.048)	(.050)	(.052)
1974	31.4	2.8	6		1.2054	2.0327	18.839	15.633	38.317
					(.119)	(.125)	(1.393)	(1.385)	(1.326)
1974+77	16.9	2.8-2.9	42	1.0025	1.2032	2.0351	18.740	15.566	38.143
					(.047)	(.059)	(.303)	(.298)	(.300)
1980	22.4	2.5-2.7	66	0.9998	1.2030	2.0360	18.847	15.666	38.370
					(.011)	(.017)	(.167)	(.156)	(.168)

APPENDIX E

Seawater Stable Lead Isotope Ratios

Table E.1 Lead isotopic composition of Sargasso Sea surface water (Station 'S'; 1983 - 1986)

Collection Date	ngs Pb	Current (amps)	# Ratios	Fractionation Factor	206/207 (95% CFL)	208/206 (95% CFL)	206/204 (95% CFL)	207/204 (95% CFL)	208/204 (95% CFL)
6/83	13.1	2.9-3.0	48	0.9991	1.1975	2.0427	18.750	15.658	38.301
					(.018%)	(.019%)	(.222%)	(.215%)	(.215%)
9/83	28.2	2.8-2.9	48	0.9997	1.2099	2.0299	18.945	15.653	38.459
					(.003)	(.008)	(.044)	(.036)	(.039)
1/84	10.9	3.2	60	0.9996	1.2021	2.0350	10.741	15.590	38.139
					(.015)	(.012)	(.140)	(.139)	(.140)
4/84	1.0	3.1	12		1.2066	2.0308	19.135	15.868	38.906
					(.086)	(.096)	(1.563)	(1.640)	(1.664)
6/84	17.3	3.0	54	1.0001	1.1954	2.0461	18.662	15.610	38.182
					(.015)	(.008)	(.110)	(.110)	(.111)
8/84 (Sta. 5)	25.1	3.1	72	0.9999	1.200	2.041	18.781	15.647	38.320
					(.014)	(.009)	(.130)	(.129)	(.130)
8/84 (Sta. 4)	19.1	3.0	24		1.208	2.033	18.896	15.641	38.426
					(.015)	(.017)	(.263)	(.254)	(.256)
12/84	3.6	3.1	18		1.1988	2.0428	18.725	15.621	38.240
					(.071)	(.050)	(.627)	(.613)	(.615)
3/85	24.1	2.9-3.0	66	0.9999	1.2033	2.0343	18.787	15.614	38.331
					(.010)	(.008)	(.059)	(.057)	(.058)
8/85	2.4	3.1-3.1	54	1.0005	1.1859	2.0621	18.872	15.908	38.896
					(.051)	(.039)	(.890)	(.874)	(.887)
10/85	9.1	3.0-3.1	48	1.0019	1.1861	2.0594	18.600	15.684	38.329
					(.051)	(.051)	(.556)	(.549)	(.561)
1/86	16.9	3.2-3.3	39	1.0014	1.1900	2.0524	18.734	15.716	38.349
					(.019)	(.125)	(.495)	(.511)	(.568)

Table E.2 Lead isotopic composition of subsurface seawater. (Station 'S', Bermuda)

Weighted Avg. Depth (m)	Sample Depths (m)	Collection Dates	Total Volume (mls.)	ngs Pb	Current (amps)	# Ratios	Fract. Factor	206/207 (95% CFL)	208/206 (95% CFL)	206/204 (95% CFL)	207/204 (95% CFL)	208/204 (95% CFL)
51	40-60	1/84-6/84	582	13.8	3.0	11		1.2030	2.0405	18.464	15.249	37.690
								(.041%)	(.074%)	(1.104%)	(1.111%)	(1.087%)
94	80-100	1/84-4/84	466	10.9	2.9-3.2	40	1.0013	1.2038	2.0338	18.859	15.666	37.362
								(.027)	(.032)	(.169)	(.176)	(.176)
173	160-180	4/84-9/84	496	11.2	2.9	60	0.9997	1.2043	2.0342	18.885	15.682	38.419
								(.017)	(.012)	(.146)	(.144)	(.142)
331	300-350	1/84-9/84	569	15.2	3.0-3.2	78	1.0005	1.2045	2.0344	18.830	15.634	38.308
								(.016)	(.012)	(.157)	(.158)	(.157)
426	390-490	1/84-9/84	427	1.8	3.3-3.4	73	1.0010	1.2030	2.0376	18.969	15.766	38.638
								(.047)	(.034)	(.341)	(.272)	(.255)
566	550-600	4/84-9/84	434	10.2	2.9-3.3	84	0.9996	1.1981	2.0442	18.737	15.640	38.307
								(.013)	(.016)	(.130)	(.132)	(.132)
649	600-692	4/84-9/84	348	6.6	3.2	12	1.0002	1.1957	2.0475	18.856	15.776	38.589
								(.034)	(.063)	(.295)	(.278)	(.281)
840	788-890	4/84-9/84	337	6.7	3.3	90	1.0002	1.1936	2.0509	18.872	15.811	38.703
								(.026)	(.020)	(.273)	(.273)	(.275)
968	900-1230	9/83-6/84	413	4.9	3.10	84	0.9998	1.1913	2.0554	18.564	15.583	38.155
								(.014)	(.008)	(.110)	(.110)	(.111)
1169	1112-1230	9/83-6/84	453	5.1	3.3	84	0.9997	1.1927	2.0544	18.648	15.635	38.309
								(.025)	(.017)	(.228)	(.231)	(.230)
1422	1387-1471	4/84-9/84	447	6.3	2.9-3.1	96	1.0009	1.1934	2.0541	18.659	15.635	38.329
								(.016)	(.015)	(.127)	(.126)	(.127)
1696	1571-1971	4/84-6/84	515	4.8	3.3	45	0.9994	1.1885	2.0577	18.545	15.600	38.149
								(.028)	(.021)	(.225)	(.221)	(.219)

Maximum blank corrections (see error bars on figures) are based on:

$$Ratio_{(meas.)} = \frac{Mass_{(sample)} Ratio_{(sample)} + Mass_{(blank)} Ratio_{(blank)}}{Mass_{(sample)} + Mass_{(blank)}}$$

$$Ratio_{(sample)} = Ratio_{(meas.)} - \left\{ \frac{Mass_{(blank)} (Ratio_{(blank)} - Ratio_{(meas.)})}{Mass_{(sample)}} \right\}$$

correction term

from NBS 981 Standard runs: $Mass_{(blank)} = 0.235$ ng

$Ratio_{(blank)} = 1.2308$ (206/207)

APPENDIX F

Sediment Trap and Rain Stable Lead Isotope Ratios

Table F.1 Lead isotopic composition of settling particles caught by sediment trap. (Station 'S', Bermuda)

Collection Date	Trap Type	Depth (m)	ngs Pb	Current (amps)	# Ratios	Fract. Factor	206/207 (95% CFL)	208/206 (95% CFL)	206/204 (95% CFL)	207/204 (95% CFL)	208/204 (95% CFL)
8/84	Shen	90	5.4	3.0-3.2	84	1.0000	1.2045	2.0365	18.796	15.604	38.278
							(.022)	(.015)	(.205)	(.205)	(.204)
		400*	1.7	3.52	18		1.2235	2.0089			
							(.087)	(.038)			
		860	~2	3.2-3.4	81	0.9997	1.2048	2.0365	19.052	16.201	39.807
							(.046)	(.040)	(.563)	(.548)	(.552)
3/85	Shen	90	2.6	3.1-3.2	77	0.9999	1.1944	2.0483	18.777	15.728	38.464
							(.044)	(.031)	(.402)	(.402)	(.404)
		400	7.5	3.0-3.1	90	0.9997	1.2021	2.0369	19.045	15.844	38.802
							(.038)	(.026)	(.313)	(.321)	(.315)
		860	11.1	2.9	54	0.9999	1.1971	2.0458	18.709	15.627	38.269
							(.011)	(.013)	(.057)	(.059)	(.059)
2/79*	Deuser	3200	863	2.4	9		1.1638	2.0941	18.246	15.643	38.131
							(.129)	(.266)	(.295)	(.490)	(.536)
5/81*	Deuser	3200	87	2.7-2.9	24		1.1707	2.0829	18.248	15.588	38.013
							(.084)	(.149)	(.176)	(.181)	(.212)
9/83*	Deuser	3200	149	2.9	24		1.1760	2.0813	18.563	15.788	38.646
							(.052)	(.111)	(.557)	(.570)	(.668)

* samples contaminated

Maximum blank corrections (see error bars on figures) are based on:

$$Ratio_{(meas.)} = \frac{Mass_{(sample)} Ratio_{(sample)} + Mass_{(blank)} Ratio_{(blank)}}{Mass_{(sample)} + Mass_{(blank)}}$$

$$Ratio_{(sample)} = Ratio_{(meas.)} - \left\{ \frac{Mass_{(blank)} (Ratio_{(blank)} - Ratio_{(meas.)})}{Mass_{(sample)}} \right\}$$

correction term

from NBS 981 Standard runs: $Mass_{(blank)} = 0.235$ ng

$Ratio_{(blank)} = 1.2308$ (206/207)

Table F.2 Lead isotopic composition of Bermuda rain.

Collection Date	ngs Pb	Current (amps)	# Ratios	Fractionation Factor	206/207 (95% CFL)	208/206 (95% CFL)	206/204 (95% CFL)	207/204 (95% CFL)	208/204 (95% CFL)
11/9/82	19.0	3.0-3.1	68	0.9995	1.1810	2.0507	18.375	15.558	38.679
					(.025%)	(.022%)	(.228%)	(.218%)	(.219%)
5/29/83	17.6	2.7-3.0	48	0.9996	1.1809	2.0655	18.404	15.583	38.012
					(.018)	(.017)	(.120)	(.122)	(.123)
5/29/83	14.3	3.0	36	0.9988	1.1813	2.0644	18.385	15.564	37.957
					(.029)	(.028)	(.191)	(.187)	(.182)
11/6/83	3.1	3.3	39	0.9988	1.1782	2.0612	18.5078	15.702	38.144
					(.059)	(.050)	(.860)	(.880)	(.866)

BIOGRAPHICAL NOTE

The author was born on July 11, 1957 in Rego Park, New York. He was raised in Dumont and Oradell, New Jersey and graduated River Dell Senior High School in 1975. In the fall of 1975, he entered the Massachusetts Institute of Technology and pursued a degree in chemical engineering. En route to the S.B. in January, 1979, he spent several semesters working for Professor John Edmond under the auspices of M.I.T.'s Undergraduate Research Opportunities Program. Upon graduating, the author was employed by the Procter and Gamble Company as a process engineer in their International Division. In September 1981, he entered the M.I.T.- W.H.O.I. Joint Program in Oceanography as a candidate for the degree of Doctor of Philosophy. The author is a member of Sigma Xi, the American Geophysical Union, the Geochemical Society, and the American Association for the Advancement of Science.

Publications

Shen, G.T., E.R. Sholkovitz and D.R. Mann (1983). The coagulation of dissolved $^{239,240}Pu$ in estuaries as determined from a mixing experiment, Earth Planet. Sci. Lett. 64: 437-444.

Boyle, E.A., S.D. Chapnick, G.T. Shen and M.P. Bacon (1986). Temporal variability of lead in the western North Atlantic, J. Geophys. Res., 91: 8573-8593.

Shen, G.T. and E.A Boyle (in preparation). Determination of lead, cadmium, and other trace metals in annually-banded corals.

Shen, G.T. and E.A. Boyle (in preparation). Lead in corals: Reconstruction of historic industrial fluxes to the surface ocean.

Shen, G.T., E.A. Boyle and D.W. Lea (in preparation). Cadmium in corals: Chronicles of historic upwelling and industrial fallout.